Palacký University Olomouc

Department of Biophysics

Centre of the Region Haná for Biotechnological and Agricultural Research

Faculty of Science

Biological Activity of Substances with Strong Antisenescence Effect

Autoreferát

Zuzana Kučerová

Olomouc 2020

Uchazeč:	Mgr. Zuzana Kučerová
	Katedra biofyziky
	Přírodovědecká fakulta Univerzity Palackého v Olomouci
Školitel:	Doc. RNDr. Martina Špundová, Ph.D.
Název práce:	Biologická aktivita látek se silným antisenescenčním účinkem
Oponenti práce:	prof. Ing. Miloš Barták, CSc.
	Přírodovědecká fakulta Masarykovy Univerzity
	Mgr. Markéta Pernisová, Ph.D.
	Přírodovědecká fakulta Masarykovy Univerzity
Místo a termín obhajoby:	

S disertační prací a posudky je možné se seznámit na Katedře biofyziky Přírodovědecké fakulty Univerzity Palackého v Olomouci.

Declaration

I hereby declare that I have written this thesis independently as the original work with the help of my supervisor doc. RNDr. Martina Špundová, Ph.D. The complete list of used literature and other information sources is included in the section References.

Olomouc, 2020   Zuzana Kučerová

Abstract

It is well known that leaf senescence can be suppressed by exogenous application of phytohormones cytokinins. Nevertheles, under specific conditions, cytokinins can have negative effects and can even accelerate senescence. For this reason there are efforts to prepare compounds (cytokinin derivatives) that lack those effects and have other advantageous properties. Recently, two aromatic cytokinin arabinosides (6-benzylamino-9-β-D-arabinofuranosylpurines; BAPAs), 3-hydroxy- (3OHBAPA) and 3-methoxy- (3MeOBAPA) derivative have been synthesized and found to possess unique effects and mechanism of action. Analysis of gene expression that was performed on detached *Arabidopsis thaliana* L. leaves treated with 3MeOBAPA revealed that 6h and 48h treatments with this compound results in a shift in gene transcription toward defence. 3MeOBAPA causes upregulation of genes involved in plant innate immunity including MAPK signalling pathway together with oxidative burst and JA-ethylene signalling, which results in effective protection of field-grown plants against fungal pathogens. Long-term incubation of leaves in 3OHBAPA and 3MeOBAPA does not impair leaf fitness which is common during prolonged activation of defence response mechanisms, but on the contrary effectively delays senescence of detached leaves. Interestingly, the anti-senescence differs quantitatively in wheat (*Triticum aestivum* L. cv. Aranka) and Arabidopsis (Col-0). In wheat, 3OHBAPA has higher protective effect than 3MeOBAPA, whereas in Arabidopsis, 3MeOBAPA is the more efficient derivative. We have found that the different anti-senescent activity of 3OHBAPA and 3MeOBAPA is coupled to different ethylene production in the treated leaves: the lower the ethylene production, the higher the anti-senescence activity. 3OHBAPA and 3MeOBAPA also protect efficiently the senescing leaves of wheat and Arabidopsis against oxidative damage induced by both H_2O_2 and high-light treatment, which could also be connected with the low level of ethylene production.

Abstrakt

Listovou senescenci lze oddálit exogenní aplikací fytohormonů cytokininů. Za určitých podmínek však mohou mít cytokininy negativní účinky a mohou naopak proces senescence urychlit. Z tohoto důvodu jsou připravovány látky na bázi cytokininů, které tyto negativní účinky nemají a mají další výhodné vlastnosti. V nedávné době byly připraveny dva aromatické cytokininové arabinosidy (6-benzylamino-9-β-D-arabinofuranosylpuriny; BAPA), 3-hydroxy-derivát (3OHBAPA) a 3-methoxyderivát (3MeOBAPA), jejichž účinky a mechanismus účinku jsou jedinečné. Analýza genové exprese, která byla provedena na oddělených listech *Arabidopsis thaliana* L. ponořených v roztoku 3MeOBAPA po dobu 6 a 48 h, odhalila, že tato látka aktivuje geny zapojené v obraně proti patogenům. 3MeOBAPA aktivuje signální dráhy spojené s MAPK, ethylenem a kyselinou jasmonovou a způsobuje přechodnou akumulaci reaktivních forem kyslíku. Tyto reakce mohou vést ke zvýšení rezistence ošetřených rostlin, jak bylo ověřeno v polních experimentech. Ačkoliv dlouhodobá aktivace mechanismů zapojených v obraně proti patogenům má zpravidla za následek zhoršení fyziologického stavu rostlin, 3OHBAPA a 3MeOBAPA naopak vykazují velmi silné antisenescenční účinky. Tyto účinky se kvantitativně liší u oddělených listů pšenice (*Triticum aestivum* L. cv. Aranka) a Arabidopsis (Col-0). Zatímco v případě pšenice má vyšší antisenescenční účinek 3OHBAPA, u listů Arabidopsis je účinnější 3MeOBAPA. Tento rozdílný efekt je spojen s různou produkcí ethylenu v ošetřených listech: čím nižší je produkce ethylenu, tím vyšší je antisenescenční aktivita daného derivátu. 3OHBAPA a 3MeOBAPA také účinně ochraňují senescentní listy pšenice a Arabidopsis před oxidativním poškozením vyvolaným působením H_2O_2 a světla, což může rovněž souviset s nízkou produkcí ethylenu po aplikaci těchto látek.

List of Publications

The thesis is based on two research articles:

1. **Kučerová Z**, Rác M, Mikulík J, Plíhal O, Pospíšil P, Bryksová M, Sedlářová M, Doležal K, Špundová M (2020) The anti-senescence activity of cytokinin arabinosides in wheat and Arabidopsis is negatively correlated with ethylene production. *International Journal of Molecular Sciences* 21: 8109. IF (2019) = 4.556

   (Kučerová Z *designed the experiments, prepared samples for all experiments, performed Chl fluorescence and ion leakage measurements, analysed and interpreted the data and wrote the article*)

2. Bryksová M*, Dabravolski S*, **Kučerová Z***, Zavadil Kokáš F, Špundová M, Plíhalová L, Takáč T, Gruz J, Hudeček M, Hloušková V, Koprna R, Novák O, Strnad M, Plíhal O, Doležal K (2020) Aromatic cytokinin arabinosides promote PAMP-like responses and positively regulate leaf longevity. *ACS Chemical Biology* 15: 1949–1963. IF (2019) = 4.434; * contributed equally

   (Kučerová Z *designed the experiments related to photosynthetic activity in the detached leaves, performed Chl fluorescence and chlorophyll content measurements, wrote the corresponding parts of the article and prepared figures throughout the article*)

Research articles by the same author that are not included in the thesis:

1. Crepin A, **Kučerová Z**, Kosta A, Durand E, Caffarri S (2020) Isolation and characterization of a large photosystem I-light harvesting complex II supercomplex with an additional lhca1-a4 dimer in Arabidopsis. *Plant Journal* 102: 398-409. IF (2019) = 6.141

   (Kučerová Z *performed the biochemical experiments*)

2. Bednaříková M, Folgar-Cameán Y, **Kučerová Z**, Lazár D, Špundová M, Hájek J, Barták M (2020) Analysis of K and L band appearance in OJIPs in Antarctic lichens in low and high temperature. *Photosynthetica* 58: 646-656. IF (2019) = 2.562

   (Kučerová Z *performed the thermostability measurements*)

3. Ilík P, Špundová M, Šicner M, Melkovičová H, **Kučerová Z**, Krchňák P, Fürst T, Večeřová K, Panzarová K, Benediktyová Z, Trtílek M (2018) Estimating heat tolerance of plants by ion leakage: A new method based on gradual heating. *New Phytologist* 218: 1278-1287. IF (2018) = 7.299

   (Kučerová Z *measured the heat tolerance of various plant species using ion leakage methods*)

Content

1 Introduction

The dissertation thesis is focused on the unique biological activity and the possible mechanism of action of aromatic cytokinin arabinosides, newly prepared derivatives of phytohormones cytokinins. Despite its benefits for the plant as such, consisting mainly in the recycling and storage of nutrients, senescence (especially premature) is one of the processes that negatively affect plant production from an agricultural point of view. Therefore, delaying senescence is desirable in this regard. The ability of cytokinins to delay senescence has been known for a long time, however, under certain conditions cytokinins can have negative effects, including accelerating senescence. For this reason, their new derivatives such as cytokinin arabinosides are synthesized. These novel compounds generally do not have cytokinin-like adverse effects and, on the contrary, are characterized by other advantageous properties.

1.1 Senescence

Plant senescence is a final stage of development that usually precedes to death of the plant itself. This highly organised and controlled process allows nutrients and organic resources mobilization and recyclation from senescing to growing, reproductive or storage organs (e.g. Smart 1994, Gan & Amasino 1997, Himelblau & Amasino 2001, Zwack & Rashotte 2013, Maillard et al. 2015, Havé et al. 2017). Typical phenomena that accompany senescence are degradation of photosynthetic pigments, proteins, membrane lipids, amino acids and related inhibition of photosynthesis and other anabolic processes that are overall substituted by catabolism (Schippers et al. 2015, Diaz-Mendoza et al. 2016, Tamary et al. 2019). The probably most apparent marker of senescence is chlorophyll (Chl) degradation accompanied by visible yellowing of leaves. However, Chl is not the only pigment whose content decreases during senescence. As carotenoids are degraded to a lesser extent than Chl, the yellow colour is typical for senescing leaves (Biswal 1995).

Genes that are they are responsible for the execution of the senescence-induced changes in plant organism are referred to as senescence-associated genes (SAGs). Expression of SAGs is activated or increases with the onset and progression of senescence (Gan & Amasino 1997, Lim et al. 2003). Majority of senescence-induced degradation processes involve SAG-encoded

proteins such as cystein and aspartic proteases, lipases, RNAses, components of ubiqutin-proteasome system or enzymes of nutrient recycling.

While nucleus and mitochondria remain intact and active to control and provide energy until the final stages of senescence, chloroplasts are first organelles that undergo senescence-induced changes and subsequently degradation. During senescence chloroplasts undergo many changes whether it is their number and volume in the cell, their structure or photochemical function (Špundová et al. 2003, Springer et al. 2016, Tamary et al. 2019). Number and also size of chloroplasts decrease and thylakoid, stromal and envelope components are dismantled. Senescence also induces changes in chloroplast shape which becomes more spherical (Špundová et al. 2003, Tamary et al. 2019).

It is well known that thylakoid membranes of chloroplast are the site of light-dependent photosynthetic reactions. The energy of photons absorbed by the photosystem II (PSII) via its light-harvesting complexes (LHCII) is further distributed in three possible ways: photochemical, fluorescent and thermal dissipation. These processes compete with each other, where a decrease in one means an increase in the representation of another (e.g. Roháček & Barták 1999, Lazár 2015). The senescence-induced changes in photosynthesis can be evaluated using measurement of Chl fluorescence parameters (e.g. Roháček & Barták 1999, Špundová et al. 2003, Vlčková et al. 2006, Prokopová et al. 2010b).

The accumulation of reactive oxygen species (ROS) is one of the early phenomena of senescence (e.g. Rosenvasser et al. 2006, Khanna-Chopra 2012). Since ROS can serve as secondary messengers or act as independent signalling molecules they are involved in almost all signalling cascades in plant organism (Mittler et al. 2004, Sewelam et al. 2016, Mayta et al. 2019). This phenomena is referred to as an oxidative signalling. Enhanced production of ROS is initiated by various physiological processes such as photosynthesis, pathogen recognition, stress or hormonal perception. ROS then activate cellular response to corresponding stimulus. ROS level is modulated by positive feedback loop and ROS-scavenging pathways (Mittler 2002). However, ROS are extremely reactive and toxic and when their accumulation overcomes the control mechanisms, they can oxidize cell components. This phenomena is called oxidative damage. Extensive formation of ROS is induced by senescence or stress-induced inhibition of photosynthesis and Chl metabolism (Thompson et al. 1987, Zimmermann & Zentgraf 2005, Rosenvasser et al. 2006, Zavaleta-Mancera et al. 2007, Del Río

2015, Zhang et al. 2016, Mayta et al. 2019). High concentrations of ROS can cause additional damage to photosynthetic apparatus and oxidative impairment of cellular components, DNA or aminoacids (Zimmermann & Zentgraf 2005).

1.2 Cytokinins

Cytokinins (CKs) are group of phytohormones that affect various plant developmental and physiological processes such as cell division, apical dominance, de-etiolization, organ formation, nutrients metabolism and defence against pathogens. CKs are considered as negative regulators of leaf senescence, i.e. they are able to delay senescence-induced changes (e.g. Mok & Mok 2001).

1.2.1 Cytokinins structure

Naturally occurring CKs are derivatives of adenine with isoprenoid or aromatic side chain at the N6 atom of purine moiety. Isoprenoid CKs are the predominant type, especially those with *trans*-hydroxylated side chain such as *trans*-zeatin (tZ) and its derivatives. The group of isoprenoid CKs also includes isopentenyladenine (iP), *cis*-zeatin (cZ) and dihydrozeatin (Mok & Mok 2001, Doležal et al. 2007). CKs with aromatic side chain were considered as an artificial compounds for a long time. However it has been proven that they naturally occur in various plant species (for review see Strnad 1997). Typical aromatic CKs are 6-furfurylaminopurine (kinetin), 6-benzylaminopurine (BAP) and its hydroxylated forms topolins. In terms of their functions, the isoprenoid CKs are considered to have a more potent effect on growth processes such as cell cycle while aromatic CKs have more pronounced effect on developmental processes, especially those involving morphogenesis and senescence (Holub et al. 1998). Beside the naturally occurring CKs there is also group of synthetic CKs derived from phenylurea represented e.g. by thidiazuron (TDZ) and diphenylurea (Mok & Mok 2001).

1.2.2 Cytokinin signalling

In the plasmatic membrane of *Arabidopsis thaliana* L., there are three highly homologous receptor histidine kinases involved in CK signal transduction, AHK2, AHK3 and CRE1/AHK4 (Inoue et al. 2001, Suzuki et al. 2001, Ueguchi et al. 2001a, b, Yamada et al. 2001). Phosphorylated histidine kinases activate histidine phosphotransfer protein (AHP) which is further translocated into nucleus. After entering nucleus, the response regulators (ARRs) are phosphorylated and then are capable to regulate the transcription of responsive genes.

The CK histidine kinases participate differently in mediating the CK action. All three receptors affect fertility, sperm size, germination, and CK metabolism. The effect on root branching and leaf cell division is mainly mediated by AHK2 and AHK3. CRE1/AHK4 plays a major role in the extension of the primary root and in the root response to the application of exogenous CKs. CK-induced photomorphogenesis as well as Chl retention are mediated primarily by the AHK3 receptor. CK-induced senescence delaying is specifically mediated via AHK3 and ARR2 (Kim et al. 2006, Riefler et al. 2006, Janečková et al. 2018). Just as the involvement of CK receptors in influencing biological responses is different, so is the affinity of individual receptors for different types of CK. *In vitro*, AHK3 and CRE1/AHK4 have the highest overall affinity for isoprenoid types of CK, tZ and iP, and also for TDZ. All three receptors are capable to bind also cZ, although with lower affinity. Sensitivity of both AHK3 and CRE1/AHK4 to aromatic CKs is very low and it is presumed that these CKs act preferably via AHK2 (Spíchal et al. 2004, Romanov et al. 2006).

1.2.3 Cytokinins and senescence-induced changes

An increase in endogenous content of CKs and also their exogenous application on plants very effectively delays senescence (e.g. Gan & Amasino 1995, Vlčková et al. 2006, Zavaleta-Mancera et al. 2007, Zwack & Rashotte 2013, Janečková et al. 2018). Exogenously applied CKs can postpone senescence-induced changes in detached senescing leaves including a decrease in Chl and carotenoid content, inhibition of photosynthesis including PSII photochemistry, degradation of proteins, pigment-protein complexes and whole chloroplasts, as well as membrane deterioration (e.g. Holub et al. 1998, Oh et al. 2005, Vlčková et al. 2006, Zavaleta-Mancera et al. 2007, Zubo et al. 2008, Liu et al. 2016, Janečková et al. 2019).

The anti-senescence activity of CKs has been found to be related to downregulation of SAGs (e.g. Weaver et al. 1998) and up-regulation of genes encoding components of photosynthetic light-harvesting complexes (Vylíčilová et al. 2016). One of the most widely used CK either in agricultural practise (for review see Koprna et al. 2016) or in biotechnological applications (for review see Plíhalová et al. 2016), is the aromatic CK BAP that is known to possess strong anti-senescence effects. However, under certain conditions, BAP can have adverse effects on primary root development, lateral root branching or shoot formation *in vitro* (Woodward & Marshal 1988, Werbrouck et al. 1996, Iqbal et al. 2006, Bairu et al. 2007, 2009). In the case of long-term exposure of plant tissues to high concentrations of BAP or in

4

combination with light, BAP can even accelerate senescence (Rulcová & Pospíšilová 2001, Carimi et al. 2004, Prokopová et al. 2010b, Vylíčilová et al. 2016).

1.3 Cytokinin derivatives

It is well known that not only CKs but also their artificially prepared derivatives can delay senescence-induced changes. Some of the derivatives are even more effective than CKs themselves, not only in the case of anti-senescence action but also in other CK activities. Biological activity of newly prepared compounds is usually tested and compared to that of CKs in three standard (tobacco callus bioassay, Amaranthus bioassay, wheat leaf senescence bioassay) and two reporter CK bioassays (bacterial receptor and ARR::GUS reporter assay). The standard bioassays are based on main CK activities such as stimulation of cell division, induction of betacyanin synthesis and delaying leaf senescence. Receptor bioassays are used for estimation of the relative activation of CK receptors and the extent of ARR promoter activation, i.e. the ability to activate the CK signalling pathway *in vitro*.

1.3.1 Anti-senescence activity of CK derivatives

Since the purine moiety of isoprenoid and aromatic CKs can be substituted at several positions such as N1, C2, N3, N6, C8 and N9, it is possible to synthetize wide range of compounds with various biological effects (for detailed review see Plíhalová et al. 2016). A number of previously prepared compounds have been shown to be more efficient in delaying senescence than unmodified CKs.

For example, derivatives of kinetin with short halogenoalkyl chains substituted on the N9 atom of purine moiety (N9-kin) possess anti-senescence activity comparable or higher than that of kinetin. The type of halogen atom and the length of the alkyl chain have been shown to determine the maintenance of Chl content during induced senescence. N9-kin with a shorter alkyl chain were more active and at the same time N9-kin containing chlorine in the alkyl chain were more active than derivatives containing bromine. The most active derivative in the wheat senescence bioassay was furfurylamino-9-(2-chloroethyl)purine, a chlorine-containing short alkyl chain kinetin derivative. This compound also significantly reduced lipid peroxidation in dark-incubated wheat leaf segments. However, in comparison to kinetin, this derivative does not have any effect on expression of analysed Arabidopsis genes related to CK metabolism and signalling (Mik et al. 2011).

It has been reported that hydroxylation of the benzyl ring in the *meta*-position increased activity of BAP in the tobacco callus and wheat senescence bioassay. Hydroxylation in the *ortho*-position leads to opposite effects of the compounds in the bioassays. Although ribosylation at the N9 position was found to lower the compound activity in tobacco callus bioassay it increased the anti-senescence activity. Glycosylation on the N9 position lowered activity in all bioassays (Holub et al. 1998).

Tarkowská et al. (2003) prepared *ortho*- and *meta*-methoxy-derivatives of mT, 6-(2-methoxybenzylamino)purine (MeoT) and 6-(3-methoxybenzylamino)purine (MemT), and also their ribosides, MeoTR and MemTR. All newly prepared derivatives had by 80-100 % higher anti-senescent activity than BAP (Tarkowská et al. 2003). Similar results were obtained by Doležal et al. (2007). They observed strong differences in activities of prepared analogues of BAP riboside with various substituents (halogen-, hydroxy- and methoxy- groups), at the benzyl ring in the CK bioassays. While activity of almost 50 % of the prepared compounds exceeded that of BAP in the wheat senescence bioassay, only few derivatives were able to interact with AHK receptors. In addition, some of the prepared compounds displayed strong cytotoxic activity (Doležal et al. 2007).

A series of 2-chloro-6-(halogenobenzylamino)purine ribosides was prepared by Vylíčilová et al. (2016). Majority of these derivatives showed high activity in all three CK bioassays, especially in the wheat senescence bioassay. Similarly to other mentioned compounds, derivatives prepared by Vylíčilová (2016) did not activate CK signalling via AHK receptors. The gene expression analysis performed in senescent Arabidopsis leaves treated by selected compounds revealed that these derivatives caused upregulation of genes related to PSI, PSII, Calvin cycle and CK signalling and metabolism together with downregulation of genes encoding Chl degradation. Application of these derivatives was accompanied also by an increase in the relative abundance of LHCII (Vylíčilová et al. 2016).

It is evident that structure-activity relationship in various CK derivatives is very complex issue, however it is possible to conclude that ribose conjugation on N9 position of adenine moiety of BAP leads to increased activity in the wheat senescence bioassay (for recent review see Vylíčilová et al. 2020).

2 Aims of research

Although a large number of different derivatives with various effects in plant organism are synthesized, there is only limited amount of information about their biological activity or mechanism of action. Newly prepared compounds are usually tested using standard and receptor CK bioassays, which provide only basic information about structure-action relationship of these substances. A more detailed approach is needed to reveal mechanisms of their action and thoroughly evaluate their potential for practical use.

In terms of the anti-senescent activity, only the ability of compounds to retain Chl content in senescing leaves is usually examined. Therefore, very little is known about their effect on photosynthetic apparatus and function and other processes affected by senescence. The main aim of our research was to evaluate the effect of novel CK derivatives, referred to as CK arabinosides, on structure and function of photosynthetic apparatus in dark-senescing leaves to propose their possible mechanism of action.

3 Results and discussion

Biological activity of 21 newly synthetized aromatic 6-benzylamino-9-β-D-arabinofuranosylpurines (BAPAs) was compared to naturally occurring aromatic CK BAP. None of the BAPAs exceeded biological activity of BAP in the tobacco callus bioassay and Amaranthus bioassay showing that their CK activity is only weak. Similarly, none of the BAPAs had ability to activate Arabidopsis CK receptors CRE1/AHK4 and AHK3 *in vitro*. Nevertheless, the activity of BAPAs in wheat leaf senescence bioassay was similar or even higher than that of BAP suggesting they possess high anti-senescence activity without triggering the CK pathway. Based on these results two compounds (3OHBAPA and 3MeOBAPA) were chosen for further testing.

3.1 Gene expression changes in 3MeOBAPA-treated Arabidopsis leaves

The high-troughput mRNA sequencing analysis of genes affected by 3MeOBAPA treatment revealed strong upregulation of genes that are related to plant defence response mechanisms such as jasmonic acid and ethylene-dependent systemic resistance (Table 1) and various cell wall modifications. In the term of downregulation, genes related to photosynthesis were the mostly affected ones. Since downregulation of photosynthetic genes is a hallmark of early responses of plants to pathogens (Bilgin et al. 2010) it is apparent that 3MeOBAPA treatment shifted the transcriptional response markedly towards defence.

Table 1. The expression level of selected genes in *Arabidopsis thaliana* L. after 48 h treatment with 10 µmol.l^{-1} 3MeOBAPA. Gene ID, name and description and log$_2$ fold change in 3MeOBAPA-treated leaves are presented.

ID	Log$_2$ fold change	Gene name	ID	Log$_2$ fold change	Gene name	ID	Log$_2$ fold change	Gene name
AT5G47910	2.20	*RBOHD*	AT4G2814	6.47	*ERF54*	AT1G0134	2.06	*CNGC10*
AT1G64060	0.66	*RBOHF*	AT1G7583	7.85	*PDF1.1*	AT2G4645	1.21	*CNGC12*
AT5G60010	5.40	*RBOHH*	AT5G4442	8.15	*PDF1.2A*	AT4G0101	1.31	*CNGC13*
AT5G07390	4.49	*RBOHA*	AT2G2602	6.04	*PDF1.2B*	AT3G1769	1.41	*CNGC19*
AT5G51060	4.26	*RBOHC*	AT5G4443	8.87	*PDF1.2C*	AT5G4589	-12.35	*SAG12*
AT4G11230	3.04	*RBOHI*	AT2G2601	8.23	*PDF1.3*	AT5G0328	-0.93	*EIN2*
AT2G14610	4.08	*PR1*	AT4G0850	1.15	*MEKK1*	AT3G2077	-0.69	*EIN3*
AT1G80460	0.52	*NHO1*	AT4G2607	0.6	*MKK1*	AT5G3961	-1.30	*ORE1*
AT3G26830	5.01	*PAD3*	AT4G2981	0.99	*MKK2*	AT2G4262	-1.66	*ORE9*
AT4G33430	1.63	*BAK1*	AT1G5166	2.08	*MKK4*	AT2G4300	4.14	*JUB1*
AT2G39660	1.55	*BIK1*	AT3G2122	0.68	*MKK5*	AT3G2284	5.02	*ELIP1*
AT5G20480	2.57	*EFR*	AT1G0156	2.57	*MPK11*	AT4G1469	3.71	*ELIP2*
AT1G06160	2.62	*ERF59*	AT4G0137	0.98	*MPK4*	AT1G3013	5.19	*JAZ8*
AT3G23240	0.32	*ERF1B*	AT3G4564	0.94	*MPK3*	AT2G3460	1.13	*JAZ7*

3.2 3MeOBAPA affects PTI via MAPK signalling modules

It is known that both exogenous and endogenous CKs can enhance plant resistance to pathogens (Choi et al. 2010, 2011, Prokopová et al. 2010b) but mechanism of their action in plant immunity is not fully understood. According to model by Choi et al. (2010) CKs increase the defence response and consequently plant resistance to pathogen via activation of AHK2/AHK3 and ARR2. We suppose that the activation of defence response by 3MeOBAPA may be different as 3MeOBAPA was not recognised by the AHK3 and AHK4 receptors *in vitro* and no upregulation of *ARR2* and most of the other CK response regulators was observed after its application. Moreover, this presumption is in line with the low cytokinin activity of 3MeOBAPA in tobacco callus and Amaranthus bioassay.

It is generally accepted that early steps in PAMP-triggered immunity (PTI) responses include MAPK signalling modules. As the main MAPKs that are involved in PTI are considered MPK4, MPK3, MPK6 and recently also MPK11 was assigned to them (Bethke et al. 2012, Bigeard et al. 2015). Upregulation of the MAPK signalling pathway (both MEKK1-MKK1/2-MPK11+MPK4 and MEKK1-MKK4/5-MPK3+MPK6, Table 1) and markers of PTI such as *RBOH*s (coding for respiratory burst oxidase homologs), *FLG22-INDUCED RECEPTOR-LIKE KINASE 1 (FRK1)*, pathogen-related WRKY transcription factors (*WRKY22, 29, 33, 53*), *PATHOGENESIS RELATED 1 (PR1)*, *NONHOST RESISTANCE TO P.S. PHASEOLICOLA 1* (*NHO1*) or *PHYTOALEXIN DEFICIENT 3* (*PAD3*) (Table 1) suggest that 3MeOBAPA induces plant responses similar to that triggered by PAMPs, thus it promotes PTI.

To corroborate the assumption that 3MeOBAPA provokes PTI response through MAPK cascade the expression profiles of *MPK3*, *MPK4*, *MPK6* and *MPK11* after 30 min, 6 h and 48 h of 3MeOBAPA treatment (10 and 50 μmol.l^{-1}) were investigated. Concentration-dependent effect of 3MeOBAPA treatment on the expression patterns of *MPK3*, *MPK4* and *MPK11* was observed while *MPK11* was the most affected (Fig. 1A). Immunoblotting experiments showed that the abundance of MPK3, MPK4 and pMPK3 in 3MeOBAPA-treated detached leaves was mostly similar either to mock- or BAP-treated leaves (both applied at concentration 10 μmol.l^{-1}, Fig. 1B-D, F). The exception was the increased abundance of MPK3, MPK6 and also its phosphorylated form pMPK6 in 3MeOBAPA-treated leaves after 6 h (Fig. 1G) indicating possible involvement of *MPK3* and *MPK6* in long-term 3MeOBAPA-induced responses.
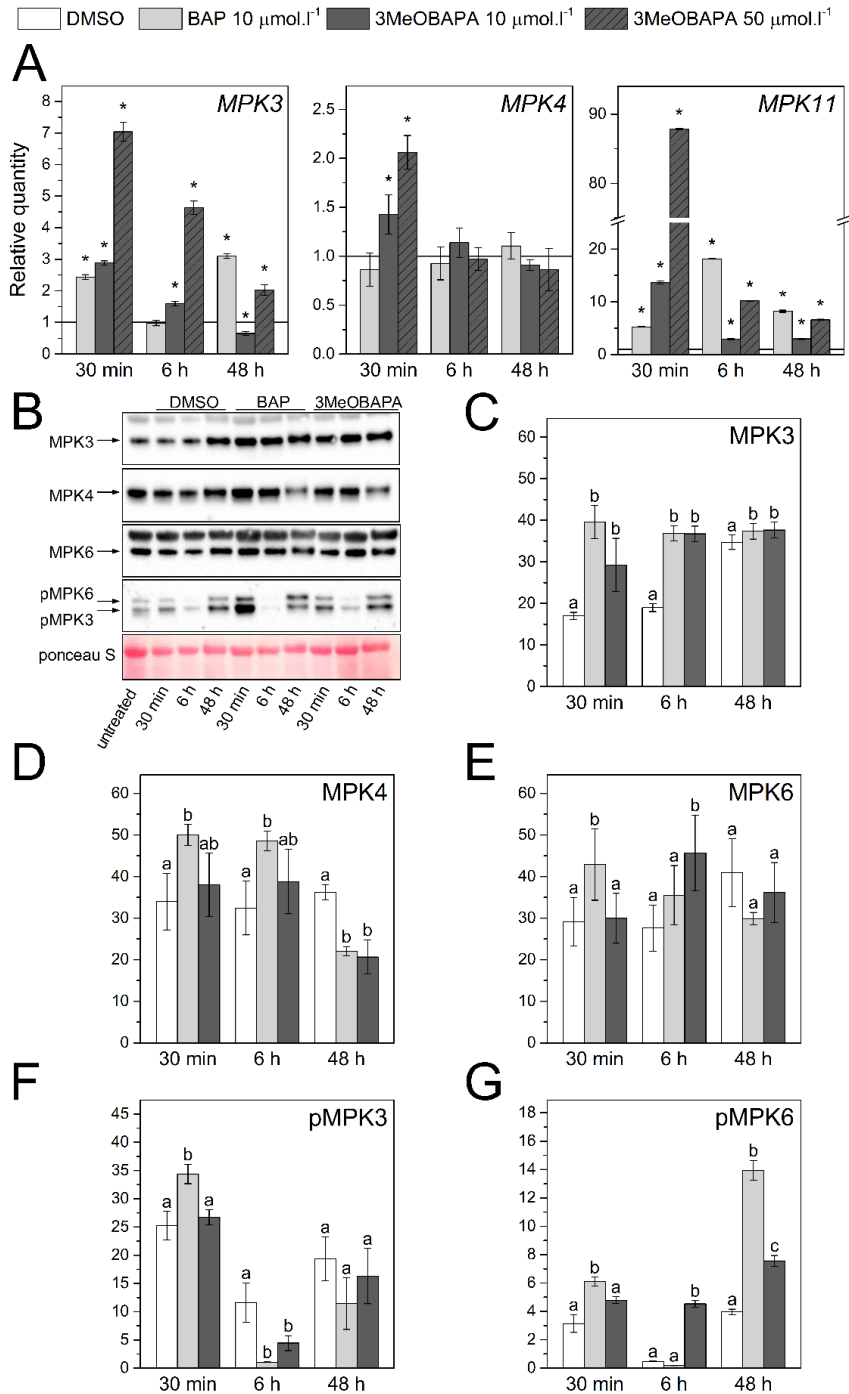
Fig. 1. (A) Expression profiles of *MPK3*, *MPK4* and *MPK11* in detached leaves treated by 0.1% DMSO or 10 μmol.l^{-1} BAP or 3MeOBAPA; or 50 μmol.l^{-1} 3MeOBAPA for 30 min, 6 h and 48 h quantified using qPCR. Means and SD are presented (n = 4). Asterisks indicate statistically significant difference of treated versus untreated (control) leaves ($p < 0.05$; Student´s unpaired *t*-test). **(B)** Immunoblots of Arabidopsis leaves incubated in 0.1% DMSO or 10 μmol.l^{-1} BAP or 3MeOBAPA for 30 min, 6 h and 48 h and probed with anti-MPK3, anti-MPK4, anti-MPK6, anti-pERK phosphospecific antibodies recognizing the phosphorylated forms of MPK3 and MPK6 (pMPK3, pMPK6). Ponceau S staining was used for loading control to verify that equal quantities of all studied proteins were loaded onto each probed membrane. **(C-G)** Quantification of band densities from immunoblots **(C)** for MPK3, **(D)** MPK4, **(E)** MPK6, **(F)** phosphorylated MPK3; pMPK3 and **(G)** phosphohorylated MPK6; pMPK6. In **(F)** and **(G)** the densities are normalized to the abundance of the corresponding MPKs. In **(C-G)** Means and SD are presented. Different letters indicate statistically significant difference between treatments ($p < 0.05$; Student´s unpaired *t*-test). Reprinted and adapted with permission from Bryksová et al. (2020). Copyright (2020) American Chemical Society.

3.3 Ethylene, jasmonic acid and ROS as signalling agents

3MeOBAPA treatment caused a strong upregulation of genes that are related to jasmonic acid (JA) and ethylene-dependent systemic resistance and upregulation of genes coding for Rbohs (respiratory burst oxidase homologs, important source of ROS production as a response to pathogen infection in plants). To confirm activation of these defence response mechanisms by 3MeOBAPA, the ethylene production in 3MeOBAPA-treated leaves (for 48 h and 72 h) and content of JA forms after 48-h treatment was compared to mock-treated leaves (Fig. 2). In the case of ethylene, 3MeOBAPA treatment increased its production after both time periods (Fig. 2A). Similarly, the content of all three JA forms (precursor *cis*-(+)-12-oxo-phytodienoic acid (*cis*-OPDA), JA itself and its major biologically active form jasmonoyl-L-isoleucine (JA-Ile)) was higher in 3MeOBAPA-treated leaves (Fig. 2B). 3MeOBAPA also induced increase in overall ROS production in 3 h of the treatment followed by a gradual decrease to pre-treatment levels (Fig. 2C) in Arabidopsis cell cultures.
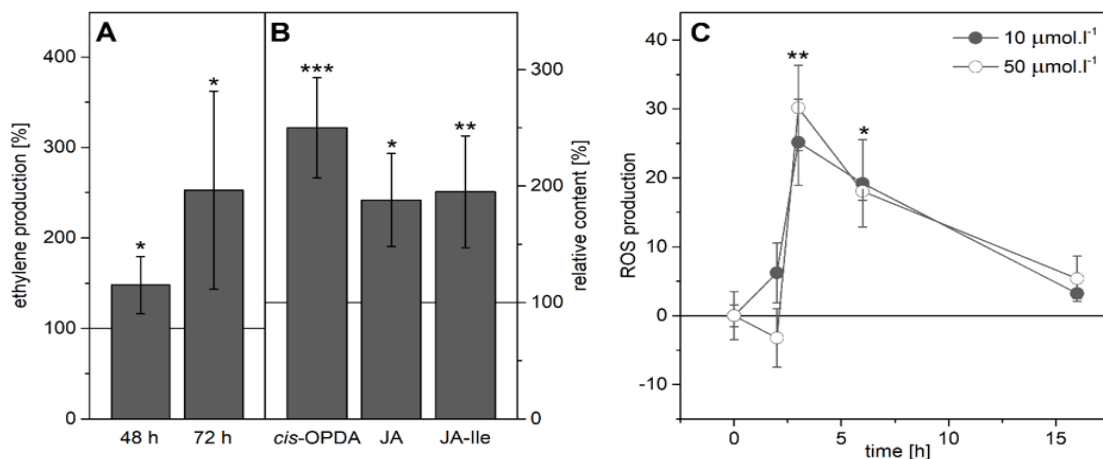

Fig. 2. (**A**) Ethylene production in detached Arabidopsis leaves treated by 10 µmol.l⁻¹ 3MeOBAPA for 48 and 72 h compared to mock-treated leaves. (**B**) Relative content of *cis*-(+)-12-oxo-phytodienoic acid (*cis*-OPDA), jasmonic acid (JA) and jasmonoyl-L-isoleucine (JA-Ile) in detached Arabidopsis leaves treated by 10 µmol.l⁻¹ 3MeOBAPA for 48 h compared to mock-treated leaves. (**C**) Overall ROS production in Arabidopsis cell cultures treated by 10 and 50 µmol.l⁻¹ 3MeOBAPA for up to 16 h. In all charts means and SD are presented (n = 4-5). Asterisks indicate statistically significant difference between 3MeOBAPA treatment and mock (DMSO) treatment (***, $p < 0.001$; **, $p < 0.01$; *, $p < 0.05$, Student's unpaired *t*-test). (B) and (C) were reprinted and adapted with permission from Bryksová et al. (2020). Copyright (2020) American Chemical Society.

3.4 Model of 3MeOBAPA action

To further confirm that 3MeOBAPA primes the PTI response in Arabidopsis seedlings, expression levels of *MPK3*, *MPK4*, *MPK6* and *MPK11* together with another PTI-responsive genes such as *FRK1* and transcription factors such as *WRKY 33* and *WRKY 53* (Eschen-Lippold et al. 2016) were evaluated using qPCR and compared with a response to flg 22 (Fig. 3).

As expected flg22 primed these PTI-responsive genes (Fig. 3). In line with results from detached leaves (Fig. 1), in the 3MeOBAPA-treated seedlings expression level of *MPK11* was strongly increased (Fig. 3). Importantly, the 3MeOBAPA-treatment profoundly increased also expression level of other PTI-responsible genes, although flg22 provoked much stronger effect, especially in the case of *FRK1*. Although treatment of 3MeOBAPA together with flg22 showed little effect in the case of *MPK*s and *WRKY*s, their downstream FRK1 proved to be very sensitive to this combined treatment. A strong synergistic effect between flg22 and 3MeOBAPA was observed in the FLS2-initiated MAPK defence pathway (Fig. 3). Based on obtained results, the model of 3MeOBAPA action was proposed (Fig. 4).

The presumed ability of 3MeOBAPA to enhance plant resistance to pathogens was confirmed by their application on field-grown plants of wheat and barley where effectively supressed infection by wheat leaf rusts and powdery mildew and foot rot diseases in the case of barley.
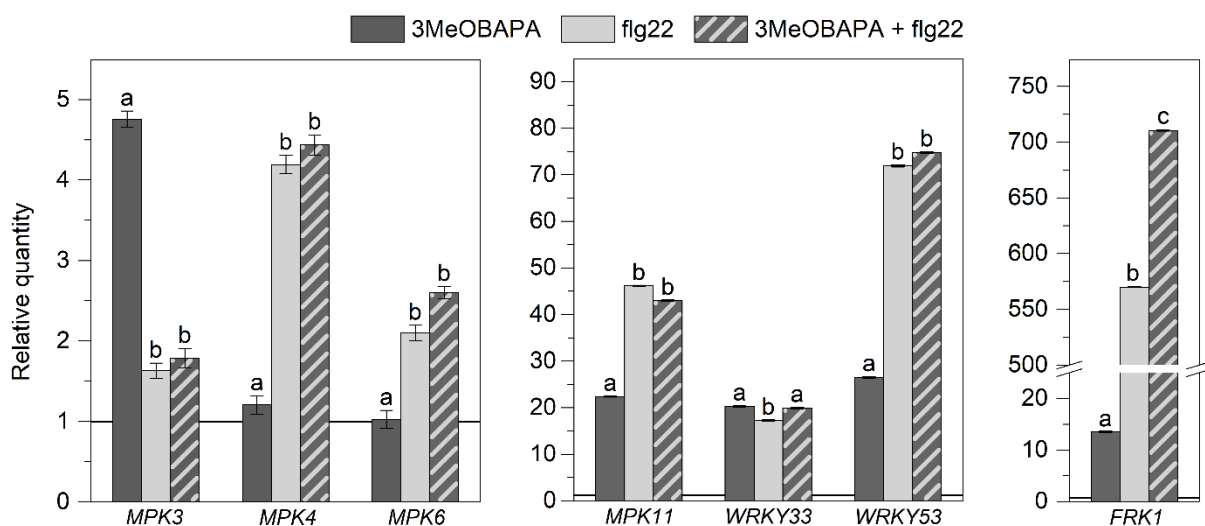

Fig. 3. The expression levels of *MPK3, MPK4, MPK6, MPK11, WRKY 33, WRKY 53* and *FRK1* in Arabidopsis seedlings treated with 10 µmol.l^{-1} 3MeOBAPA and/or 1 µmol.l^{-1} flg22 for 2 h in comparison with mock-treated seedlings. Genes for elongation factor 1 alpha and actin 7 were used as reference genes. Means and SD are presented (each bar represents a biological pool of approximately 50 seedlings, n ≥ 4). Different letters indicate statistically significant difference between treatments ($p < 0.05$; Student's unpaired t-test). Reprinted and adapted with permission from Bryksová et al. (2020). Copyright (2020) American Chemical Society.
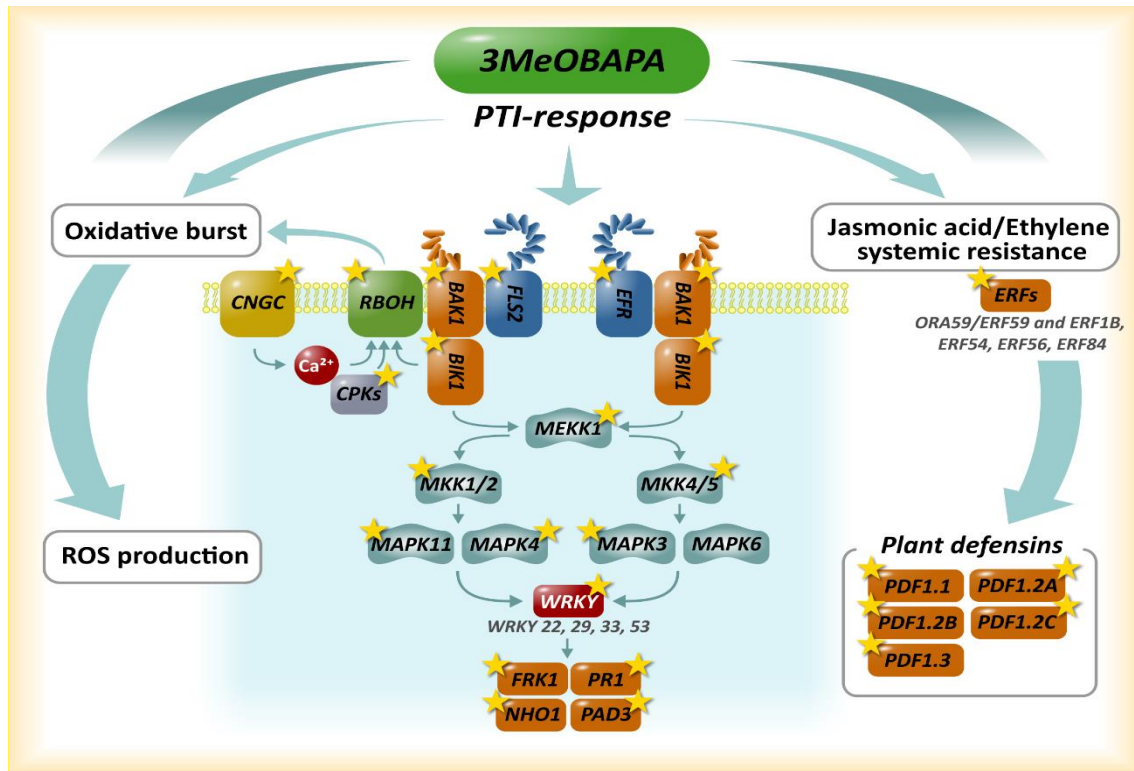
Fig. 4. Model of 3MeOBAPA mediated priming in Arabidopsis plants. Significantly upregulated genes (data from RNA-seq analysis and gene expression studies) are marked with a star. *ERF, ETHYLENE RESPONSIVE FACTOR; PDF, PLANT DEFENSIN; FRK1, FLG-INDUCED RECEPTOR-LIKE KINASE; PR1, PATHOGENESIS RELATED1; NHO1, NONHOST RESISTANCE TO P.S. PHASEOLICOLA 1; PAD3, PHYTOALEXIN DEFICIENT 3*). Reprinted and adapted with permission from Bryksová et al. (2020). Copyright (2020) American Chemical Society.

3.5 Anti-senescence activity of CK arabinosides

Since defence mechanisms are high-cost, energy demanding and are accompanied by photosynthesis inhibition, long-term exposure to PAMP usually leads to plant fitness impairment (Gómez-Gómez et al. 1999, Göhre et al. 2012). In spite of that, 3OHBAPA and 3MeOBAPA possess high anti-senescence activity in wheat and Arabidopsis. In the case of wheat the results were resembling wheat senescence bioassay – 3OHBAPA maintained Chl and also preserved PSII function very effectively while effect of 3MeOBAPA was similar to that of BAP (Table 2). In Arabidopsis the Chl content was most effectively maintained in BAP-treated leaves. On the contrary, F_V/F_M was highest in 3MeOBAPA-treated leaves (Table 2).

Table 2. Chlorophyll (Chl) content, Chl *a/b* ratio and maximum quantum yield of photosystem II photochemistry (F_V/F_M) of freshly detached (0.dad) leaves of wheat and Arabidopsis and leaves incubated in 0.1% DMSO or BAP, 3OHBAPA and 3MeOBAPA at various concentrations in the dark for 6 days. Different letters indicate statistically significant difference. Means ± SD are presented (n = 5).

treatment	wheat			Arabidopsis		
	Chl content	Chl *a/b*	F_V/F_M	Chl content	Chl *a/b*	F_V/F_M
0.dad	28.24 ± 0.44 [a]	3.42 ± 0.03 [a]	0.80 ± 0.00 [a]	15.24 ± 2.61 [a]	2.98 ± 0.05 [a]	0.79 ± 0.01 [a]
DMSO	9.69 ± 2.14 [b]	2.99 ± 0.04 [b]	0.06 ± 0.02 [b]	0.50 ± 0.16 [b]	3.76 ± 0.81 [b]	0.14 ±0.07 [b]
BAP	15.55 ± 2.39 [c]	2.97 ± 0.08 [b]	0.59 ± 0.04 [c]	10.44 ± 2.71 [c]	3.37 ± 0.16 [b]	0.24 ± 0.05 [c]
3OHBAPA	23.10 ± 2.79[d]	3.21 ± 0.12 [c]	0.72 ± 0.01 [d]	3.74 ± 1.76 [d]	4.95 ± 0.50 [c]	0.24 ± 0.13 [c]
3MeOBAPA	12.90 ± 1.63[c]	2.50 ± 0.14 [d]	0.61 ± 0.07 [c]	8.87 ± 0.78 [e]	4.66 ± 0.44 [c]	0.53 ± 0.11 [d]

3.6 PSII function

Measuring F_V/F_M affirmed that the CK arabinosides (especially 3OHBAPA in wheat and 3MeOBAPA in Arabidopsis) effectively maintain PSII function. To determine this action in more detailed way other Chl fluorescence parameters such as Chl fluorescence induction transient (OJIP curve) and quantum yields of Φ_P, Φ_{NPQ} and $\Phi_{f,D}$ (Fig. 5) were used.

The OJIP curve was measured to monitor the rate of excitation supply to reaction center (RCII), reduction of primary electron acceptor of PSII (Q_A), and subsequent electron transport behind Q_A (Strasser et al. 2000) during the first (milli)seconds of illumination of dark-adapted leaves. In the mock-treated wheat leaves, both $(dV/dt)_0$ and V_J parameters increased indicating an acceleration of both excitation supply to RCII and Q_A reduction together with inhibition of electron transport behind Q_A. Almost the same increase in both parameters was found in the BAP- and 3MeOBAPA-treated leaves, but it was eliminated completely by 3OHBAPA (Fig. 5A, B). In the mock-treated Arabidopsis leaves $(dV/dt)_0$ decreased, while V_J increased to its maximal value (= 1). These changes indicate a strong impairment of PSII including minimal delivery of excitations to RCII and extreme inhibition of electron transfer from Q_A^-. The inhibition of the excitation supply to RCII could be related to the increased Chl *a/b* ratio (Table 2), which reflects higher degradation of light-harvesting complexes of PSII (LHCII) compared to RCII (Leong & Anderson 1984). In the BAP-treated leaves, $(dV/dt)_0$ increased pronouncedly indicating stimulation of the excitation supply to RCII probably due to the suppression of preferential degradation of LHCII observed in mock-treated leaves, whereas

the electron transport behind Q_A^- was inhibited as $V_J = 0.98$ (Fig. 5A, B). 3OHBAPA maintained $(dV/dt)_0$ close to the value of freshly detached leaves, but it did not reduce the senescence-induced inhibition of electron transport behind Q_A ($V_J = 0.98$). On the other hand, 3MeOBAPA maintained both excitation supply to RCII and electron transport behind Q_A as values of $(dV/dt)_0$ and V_J were very similar to those of freshly detached leaves (Fig. 5A, B). The non-accelerated excitation supply to RCII corresponds to a higher degradation of LHCII in comparison to RCII indicated by the increased Chl a/b ratio (Table 2).
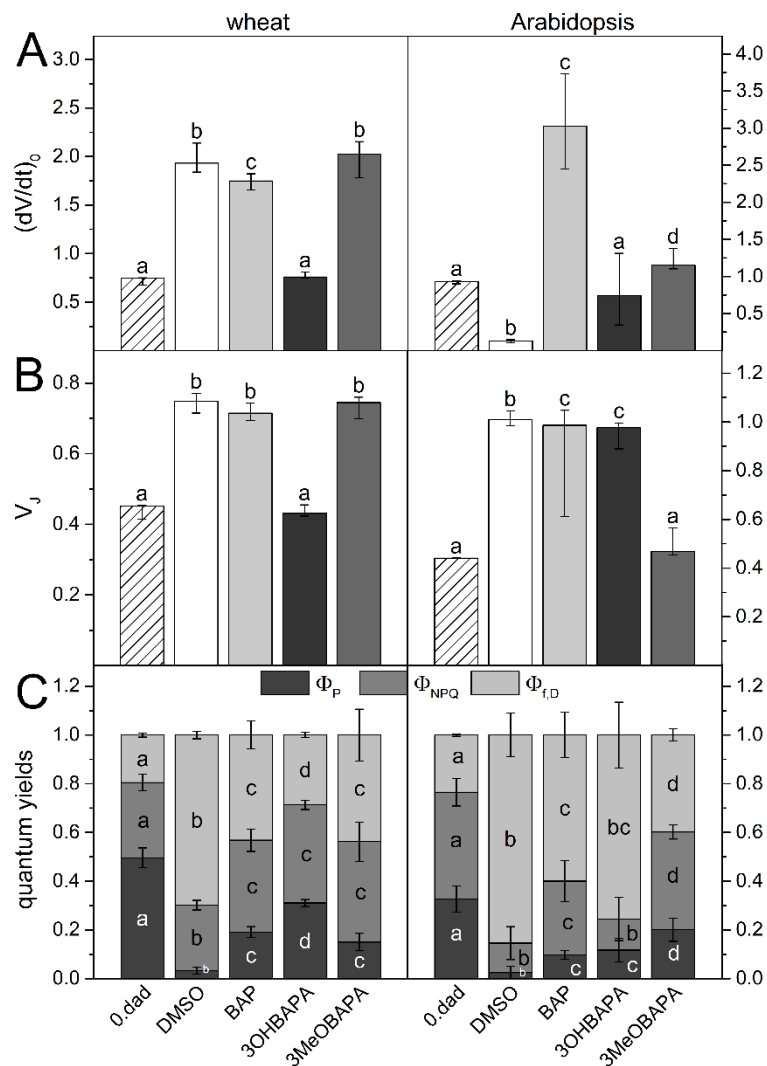

Fig. 5. (**A**) The initial slope of the O–J Chl fluorescence rise $(dV/dt)_0$, (**B**) the relative variable fluorescence at the J step (V_J) and (**C**) quantum yields of photosystem II photochemistry (Φ_P), regulatory non-photochemical quenching (Φ_{NPQ}) and non-regulatory dissipation processes ($\Phi_{f,D}$) in freshly detached (0.dad) leaves and in detached leaves of wheat and Arabidopsis after six days in the dark-incubation in 0.1% DMSO, 10 µmol.l^{-1} solution of BAP, 3OHBAPA and 3MeOBAPA. Medians and quartiles are presented (n = 5-12). Different letters indicate a statistically significant difference between treatments within a plant species ($p < 0.05$; Student's unpaired t-test). Reprinted from Kučerová et al. (2020).

Further information on senescence-induced changes in the PSII function was obtained by measurement of quantum yields Φ_P, Φ_{NPQ} and $\Phi_{f,D}$. These parameters, measured during exposition of leaves to actinic light, reflect the partitioning of absorbed light energy for PSII photochemistry (Φ_P) and for regulated (Φ_{NPQ}) and non-regulated ($\Phi_{f,D}$) non-photochemical processes (Lazár 2015). Steady-state values of Φ_P, Φ_{NPQ}, and $\Phi_{f,D}$ measured after a 7-min exposition of the senescent leaves to actinic light are discussed (Fig. 5C). Decrease in Φ_P and Φ_{NPQ} and increase in $\Phi_{f,D}$ was found in mock-treated leaves of both wheat and Arabidopsis, while in Arabidopsis those changes were more pronounced (Fig. 5C). The senescence-induced changes in the partitioning of absorbed light energy were partially reduced in the BAP-treated leaves of both wheat and Arabidopsis. The PSII photochemistry and regulatory non-photochemical quenching (Φ_P and Φ_{NPQ}, respectively) were more effective and the increase in the yield of non-regulated energy dissipation ($\Phi_{f,D}$) was lower compared to the mock-treated leaves (Fig. 5C). Similarly to F_V/F_M (Table 2) and OJIP transient parameters, the senescence-induced changes in the partitioning of absorbed light energy observed in mock-treated leaves were suppressed very effectively by 3OHBAPA in wheat and 3MeOBAPA in Arabidopsis (Fig. 5C). While in these two cases CK arabinosides maintained the PSII function more effectively than BAP, protective effect of 3MeOBAPA in wheat and 3OHBAPA in Arabidopsis was comparable to that of BAP (Fig. 5C).

In summary to the anti-senescence action of BAP and CK arabinosides, 3OHBAPA had the highest activity in wheat, followed by 3MeOBAPA and BAP, whose activity was similar. In Arabidopsis, 3MeOBAPA was less efficient than BAP in the maintenance of photosynthetic pigment content, but it was more effective in the maintenance of PSII function. At the same time, when compared to 3OHBAPA, 3MeOBAPA had higher anti-senescence activity, as documented by the changes in all studied parameters.

3.7 Ethylene production

It has been shown that different activity of anti-senescence compounds can be associated with their influence on ethylene production in the detached dark-incubated leaves (Nisler et al. 2018). As opposed to the positive effect of CKs on plant and leaf longevity, ethylene is known for being the accelerator of senescence (for recent review see Ceusters & Van de Poel 2018) and exogenous application of CKs stimulates the production of ethylene (Cary et al. 1995, for

review see Zdarska et al. 2015). Thus, the rate of the stimulation of ethylene production by exogenously applied CK can co-determine a resultant senescence-delaying effect—i.e., the anti-senescence activity of CK. Therefore, we evaluated the effect of the compounds on ethylene production in wheat and Arabidopsis leaves. As expected, the ethylene production in BAP-treated leaves was higher compared to the mock-treated leaves in both wheat and Arabidopsis (Fig. 6). Interestingly, no stimulation of ethylene production was observed in the wheat leaves treated by 3OHBAPA and, despite the increased ethylene production in Arabidopsis leaves treated by 3MeOBAPA for 48 and 72 h (Fig. 2), also in Arabidopsis leaves treated by 3MeOBAPA. A moderately stimulated ethylene production was observed in the 3MeOBAPA-treated wheat leaves and 3OHBAPA-treated leaves of Arabidopsis (Fig. 6). Thus, the differences in the rate of ethylene production corresponded generally to the quantitative differences of anti-senescence activity between BAP and CK arabinosides, as well as between 3OHBAPA and 3MeOBAPA: the lower the ethylene production, the higher the anti-senescence action.
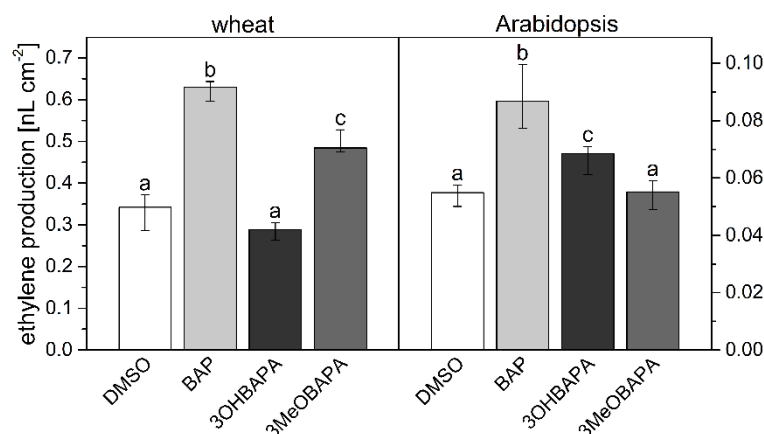

Fig. 6. Ethylene production in detached leaves of wheat and Arabidopsis incubated in 0.1% DMSO or 10 μmol.l^{-1} solutions of BAP, 3OHBAPA and 3MeOBAPA and kept sealed in 8 ml vials in darkness for 6 days. Medians and quartiles are presented (n = 5–9). Different letters indicate a statistically significant difference between treatments within a plant species ($p < 0.05$; Student′s unpaired t-test). Reprinted Kučerová et al. (2020)

3.8 Protection against induced oxidative damage

The gene expression analysis revealed downregulation of positive regulators of senescence such as *SAG12*, *ORE1*, *ORE3* and *ORE9* and upregulation of some negative regulators of senescence such as *JAZ7* and *JAZ8* (Table 1) confirming the anti-senescent effect of 3MeOBAPA at the molecular level. *JUB1*, *ELIP1* and *ELIP2* that are known to be involved

in regulation of leaf longevity and in protection against oxidative damage were also upregulated (Table 1). It has been shown that the inhibition of ethylene production not only delays leaf senescence but also enhances tolerance of plants to abiotic stresses, including H_2O_2- or HL- induced oxidative stress (Wi et al. 2010). Since no ethylene stimulation was found in 3OHBAPA-treated wheat leaves and 3MeOBAPA-treated Arabidopsis leaves (Fig. 6), this suggests, along with downregulation of *ORE*s and upregulation of *ELIP*s and *JUB1* in 3MeOBAPA-treated Arabidopsis leaves, protective function of CK arabinosides against oxidative damage. To confirm this hypothesis, we exposed the senescent leaves (kept in the dark for 6 days while incubated in BAP or CK arabinosides) to subsequent H_2O_2 or HL treatment to induce oxidative stress and investigated how the CK arabinosides affect a level of oxidative damage. For those experiments only the more effective CK arabinoside (meaning 3OHBAPA in wheat and 3MeOBAPA in Arabidopsis) was used to compare their effect with BAP.

The level of oxidative damage in senescent leaves exposed to subsequent H_2O_2 treatment was evaluated using ultra-weak photon emission (UPE) as its intensity correlates with an extent of oxidative damage (Pospíšil et al. 2014). In wheat, the protective effect indicated by the lower UPE ratio was observed only in leaves treated with 3OHBAPA. In Arabidopsis, both BAP and 3MeOBAPA reduced the oxidative damage, 3MeOBAPA being more effective (Fig. 7).
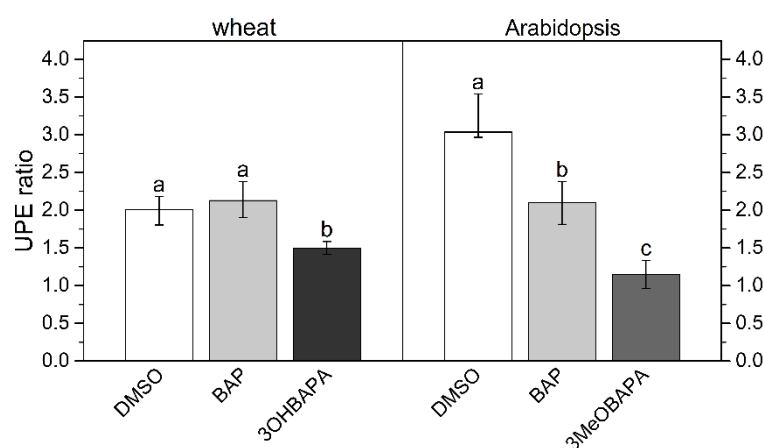

Fig. 7. Ratio of ultra-weak photon emission (UPE) intensity after/before application of H_2O_2 in detached leaves of wheat and Arabidopsis dark-incubated for 6 days in 0.1% DMSO or 10 μmol.l^{-1} solutions of BAP, 3OHBAPA or 3MeOBAPA. Medians and quartiles are presented (n = 4). Different letters indicate a statistically significant difference between treatments within a plant species ($p < 0.05$; Student´s unpaired *t*-test). Reprinted from Kučerová et al. (2020).

Additionally, we exposed the senescent leaves to HL (500 μmol photons.m^{-2}.s^{-1}) and estimated cell membrane damage using the measurement of ion leakage by conductivity and maintenance of the maximal quantum yield of PSII photochemistry (Fv/Fm), which reflects the extent of photoinhibition or photodamage of PSII. The exposure of senescing mock-treated leaves to HL led to a strong oxidative damage, as indicated by progressive deterioration of cell membranes during 8 h of HL treatment (Fig. 8) and photoinhibition of PSII (Fig. 9) after 4 h of HL treatment.
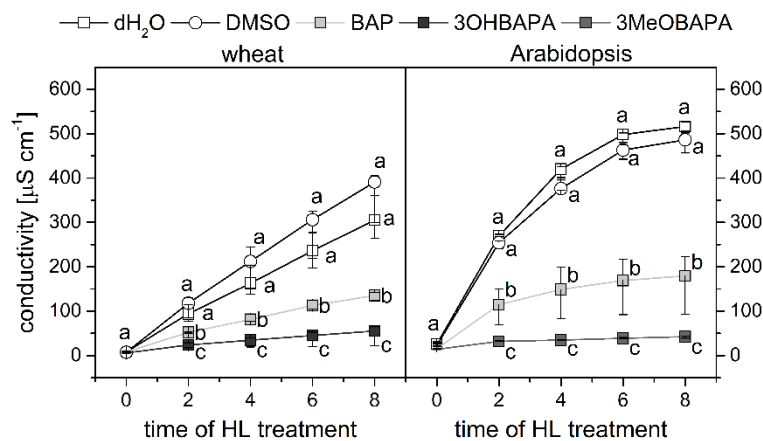

Fig. 8. Conductivity as a measure of cell membrane damage in wheat and Arabidopsis detached leaves incubated in deionized water (dH2O), 0.1% DMSO, 10 μmol.l^{-1} solutions of BAP, 3OHBAPA or 3MeOBAPA. Before high-light treatment (HL; 500 μmol photons.m^{-2}.s^{-1}) for up to 8 h leaves were incubated in the dark for 6 days. Medians and quartiles are presented (n = 7). Different letters indicate a statistically significant difference between treatments within a plant species (p < 0.05; Student´s unpaired t-test). Reprinted from Kučerová et al. (2020).

The oxidative damage was suppressed by the exogenous application of BAP, although its protective effect was quite low. The HL-induced membrane deterioration and PSII photoinhibition were attenuated in the BAP-treated leaves of both wheat and Arabidopsis (Figs. 8 and 9). It has been previously reported that action of CKs (including BAP) can switch from protective to damaging when their application is combined with excessive light conditions (Vlčková et al. 2006, Prokopová et al. 2010a). This negative CK effect is supposed to be a result of over-excitation of photosynthetic apparatus and related oxidative damage (Vlčková et al. 2006). We presume that was the case of the BAP-treated Arabidopsis leaves exposed to HL as the excitation supply to RCII in senescent leaves was increased (indicated by increased (dV/dt)$_0$; Fig. 5A) due to the higher LHCII/RCII ratio. The mentioned negative effect

could reduce a protective action of BAP resulting in the relatively high oxidative damage and decrease in xanthophyll content (Fig. 10).

As we presumed, the CK arabinosides were more efficient than BAP in the protection of wheat and Arabidopsis leaves against HL-induced oxidative damage as indicated by the lower cell membrane deterioration and PSII photoinhibition (Figs. 8 and 9).
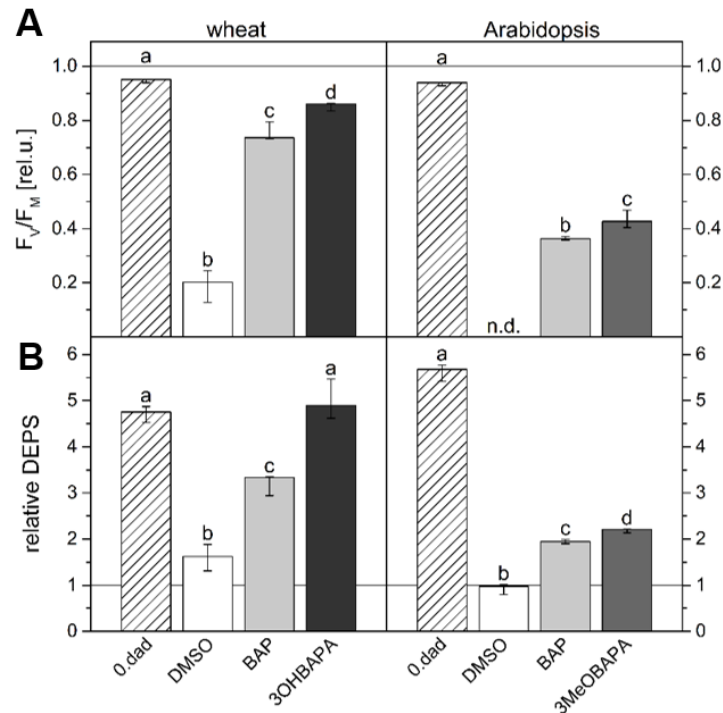

Fig. 9. (A) Relative F_V/F_M values and (**B**) relative de-epoxidation state of xanthophylls (DEPS) after high-light treatment (HL; 500 μmol photons.m^{-2}.s^{-1} for 4 h) of freshly detached leaves and leaves incubated for 6 days in 0.1% DMSO or 10 μmol.l^{-1} solutions of BAP, 3OHBAPA or 3MeOBAPA. The relative F_V/F_M and DEPS were calculated as a ratio of values measured after and before exposure to high light. Medians and quartiles are presented (n = 5). Different letters indicate a statistically significant difference between treatments within a plant species ($p < 0.05$; Student's unpaired t-test). Reprinted and adapted from Kučerová et al. (2020).

Nevertheless, we suppose that in case of the HL-treated wheat leaves the high protective effect of 3OHBAPA against oxidative damage consisted mainly in the completely maintained xanthophyll cycle (Fig. 9B) together with the high content of xanthophylls (Fig. 10).

Unlike wheat, the xanthophyll cycle was only moderately more efficient in the 3MeOBAPA-treated Arabidopsis leaves in comparison with the BAP-treated ones (Fig. 9B), which corresponds to only slightly lower decrease in F_V/F_M after HL treatment (Fig. 9A). We suppose that the protective effect of 3MeOBAPA from PSII photoinhibition was related rather to the lower LHCII/RCII ratio and to the higher maintenance of xanthophylls during HL treatment (Fig. 10). The difference in the Chl a/b ratio observed in senescent leaves treated

by BAP and 3MeOBAPA (Table 2) was deepened due to HL treatment (Fig. 10). The higher Chl a/b ratio in 3MeOBAPA-treated leaves reflects higher degradation of LHCII compared to RCII (Leong & Anderson 1984). Unlike only a little increased PSII photoprotection, 3MeOBAPA clearly surpassed BAP in the overall antioxidative effect (Figs. 7 and 8). This effective protection could be related to the above mentioned changes in gene expression, i.e., upregulation of *ELIPs* and *JUB1* and downregulation of *OREs* (Table 2).
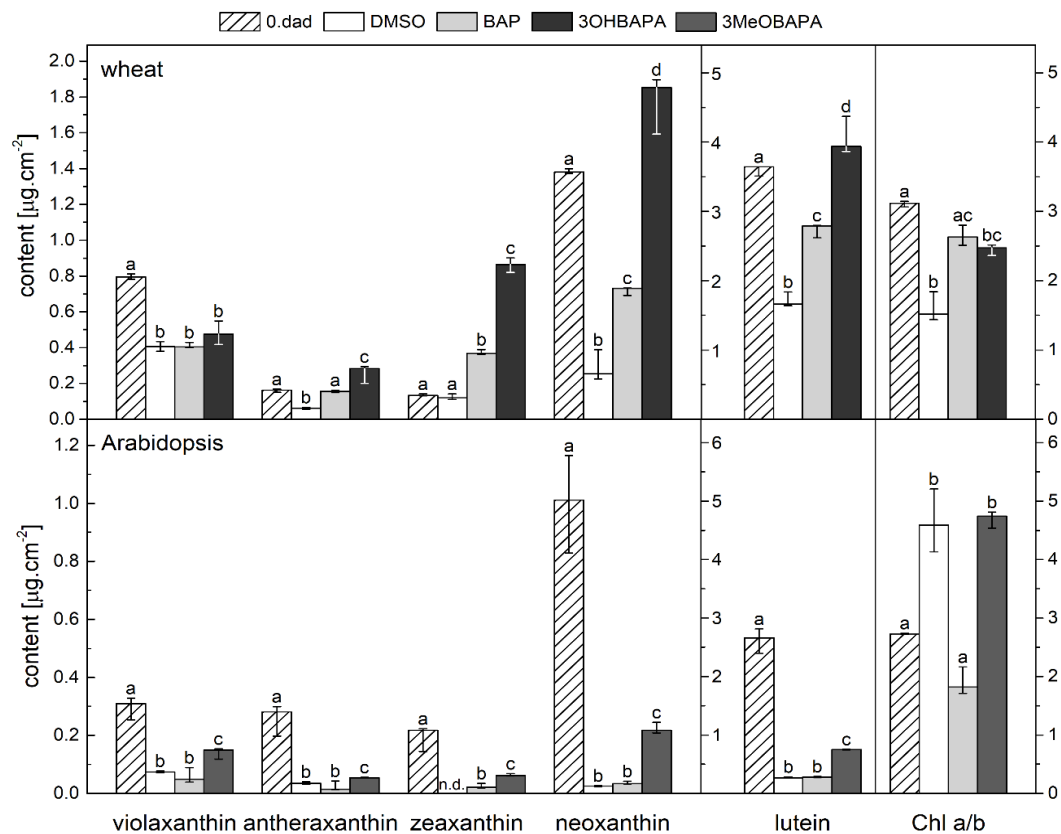

Fig. 10. Content of violaxanthin, antheraxanthin, zeaxanthin, neoxanthin and lutein; and chlorophyll a/b ratio in freshly detached leaves of wheat and Arabidopsis (0. dad) and in detached leaves incubated in 10 µmol.l^{-1} solutions of BAP, 3OHBAPA or 3MeOBAPA. Leaves were kept in the dark for 6 days and subsequently exposed to high light (500 µmol photons.m^{-2}.s^{-1} for 4 h). Medians and quartiles are presented (n = 3-5). Different letters indicate a statistically significant difference between treatments within a plant species (p<0.05, Student's unpaired *t*-test). n.d., not detectable.

3.9 On the mechanism of anti-senescence action of CK arabinosides

The upregulation of genes of defence regulons in the 3MeOBAPA-treated Arabidopsis leaves included jasmonate/ethylene-driven upregulation of PDFs and was accompanied by a significant elevation of endogenous levels of ethylene and ROS together with JA and its metabolites (Fig. 2).

However, despite the increased ethylene production in Arabidopsis leaves treated by 3MeOBAPA for 48 and 72 h, the ethylene production after 6 days of dark-incubation in appropriate solutions of the CK arabinosides was low (Fig. 6). As ethylene is known to promote leaf senescence (Ceusters & Van de Poel 2018), low ethylene production by CK arabinosides-treated senescing leaves might be one of the main reasons for the CK arabinosides' high anti-senescence activity.

Similarly to ethylene, JA is considered to be a positive regulator of leaf senescence. As mentioned, the level of JA and its metabolites was found to be increased in the 3MeOBAPA-treated Arabidopsis leaves (Fig. 2). However, this increase was only temporary – it was observed after 48 h of the treatment (Fig. 2), while after 4 and 8 days the JA level was lower than that in the mock-treated leaves (Fig. 11).

The transient increase in ethylene and JA content appears to be involved in triggering the defence response by 3MeOBAPA and does not stimulate, but rather suppresses leaf senescence. The differences in ethylene and JA production between early and long-term response to 3MeOBAPA treatment suggest that elevated production of ethylene and JA have only signalling function and later it is attenuated.
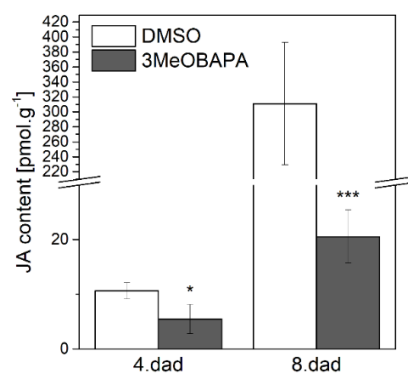

Fig. 11. Content of jasmonic acid (JA) in detached Arabidopsis leaves in 0.1% DMSO or 10 µmol.l^{-1} 3MeOBAPA for 4 and 8 days. Means and SD are presented (n = 4-5). Asterisks indicate statistically significant difference between 3MeOBAPA treatment and mock (DMSO) treatment (***, $p < 0.001$; **, $p < 0.01$; *, $p < 0.05$, Student´s unpaired t-test).

4 Conclusion

It is well-known that leaf senescence can be suppressed by exogenous application of CKs. Nevertheles, under specific conditions CKs can possess negative effects and can even accelerate senescence. For this reason there are efforts to prepare compounds based on CKs that lack those effects and have other advantageous properties. Recently, two aromatic CK arabinosides, 3OHBAPA and 3MeOBAPA, have been synthesized and found to possess unique effects and mechanism of action. The RNA-seq profiling study that was performed on detached Arabidopsis leaves revealed that treatment with 3MeOBAPA results in the shift in transcriptional response toward defence. 3MeOBAPA affects genes involved in processes associated with plant innate immunity and its activation of MAPK signalling pathway together with oxidative burst and JA-ethylene signalling results in the effective protection of field-grown plants against fungal pathogens. Interestingly, the long-term incubation of leaves in 3OHBAPA and 3MeOBAPA solutions does not impair leaf fitness which is common in prolonged activation of defence response mechanisms, but on the contrary effectively delays senescence. CK arabinosides anti-senescence action in detached dark-adapted leaves differs quantitatively in wheat and Arabidopsis. In wheat, 3OHBAPA has higher protective effect than 3MeOBAPA, whereas in Arabidopsis, 3MeOBAPA is the more efficient derivative. We have found that the different anti-senescent activity of 3OHBAPA and 3MeOBAPA is coupled to different ethylene production in the treated leaves: the lower the ethylene production, the higher the anti-senescence activity. 3OHBAPA and 3MeOBAPA also protects efficiently the senescing leaves against oxidative damage induced by both H_2O_2 and high-light treatment, which could also be connected with the low level of ethylene production.

The specific effects described in this work represent evidence that CK arabinosides possess unique activity while acting through a mechanism different from that of classical CKs. Since they have high anti-senescence activity and protective effects under biotic and abiotic stress conditions they are promising substances for plant protection. However, further study is needed to elucidate the exact mechanism of their action.

5 References

Bairu MW, Jain N, Stirk WA, Doležal K, Van Staden J (2009) Solving the problem of shoot-tip necrosis in Harpagophytum procumbens by changing the cytokinin types, calcium and boron concentrations in the medium. *South African Journal of Botany* 75: 122–127.

Bairu MW, Stirk WA, Doležal K, Van Staden J (2007) Optimizing the micropropagation protocol for the endangered *Aloe polyphylla*: Can meta-topolin and its derivatives serve as replacement for benzyladenine and zeatin? *Plant Cell, Tissue and Organ Culture* 90: 15–23.

Bethke G, Pecher P, Eschen-Lippold L, Tsuda K, Katagiri F, Glazebrook J, Scheel D, Lee J (2012) Activation of the *Arabidopsis thaliana* mitogen-activated protein kinase MPK11 by the flagellin-derived elicitor peptide, flg22. *Molecular Plant-Microbe Interactions* 25: 471–480.

Bigeard J, Colcombet J, Hirt H (2015) Signaling mechanisms in pattern-triggered immunity (PTI). *Molecular Plant* 8: 521–539.

Bilgin DD, Zavala JA, Zhu J, Clough SJ, Ort DR, Delucia EH (2010) Biotic stress globally downregulates photosynthesis genes. *Plant, Cell and Environment* 33: 1597–1613.

Biswal B (1995) Carotenoid catabolism during leaf senescence and its control by light. *Journal of Photochemistry and Photobiology, B: Biology* 30: 3–13.

Carimi F, Terzi M, De Michele R, Zottini M, Lo Schiavo F (2004) High levels of the cytokinin BAP induce PCD by accelerating senescence. *Plant Science* 166: 963–969.

Cary AJ, Liu Wennuan, Howell SH (1995) Cytokinin action is coupled to ethylene in its effects on the inhibition of root and hypocotyl elongation in *Arabidopsis thaliana* seedlings. *Plant Physiology* 107: 1075–1082.

Ceusters J, Van de Poel B (2018) Ethylene exerts species-specific and age-dependent control of photosynthesis. *Plant Physiology* 176: 2601–2612.

Choi J, Choi D, Lee S, Ryu CM, Hwang I (2011) Cytokinins and plant immunity: Old foes or new friends? *Trends in Plant Science* 16: 388–394.

Choi J, Huh SU, Kojima M, Sakakibara H, Paek KH, Hwang I (2010) The cytokinin-activated transcription factor ARR2 promotes plant immunity via TGA3/NPR1-dependent salicylic acid signaling in arabidopsis. *Developmental Cell* 19: 284–295.

Diaz-Mendoza M, Velasco-Arroyo B, Santamaria ME, González-Melendi P, Martinez M, Diaz I (2016) Plant senescence and proteolysis: Two processes with one destiny. *Genetics and Molecular Biology* 39: 329–338.

Doležal K, Popa I, Hauserová E, Spíchal L, Chakrabarty K, Novák O et al. (2007) Preparation, biological activity and endogenous occurrence of N6-benzyladenosines. *Bioorganic and Medicinal Chemistry* 15: 3737–3747.

Eschen-Lippold L, Jiang X, Elmore JM, Mackey D, Shan L, Coaker G, Scheel D, Lee J (2016) Bacterial AvrRpt2-like cysteine proteases block activation of the arabidopsis mitogen-activated protein kinases, MPK4 and MPK11. *Plant Physiology* 171: 2223–2238.

Gan S, Amasino RM (1995) Inhibition of leaf senescence by autoregulated production of cytokinin. *Science* 270: 1986–1988.

Gan S, Amasino RM (1997) Making sense of senescence: Molecular genetic regulation and manipulation of leaf senescence. *Plant Physiology* 113: 313–319.

Göhre V, Jones AME, Sklenář J, Robatzek S, Weber APM (2012) Molecular crosstalk between PAMP-triggered immunity and photosynthesis. *Molecular Plant-Microbe Interactions* 25: 1083–1092.

Gómez-Gómez L, Felix G, Boller T (1999) A single locus determines sensitivity to bacterial flagellin in *Arabidopsis thaliana*. *Plant Journal* 18: 277–284.

Havé M, Marmagne A, Chardon F, Masclaux-Daubresse C (2017) Nitrogen remobilization during leaf senescence: Lessons from Arabidopsis to crops. *Journal of Experimental Botany* 68: 2513–2529.

Himelblau E, Amasino RM (2001) Nutrients mobilized from leaves of *Arabidopsis thaliana* during leaf senescence. *Journal of Plant Physiology* 158: 1317–1323.

Holub J, Hanuš J, Hanke DE, Strnad M (1998) Biological activity of cytokinins derived from Ortho- and Meta-hydroxybenzyladenine. *Plant Growth Regulation* 26: 109–115.

Inoue T, Higuchi M, Hashimoto Y, Seki M, Kobayashi M, Kato T, Tabata S, Shinozaki K, Kakimoto T (2001) Identification of CRE1 as a cytokinin receptor from Arabidopsis. *Nature* 409: 1060–1063.

Iqbal M, Ashraf M, Jamil A (2006) Seed enhancement with cytokinins: Changes in growth and grain yield in salt stressed wheat plants. *Plant Growth Regulation* 50: 29–39.

Janečková H, Husičková A, Ferretti U, Prčina M, Pilařová E, Plačková L, Pospíšil P, Doležal K, Špundová M (2018) The interplay between cytokinins and light during senescence in detached Arabidopsis leaves. *Plant Cell and Environment* 41: 1870–1885.

Janečková H, Husičková A, Lazár D, Ferretti U, Pospíšil P, Špundová M (2019) Exogenous application of cytokinin during dark senescence eliminates the acceleration of photosystem II impairment caused by chlorophyll *b* deficiency in barley. *Plant Physiology and Biochemistry* 136: 43–51.

Khanna-Chopra R (2012) Leaf senescence and abiotic stresses share reactive oxygen species-mediated chloroplast degradation. *Protoplasma* 249: 469–481.

Kim HJ, Ryu H, Hong SH, Woo HR, Lim PO, Lee IC, Sheen J, Nam HG, Hwang I (2006) Cytokinin-mediated control of leaf longevity by AHK3 through phosphorylation of ARR2 in Arabidopsis. *Proceedings of the National Academy of Sciences of the United States of America* 103: 814–819.

Koprna R, De Diego N, Dundálková L, Spíchal L (2016) Use of cytokinins as agrochemicals. *Bioorganic and Medicinal Chemistry* 24: 484–492.

Kučerová Z, Rác M, Mikulík J, Plíhal O, Pospíšil P, Bryksová M, Sedlářová M, Doležal K, Špundová M (2020) The Anti-Senescence activity of cytokinin arabinosides in wheat and Arabidopsis is negatively correlated with ethylene production. *International Journal of Molecular Sciences* 21: 8109.

Lazár D (2015) Parameters of photosynthetic energy partitioning. *Journal of Plant Physiology* 175: 131–147.

Leong TY, Anderson JM (1984) Adaptation of the thylakoid membranes of pea chloroplasts to light intensities. II. Regulation of electron transport capacities, electron carriers, coupling factor (CF1) activity and rates of photosynthesis. *Photosynthesis Research* 5: 117–128.

Lim PO, Woo HR, Nam HG (2003) Molecular genetics of leaf senescence in Arabidopsis. *Trends in Plant Science* 8: 272–278.

Liu L, Li H, Zeng H, Cai Q, Zhou X, Yin C (2016) Exogenous jasmonic acid and cytokinin antagonistically regulate rice flag leaf senescence by mediating chlorophyll degradation, membrane deterioration, and senescence-associated genes expression. *Journal of Plant Growth Regulation* 35: 366–376.

Maillard A, Diquélou S, Billard V, Laîné P, Garnica M, Prudent M, Garcia-Mina JM, Yvin JC, Ourry A (2015) Leaf mineral nutrient remobilization during leaf senescence and

modulation by nutrient deficiency. *Frontiers in Plant Science* 6: 1–15.

Mayta ML, Hajirezaei MR, Carrillo N, Lodeyro AF (2019) Leaf senescence: the chloroplast connection comes of age. *Plants* 8: 1–18.

Mik V, Szüčová L, Šmehilová M, Zatloukal M, Doležal K, Nisler J et al. (2011) N9-substituted derivatives of kinetin: Effective anti-senescence agents. *Phytochemistry* 72: 821–831.

Mittler R (2002) Oxidative stress, antioxidants and stress tolerance. *Trends in Plant Science* 7: 405–410.

Mittler R, Vanderauwera S, Gollery M, Van Breusegem F (2004) Reactive oxygen gene network of plants. *Trends in Plant Science* 9: 490–498.

Mok DW, Mok MC (2001) Cytokinin metabolism and action. *Annual Review of Plant Physiology and Plant Molecular Biology* 52: 89–118.

Nisler J, Zatloukal M, Sobotka R, Pilný J, Zdvihalová B, Novák O, Strnad M, Spíchal L (2018) New urea derivatives are effective anti-senescence compounds acting most likely via a cytokinin-independent mechanism. *Frontiers in Plant Science* 9: 1225.

Oh MH, Kim JH, Zulfugarov IS, Moon YH, Rhew TH, Lee CH (2005) Effects of benzyladenine and abscisic acid on the disassembly process of photosystems in an Arabidopsis delayed-senescence mutant, ore9. *Journal of Plant Biology* 48: 170–177.

Plíhalová L, Vylíčilová H, Doležal K, Zahajská L, Zatloukal M, Strnad M (2016) Synthesis of aromatic cytokinins for plant biotechnology. *New Biotechnology* 33: 614–624.

Pospíšil P, Prasad A, Rác M (2014) Role of reactive oxygen species in ultra-weak photon emission in biological systems. *Journal of Photochemistry and Photobiology B: Biology* 139: 11–23.

Prokopová J, Mieslerová B, Hlaváčková V, Hlavinka J, Lebeda A, Nauš J, Špundová M (2010a) Changes in photosynthesis of *Lycopersicon* spp. plants induced by tomato powdery mildew infection in combination with heat shock pre-treatment. *Physiological and Molecular Plant Pathology* 74: 205–213.

Prokopová J, Špundová M, Sedlářová M, Husičková A, Novotný R, Doležal K, Nauš J, Lebeda A (2010b) Photosynthetic responses of lettuce to downy mildew infection and cytokinin treatment. *Plant Physiology and Biochemistry* 48: 716–723.

Riefler M, Novak O, Strnad M, Schmülling T (2006) Arabidopsis cytokinin receptors mutants reveal functions in shoot growth, leaf senescence, seed size, germination, root development, and cytokinin metabolism. *Plant Cell* 18: 40–54.

Del Río LA (2015) ROS and RNS in plant physiology: An overview. *Journal of Experimental Botany* 66: 2827–2837.

Roháček K, Barták M (1999) Technique of the modulated chlorophyll fluorescence: Basic concepts, useful parameters, and some applications. *Photosynthetica* 37: 339–363.

Romanov GA, Lomin SN, Schmülling T (2006) Biochemical characteristics and ligand-binding properties of Arabidopsis cytokinin receptor AHK3 compared to CRE1/AHK4 as revealed by a direct binding assay. *Journal of Experimental Botany* 57: 4051–4058.

Rosenvasser S, Mayak S, Friedman H (2006) Increase in reactive oxygen species (ROS) and in senescence-associated gene transcript (SAG) levels during dark-induced senescence of *Pelargonium* cuttings, and the effect of gibberellic acid. *Plant Science* 170: 873–879.

Rulcová J, Pospíšilová J (2001) Effect of benzylaminopurine on rehydration of bean plants after water stress. *Biologia Plantarum* 44: 75–81.

Schippers JHM, Schmidt R, Wagstaff C, Jing HC (2015) Living to die and dying to live: The survival strategy behind leaf senescence. *Plant Physiology* 169: 914–930.

Sewelam N, Kazan K, Schenk PM (2016) Global plant stress signaling: Reactive oxygen species at the cross-road. *Frontiers in Plant Science* 7: 1–21.

Smart BYCM (1994) Tansley Review No. 64 Gene expression during leaf senescence. *New Phytologist*: 419–448.

Spíchal L, Rakova NY, Riefler M, Mizuno T, Romanov GA, Strnad M, Schmülling T (2004) Two cytokinin receptors of Arabidopsis thaliana, CRE1/AHK4 and AHK3, differ in their ligand specificity in a bacterial assay. *Plant and Cell Physiology* 45: 1299–1305.

Springer A, Kang C, Rustgi S, Von Wettstein D, Reinbothe C, Pollmann S, Reinbothe S (2016) Programmed chloroplast destruction during leaf senescence involves 13-lipoxygenase (13-LOX). *Proceedings of the National Academy of Sciences of the United States of America* 113: 3383–3388.

Špundová M, Popelkova H, Ilik P, Skotnica J, Novotný R, Nauš J (2003) Ultra-structural and functional changes in the chloroplasts of detached barley leaves senescing under dark and light conditions. *Journal of Plant Physiology* 160: 1051–1058.

Strasser R, Srivastava A, Tsimilli-Michael M (2000) The fluorescence transient as a tool to characterize and screen photosynthetic samples. *In: Probing Photosynthesis: Mechanism, Regulation & Adaptation; Yunus M, Pathre U, Mohanty P, Eds.* Taylor & Francis: New York, NY, USA. pp.445-483.

Strnad M (1997) The aromatic cytokinins. *Physiologia Plantarum* 101: 674–688.

Suzuki T, Miwa K, Ishikawa K, Yamada H, Aiba H, Mizuno T (2001) The Arabidopsis sensor His-kinase, AHK4, can respond to cytokinins. *Plant and Cell Physiology* 42: 107–113.

Tamary E, Nevo R, Naveh L, Levin-Zaidman S, Kiss V, Savidor A et al. (2019) Chlorophyll catabolism precedes changes in chloroplast structure and proteome during leaf senescence. *Plant Direct* 3: 1–18.

Tarkowská D, Doležal K, Tarkowski P, Åstot C, Holub J, Fuksová K, Schmülling T, Sandberg G, Strnad M (2003) Identification of new aromatic cytokinins in Arabidopsis thaliana and Populus x canadensis leaves by LC-(+)ESI-MS and capillary liquid chromatography/frit-fast atom bombardment mass spectrometry. *Physiologia Plantarum* 117: 579–590.

Thompson JE, Legge RL, Barber RF (1987) The role of free radicals in senescence and wounding. *New Phytologist* 105: 317–344.

Ueguchi C, Koizumi H, Suzuki T, Mizuno T (2001a) Novel family of sensor histidine kinase genes in *Arabidopsis thaliana*. *Plant and Cell Physiology* 42: 231–235.

Ueguchi C, Sato S, Kato T, Tabata S (2001b) The AHK4 gene involved in the cytokinin-signaling pathway as a direct receptor molecule in *Arabidopsis thaliana*. *Plant and Cell Physiology* 42: 751–755.

Vlčková A, Špundová M, Kotabová E, Novotný R, Doležal K, Nauš J (2006) Protective cytokinin action switches to damaging during senescence of detached wheat leaves in continuous light. *Physiologia Plantarum* 126: 257–267.

Vylíčilová H, Bryksová M, Matušková V, Doležal K, Plíhalová L, Strnad M (2020) Naturally occurring and artificial N9-cytokinin conjugates: From synthesis to biological activity and back. *Biomolecules* 10: 832.

Vylíčilová H, Husičková A, Spíchal L, Srovnal J, Doležal K, Plíhal O, Plíhalová L (2016) C2-substituted aromatic cytokinin sugar conjugates delay the onset of senescence by maintaining the activity of the photosynthetic apparatus. *Phytochemistry* 122: 22–33.

Weaver LM, Gan S, Quirino B, Amasino RM (1998) A comparison of the expression patterns of several senescence-associated genes in response to stress and hormone treatment. *Plant*

Molecular Biology 37: 455–469.

Werbrouck SPO, Strnad M, Van Onckelen HA, Debergh PC (1996) Meta-topolin, an alternative to benzyladenine in tissue culture? *Physiologia Plantarum* 98: 291–297.

Wi SJ, Jang SJ, Park KY (2010) Inhibition of biphasic ethylene production enhances tolerance to abiotic stress by reducing the accumulation of reactive oxygen species in *Nicotiana tabacum*. *Molecules and Cells* 30: 37–49.

Woodward EJ, Marshal C (1988) Effects of plant growth regulators on tiller bud outgrowth in Barley (Hordeum distichum L.). *Annals of Botany* 61: 347–354.

Yamada H, Suzuki T, Terada K, Takei K, Ishikawa K, Miwa K, Yamashino T, Mizuno T (2001) The arabidopsis AHK4 histidine kinase is a cytokinin-binding receptor that transduces cytokinin signals across the membrane. *Plant and Cell Physiology* 42: 1017–1023.

Zavaleta-Mancera HA, López-Delgado H, Loza-Tavera H, Mora-Herrera M, Trevilla-García C, Vargas-Suárez M, Ougham H (2007) Cytokinin promotes catalase and ascorbate peroxidase activities and preserves the chloroplast integrity during dark-senescence. *Journal of Plant Physiology* 164: 1572–1582.

Zdarska M, Dobisová T, Gelová Z, Pernisová M, Dabravolski S, Hejátko J (2015) Illuminating light, cytokinin, and ethylene signalling crosstalk in plant development. *Journal of Experimental Botany* 66: 4913–4931.

Zhang J, Li H, Xu B, Li J, Huang B (2016) Exogenous melatonin suppresses dark-induced leaf senescence by activating the superoxide dismutase-catalase antioxidant pathway and down-regulating chlorophyll degradation in excised leaves of perennial ryegrass (*Lolium perenne* L.). *Frontiers in Plant Science* 7: 1500.

Zimmermann P, Zentgraf U (2005) The correlation between oxidative stress and leaf senescence during plant development. *Cellular and Molecular Biology Letters* 10: 515–534.

Zwack PJ, Rashotte AM (2013) Cytokinin inhibition of leaf senescence. *Plant Signaling and Behavior* 8: e24737.

Palacký University Olomouc

Department of Biophysics

Centre of the Region Haná for Biotechnological and Agricultural Research

Faculty of Science

Biological Activity of Substances with Strong Antisenescence Effect

Doctoral Thesis

Zuzana Kučerová

Supervisor: Martina Špundová

Olomouc 2020

Bibliographical identification

Author´s first name and surname	Zuzana Kučerová
Title of thesis	Biological Activity of Substances with Strong Antisenescence Effect
Type of thesis	doctoral
Department	Department of Biophysics
Supervisor	doc. RNDr. Martina Špundová, Ph.D.
The year of presentation	2021
Abstract	

It is well known that leaf senescence can be suppressed by exogenous application of phytohormones cytokinins. Nevertheles, under specific conditions, cytokinins can have negative effects and can even accelerate senescence. For this reason there are efforts to prepare compounds (cytokinin derivatives) that lack those effects and have other advantageous properties. Recently, two aromatic cytokinin arabinosides (6-benzylamino-9-β-D-arabinofuranosylpurines; BAPAs), 3-hydroxy- (3OHBAPA) and 3-methoxy- (3MeOBAPA) derivative have been synthesized and found to possess unique effects and mechanism of action. Analysis of gene expression that was performed on detached *Arabidopsis thaliana* L. leaves treated with 3MeOBAPA revealed that 6h and 48h treatments with this compound results in a shift in gene transcription toward defence. 3MeOBAPA causes upregulation of genes involved in plant innate immunity including MAPK signalling pathway together with oxidative burst and JA-ethylene signalling, which results in effective protection of field-grown plants against fungal pathogens. Long-term incubation of leaves in 3OHBAPA and 3MeOBAPA does not impair leaf fitness which is common during prolonged activation of defence response mechanisms, but on the contrary effectively delays senescence of detached leaves. Interestingly, the anti-senescence differs quantitatively in wheat (*Triticum aestivum* L. cv. Aranka) and Arabidopsis (Col-0). In wheat, 3OHBAPA has higher protective effect than 3MeOBAPA, whereas in Arabidopsis, 3MeOBAPA is the more efficient derivative. We have found that the different anti-senescent activity of 3OHBAPA and 3MeOBAPA is coupled to different ethylene production in the treated leaves: the lower the ethylene production, the higher the anti-senescence activity. 3OHBAPA and 3MeOBAPA also protect efficiently the senescing leaves of wheat and Arabidopsis against oxidative damage induced by both H_2O_2 and high-light treatment, which could also be connected with the low level of ethylene production.

Keywords	cytokinin derivatives, senescence, wheat, Arabidopsis, photosynthesis
Number of pages including references	86
Language	English

Bibliografická identifikace

Jméno a příjmení autora	Zuzana Kučerová
Název práce	Biologická aktivita látek se silným antisenescenčním účinkem
Typ práce	disertační
Pracoviště	Katedra biofyziky
Vedoucí práce	doc. RNDr. Martina Špundová, Ph.D.
Rok obhajoby práce	2021
Abstrakt	

Listovou senescenci lze oddálit exogenní aplikací fytohormonů cytokininů. Za určitých podmínek však mohou mít cytokininy negativní účinky a mohou naopak proces senescence urychlit. Z tohoto důvodu jsou připravovány látky na bázi cytokininů, které tyto negativní účinky nemají a mají další výhodné vlastnosti. V nedávné době byly připraveny dva aromatické cytokininové arabinosidy (6-benzylamino-9-β-D-arabinofuranosylpuriny; BAPA), 3-hydroxy-derivát (3OHBAPA) a 3-methoxyderivát (3MeOBAPA), jejichž účinky a mechanismus účinku jsou jedinečné. Analýza genové exprese, která byla provedena na oddělených listech *Arabidopsis thaliana* L. ponořených v roztoku 3MeOBAPA po dobu 6 a 48 h, odhalila, že tato látka aktivuje geny zapojené v obraně proti patogenům. 3MeOBAPA aktivuje signální dráhy spojené s MAPK, ethylenem a kyselinou jasmonovou a způsobuje přechodnou akumulaci reaktivních forem kyslíku. Tyto reakce mohou vést ke zvýšení rezistence ošetřených rostlin, jak bylo ověřeno v polních experimentech. Ačkoliv dlouhodobá aktivace mechanismů zapojených v obraně proti patogenům má zpravidla za následek zhoršení fyziologického stavu rostlin, 3OHBAPA a 3MeOBAPA naopak vykazují velmi silné antisenescenční účinky. Tyto účinky se kvantitativně liší u oddělených listů pšenice (*Triticum aestivum* L. cv. Aranka) a Arabidopsis (Col-0). Zatímco v případě pšenice má vyšší antisenescenční účinek 3OHBAPA, u listů Arabidopsis je účinnější 3MeOBAPA. Tento rozdílný efekt je spojen s různou produkcí ethylenu v ošetřených listech: čím nižší je produkce ethylenu, tím vyšší je antisenescenční aktivita daného derivátu. 3OHBAPA a 3MeOBAPA také účinně ochraňují senescentní listy pšenice a Arabidopsis před oxidativním poškozením vyvolaným působením H_2O_2 a světla, což může rovněž souviset s nízkou produkcí ethylenu po aplikaci těchto látek.

Klíčová slova	cytokininy, deriváty, senescence, pšenice, Arabidopsis, fotosyntéza
Počet stran včetně seznamu literatury	86
Jazyk	anglický

Declaration

I hereby declare that I have written this thesis independently as the original work with the help of my supervisor doc. RNDr. Martina Špundová, Ph.D. The complete list of used literature and other information sources is included in the section References.

Olomouc, 2020   Zuzana Kučerová

Acknowledgement

First of all, I would like to address my deepest thanks to my supervisor Martina Špundová for everything she did for me. Especially for her kind support, unvaluable advices, patient guidance and, most importantly, for her friendship and for all the corrections! ☺

It is a pleasure to have such great colleagues as Pavla Ocvirková and Marek Rác. I would like to thank them for all the help they have given me. Pavla and Marek, you are one of the reasons why I love my job!

Furthermore, I would like to thank all the members of the Department of Biophysics for the collaboration and for creating a pleasant and kind environment. Special thanks belong to prof. Petr Ilík for giving me the opportunity to pursue my doctoral studies at the Department of Biophysics. I am thankful to prof. Stefano Caffarri for allowing me to be involved in his projects during my three months research stay at the Laboratory of Plant Genetics and Biophysics at Aix-Marseille University and for all the things he taught me (and also for the 2 kg of Parmigiano-Reggiano!).

Nevertheless, there would never have been any doctoral study without my husband. Thank you for convincing me that I can do it and for all of your love, support, encouragement and compromises that allow me to do what I enjoy. I am grateful to have you. My deepest gratitude belongs to my parents for everything they have ever done for me. I am the luckiest child in the world to have you. Thank you all for believing in me.

List of Publications

This thesis is based on two research articles enclosed at the end of the thesis.

1. **Kučerová Z**, Rác M, Mikulík J, Plíhal O, Pospíšil P, Bryksová M, Sedlářová M, Doležal K, Špundová M (2020) The anti-senescence activity of cytokinin arabinosides in wheat and Arabidopsis is negatively correlated with ethylene production. *International Journal of Molecular Sciences* 21: 8109. IF (2019) = 4.556
(Kučerová Z *designed the experiments, prepared samples for all experiments, performed Chl fluorescence and ion leakage measurements, analysed and interpreted the data and wrote the article*)

2. Bryksová M*, Dabravolski S*, **Kučerová Z***, Zavadil Kokáš F, Špundová M, Plíhalová L, Takáč T, Gruz J, Hudeček M, Hloušková V, Koprna R, Novák O, Strnad M, Plíhal O, Doležal K (2020) Aromatic cytokinin arabinosides promote PAMP-like responses and positively regulate leaf longevity. *ACS Chemical Biology* 15: 1949–1963. IF (2019) = 4.434; * contributed equally
(Kučerová Z *designed the experiments related to photosynthetic activity in the detached leaves, performed Chl fluorescence and chlorophyll content measurements, wrote the corresponding parts of the article and prepared figures throughout the article*)

Research articles by the same author that are not included in this thesis:

1. Crepin A, **Kučerová Z**, Kosta A, Durand E, Caffarri S (2020) Isolation and characterization of a large photosystem I-light harvesting complex II supercomplex with an additional lhca1-a4 dimer in Arabidopsis. *Plant Journal* 102: 398-409. IF (2019) = 6.141
(Kučerová Z *performed the biochemical experiments*)

2. Bednaříková M, Folgar-Cameán Y, **Kučerová Z**, Lazár D, Špundová M, Hájek J, Barták M (2020) Analysis of K and L band appearance in OJIPs in Antarctic lichens in low and high temperature. *Photosynthetica* 58: 646-656. IF (2019) = 2.562
(Kučerová Z *performed the thermostability measurements*)

3. Ilík P, Špundová M, Šicner M, Melkovičová H, **Kučerová Z**, Krchňák P, Fürst T, Večeřová K, Panzarová K, Benediktyová Z, Trtílek M (2018) Estimating heat tolerance of plants by ion leakage: A new method based on gradual heating. *New Phytologist* 218: 1278-1287. IF (2018) = 7.299

(Kučerová Z *measured the heat tolerance of various plant species using ion leakage methods*)

Abbreviations

A	antheraxanthin
ADP	adenosine diphosphate
AHK	Arabidopsis histidine kinase
AHP	Arabidopsis histidine phosphotransfer protein
ARR	Arabidopsis response regulator
ATP	adenosine triphosphate
BAK	brassinosteroid-insensitive-associated receptor kinase
BIK	Botrytis-induced kinase
BAP	6-benzylaminopurine
BAPA	6-benzylamino-9-β-D-arabinofuranosylpurine
car	carotenoid
CCD4	carotenoid cleavage dioxygenase 4
CHASE	cyclase/histidine kinase associated sensors extracellular
Chl	chlorophyll
cis-OPDA	*cis*-12-oxo-phytodienoic acid
CK	cytokinin
CNGC	calcium-nucleotide-gated channel
CPK	calcium-dependent protein kinase
CRF	cytokinin responsive factor
cZ	*cis*-zeatin
dad	day after detachment
dai	day after inoculation
DCFH-DA	2′-7′-dichlorodihydrofluorescein diacetate
DEPS	de-epoxidation state of xanthophylls
DFCC	dioxobilin-type fluorescent chlorophyll catabolite
DHE	dihydroethidium
DIC	differential interference contrast
DMSO	dimethylsulfoxide
DNCC	formyloxobillin-type non-fluorescent chlorophyll catabolite
$(dV/dt)_0$	the initial slope of the O–J Chl fluorescence rise
F_0	the minimal fluorescence of the dark-adapted state
FCC	formyloxobillin-type fluorescent chlorophyll catabolite
F_V/F_M	the maximum quantum yield of photosystem II photochemistry
F_M	the maximal fluorescence of the dark-adapted state
$F_M{}'$	the maximal fluorescence of the light-adapted state
F_t	the actual fluorescence signal at the time t of actinic illumination
FW	fresh weight

GO	Gene Ontology
GUS	β-glucuronidase
H_2O_2	hydrogen peroxide
HCAR	7-hydroxymethyl Chl *a* reductase
HL	high light
iP	isopentenyladenine
JA	jasmonic acid
JA-Ile	jasmonoyl-L-isoleucine
kinetin	6-furfurylaminopurine
LHCII	light-harvesting complexes of photosystem II
LOOH	lipid hydroperoxide
MAPK	mitogen-activated protein kinase
MemT	6-(3-methoxybenzylamino)purine
MeoT	6-(2-methoxybenzylamino)purine
MemT	6-(3-methoxybenzylamino)purine riboside
MeoT	6-(2-methoxybenzylamino)purine riboside
N9-iP	isopentenyladenine with substitution on the N9 atom of purine moiety
N9-kin	6-furfurylaminopurine with substitution on the N9 atom of purine moiety
NCC	formyloxobillin-type non-fluorescent chlorophyll catabolite
NPQ	non-photochemical quenching
$^1O_2$	singlet oxygen
$O_2^{\cdot-}$	superoxide anion radical
OJIP	chlorophyll fluorescence induction transient
PAMP	pathogen-associated molecular pattern
PAO	pheophorbide *a* oxygenase
PAR	photosynthetically active radiation
PDF	plant defensin
pFFC	phyllobillin
PPH	pheophytinase
PRR	pattern recognition receptor
PSII	photosystem II
PTI	pathogen-associated molecular pattern-triggered immunity
PUFA	polyunsaturated fatty acid
Q_A	primary electron acceptor of photosystem II
Rboh	respiratory burst oxidase homolog
RCC	red chlorophyll catabolite
RCCR	red chlorophyll catabolite reductase
RCII	reaction center of photosystem II
ROS	reactive oxygen species

SAG	senescence-associated gene
SDG	senescence-downregulated gene
TF	transcription factor
TIC55	translocon at the inner chloroplast envelope 55
TDZ	thidiazuron
tZ	*trans*-zeatin
UPE	ultra-weak photon emission
V	violaxanthin
V_J	relative variable fluorescence at the J step of OJIP curve
Z	zeaxanthin
ZmHK	*Zea mays* histidine kinase
3OHBAPA	6-(3-hydroxybenzylamino)-9-β-D-arabinofuranosylpurine
3MeOBAPA	6-(3-methoxybenzylamino)-9-β-D-arabinofuranosylpurine
$\Phi_{f,D}$	quantum yield of constitutive non-regulatory dissipation processes
Φ_{NPQ}	quantum yield of regulatory light-induced non-photochemical quenching
Φ_P	effective quantum yield of photosystem II photochemistry (for the light-adapted state)

Content

1 Introduction

This dissertation thesis is focused on the unique biological activity and the possible mechanism of action of aromatic cytokinin arabinosides, newly prepared derivatives of phytohormones cytokinins. The theoretical part of the thesis represents a brief introduction with respect to the experimental part. The introductory part deals with leaf senescence, its accompanying phenomena, mechanisms and signalling together with description of cytokinins and their derivatives, their structure, signalling and antisenescent effect.

Despite its benefits for the plant as such, consisting mainly in the recycling and storage of nutrients, senescence (especially premature) is one of the processes that negatively affect plant production from an agricultural point of view. Therefore, delaying senescence is desirable in this regard. The ability of cytokinins to delay senescence has been known for a long time, however, under certain conditions cytokinins can have negative effects, including accelerating senescence. For this reason, their new derivatives with improved effects on plants are being synthetized. Newly prepared cytokinin arabinosides have been found to have no cytokinin-like adverse actions. On the contrary, they are characterized by other advantageous effects such as increased plant protection from biotic and abiotic stress. The experimental part of the thesis includes results of the study of biological activity and the possible mechanism of action of cytokinin arabinosides which were partly published in two original articles enclosed in the Appendix. The biological properties of cytokinin arabinosides combine defence and anti-senescent effect while having no observable adverse effects on the overall fitness of the plant and minimal interaction with the cytokinin signalling pathway. For their unique activity, cytokinin arabinosides are reasonable candidates for efficient use, for example in biotechnological or agronomic practice.

1.1 Senescence

Plant senescence is a final stage of development that usually precedes to death of the plant itself. This highly organised and controlled process allows nutrients and organic resources mobilization and recyclation from senescing to growing, reproductive or storage organs (e.g. Smart 1994, Gan & Amasino 1997, Himelblau & Amasino 2001, Zwack & Rashotte 2013, Maillard et al. 2015, Havé et al. 2017). During this process of programmed degradation cells remain viable (Smart 1994) nevertheless senescence also includes some processes that are typical for programmed cell death such as chromatin condensation or fragmentation of DNA (Simeonova et al. 2000). Typical phenomena that accompany senescence are degradation of photosynthetic pigments, proteins, membrane lipids, amino acids and related inhibition of photosynthesis and other anabolic processes that are overall substituted by catabolism (Schippers et al. 2015, Diaz-Mendoza et al. 2016, Tamary et al. 2019). The probably most apparent marker of senescence is chlorophyll (Chl) degradation accompanied by visible yellowing of leaves. However, Chl is not the only pigment whose content decreases during senescence. As carotenoids are degraded to a lesser extent than Chl, the yellow colour is typical for senescing leaves (Biswal 1995).

While natural senescence is usually associated with plant age, it can also be affected (and induced) by many external and internal factors. External (environmental) factors include photosynthetically active radiation (PAR), darkness, temperature, water availability, amount of nutrients, soil salinity or infection by pathogens. Internal factors include levels of plant hormones and growth regulators, antioxidants, reproduction, the age of the plant or its physiological state (Noodén et al. 1996, 1997, Špundová et al. 2003, Yoshida 2003, Špundová et al. 2005, Zwack & Rashotte 2013, Zhang et al. 2016, Janečková et al. 2018, Mayta et al. 2019). When the metabolic threshold of these signals is exceeded, senescence-associated genes (SAGs) are expressed, which results in the onset of senescence in the plant organ or organism and possibly its death (Smart 1994, Gan & Amasino 1997, Guo et al. 2004). The possibility to induce senescence using either internal or external factors is widely used for studies of senescence mechanisms, processes, signalling or biological activity of compounds with senescence-related effects.

1.1.1 Senescence-associated genes

As has been already mentioned, SAGs play an important role during senescence. SAGs are genes whose expression is activated or increases with the onset and progression of senescence (Gan & Amasino 1997, Lim et al. 2003), they are responsible for the execution of the senescence-induced changes in plant organism. Majority of senescence-induced degradation processes involve SAG-encoded proteins such as cystein and aspartic proteases, lipases, RNAses, components of ubiqutin-proteasome system or enzymes of nutrient recycling. However, SAGs also encode various transcription factors (TFs) such as WRKY or NAC, regulatory genes, stress and secondary metabolites or antioxidants.

Expression profiles of SAGs are more or less different when compared developmental and induced senescence, and in the latter case they depend on what caused the senescence. In other words, as senescence can be induced by many factors, there are multiple regulatory pathways of this process. Expression of SAGs differs in attached and detached leaves, in leaves senescing under dark or light conditions, in monocarpic and perennial trees, etc. (Gan & Amasino 1997, Gepstein et al. 2003, Buchanan-Wollaston et al. 2005, Breeze et al. 2011, Kim et al. 2016). For example, in Arabidopsis plants with knockout in *ORE4* (*RPS17*) gene, that play a critical role in biosynthesis of thylakoid membrane proteins, the mutation delayed many age-dependent senescence-induced changes. On the contrary, its effect on the induced senescence (by darkness or exogenously applied phytohormones) was only low (Woo et al. 2002). However, there are genes that can be used as markers of senescence such as *SAG12* coding for cysteine protease in Arabidopsis (Gan & Amasino 1995) or *LSC54* in *Brassica napus* L (Buchanan-Wollaston 1994). Beside SAGs that are typically upregulated during senescence, there are senescence-downregulated genes (SDGs) that include genes encoding photosynthetic proteins such as Chl *a/b* binding protein and small subunit of Rubisco (Gan & Amasino 1997), Chl and carotenoid biosynthesis genes, genes encoding carbon fixation, cell cycle or cellular metabolism (Breeze et al. 2011).

1.1.2 Senescence and chloroplasts

While nucleus and mitochondria remain intact and active to control and provide energy until the final stages of senescence, chloroplasts are first organelles that undergo senescence-induced changes and subsequently degradation. Since chloroplasts contain

a majority of cellular lipids and proteins, their degradation is in particular important for effective recyclation of nutrients (Lim et al. 2003, Schippers et al. 2015, Tamary et al. 2019), especially of nitrogen (Girondé et al. 2015). During senescence chloroplasts undergo many changes whether it is their number and volume in the cell, their structure or photochemical function (Špundová et al. 2003, Springer et al. 2016, Tamary et al. 2019). Number and also size of chloroplasts decrease and thylakoid, stromal and envelope components are dismantled. Senescence also induces changes in chloroplast shape which becomes more spherical (Špundová et al. 2003, Tamary et al. 2019). Dissintegration of thylakoids is accompanied by a release of plastoglobuli, whose number and size increase during senescence, to the cytosol through small holes in the chloroplast envelope (Špundová et al. 2003, Zavaleta-Mancera et al. 2007, Springer et al. 2016, Tamary et al. 2019). Although plastoglobuli were considered as a lipid storage site, it is now known that they play active role in lipid metabolism (e.g. Spicher & Kessler 2015). Recently, it has been found that carotenoid cleavage dioxygenase 4 (CCD4), enzyme involved in carotenoid senescence-induced degradation, is functionally active in plastoglobuli. Mutant Arabidopsis plants that constitutively express CCD4 have reduced content of carotenoids such as β-carotene, lutein or violaxanthin. Carotenoids accumulate in plastoglobuli of CCD4 mutant plants suggesting their active translocation during dark-induced senescence (Rottet et al. 2016).

It is well known that thylakoid membranes of chloroplast are the site of light-dependent photosynthetic reactions. The energy of photons absorbed by the photosystem II (PSII) via its light-harvesting complexes (LHCII) is further distributed in three possible ways: photochemical, fluorescent and thermal dissipation. These processes compete with each other, where a decrease in one means an increase in the representation of another (e.g. Roháček & Barták 1999, Lazár 2015). The senescence-induced changes in photosynthesis can be evaluated using measurement of Chl fluorescence parameters such as the maximum quantum yield of PSII photochemistry (F_V/F_M; for definitions of the Chl fluorescence parameters see chapter 3.15) which is the most commonly used Chl fluorescence parameter. F_V/F_M is measured in samples adapted to darkness and it is used as an indicator of photoinhibition or other PSII damage. In stressed plants F_V/F_M is significantly reduced and it also decreases during senescence

4

(e.g. Roháček & Barták 1999, Špundová et al. 2003, Vlčková et al. 2006, Prokopová et al. 2010b).

Other used parameters are non-photochemical quenching (NPQ; calculated as $NPQ = (F_M-F_M')/F_M'$) of chlorophyll fluorescence and also the quantum yield of regulatory light-induced non-photochemical quenching (Φ_{NPQ}). Both are measured during the transition of leaves from a dark-adapted state to light-adapted state. The non-photochemical quenching which is associated with the dissipation of absorbed energy to heat, increases at the beginning of senescence and then decreases in the last phase of leaf life (Roháček & Barták 1999, Roháček 2002, Dai et al. 2004, Hendrickson et al. 2004). Thermal energy dissipation is a very effective process of protecting the photosynthetic apparatus against photo-damage. If the use of absorbed energy for photosynthesis is reduced (due to stress or senescence), i.e. the energy input exceeds the photosynthetic capacity, deepoxidation of xanthophylls in xanthophyll cycle is stimulated (Arnoux et al. 2009, Järvi et al. 2013). As mentioned above, at the beginning of senescence non-photochemical quenching usually increases due to stimulation of the xanthophyll cycle, but with advancing senescence, the effectiveness of this process decreases and therefore the photoprotection decreases (Dai et al. 2004).

The chlorophyll fluorescence parameters reflecting PSII photochemistry include the effective quantum yield of PSII photochemistry (Φ_P) that may be substituted by the parameter Φ_{PSII}, referred to as the actual quantum yield of PSII photochemistry for the light-adapted state. Both Φ_P and Φ_{PSII} decrease relatively significantly during senescence (Dai et al. 2004, Hendrickson et al. 2004, Kalaji et al. 2014, 2017, Lazár 2015, Janečková et al. 2019). The complementary parameter to Φ_P and Φ_{NPQ} is quantum yield of constitutive non-regulatory dissipation processes ($\Phi_{f,D}$) that indicates how much of the absorbed energy is lost by constitutive thermal dissipation and fluorescence, with the greater part being thermal dissipation (Hendrickson et al. 2004). Senescence usually induces increase in $\Phi_{f,D}$ (Janečková et al. 2019).

1.1.3 Role of ROS in senescence

The accumulation of reactive oxygen species (ROS) such as hydrogen peroxide (H_2O_2), singlet oxygen ($^1O_2$) and the superoxide anion radical (O_2^-), is one of the early phenomena of senescence (e.g. Rosenvasser et al. 2006, Khanna-Chopra 2012). The

increased level of ROS is usually caused either by their enhanced production or decline in activity of antioxidative system. ROS are formed as byproducts of oxido-reductive reactions especially in chloroplasts, mitochondria and peroxisome (e.g. Bhattacharjee 2005, Guo & Crawford 2005), due to activity of oxidases such as membrane-localized NADPH oxidases, cell wall-bounded peroxidases or via fatty acid oxidation pathways (Del Río 2015). Since ROS can serve as secondary messengers or act as independent signalling molecules they are involved in almost all signalling cascades in plant organism (Mittler et al. 2004, Sewelam et al. 2016, Mayta et al. 2019). This phenomena is referred to as an oxidative signalling. Enhanced production of ROS is initiated by various physiological processes such as photosynthesis, pathogen recognition, stress or hormonal perception. ROS then activate cellular response to corresponding stimulus. ROS level is modulated by positive feedback loop and ROS-scavenging pathways (Fig. 1; Mittler 2002).

However, ROS are extremely reactive and toxic and when their accumulation overcomes the control mechanisms, they can oxidize cell components. This phenomena is called oxidative damage. The extensive formation of ROS is induced by senescence or stress-induced inhibition of photosynthesis and Chl metabolism (Thompson et al. 1987, Zimmermann & Zentgraf 2005, Rosenvasser et al. 2006, Zavaleta-Mancera et al. 2007, Del Río 2015, Zhang et al. 2016, Mayta et al. 2019). High concentrations of ROS can cause additional damage to photosynthetic apparatus and impairment of cellular components, DNA or aminoacids (Zimmermann & Zentgraf 2005).
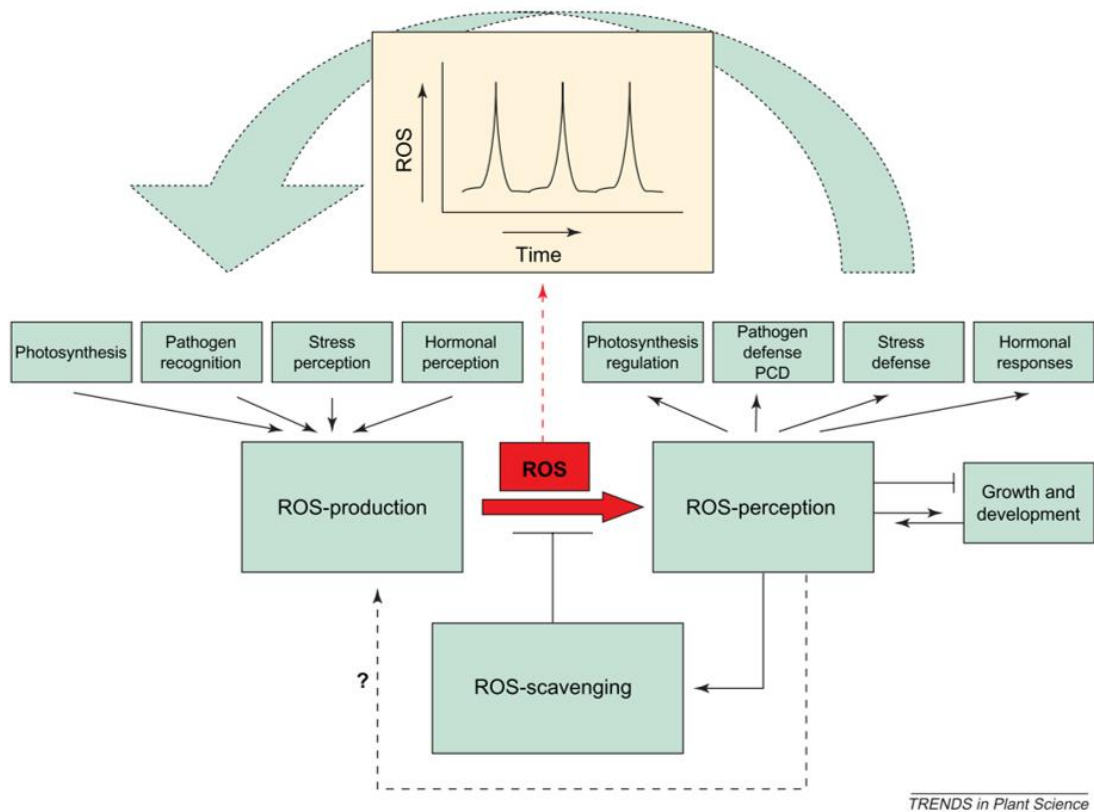
Fig. 1 Reactive oxygen species (ROS) signalling network in plants. Reprinted with permission from Mittler (2002).

Since cell membrane-forming polyunsaturated fatty acids (PUFA) are very prone to oxidative damage, the accumulation of ROS can cause peroxidation of membrane lipids that leads to leakage of cell content outside of the cell and subsequently cell death (Zimmermann & Zentgraf 2005). During senescence PUFAs are transformed via lipoxygenases to lipid hydroperoxides (LOOHs) which are considered as primary products of lipid peroxidation (Spiteller 2003). Accumulation of ROS and related oxidative damage including lipid peroxidation are considered to be one of the major contributors to senescence. ROS together with proteases are also responsible for chloroplast proteolysis, especially of large subunit of Rubisco that is selectively degraded during senescence (Khanna-Chopra 2012, Del Río 2015). In summary, the accumulation of ROS plays very important role in signalling pathways at the onset of senescence and also in sense of extensive oxidative degradation of cellular components, especially in the later phases of senescence.

1.1.4 Chlorophyll degradation

As has been already mentioned, important and most visible phenomenon of leaf senescence is gradual loss of Chl. Chl is metabolised to colourless catabolites. One of the major purposes of this process is to remove Chl molecules and protect of chloroplasts and cells against oxidative damage, as Chl can be a source of ROS (Triantaphylidès & Havaux 2009, Kuai et al. 2018). Also, Chl degradation makes accessible other important sources of nitrogen such as light-harvesting complexes for nitrogen recyclation. First steps of Chl degradation in Arabidopsis take place in chloroplasts (Fig. 2A) and then it proceeds in cytosol and vacuole (Fig. 2B). During the first steps, reactions with coloured pigments as substrates are occurring, the latest are reactions that lead to diversification of phyllobillins (pFCCs). Senescence-induced Chl degradation starts with two-step reduction of Chl *b* to Chl *a:* conversion of Chl *b* to 7-hydroxymethyl Chl *a* catalysed by Chl *b* reductase (encoded by *NON-YELLOW COLORING, NYC1/NOL*) and conversion of 7-hydroxymethyl Chl *a* to Chl *a* catalysed by 7-hydroxymethyl Chl *a* reductase (HCAR). Central Mg is then removed from Chl *a* via Mg-dechelatase (encoded by STAY-GREEN, SGR) and pheophytin *a* is formed. Removal of phytol chain from pheophytin *a* subsequently forms pheophorbide *a*. This reaction is catalysed by pheophytinase (PPH). Pheophorbide *a* is then converted via chloroplast envelope-bound pheophorbide *a* oxygenase (PAO) to red Chl catabolites (RCCs) which are converted via red Chl catabolite reductase (RCCR) to pFCCs (also referred to as primary fluorescent catabolites). Once Chl is transformed to pFCC its potential phototoxicity is removed because ability of pFCC to produce ROS is only low in comparison to Chl, pheophorbide or RCC (Pružinská et al. 2005, Hörtensteiner & Kräutler 2011, Hauenstein et al. 2016, Kuai et al. 2018). Approximately 50% of pFCCs are hydroxylated via translocon at the inner chloroplast envelope 55 (TIC55). Probably due to their non-phototoxicity pFCCs and also hydroxy-pFCCs are able to leave the chloroplast, although the exact transporting mechanism is not yet known (Hauenstein et al. 2016). Both pFCCs and hydroxy-pFCCs can be variously modified. When they are demethylated via MES16 (in cytosol), formyloxobillin-type fluorescent Chl catabolites (FCCs) are formed, which are in low pH isomerized to formyloxobillin-type non-fluorescent Chl catabolites (NCCs). Deformylation of pFCCs and hydroxy-pFCCs via ER-localized CYP89A9 followed by

demethylation via MES16 leads to formation of dioxobilin-type fluorescent Chl catabolites (DFCCs) which are in low pH converted to non-fluorescent isomers formyloxobillin-type non-fluorescent Chl catabolites (DNCCs). The isomerisation of FCCs to NCCs and DFCCs to DNCCs takes place in vacuole (as indicated by the needed low pH) (Hörtensteiner & Kräutler 2011, Hauenstein et al. 2016, Kuai et al. 2018).
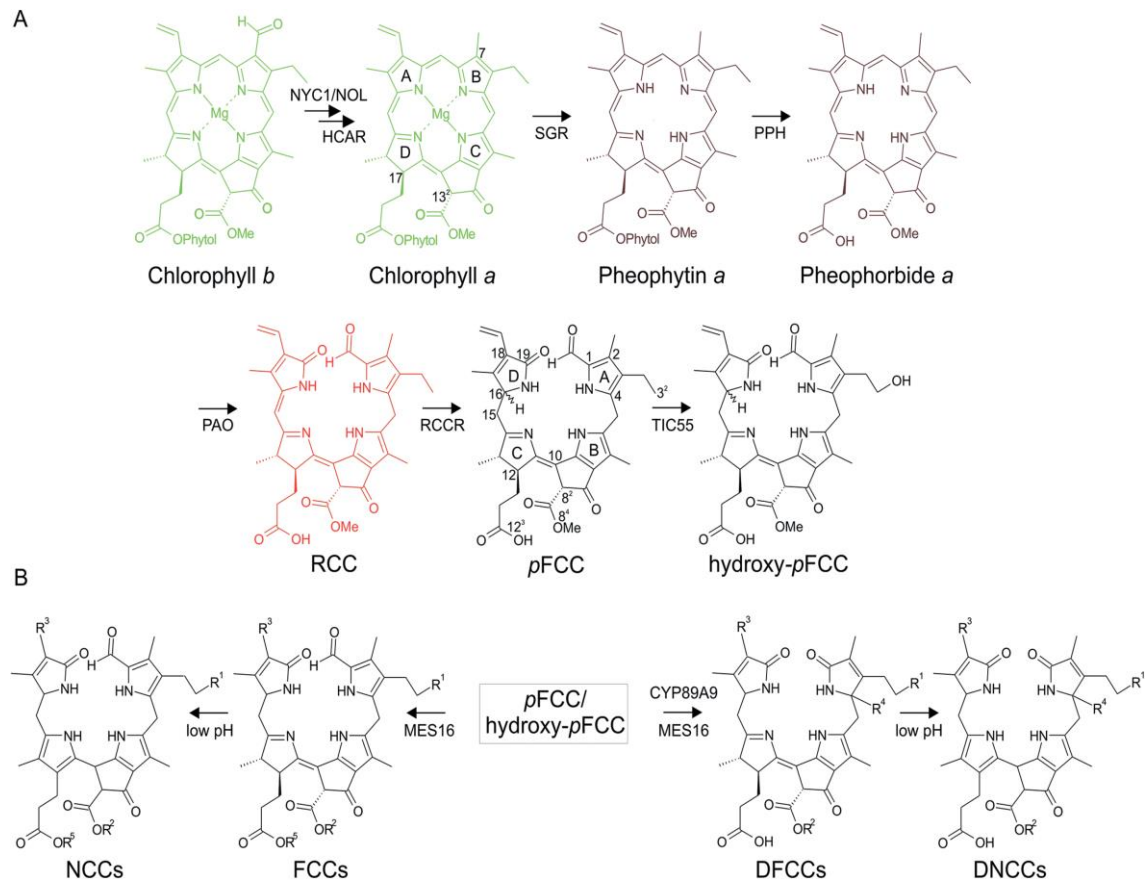
Fig. 2. Senescence-induced Arabidopsis chlorophyll degradation pathway. (**A**) Reactions in chloroplasts. Letters A, B, C and D are pyrrole rings labels. (**B**) Reactions diversifying phyllobillins outside chloroplast. NYC/NOL1, NON-YELLOW COLORING; HCAR, 7-hydroxymethyl Chl *a* reductase; SGR, STAY-GREEN; PPH, pheophytinase; PAO, pheophorbide *a* oxygenase; RCC, red chlorophyll catabolite; RCCR red chlorophyll catabolite reductase; pFCC, phyllobillin; TIC55, TRANSLOCON AT THE INNER CHLOROPLAST ENVELOPE55; DFCCs, dioxobilin-type fluorescent chlorophyll catabolites; DNCCs, dioxobilin-type non-fluorescent chlorophyll catabolites; FCCs, formyloxobilin-type fluorescent chlorophyll catabolites; NCCs, formyloxobilin-type non-fluorescent chlorophyll catabolites; pFCC, primary fluorescent chlorophyll catabolite; RCC, red chlorophyll catabolite. Reprinted with permission from Kuai et al. (2018).

1.2 Cytokinins

Cytokinins (CK) are group of phytohormones that are evolutionary very old and conservative substances. They were identified in almost all known living organisms (Spíchal 2012). First CK was discovered and identified by Miller and his co-workers as 6-furfurylaminopurine in 1950s in autoclaved herring sperm as a DNA degradation product. Based on the compound ability to promote cell division in tobacco (*Nicotiana tabacum* L.) they named it kinetin. First naturally occurring plant CK was *trans*-zeatin in 1960s which was purified from immature maize endosperm by Letham & Miller. To avoid misunderstanding with kinins, animal polypeptides, this group of phytohormones was named cytokinins by Skoog and his co-workers in 1965 (Amasino 2005). In plants, CKs are very important phytohormones that affect various plant developmental and physiological processes such as cell division, apical dominance, de-etiolization, organ formation, nutrients metabolism and defence against pathogens. CKs are considered to be negative regulators of leaf senescence, i.e. they are able to delay senescence-induced changes (e.g. Mok & Mok 2001).
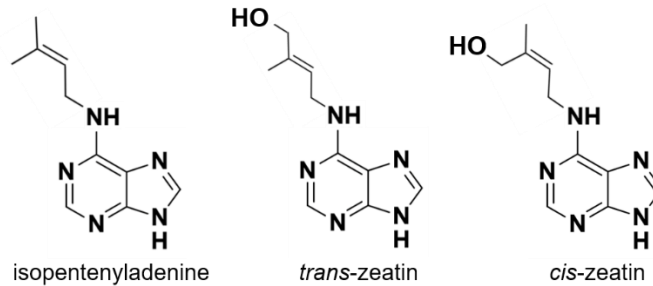
1.2.1 Cytokinins structure

Naturally occurring CKs are derivatives of adenine with isoprenoid or aromatic side chain at the N6 atom of purine moiety. CKs in plant organism are usually present in low concentrations in the forms of free bases, nucleosides, glucosides and nucleotides. Isoprenoid CKs are the predominant type, especially those with *trans*-hydroxylated side chain such as *trans*-zeatin (tZ) and its derivatives (Fig. 3). The group of isoprenoid CKs also includes isopentenyladenine (iP), *cis*-zeatin (cZ) and dihydrozeatin (Mok & Mok 2001, Doležal et al. 2007). While tZ shows extensive biological activity, function of cZ is not fully elucidated despite its considerable prevalence. It is presumed that cZ preferably acts in developmental phases associated with limited growth (Gajdošová et al. 2011, Janečková et al. 2018).

CKs with aromatic side chain were considered as artificial compounds for a long time. However it has been proven that they naturally occur in various plant species (for review see Strnad 1997). Typical aromatic CKs are 6-furfurylaminopurine (kinetin), 6-benzylaminopurine (BAP) and its hydroxylated forms topolins (Fig. 3). In terms of their

functions, the isoprenoid CKs are considered to have a more potent effect on growth processes such as cell cycle while aromatic CKs have more pronounced effect on developmental processes, especially those involving morphogenesis and senescence (Holub et al. 1998). Beside the naturally occurring CKs there is also group of synthetic CKs derived from phenylurea represented e.g. by thidiazuron (TDZ) and diphenylurea (Mok & Mok 2001).
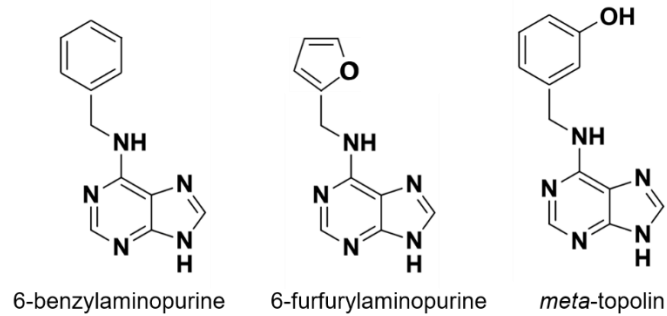
Fig. 3. Chemical structure of selected isoprenoid, aromatic and phenylurea cytokinins.

1.2.2 Cytokinin signalling

With respect to experimental part of the thesis and the long-standing use of this plant as a model system, this chapter is focused on CK signalling in *Arabidopsis thaliana*.

In the plasmatic membrane of Arabidopsis, there are three highly homologous receptor histidine kinases involved in CK signal transduction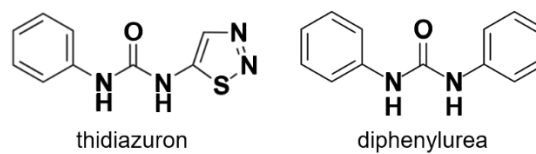, AHK2, AHK3 and CRE1/AHK4 (Inoue et al. 2001, Suzuki et al. 2001, Ueguchi et al. 2001a, b, Yamada et al. 2001). These transmembrane proteins have similar multidomain structure and a molecular weight exceeding 100 kDa. At the N-terminus of the receptor molecule is the CK-binding extracellular CHASE domain (Cyclase/Histidine kinase associated sensors extracellular). There is transmembrane domain on each side of CHASE, one is followed by a catalytic domain with histidine kinase activity. This catalytic domain consists of two parts, a dimerization domain that is formed by two adjacent antiparallel helices and an ATP/ADP binding phosphotransfer domain, which contains a conserved histidine residue (H-box). At the receptor C-terminus is an acceptor domain containing a conserved aspartate residue. High-energy phosphate groups are transferred between histidine and aspartate. Between the receptor and histidine kinase domains, a pseudo-receiver domain is present whose function has not yet been fully elucidated (Fig. 4) (summarized in Lomin et al. 2012).
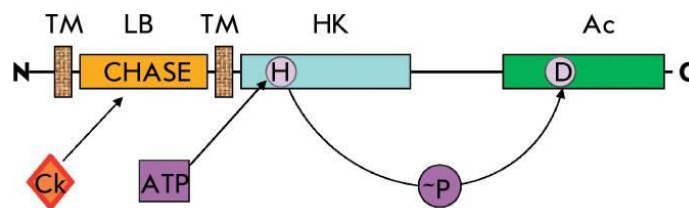
Fig. 4 Domain structure of Arabidopsis cytokinin receptor. Protein domains: TM, transmembrane; LB, ligand-binding (CHASE); HK, histidine kinase; Ac, acceptor; Ck, cytokinin; H, conserved histidine; D, conserved aspartate; N and C denote the N- and C-terminus of the receptor. Reprinted from Lomin et al. (2012; open access).

CK binding on the CHASE domain causes phosphorylation of the histidine residue which results in histidine kinase dimer formation. The phosphate group is then transferred to the histidine residue of histidine phosphotransfer protein (AHP) which is further translocated into nucleus. While AHP 1-5 are positive regulators of CK signalling, AHP 6 does not transfer the phosphate group and is considered as a negative

regulator of CK signalling. After entering nucleus, the phosphate group is transferred on the aspartate residue of the acceptor domain of response regulator (ARR). The activated ARR is capable to regulate the transcription of responsive genes. Based on their function, there are three groups of ARRs: type A, B and C (ARR A, B, C, respectively; Fig. 5). ARR A are negative regulators of CK signalling responsible for regulation circadian rhythms (ARR3, 4, 8, 9) and phytochromes function (ARR4). They compete for the phosphate group with ARR B that are effectors of CK signal. ARR B activate transcription of genes that are involved in root and shoot formation, de-etiolization, leaf growth, senescence, CK homeostasis and also genes coding for ARR A and CK responsive factors (CRF; Fig. 5). CRFs are APETALA2-like genes and are related to ethylene responsive factors, together with ARR B they affect transcription of CK-responsive genes. ARR C are not CK-induced and they probably do not have any significant effect in CK signalling pathway (for review see To & Kieber 2008, Lomin et al. 2012).
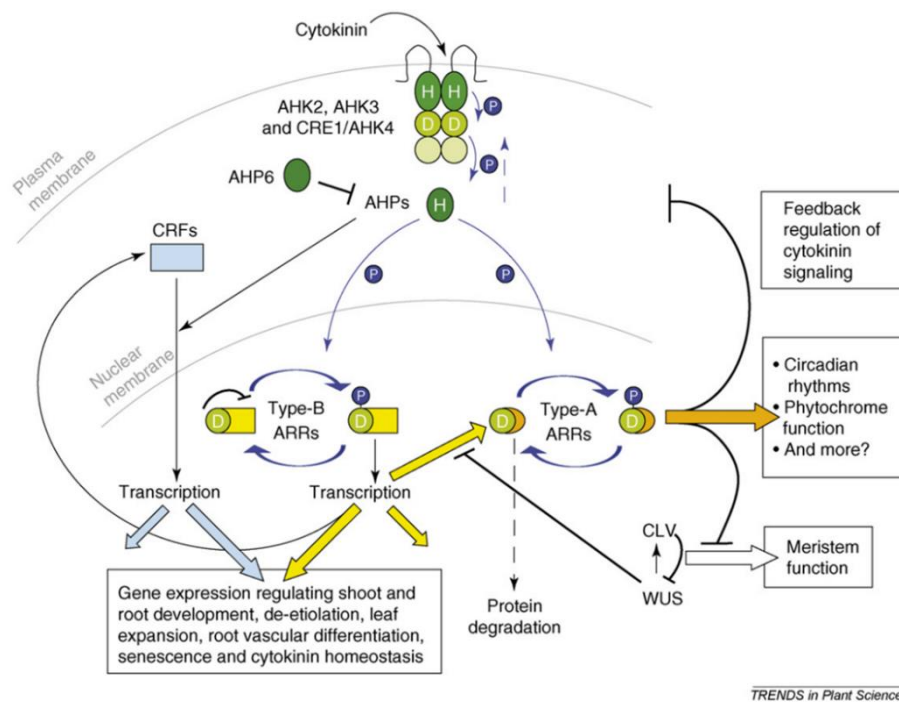

Fig. 5. Model of cytokinin signalling. AHK, Arabidopsis histidine kinase; AHPs, Arabidopsis histidine phosphotransfer proteins; ARRs, Arabidopsis response regulators; CRFs, cytokinin responsive factors. Reprinted with permission from To & Kieber (2008).

The CK histidine kinases participate differently in mediating the CK action. All three receptors affect fertility, sperm size, germination, and CK metabolism. The effect on root branching and leaf cell division is mainly mediated by AHK2 and AHK3. CRE1/AHK4 plays a major role in the extension of the primary root and in the root response to the application of exogenous CKs. CK-induced photomorphogenesis as well as Chl retention are mediated primarily by the AHK3 receptor. CK-induced senescence delaying is specifically mediated via AHK3 and ARR2 (Kim et al. 2006, Riefler et al. 2006, Janečková et al. 2018). Just as the involvement of CK receptors in influencing biological responses is different, so is the affinity of individual receptors for different types of CK. *In vitro*, AHK3 and CRE1/AHK4 have the highest overall affinity for isoprenoid types of CK, tZ and iP, and also for TDZ. All three receptors are capable to bind also cZ, although with lower affinity. Sensitivity of both AHK3 and CRE1/AHK4 to aromatic CKs is very low and it is presumed that these CKs act preferably via AHK2 (Spíchal et al. 2004, Romanov et al. 2006).

1.2.3 Cytokinins and senescence-induced changes

The increase in endogenous content of CKs and also their exogenous application on plants very effectively delays senescence (e.g. Gan & Amasino 1995, Vlčková et al. 2006, Zavaleta-Mancera et al. 2007, Zwack & Rashotte 2013, Janečková et al. 2018). Exogenously applied CKs can postpone senescence-induced changes in detached senescing leaves including decrease in Chl and carotenoid content, inhibition of photosynthesis including PSII photochemistry, degradation of proteins, pigment-protein complexes and whole chloroplasts, as well as membrane deterioration (e.g. Holub et al. 1998, Oh et al. 2005, Vlčková et al. 2006, Zavaleta-Mancera et al. 2007, Zubo et al. 2008, Liu et al. 2016, Janečková et al. 2019).

The anti-senescence activity of CKs has been found to be related to downregulation of SAGs (e.g. Weaver et al. 1998) and up-regulation of genes encoding components of photosynthetic light-harvesting complexes (Vylíčilová et al. 2016). One of the most widely used CK either in agricultural practise (for review see Koprna et al. 2016) or in biotechnological applications (for review see Plíhalová et al. 2016), is the aromatic CK BAP that is known to possess strong anti-senescence effects. The exogenous application of BAP activates expression of chloroplast genes such as *petD* and *petLG*

coding for cytochrome b6f subunits, *rbcL* coding for large subunit of Rubisco, *psbD* and *psbA* coding for PSII D proteins or *atpB* coding for ATP synthase subunit (Zubo et al. 2008). However, under certain conditions, BAP can have adverse effects on primary root development, lateral root branching or shoot formation *in vitro* (Woodward & Marshal 1988, Werbrouck et al. 1996, Iqbal et al. 2006, Bairu et al. 2007, 2009). In the case of long-term exposure of plant tissues to high concentrations of BAP or in combination with light, BAP can even accelerate senescence (Rulcová & Pospíšilová 2001, Carimi et al. 2004, Prokopová et al. 2010b, Vylíčilová et al. 2016).

1.2.4 Cytokinins and pathogens

CKs play an important role in plant interaction with symbiotic organisms, e.g. plants of *Medicago truncatula* Gaertn. with non-functional CK signalling show reduced nodulation and nitrogen fixation due to reduced symbiosis with *Sihorhizobium melilotti* bacteria (Gonzalez-Rizzo et al. 2006). In the case of *Agrobacterium tumefaciens*-infected plants an upregulation in genes coding for CK degradation enzymes was observed. Since *A. tumefaciens* produces CKs to support growth of crown-gall tumours, this upregulation suggests an activation of plants inner regulation of endogenous CK levels as a defence mechanism (Werner et al. 2006). However, an increased level of endogenous CKs can also serve as a defence mechanism. In mutant tobacco plants overexpressing gene coding for isopentenyltrasferase, CK biosynthesis enzyme, the related increase in CK content caused symptoms of hypersensitive reaction such as necrosis, inhibition of photosynthesis, increased level of stress hormones, membrane oxidative damage and stomatal closure. The hypersensitive reaction is a plant defence mechanism in which the controlled and induced death of the affected cells prevents the spread of the pathogen.

In addition to the endogenous CKs, exogenously applied CKs can also be used in defence against pathogens. For example, application of BAP and mT on leaves of *Lactuca sativa* L. prior to infection of *Bremia lactucae* leads to deceleration of pathogen sporulation without any adverse effect on photosynthetic apparatus (Prokopová et al. 2010b). Similarly, Arabidopsis plants sprayed with *trans*-zeatin show increased resistance to bacterial pathogen *Pseudomonas syringae* (DC3000) (Choi et al. 2010). However, in some cases CKs can cause increased plant susceptibility to pathogens. This process is usually initiated by pathogen that manipulates CK signalling *in planta* for its benefit. For

example, exogenous application of low concentrations of BAP (< 1 µmol.l^{-1}) led to increased growth of *Hyaloperonospora arabidopsidis* (isolate Noco2) on Arabidopsis plants (Argueso et al. 2012). The CK-increased susceptibility to pathogens can also be caused by lowered defence mechanisms. HopQ1, a *Pseudomonas syringae* DC3000 effector protein, subtly increases endogenous CK levels which in turn leads to reduced defence response via attenuated expression of pathogen recognition receptors (Hann et al. 2014).

1.3 Cytokinin derivatives

It is well known that not only CKs but also their artificially prepared derivatives can delay senescence-induced changes. Some of the derivatives are even more effective than CKs themselves, not only in the case of anti-senescence action but also in other CK activities.

1.3.1 Cytokinin bioassays

Biological activity of newly prepared compounds is usually tested and compared to that of CKs in three standard (tobacco callus bioassay, Amarathus bioassay, wheat leaf senescence bioassay) and two reporter CK bioassays (bacterial receptor and ARR::GUS reporter assay).

1.3.1.1 Tobacco callus bioassay

The callus bioassay is based on the ability of CKs to stimulate cell division and thus the growth of tobacco callus. According to Holub et al. (1998) the callus of *Nicotiana tabacum* L. is grown at 25 °C on a modified MS medium containing, *inter alia*, the CK or derivative to be tested. Subculturing is performed every three weeks, and two weeks before the bioassay itself, the callus is transferred to a CK-free medium. The biological activity of the tested compound is derived from the increase in fresh weight (FW) of the callus, four weeks after cultivation (Holub et al. 1998).

1.3.1.2 Amaranthus bioassay

The Amaranthus bioassay is based on the induction of betacyanin synthesis by CK in the cotyledons of *Amaranthus caudatus* L. cv. Atropurpurea in the dark (Biddington & Thomas 1973). The seeds are cultivated in the dark for 72 hours. Young plants consisting of hypocotyl and cotyledons are then transferred to an incubation medium containing

the compound to be tested, and subsequently incubated again in the dark (for 48 h). Betacyanin is extracted from plants by freezing them in acetic acid solution, and betacyanin concentration is determined by comparing the absorbance at 537 nm and 620 nm ($\Delta A = A537$ nm-A620 nm) (summarized in Holub et al. 1998, Doležal et al. 2007).

1.3.1.3 Wheat senescence bioassay

The senescence bioassay is based on the ability of CKs to delay senescence-induced decrease in Chl content. The modified bioassay according to Holub et al. 1998 is performed on the leaves of seven days old wheat plants (*Triticum aestivum* L.). At this stage of development the first leaves are already fully developed and the second leaves begin to grow. The tips of the first leaves are separated (the segments are about 35 mm long) and the basal ends of the segments are immersed in a solution of the tested compound. The segments are incubated in the dark for 96 h at 25 °C, afterwards Chl is extracted from them using 80% ethanol or acetone and its concentration is estimated from the absorbance of the extract at 665 nm (Holub et al. 1998) or according to Lichtenthaler (1987).

1.3.1.4 Bacterial receptor bioassay

An *Escherichia coli* strain KMI001 containing plasmids encoding the histidine kinases AHK3 and CRE1/AHK4 or ZmHK1 and ZmHK3 (CK receptors from *Zea mays* L.) is used to perform this assay (Suzuki et al. 2001, Yamada et al. 2001, Mik et al. 2011b, Podlešáková et al. 2012). Thus, this bacterial strain contains functional CK receptors and the bioassay allows rapid determination of CK activity. The signal from the receptors is associated with a signaling pathway in *E. coli* that leads to activation of the cps::lacZ fusion reporter gene (Spíchal et al. 2004).

A common intracellular signal transduction in prokaryotes is via His→Asp phosphorylation (e.g. Suzuki et al. 2001, Yamada et al. 2001). A homologous signalling system also applies in Arabidopsis CK signalling pathway (for review see Lomin et al. 2012) which is used in the bacterial receptor bioassay. One of the *E. coli* signalling pathway based on His→Asp transduction is the pathway RcsC→YojN→RcsB which is part of the regulatory mechanism of extracellular polysaccharide synthesis activated via cps operon. RcsC is a hybrid receptor with similar structure as the CRE1/AHK4, YojN is

a histidine phosphotransfer factor, and RcsB is a response regulator. Activation of this signalling pathway can be easily monitored by measuring β-galactosidase activity in *E. coli* cells containing cps::lacZ (Suzuki et al. 2001). The lacZ gene encodes β-galactosidase, an enzyme that cleaves lactose. The culture medium contains X-Gal (5-bromo-4-chloro-3-indoyl-β-D-galactopyranoside) colorless lactose analogue, that is cleaved by β-galactosidase to release a blue product (for review see Juers et al. 2012). This reporter system was used also by Suzuki et al. (2001) who constructed an *E. coli* strain containing cps::lacZ and then introduced CRE1/AHK4 receptor gene into the bacterium. The *E. coli* cells were then cultured on medium containing X-Gal. If the medium contains CK (or compound that activates CRE1/AHK4) the colonies are blue due to activation CRE1/AHK4→YojN → RcsB → cps :: lacZ signalling pathway (Suzuki et al. 2001).

Currently, this bioassay is used for estimation of the relative activation of CK receptors that is determined by measuring OD_{600} and β-galactosidase activity using the fluorescent substrate 4-methylumbelliferyl-β-D-galactoside. Fluorescence is measured at emission and excitation wavelengths of 365 and 460 nm, respectively (Spíchal et al. 2004, Doležal et al. 2007, Szüčová et al. 2009, Mik et al. 2011b).

1.3.1.5 ARR::GUS reporter bioassay

This bioassay is based on CK-induced increase in ARR content. It is very fast, sensitive, dose-dependent, and highly specific for both adenine and phenylurea CKs (Romanov et al. 2002). In this bioassay, tested compound is applied on transgenic Arabidopsis plants containing the ARR::GUS gene construct (ARR promoter and reporter gene for β-glucuronidase). Then proteins are isolated from the plants and quantified (by various methods). β-glucuronidase (GUS) activity is determined using the fluorogenic substrate 4-methylumbelliferyl glucuronide followed by measurement of fluorescence intensity at 365 nm and 450 nm. The specific activity of GUS is then expressed in nmol of 4-methylumbelliferone.mg^{-1} protein.h^{-1}. The extent of ARR promoter activation by the tested compound is determined based on the results of this bioassay (Romanov et al. 2002, Nisler et al. 2010).

1.3.2 Anti-senescence activity of CK derivatives

Since the purine moiety of isoprenoid and aromatic CKs can be substituted at several positions such as N1, C2, N3, N6, C8 and N9 (Fig. 6), it is possible to synthetize wide range of compounds with various biological effects (for detailed review see Plíhalová et al. 2016). Additionally, derivatives of artificial phenylurea CKs are also prepared. However, it is beyond scope of this thesis to deal with biological properties of such a great amount of compounds, so only few selected derivatives will be described in more detail.
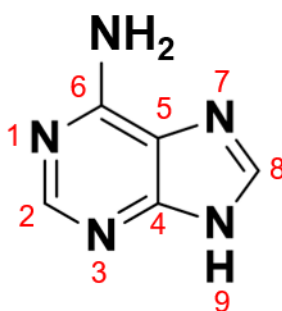
Fig. 6. Adenine structure with numbered positions.

The biological activity of iP derivatives with substitution on the N9 atom of purine moiety (N9-iP) was studied by Mik et al. (2011). While majority of iP derivatives was highly active in the tobacco callus and Amaranthus bioassay, in wheat senescence bioassay their activity was only low. Anti-senescence activity of none of the derivatives exceeded iP which itself is only low. The N9-iP derivatives were practically inactive in this bioassay and majority of them did not activate CRE1/AHK4 receptor in the bacterial receptor bioassay.

In contrast to N9-iP derivatives, derivatives of kinetin with short halogenoalkyl chains substituted on the N9 atom of purine moiety (N9-kin) possess anti-senescence activity comparable or higher than that of kinetin. The type of halogen atom and the length of the alkyl chain have been shown to determine the maintenance of Chl content during induced senescence. N9-kin with a shorter alkyl chain were more active and at the same time N9-kin containing chlorine in the alkyl chain were more active than derivatives containing bromine. The most active derivative in the wheat senescence bioassay was furfurylamino-9-(2-chloroethyl)purine, a chlorine-containing short alkyl

chain kinetin derivative. This compound also significantly reduced lipid peroxidation in dark-incubated wheat leaf segments. However, in comparison to kinetin, this derivative does not have any effect on expression of analysed Arabidopsis genes related to CK metabolism and signalling (Mik et al. 2011a).

It has been reported that hydroxylation of the benzyl ring in the *meta*-position increased activity of BAP in the tobacco callus and wheat senescence bioassay. On the contrary, activity in the Amaranthus bioassay was lower. Hydroxylation in the *ortho*-position leads to opposite effects of the compounds in the bioassays. Although ribosylation at the N9 position was found to lower the compound activity in tobacco callus bioassay, it increased the anti-senescence activity. Glycosylation on the N9 position lowered activity in all bioassays (Holub et al. 1998).

Tarkowská et al. (2003) prepared *ortho*- and *meta*-methoxy-derivatives of mT, 6-(2-methoxybenzylamino)purine (MeoT) and 6-(3-methoxybenzylamino)purine (MemT), and also their ribosides, MeoTR and MemTR. All newly prepared derivatives had by 80-100% higher anti-senescent activity than BAP, but lower activity in the tobacco callus and Amaranthus bioassay (except for MeoTR in tobacco callus bioassay) (Tarkowská et al. 2003). Similar results were obtained by Doležal et al. (2007). They observed strong differences in activities of prepared analogues of BAP riboside with various substituents (halogen-, hydroxy- and methoxy- groups), at the benzyl ring in the CK bioassays. While activity of almost 50% of the prepared compounds exceeded that of BAP in the wheat senescence bioassay, only few derivatives were able to interact with AHK receptors. At the same time, only one derivative was more effective than BAP in the tobacco callus bioassay. In addition, some of the prepared compounds displayed strong cytotoxic activity (Doležal et al. 2007).

Derivatives of tetrahydropyran-2-yl and tetrahydrofuran-2-yl with various substituents at the N9 position of adenine moiety and at the benzyl ring were prepared by Szüčová et al. (2009). Interestingly, the substitutions did not improve the compounds activity in CK bioassays. Only 6-(3-hydroxybenzylamino)-9-tetrahydropyran-2-ylpurine and 6-(3-hydroxybenzylamino)-9-tetrahydrofuran-2-ylpurine possess higher anti-senescent activity than BAP (Szüčová et al. 2009).

A series of 2-chloro-6-(halogenobenzylamino)purine ribosides was prepared by Vylíčilová et al. (2016). Majority of these derivatives showed high activity in all three CK bioassays, especially in the wheat senescence bioassay. Similarly to the other mentioned compounds, derivatives prepared by Vylíčilová did not activate CK signalling via AHK receptors. However, some of them were able to activate the ZmHK1 receptor. The gene expression analysis performed in senescent Arabidopsis leaves treated by selected compounds, 2-chloro-6-(3-fluorobenzylamino)purine riboside and 2-chloro-6-(3-chlorobenzylamino)purine riboside, revealed that these compounds caused upregulation of genes related to PSI, PSII, Calvin cycle and CK signalling and metabolism together with downregulation of genes encoding Chl degradation. Application of these derivatives was accompanied also by an increase in the relative abundance of LHCII (Vylíčilová et al. 2016).

It is evident that structure-activity relationship in various CK derivatives is very complex issue, however it is possible to conclude that ribose conjugation on the N9 position of adenine moiety of BAP leads to increased activity in the wheat senescence bioassay (for recent review see Vylíčilová et al. 2020).

2 Aims of research

Although a large number of different derivatives with various effects in plant organism are synthesized, there is only limited amount of information about their biological activity or mechanism of action. Newly prepared compounds are usually tested using standard and receptor CK bioassays, which provide only basic information about structure-action relationship of these substances. A more detailed approach is needed to reveal mechanisms of their action and thoroughly evaluate their potential for practical use.

In terms of the anti-senescent activity, only the ability of compounds to retain Chl content in senescing leaves is usually examined. Therefore, very little is known about their effect on photosynthetic apparatus and function and other processes affected by senescence. The main aim of our research was to evaluate the effect of novel CK derivatives, referred to as CK arabinosides, on structure and function of photosynthetic apparatus in dark-senescing leaves to propose their possible mechanism of action.

3 Experimental approach

3.1 Solutions of CK and CK arabinosides

Group of 6-benzylamino-9-β-D-arabinofuranosylpurines (BAPA) was synthesized by M. Bryksová at the Department of Chemical Biology and Genetics of the Centre of the region Haná for Biotechnological and Agricultural Research. Two compounds, 3-hydroxy- (3OHBAPA) and 3-methoxy- (3MeOBAPA) (see Fig. 7) were subsequently selected for more detailed analysis of their biological activity *in planta* and their effect was compared to that of BAP. For detailed synthesis, physicochemical properties and chemical purity of 3OHBAPA and 3MeOBAPA see supplementary material of Bryksová et al. (2020) in Appendix, section Synthesis of prepared derivatives. Solutions of BAP and cytokinin arabinosides were prepared by dissolving in dimethylsulfoxide (DMSO; Sigma-Aldrich, USA) and used in concentrations 100 nmol.l^{-1}, 1 μmol.l^{-1} and 10 μmol.l^{-1}. The concentration of DMSO in BAP and CK arabinosides´ solutions did not exceed 0.1% (v/v) and 0.1% solution of DMSO in deionized water was used as mock control.
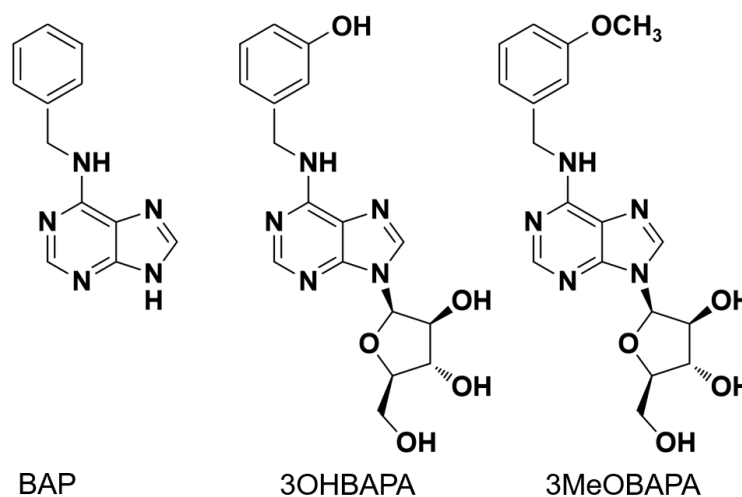

Fig. 7 Structure of 6-benzylaminopurine (BAP), 6-(3-hydroxybenzylamino)-9-β-D-arabinofuranosylpurine (3OHBAPA) and 6-(3-methoxybenzylamino)-9-β-D-arabinofuranosylpurine (3MeOBAPA).

3.2 CK bioassays

The prepared compounds were tested in three classical CK bioassays: the tobacco callus bioassay, Amaranthus bioassay, and detached wheat leaf senescence bioassay. In all cases biological activity of CK arabinosides was compared to that of BAP. The bioassays were performed as described by Holub et al. (1998) with minor modifications in the tobacco callus bioassay (using 6-well plates with each well containing 3 ml of MS medium and 0.1 g of callus tissue). The ability of CK arabinosides to activate CRE1/AHK4 or AHK3 signalling cascade *in vitro* was tested in the bacterial CK bioassay. An *E. coli* strain KMI001 (*ΔrcsC, cps::lacZ*), harboring either the plasmid pIN-III-AHK4 or pSTV28-AHK3, which expressess the Arabidopsis CRE1/AHK4 or AHK3 was used in the experiments. Activity of β-galactosidase was measured using 4-methylumbelliferyl-β-D-galactopyranoside as a substrate after overnight growth in the presence of CK. In addition, live-cell cytokinin-binding assay with radiolabeled tZ as a competitor was performed as previously described by Zatloukal et al. (2008). Homogenous bacterial suspensions with OD_{600} values of 0.8 and 1.2 were found to be optimal for CRE1/AHK4 and AHK3 cultures, respectively. The competition reaction was allowed to proceed with 2 nmol.l^{-1} [2-^{3}H]*t*Z and various concentrations of the tested compounds for 30 min at 4 °C. When binding equilibrium was reached, the suspension was centrifuged and the bacterial pellet was resuspended in the scintillation cocktail (Beckman Coulter, USA). *Performed by J. Balonová*

3.3 Plant material and growth conditions

Plants of spring wheat (*Triticum aestivum* L. cv. Aranka) were grown on an artificial medium composed of perlite and Hoagland´s solution (for composition see Table 1) in a growth chamber at 25 °C under a 16-h light (120 μmol photons.m^{-2}.s^{-1})/8-h dark cycle for 7 days. Then segments were cut off from the primary leaves, 4 cm from the leaf tip. The basal end of the leaf segment was placed into a well of 96-well plate with 200 μl of solutions of BAP, 3OHBAPA or 3MeOBAPA (each solution on one plate). Plates with leaf segments were individually packed in airtight plastic bags to avoid being affected by the volatile compounds produced by the detached segments of the individual

variants. The detached segments were subsequently kept in darkness at 24 °C for 6 days. Freshly detached wheat leaves were used as control (0. day after detachment; dad).

Table 1 Nutritional composition of Hoagland´s solution

chemical component	concentration
macronutrients	**g.l^{-1}**
$Ca(NO_3)_2$	9.4
$MgSO_4.7H_2O$	5.2
KNO_3	6.6
$NH_4H_2PO_4$	1.2
micronutrients	**mg.l^{-1}**
H_3BO_3	2.80
$MnSO_4.H_2O$	3.40
$CuSO_4.5H_2O$	0.10
$ZnSO_4.7H_2O$	0.22
$(NH_4)_6Mo_7O_{24}.4H_2O$	0.10
	mg.l^{-1}
Na2EDTA	37
$FeSO_4.7H_2O$	27
	µl.l^{-1}
H_2SO_4	25

For RNA or protein isolation, plants of *Arabidopsis thaliana* L. (Col-0) were grown in a soil in a growth chamber under an 8-h light (120 µmol photons.m^{-2}.s^{-1})/16-h dark cycle and at 22 °C/20 °C for 6 weeks. Then the rosette leaves of similar size and Chl content were detached from the plants and incubated in MS medium supplemented with 0.1% DMSO or 10 µmol.l^{-1} 3MeOBAPA for 30 min, 6 h or 48 h in darkness. Subsequently, leaves were frozen in liquid nitrogen and used for RNA or protein isolation. In case of RNA isolation from seedlings, Arabidopsis plants were grown on ½ MS agar plates in growth chamber under an 16-h light (120 µmol photons.m^{-2}.s^{-1})/8-h dark cycle for 5 days. Seedlings were then transferred into liquid ½ MS medium for another 3 days under constant shaking (60 rpm) and treated with 0.1% DMSO, 10 µmol.l^{-1} 3MeOBAPA or 1 µmol.l^{-1} flg22 (Anaspec, USA) or both for 2 h. After that, seedlings were frozen in liquid nitrogen and used for RNA isolation.

For measurements using detached leaves, plants of *Arabidopsis thaliana* L. (Col-0) were grown in a soil (Potgrond H, Klasmann-Deilmann, Germany) in a growth chamber under an 8-h light (120 µmol photons.m^{-2}.s^{-1})/16-h dark cycle and at 22 °C/20 °C for

6 weeks. Then the 7th and 8th rosette leaves were detached from the plants and incubated in a six-well plate with 5 ml of the solutions of BAP, 3OHBAPA or 3MeOBAPA. Similarly to wheat, the plates were then closed with a lid to avoid contact with volatile compounds from different variants. The detached leaves were kept in darkness at 24 °C for 6 h or 6 days. Freshly detached Arabidopsis leaves were used as control.

3.4 RNA-seq analysis

Plant cDNA sequencing libraries were prepared using 3.5 µg of total RNA per sample with the Illumina® TruSeq® Stranded mRNA Sample Preparation Kit (Illumina, San Diego, USA) in accordance with the standard procedure. Two independent replicate samples per condition were used to generate cDNA libraries. Prepared libraries were validated using a DNA 1000 chip with a 2100 Bioanalyzer (Agilent Technologies, USA) instrument, and all concentrations were assessed using a Kapa Library Quantification Kit (Kapa Biosystems, Roche, Switzerland). Prepared libraries were pooled to a final concentration of 12 pmol.l^{-1} for cluster generation and sequencing. The clusters were generated using an Illumina® TruSeq® SR Cluster Kit v3 cBot HS and sequenced on a HiSeq SR Flow Cell v3 (50 bp reads) with a HiSeq 2500 Sequencing System (Illumina, USA). Two independent libraries were prepared for each condition at each time point from two biological replicates. The quality control of reads generated by sequencing was performed with FASTQC v.0.11.5 and reads were mapped to the reference genome of *Arabidopsis thaliana* v.25 obtained from Ensembl using a TopHat v.2.0.12 splice-read mapper with default parameters. The reads mapped to the transcripts annotated in the reference genome were quantified using HTSeq v.0.6.0 with respect to the stranded library. The tests for differential gene expression were performed using the DESeq2 package. Gene ontology (GO) analysis was performed using the Blas2GO v.3.0 program. HemI software was used to generate heatmaps.

Performed by S. Dabravolski and O. Plíhal

3.5 Quantitative PCR analysis

Expression profiling of genes coding for MPKs and PAMP-triggered immunity (PTI)-marker genes was done as described by Zatloukal et al. (2008). Briefly, 5 μg of total RNA isolated using RNAqueousH kit and treated twice with TURBO DNase-freeTM kit (Life Technologies, USA) was used for first strand cDNA synthesis by RevertAidTM H Minus M-MuLV RT and oligo-dT (Fermentas, Lithuania). Diluted cDNA samples were used as templates in real-time PCR reactions containing gb SG PCR Master Mix (Generi Biotech, Czech Republic) and 300 nmol.l^{-1} of each primers. RNA samples were isolated from four biological replicates and transcribed in four independent reactions and each cDNA sample was run in at least two technical replications on StepOnePlusTM Real-Time PCR System in a default program (Life Technologies, USA). Ct values were normalized with respect to Actin 2 and Elongation factor 1 genes. Expression values were determined and statistically evaluated with DataAssist v3.0 Software (Life Technologies, USA).

Performed by F. Zavadil Kokáš, M. Hudeček and V. Hloušková

3.6 Immunoblotting analyses of mitogen-activated protein kinases (MAPKs)

Detached Arabidopsis leaves were homogenized in liquid nitrogen to a fine powder. Proteins were extracted by adding ice-cold 50 mM HEPES (pH 7.5) containing 75 mmol.l^{-1} NaCl, 1 mmol.l^{-1} EGTA, 1 mmol.l^{-1} MgCl$_2$, 10% (v/v) glycerol, 1 mmol.l^{-1} DTT, and Complete® EDTA-free protease inhibitor cocktail (Roche, Switzerland). After 15 min incubation on ice, the extracts were centrifuged at 13000 g at 4 °C for 15 min and the protein amount was quantitated in supernatants. Extracts were proportionally mixed to give a protein concentration of 1.5 mg protein/ml with 4-fold concentrated Laemmli buffer (final concentration 62.5 mmol.l^{-1} Tris-HCl, pH 6.8, 2% (w/v) SDS, 10% (v/v) glycerol, 300 mmol.l^{-1} 2-mercaptoethanol), heat-denatured at 95°C for 5 min, and centrifuged to remove undissolved components. Fifteen μg of each protein was loaded on 1% PAGE gels. After electrophoresis, the proteins were transferred to nitrocellulose membranes using the TransBlot™ Turbo (BioRad, USA) semidry transfer system. To validate the protein transfer, membranes were stained with Ponceau S. Afterwards, they were blocked overnight in 15% (v/v) commercial blocking

solution (Western blocking reagent; Roche, Switzerland) diluted in Tris-HCl buffered saline with 0.1% (v/v) Tween-20 (TBS-T), then incubated overnight with anti-MPK3 (1:3000), anti-MPK4 (1:1000), and anti-MPK6 (1:10000) antibodies (all from Sigma-Aldrich, USA), and anti-phospho p44/42 MAPK antibody (Erk1/2,Thr202/Tyr204) (Cell Signalling Technology, USA), all prepared in TBS-T with 4% (v/v) Western blocking reagent (Roche, Switzerland). After repeated washing in TBS-T, membranes were incubated with a HRP-conjugated secondary antibody (F(ab')2-goat anti-rabbit IgG (H+L) Secondary Antibody, HRP; Thermo Fisher Scientific, USA) diluted to 1:5000 in 4% (v/v) Western blocking reagent (Roche, Switzerland). The signal was developed after washing with TBS-T using Clarity™ ECL Western Blotting Substrate (BioRad, USA) and recorded with the ChemiDoc™ documentation system (BioRad, USA). Band densities were quantified using ImageLab (BioRad, USA). The densities of phosphorylated MPK3 and MPK6 were normalized to the abundance of the corresponding MPKs. All immunoblot analyses were performed using at least 3 biological replicates.

Performed by T. Takáč

3.7 Ethylene production

The detached leaves of wheat and Arabidopsis were put into 10 µmol.l^{-1} solutions of BAP, 3OHBAPA, 3MeOBAPA, or into 0.1% DMSO and kept sealed in 8-ml vials in darkness for 48 h, 72 h or 6 days. Subsequently, 1.5 ml of air was collected from each vial and reduced to 1 ml before injection to gas-chromatograph Agilent GC 6890 (Agilent Technologies, USA) equipped with a flame-ionization detector and 50-m capillary column (HP-AL/S stationary phase, 15 µm, i.d. = 0.535). The injection temperature was set to 200 °C, oven temperature to 40 °C, and the detector temperature to 220 °C. The measurements were performed in triplicate from three different test tubes of each variant.

Performed by M. Mikulík and Z. Kučerová

3.8 Quantification of jasmonic acid forms

Detached 7th or 8th leaves of Arabidopsis plants were put into 0.1% DMSO or 10 µmol.l^{-1} 3MeOBAPA solutions by a petiole for 2, 4 or 8 days. Subsequently, the samples were

frozen in liquid nitrogen and stored at −80 °C before measurement. Endogenous levels of jasmonates (jasmonic acid, JA; jasmonoyl-L-isoleucine, JA-Ile; and *cis*-12-oxo-phytodienoic acid, *cis*-OPDA) were determined in 30-40 mg of plant material according to the method described by Floková et al. (2014). Briefly, the phytohormones were extracted using 10% methanol with a cocktail of stable isotope-labelled standards added as follows: 10 pmol of [^{2}H$_6$]JA, [^{2}H$_2$]JA-Ile, and 20 pmol of [^{2}H$_5$]OPDA (all from Olchemim, Czech Republic) per sample. The extracts were purified using Oasis HLB columns (30 mg/1 ml, Waters, USA) and then evaporated to dryness under a stream of nitrogen. Jasmonate levels were quantified by ultra-high performance liquid chromatography-electrospray tandem mass spectrometry (an Acquity UPLC I-Class System coupled to a Xevo TQ-S MS, all from Waters, USA) using stable isotope-labelled internal standards as a reference. All experiments were repeated in five biological replicates.

Performed by O. Novák and Z. Kučerová

3.9 ROS measurements

Arabidopsis cells of PSB-D suspension culture in conical flasks were cultivated in the dark at 25 °C, under constant shaking (130 rpm) and sub-cultured every 7 days (1:5) in a cell suspension medium (MS medium with 3% sucrose, 1 mg.ml^{-1} NAA, 50 µg.ml^{-1} kinetin). The generation of ROS in PSB-D culture was determined by DCFH-DA (2′,7′-dichlorofluorescin diacetate) (Merck, Germany). Cells were treated with either 10 µmol.l^{-1} or 50 µmol.l^{-1} 3MeOBAPA, or 0.1% DMSO (negative control) for up to 16 h. Briefly, cells were loaded with 10 µmol.l^{-1} DCFH-DA and the fluorescence was detected after 10 min using a microplate reader (Tecan Infinite M200, Switzerland) operating at excitation and emission wavelengths of 485 and 525 nm, respectively.

Performed by J. Grúz

3.10 Field trial experiments

An effect of 3MeOBAPA and 3OHBAPA was tested in field trials on winter wheat (*Triticum aestivum* L. cv. Turandot) and spring barley (*Hordeum vulgare* L. cv. Francin) performed near Olomouc, Czech Republic (GPS: 49.5748542N, 17.2851261E; altitude

218 m) in a growth season 2017/2018. The 5 μmol.l^{-1} solution of 3OHBAPA or 3MeOBAPA was applied as a foliar spray on wheat at a growth stage of tillering and on barley at stage of beginning of stem elongation or start of flag leaf extending in amount of 300 ml per 10 m^2. A level of infection was evaluated at a growth stage of beginning of heading in the case of wheat and leaf rusts and barley and powdery mildew or at growth stage of early milk ripeness in the case of barley and foot rot diseases. The evaluation of each variant was carried out on 5 plots (n = 5), 20 plants were evaluated from each plot. The level of infection was evaluated according the following scales:

1) for wheat and leaf rusts (namely *Puccinia striiformis* syn. *Puccinia glumarum*, *Puccinia recondita* f. sp. *tritici*, *Puccinia graminis*): 1 – without infection; 2 – a few clusters of chlorosis; 3 – clusters to 1% of leaf area; 4 – clusters from 1 to 3% of leaf area; 5 - clusters from 3 to 5% of leaf area, beginning of strips; 6 – clusters and strips from 5 to 15% of leaf area;

2) for barley and powdery mildew (*Blumeria graminis* syn. *Erysiphe graminis*): 1 – without symptoms; 2 – mycelium at max. 1% of leaf area; 3 – mycelium at 1 – 5% of leaf area; 4 – mycelium at 5 – 10% of leaf area; 5 - mycelium at 10 – 30% of leaf area;

3) for barley and foot rot diseases (*Gaeumannomyces graminis* syn. *Ophiobolus graminis*, *Ramulispora herpotrichoides* syn. *Pseudocercosporella herpotrichoides*, teleomorpha *Tapesia yallundae*, *Fusarium* spp., *Rhizoctonia* spp.): 1 – without symptoms; 3 – brown spots to 5 % of stem perimeter; 5 – brown spots from 5 to 25% of stem perimeter.

Performed by R. Koprna

3.11 *Botrytis cinerea* inoculation

Detached Arabidopsis leaves were treated by DMSO, 10 μmol.l^{-1} BAP or 3MeOBAPA in two different ways: leaves were either placed into 5 ml of the solution in a well of 6-well plate or were put into the solution in 2 ml-microtube by a petiole. Then the leaves were incubated in the dark, in the case of leaves floating on the surface of the solution for 24 h and for 48 h in the case of leaves treated by a petiole. Subsequently, the leaves were inoculated by *Botrytis cinerea* strain B05.10 by placing of 5 μl of conidia suspension in PDB medium into the middle of the leaf (5 μl of PDB medium without conidia was used as a control). After inoculation, the leaves were put back into DMSO, BAP or

3MeOBAPA solutions, packed in airtight plastic bags to avoid drying out and incubated in a growth chamber under a 8-h light (30 μmol photons.m^{-2}.s^{-1})/16-h dark cycle and at 22/20 °C. The development of *B. cinerea* was evaluated 4 days after inoculation (dai) in the case of leaves floating on the surface of the solutions and 7 dai in the case of leaves put in the solution by a petiole.

Performed by Z. Kučerová and M. Sedlářová

3.12 High light treatment

After six days in the dark, detached wheat leaf segments and Arabidopsis leaves incubated in 0.1% DMSO or 10 μmol.l^{-1} solutions of BAP, 3MeOBAPA and 3OHBAPA were exposed to high-light (HL; white light, 500 μmol photons·m^{-2}·s^{-1}) for up to 8 h to induce photo-oxidative stress. In the case of wheat, edges of the segments were cut off and the rectangular middle part (2 cm long) of the leaf segment was placed into 6-well plates with solutions prior to the HL treatment.

Performed by Z. Kučerová

3.13 Determination of chlorophyll, carotenoid and xanthophyll content

Following estimation of their area, leaf samples were frozen in liquid nitrogen, stored at −80 °C and subsequently homogenized using 80% acetone and a small amount of MgCO$_3$. Homogenate was centrifuged at 3600 g for 15 min at 4 °C. The supernatant was used for spectrophotometric (Unicam UV 500, Thermo Spectronics, UK) estimation of Chl and carotenoid contents according to Lichtenthaler (1987) and for quantification of xanthophylls (violaxantin, V; anteraxantin, A; zeaxantin, Z; neoxantin; lutein) by a reversed-phase high-performance liquid chromatography (HPLC) using Alliance e 2695 HPLC System (Waters, USA) equipped with 2998 Photodiode Array detectors. The separation was carried out using a gradient system (1.5 mL·min^{-1} at 25 °C) on a LiChrospher® 100 RP-18 column (5 μm particle size) (L×I.D., 2 mm×4.6 mm) (Merck, Germany). Quantification was performed by absorbance at the following wavelength: 437 nm (neoxanthin), 441 nm (violaxanthin), 446 nm (antheraxanthin), 447 nm (lutein), and 454 nm (zeaxanthin) using standards purchased from DHI Lab Products (Hørsholm,

Denmark). The de-epoxidation state of xanthophylls (DEPS) was calculated as DEPS = (A+Z)/(V+A+Z) (Gilmore & Björkman 1994).

Performed by Z. Kučerová and P. Pospíšil

3.14 Confocal laser scanning microscopy

Confocal microscopy was performed on detached Arabidopsis leaves treated by 3MeOBAPA (10 µmol.l^{-1}) for 30 min in which O_2^- were visualized using fluorescent probe dihydroethidium (DHE) and on senescing leaves of wheat and Arabidopsis kept in the dark for 6 days and on leaves subsequently exposed to HL for 4 h. Using fluorescent probe SPY-LHP (Dojindo Molecular Technologies, USA) LOOHs were localized in leaves of wheat and Arabidopsis. Leaves were cut into pieces (approximately 2 mm × 2 mm) and incubated in 50 µmol.l^{-1} SPY-LHP in HEPES buffer (10 mmol.l^{-1}, pH 7.5) in the dark at room temperature for 30 min. Afterward, the samples were visualized by a confocal microscope (FV1000, Olympus Czech Group, Czech Republic). The excitation of fluorochrome was performed using a 488-nm line of argon laser. The signal was detected through a 505–550-nm emission filter. The morphology of tissues was visualized by a 405-nm diode laser excitation in transmitted light detection module with differential interference contrast (DIC) filters, while chloroplasts were visualised by a 543-nm helium–neon laser excitation with emission recorded with a 655–755-nm bandpass filter. The proper intensity of the laser was set according to unstained samples at the beginning of each experiment (Sedlářová et al. 2011). During the image postprocessing in FV10-ASW 4.0 Viewer software (Olympus Czech Group, Czech Republic), the contrast of the SPY-LHP channel was increased to 3 in the case of wheat and to 4 in the case of Arabidopsis. Five replicates were performed and representative images were presented. The visualisation of O_2^- using DHE fluorescent probe was performed as described for SPY-LHP probe with only minor changes. The DHE probe was diluted in 0.1% DMSO or 10 µmol.l^{-1} 3MeOBAPA solution (4 µl of DHE in 396 µl DMSO or 3MeOBAPA) and MES buffer (10 mmol.l^{-1}, pH 5.5) was applied at slide glass under the sample.

Performed by M. Rác and Z. Kučerová

3.15 Chlorophyll fluorescence parameters (PSII functioning)

Chl fluorescence induction transient (OJIP curve) and Chl fluorescence quenching analysis were measured at room temperature from the adaxial side of the leaves using a Plant Efficiency Analyser (Hansatech Instruments, UK) and FluorCam imaging system (PSI, Czech Republic), respectively. The control leaves and HL-treated leaves were dark-adapted for 30 min prior to the measurement. In the case of senescent leaves, dark adaptation was not necessary due to their incubation in the dark.

The OJIP transient was measured in the middle of leaf segments with excitation light (red light, 4300 µmol photons·m^{-2}·s^{-1}) lasting 1 s. The initial slope of the O–J Chl fluorescence rise $(dV/dt)_0$ and the relative variable fluorescence at the J step (V_J) were evaluated. The $(dV/dt)_0$ parameter, defined as the maximal rate of accumulation of closed (i.e., reduced) RCII, was calculated as $(dV/dt)_0 = 4 (F_{300\mu s} - F_{50\mu s})/F_V$, where $F_{300\mu s}$ and $F_{50\mu s}$ are fluorescence intensities at the indicated times of the transient, and F_V is variable fluorescence ($F_V = F_P - F_0$, where F_P is fluorescence intensity at P step and F_0 is minimal fluorescence) (Strasser et al. 2000). The V_J parameter reflects a fraction of reduced RCII and was calculated as $V_J = (F_J - F_0)/F_V$, where F_J is fluorescence intensity at 2 ms (J-step).

A FluorCam imaging system was used for measurement of maximum quantum yield of PSII photochemistry ($F_V/F_M = (F_M - F_0)/F_M$) in dark-adapted state and for measurement of quantum yields Φ_P, Φ_{NPQ} and $\Phi_{f,D}$ in light-adapted state reflecting the proportion of three different types of energy usage by PSII (their sum equals 1; (Lazár 2015)), . The effective quantum yield of PSII photochemistry for the light-adapted state was calculated as $\Phi_P = (F_M' - F_t)/F_M'$. The quantum yield of regulatory light-induced non-photochemical quenching was calculated as $\Phi_{NPQ} = (F_t/F_M') - (F_t/F_M)$. The quantum yield of constitutive non-regulatory dissipation processes was calculated as $\Phi_{f,D} = F_t/F_M$. The minimal fluorescence of the dark-adapted leaf sample (F_0) was determined by applying several µ-seconds-long measuring flashes (red light, 0.1 µmol photons.m^{-2}.s^{-1}) at the beginning of the procedure. The maximal fluorescence of the dark-adapted sample (F_M) was measured using the 1.6-s saturating pulse (white light, 850 µmol photons.m^{-2}.s^{-1}). After 2 min of dark relaxation the sample was exposed to

actinic light (red light, 200 µmol photons.m^{-2}.s^{-1}) and series of saturating pulses (the 1st pulse at the 3rd second of actinic light, 6 pulses in a 23-s interval, 3 pulses in a 47-s interval and the last 2 pulses in a 70-s interval) to measure the maximal fluorescence in the light-adapted sample (F_M'). The actual fluorescence signal at the time t of actinic illumination (F_t) was measured immediately prior to the application of saturating pulse.

Performed by Z. Kučerová

3.16 Ultra-weak photon emission

Two-dimensional imaging of ultra-weak photon emission (UPE) was measured from the adaxial side of the leaves kept in the dark for 6 days before and after their treatment with 5 mmol l^{-1} H$_2$O$_2$. After the first UPE measurement, the leaf segments were let to dry off for 30 min under common laboratory conditions and then put into the H$_2$O$_2$ solution. After 3 h of H$_2$O$_2$ incubation, the second UPE measurement was performed while the leaves remained in the H$_2$O$_2$ solution. A ratio of UPE of the leaf after and before the H$_2$O$_2$ incubation was estimated. The UPE was detected by a highly sensitive CCD camera VersArray 1300B (Princeton Instruments, USA) equipped with an objective (F mount Nikkor 50 mm, f/1.2, Nikon, Japan). The CCD element was cooled down to −104 °C to reduce the background noise, the accumulation time of each measurement was 30 min. The UPE of the leaf represents the average number of counts from the leaf surface (n = 5).

Performed by M. Rác and Z. Kučerová

3.17 Ion leakage

For the determination of the extent of ion leakage from leaf tissue as a measure of cell membrane damage, circular (diameter of 1 cm) or rectangular (2 cm long) segments were cut out from Arabidopsis leaves or wheat leaf segments, respectively. Groups of six leaf discs or eight rectangular segments (one group represents one sample) were put into 6-well plates containing 3.5 ml of deionized water and incubated under HL (500 µmol photons.m^{-2}.s^{-1}) for up to 8 h to induce oxidative damage in cell membranes. The conductivity of the solutions was measured after 2, 4, 6 and 8 h of the HL treatment with a conductivity meter (GMH 3430, Greisinger, Germany). As DMSO is known

to affect the membrane fluidity and permeability for ions, deionized water was used as a mock control as well to exclude effect of DMSO on the membrane permeability.

Performed by Z. Kučerová

4 Results and discussion

Newly prepared compounds derived from CKs are usually tested by standard CK bioassays to compare their CK-like biological activity to that of commonly used CKs. In our case, biological activity of 21 newly synthetized aromatic 6-benzylamino-9-β-D-arabinofuranosylpurines (BAPA) was compared to naturally occurring aromatic CK BAP. None of the BAPAs exceeded biological activity of BAP in tobacco callus bioassay and Amaranthus bioassay showing that their CK activity is only weak (for detailed results please see Table 1 in Bryksová et al. 2020 in Appendix). Similarly, none of the BAPAs had ability to activate Arabidopsis CK receptors CRE1/AHK4 and AHK3 *in vitro.* AHK3 is considered to be the main receptor involved in mediating leaf senescence (Riefler et al. 2006, Janečková et al. 2018). Nevertheless, the activity of BAPAs in wheat leaf senescence bioassay was similar or even higher than that of BAP suggesting they possess high anti-senescence activity without triggering the CK pathway. Based on these results, two compounds (3OHBAPA and 3MeOBAPA) were chosen for further, more detailed, testing. 3OHBAPA is structurally related to aromatic CK *meta*-topolin which does not have negative effects on root development and therefore is widely used in *in vitro* tissue cultures (Werbrouck et al. 1996, Aremu et al. 2012) and 3MeOBAPA is its methoxy- derivative. Hydroxy- and methoxy- derivatives of BAP have been shown previously to be more effective in delaying senescence than unmodified BAP (Holub et al. 1998, Tarkowská et al. 2003, Szüčová et al. 2009).

4.1 Gene expression changes in 3MeOBAPA-treated Arabidopsis leaves

To characterize changes in gene transcription caused by 3MeOBAPA in Arabidopsis leaves a high-troughput mRNA sequencing analysis was performed. Detached Arabidopsis leaves were incubated in the dark in 10 μmol.l^{-1} 3MeOBAPA for 6 and 48 h. In the case of 6-h treatment 1102 genes were upregulated and 1119 downregulated in comparison with mock-treated leaves. In the case of 48-h treatment the number of genes affected by 3MeOBAPA was higher than in the shorter treatment, 7509 upregulated and 7095 downregulated in comparison with the mock-treatment (Fig. 7).
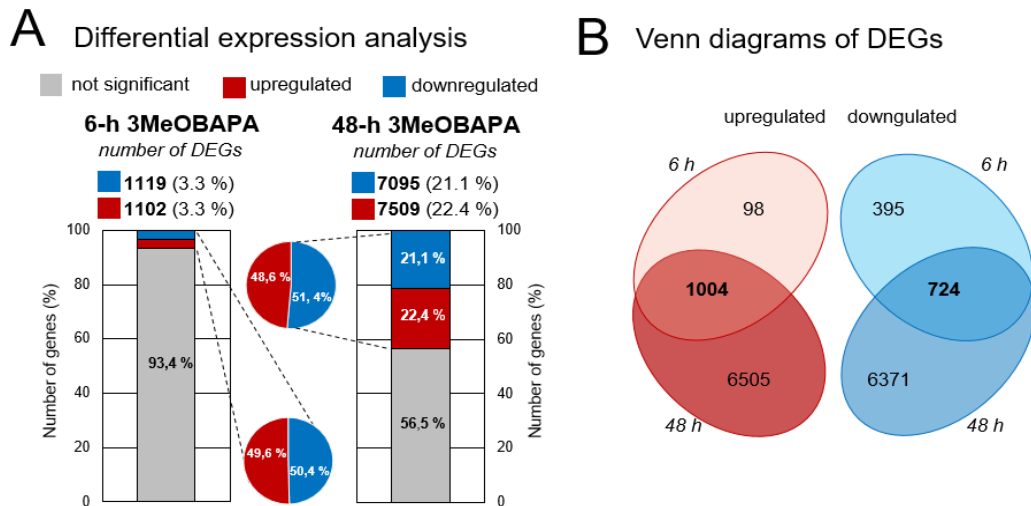
Fig. 7. Transcriptional reprogramming in Arabidopsis leaves treated by 10 μmol.l⁻¹ 3MeOBAPA (**A**) in comparison to mock-treated leaves (0.1% DMSO; p<0.05). Venn diagrams comparing gene expression after 6-h and 48-h treatment with 3MeOBAPA (**B**). Reprinted and adapted with permission from Bryksová et al. (2020). Copyright (2020) American Chemical Society.

To characterize the biological function of genes that were affected by 3MeOBAPA treatment, all genes were analysed according to Gene Ontology (GO) project (for complex and more detailed information about affected genes see Supplementary table 2 and 3 of Bryksová et al. 2020 in Appendix) and KEGG database resource. The GO analysis of genes affected by 6-h treatment by 3MeOBAPA revealed strong upregulation of genes that are related to plant defence response mechanisms such as jasmonic acid and ethylene-dependent systemic resistance and various cell wall modifications. The KEGG pathway analysis was performed to decipher biological consequences of the observed changes in gene expression under 6-h and 48-h 3MeOBAPA treatment. Similarly to GO analysis, plant defence elements such as Plant-pathogen interactions, Phenylpropanoid biosynthesis and Glutathione metabolism were upregulated after 48-h 3MeOBAPA treatment (Fig. 8). In the term of downregulation, in both GO and KEGG analysis genes related to photosynthesis were the mostly affected ones (GO categories such as Light-harvesting complex, Photosystem I and Non-photochemical quenching and KEGG pathways Carbon fixation, Photosynthesis-antenna proteins and Photosynthesis). Since downregulation of photosynthetic genes is a hallmark of early responses of plants to pathogens (Bilgin et al. 2010) it is apparent that 3MeOBAPA treatment shifted the transcriptional response markedly towards defence.
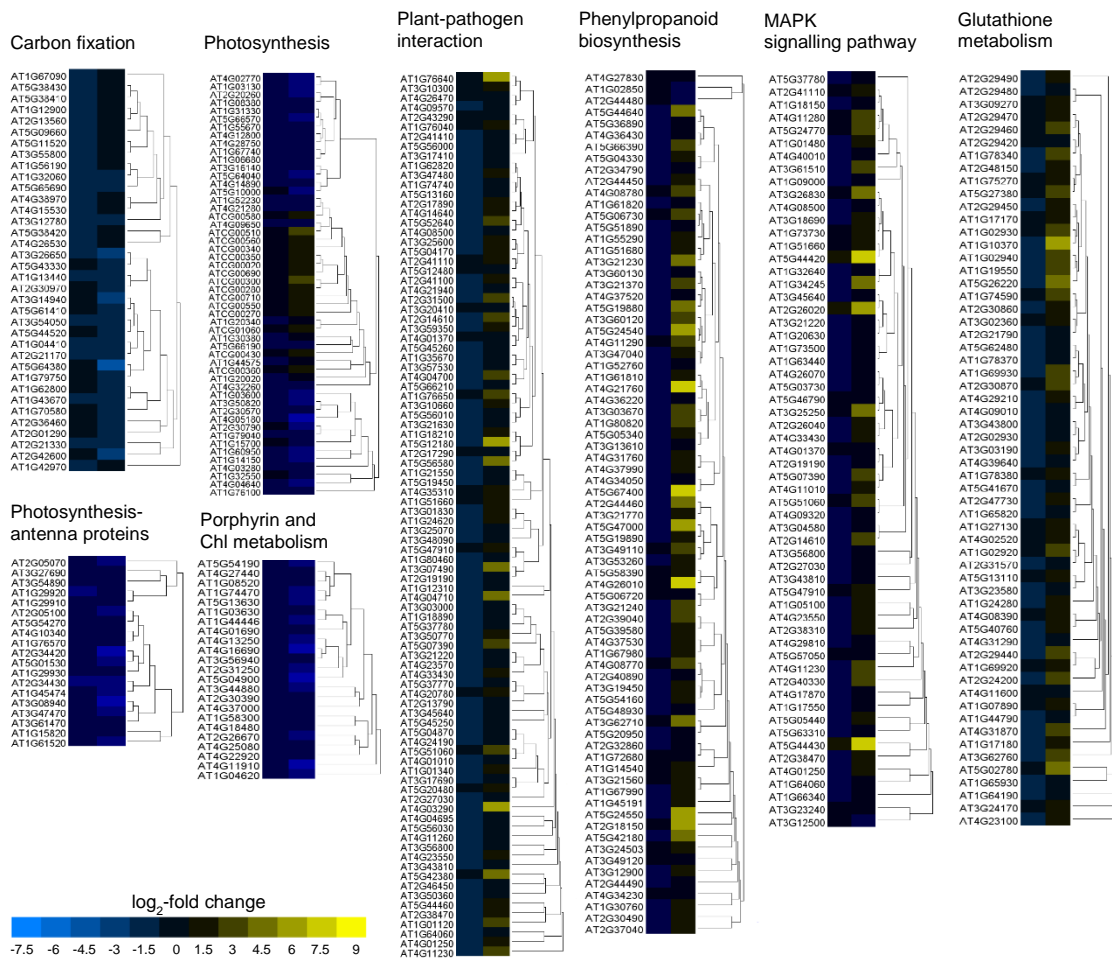
Fig. 8. KEGG pathways over-representation analysis. Fold changes (log$_2$ scale) in expression of selected metabolic pathway genes are shown for the 6h- (left columns) and 48h- (right columns) treatment with 3MeOBAPA. Genes were clustered using average-linkage hierarchical clustering. The metabolic pathways shown in the figure represent the most significantly affected group of genes related to carbon fixation (map00710), photosynthetic machinery (map00195 'Photosynthesis', map00196 'Photosynthesis - antenna proteins', map00860 'Porphyrin and chlorophyll (Chl) metabolism'), plant-pathogen interactions (map04626), mitogen-activated protein kinase (MAPK) signaling (map04016), phenylpropanoid biosynthesis (map00940), and glutathione metabolism (map00480) according to KEGG database. The log2 fold change values are expressed as negative or positive numbers on the bar, and the colour scale indicates which genes are up- (yellow) and down-regulated (blue). Reprinted and adapted with permission from Bryksová et al. (2020). Copyright (2020) American Chemical Society.

However, the downregulation of genes related to photosynthesis was not accompanied by a decrease in photosynthetic function in any time point. On the contrary, a mild stimulation of photosynthetic electron transport occurred in the leaves treated by 3MeOBAPA for 6 h as a more rapid induction of Φ_P (representing PSII photochemistry) during transition of the leaves from the dark- to light-adapted state was observed when compared with mock or BAP-treated leaves (Fig. 9A). It has been shown previously that a reprogramming of the leaf transcriptome from photosynthesis towards defence can occur without a significant decrease in the photosynthetic function (Attaran et al. 2014). The maintenance of functional photosynthesis is very important during critical early stages of the defence response (Bilgin et al. 2010, Attaran et al. 2014) because this response is associated with an increased demand for energy and carbon skeletons. In our case, an increased demand for ATP typical for the activation of defence response (Swarbrick et al. 2006) was indicated by changes in the Φ_{NPQ} induction (representing regulatory non-photochemical quenching; Fig. 9B): a slightly lower Φ_{NPQ} values from approximately the 3rd minute of the induction reflected an increased consumption of trans-thylakoid proton gradient, probably due to stimulation of ATP synthase. Decrease in photochemical quenching caused by activation of defence response was also reported by (Göhre et al. 2012).
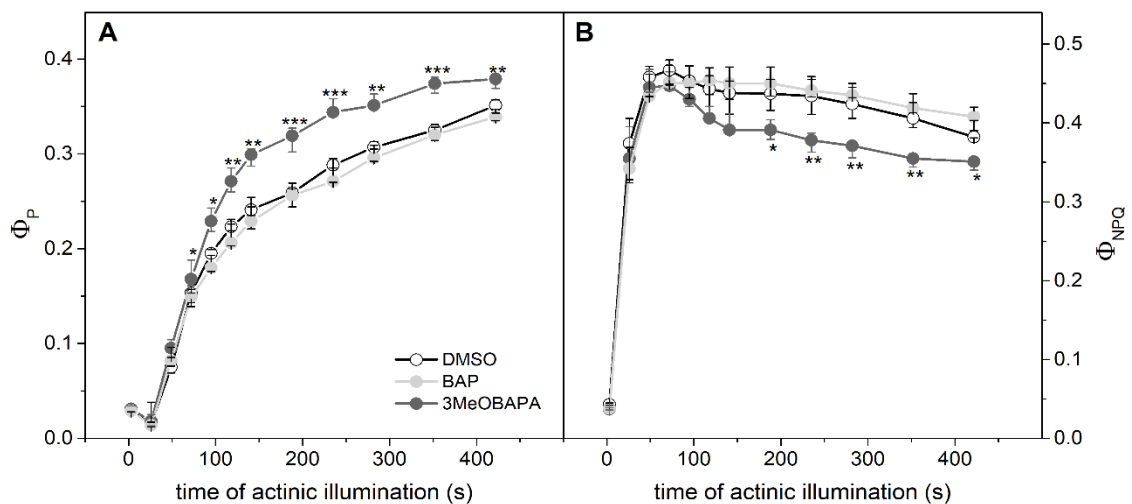
Fig. 9. (**A**) Induction of the effective quantum yield of photochemistry of photosystem II (ΦP) and (**B**) the quantum yield of regulatory non-photochemical quenching (ΦNPQ) during transition of Arabidopsis leaves from the dark- to light-adapted state. The leaves were dark-incubated in 0.1% DMSO or 10 μmol.l^{-1} solution of BAP or 3MeOBAPA for 6 h. Medians and quartiles are presented (n = 5). Asterisks mean statistically significant difference; ***, $p < 0.001$; **, $p < 0.01$; *, $p < 0.05$ (Student´s unpaired t-test).

Table 2. The expression level of selected genes in *Arabidopsis thaliana* L. after 48 h treatment with 10 µmol.l^{-1} 3MeOBAPA. Gene ID, name and description and log$_2$ fold change in 3MeOBAPA-treated leaves are presented.

ID	Log$_2$ fold change	Gene name	
AT5G47910	2.20	*RBOHD*	*RESPIRATORY BURST OXIDASE HOMOLOG D*
AT1G64060	0.66	*RBOHF*	*RESPIRATORY BURST OXIDASE HOMOLOG F*
AT5G60010	5.40	*RBOHH*	*RESPIRATORY BURST OXIDASE HOMOLOG H*
AT5G07390	4.49	*RBOHA*	*RESPIRATORY BURST OXIDASE HOMOLOG A*
AT5G51060	4.26	*RBOHC*	*RESPIRATORY BURST OXIDASE HOMOLOG C*
AT4G11230	3.04	*RBOHI*	*RESPIRATORY BURST OXIDASE HOMOLOG I*
AT2G14610	4.08	*PR1*	*PATHOGENESIS RELATED 1*
AT1G80460	0.52	*NHO1*	*NONHOST RESISTANCE TO P. S. PHASEOLICOLA 1*
AT3G26830	5.01	*PAD3*	*PHYTOALEXIN DEFICIENT 3*
AT4G33430	1.63	*BAK1*	*BRASSINOSTEROID-INSENSITIVE 1-associated receptor kinase*
AT2G39660	1.55	*BIK1*	*BOTRYTIS-INDUCED KINASE 1*
AT5G20480	2.57	*EFR*	*EF-TU RECEPTOR*
AT1G06160	2.62	*ERF59*	*ETHYLENE RESPONSIVE FACTOR 59*
AT3G23240	0.32	*ERF1B*	*ETHYLENE RESPONSIVE FACTOR 1B*
AT4G28140	6.47	*ERF54*	*ETHYLENE RESPONSIVE FACTOR 54*
AT1G75830	7.85	*PDF1.1*	*PLANT DEFENSIN 1.1*
AT5G44420	8.15	*PDF1.2A*	*PLANT DEFENSIN 1.2A*
AT2G26020	6.04	*PDF1.2B*	*PLANT DEFENSIN 1.2B*
AT5G44430	8.87	*PDF1.2C*	*PLANT DEFENSIN 1.2C*
AT2G26010	8.23	*PDF1.3*	*PLANT DEFENSIN 1.3*
AT4G08500	1.15	*MEKK1*	*MITOGEN-ACTIVATED PROTEIN KINASE KINASE KINASE 1*
AT4G26070	0.6	*MKK1*	*MITOGEN-ACTIVATED PROTEIN KINASE KINASE 1*
AT4G29810	0.99	*MKK2*	*MITOGEN-ACTIVATED PROTEIN KINASE KINASE 2*
AT1G51660	2.08	*MKK4*	*MITOGEN-ACTIVATED PROTEIN KINASE KINASE 4*
AT3G21220	0.68	*MKK5*	*MITOGEN-ACTIVATED PROTEIN KINASE KINASE 5*
AT1G01560	2.57	*MPK11*	*MITOGEN-ACTIVATED PROTEIN KINASE 11*
AT4G01370	0.98	*MPK4*	*MITOGEN-ACTIVATED PROTEIN KINASE 4*
AT3G45640	0.94	*MPK3*	*MITOGEN-ACTIVATED PROTEIN KINASE 3*
AT1G01340	2.06	*CNGC10*	*CYCLIC NUCLEOTIDE GATED CHANNEL 10*
AT2G46450	1.21	*CNGC12*	*CYCLIC NUCLEOTIDE GATED CHANNEL 12*
AT4G01010	1.31	*CNGC13*	*CYCLIC NUCLEOTIDE GATED CHANNEL 13*
AT3G17690	1.41	*CNGC19*	*CYCLIC NUCLEOTIDE GATED CHANNEL 19*
AT5G45890	-12.35	*SAG12*	*SENESCENCE-ASSOCIATED GENE 12*
AT5G03280	-0.93	*EIN2, ORE3*	*ETHYLENE INSENSITIVE 2. ORESARA 3*
AT3G20770	-0.69	*EIN3*	*ETHYLENE INSENSITIVE 3*
AT5G39610	-1.30	*ORE1*	*ORESARA 1*
AT2G42620	-1.66	*ORE9*	*ORESARA 9*
AT2G43000	4.14	*JUB1*	*JUNGBRUNNEN 1*
AT3G22840	5.02	*ELIP1*	*EARLY-LIGHT INDUCED PROTEIN 1*
AT4G14690	3.71	*ELIP2*	*EARLY-LIGHT INDUCED PROTEIN 2*
AT1G30135	5.19	*JAZ8*	*JASMONATE-ZIM-DOMAIN PROTEIN 7*
AT2G34600	1.13	*JAZ7*	*JASMONATE-ZIM-DOMAIN PROTEIN 8*

4.2 3MeOBAPA affects PTI via MAPK signalling modules

It is known that both exogenous and endogenous CKs can enhance plant resistance to pathogens (Choi et al. 2010, 2011, Prokopová et al. 2010b) but mechanism of their action in plant immunity is not fully understood. Nevertheless, the promoting effect of CKs on pathogen-associated molecular patterns (PAMP)-triggered immunity of Arabidopsis has been reported (Choi et al. 2010, Naseem et al. 2012). According to model by Choi et al. (2010) CKs increase the defence response and consequently plant resistance to pathogen via activation of AHK2/AHK3 and ARR2. We suppose that the activation of defence response by 3MeOBAPA may be different as 3MeOBAPA was not recognised by the AHK3 and AHK4 receptors *in vitro* and no upregulation of *ARR2* and most of the other CK response regulators was observed after its 6-h and 48-h application. Moreover, this presumption is in line with low cytokinin activity of 3MeOBAPA in the tobacco callus and Amaranthus bioassay.

It is generally accepted that early steps in PAMP-triggered immunity (PTI) responses include mitogen-activated protein kinase (MAPK) signalling modules. The activation of pattern recognition receptors (PRR) localized on plasma membrane triggers defence response in affected cells through activation of MAPK signalling cascade (for review see Bigeard et al. 2015). As the main MAPKs that are involved in PTI are considered MPK4, MPK3, MPK6 and recently also MPK11 was assigned to them (Bethke et al. 2012, Bigeard et al. 2015). Expression of *MPK11* was showed to be strongly upregulated in response to flg22 (the PAMP derived from the bacterial protein flagellin) and others PAMP such as elf18 and ch8 (Gómez-Gómez et al. 1999, Bethke et al. 2012, Eschen-Lippold et al. 2012). Upregulation of the MAPK signalling pathway (both MEKK1-MKK1/2-MPK11+MPK4 and MEKK1-MKK4/5-MPK3+MPK6, Table 2) and Plant-pathogen interaction module in response to the 3MeOBAPA treatment together with reprogramming of the transcriptome from photosynthesis towards defence (Fig. 8) suggest that 3MeOBAPA induces plant responses similarly to that triggered by PAMPs and thus promotes PTI. This suggestion is supported by the observation that another markers of PTI such as *RBOH*s (coding for respiratory burst oxidase homologs), *FLG22-INDUCED RECEPTOR-LIKE KINASE 1 (FRK1)*, pathogen-related WRKY transcription

factors (*WRKY22, WRKY29, WRKY33, WRKY53*), *PATHOGENESIS RELATED 1* (*PR1*), *NONHOST RESISTANCE TO P.S. PHASEOLICOLA 1* (*NHO1*) or *PHYTOALEXIN DEFICIENT 3* (*PAD3*) were also upregulated by 3MeOBAPA (Table 2).

To corroborate the assumption that 3MeOBAPA provokes PTI response through MAPK cascade, the expression profiles of *MPK3*, *MPK4*, *MPK6* and *MPK11* after 30 min, 6 h and 48 h of 3MeOBAPA treatment (10 and 50 μmol.l^{-1}) were further investigated. Concentration-dependent effect of 3MeOBAPA treatment on the expression patterns of *MPK3*, *MPK4* and *MPK11* was observed while *MPK11* was the most affected (especially after 30 min treatment with 50 μmol.l^{-1} 3MeOBAPA suggesting a fast response mechanism; Fig. 10A). Immunoblotting experiments showed that the abundance of MPK3, MPK4 and pMPK3 in 3MeOBAPA-treated detached leaves was mostly similar either to mock- or BAP-treated leaves (both applied at concentration 10 μmol.l^{-1}, Fig. 10B-D, F). The exception was the increased abundance of MPK3, MPK6 and also its phosphorylated form pMPK6 in 3MeOBAPA-treated leaves after 6 h (Fig. 10E, G) indicating possible involvement of *MPK3* and *MPK6* in long-term 3MeOBAPA-induced responses. Unfortunately, the abundance of the protein product of the highly responsive *MPK11* could not be assessed due to unavailability of the respective antibody.
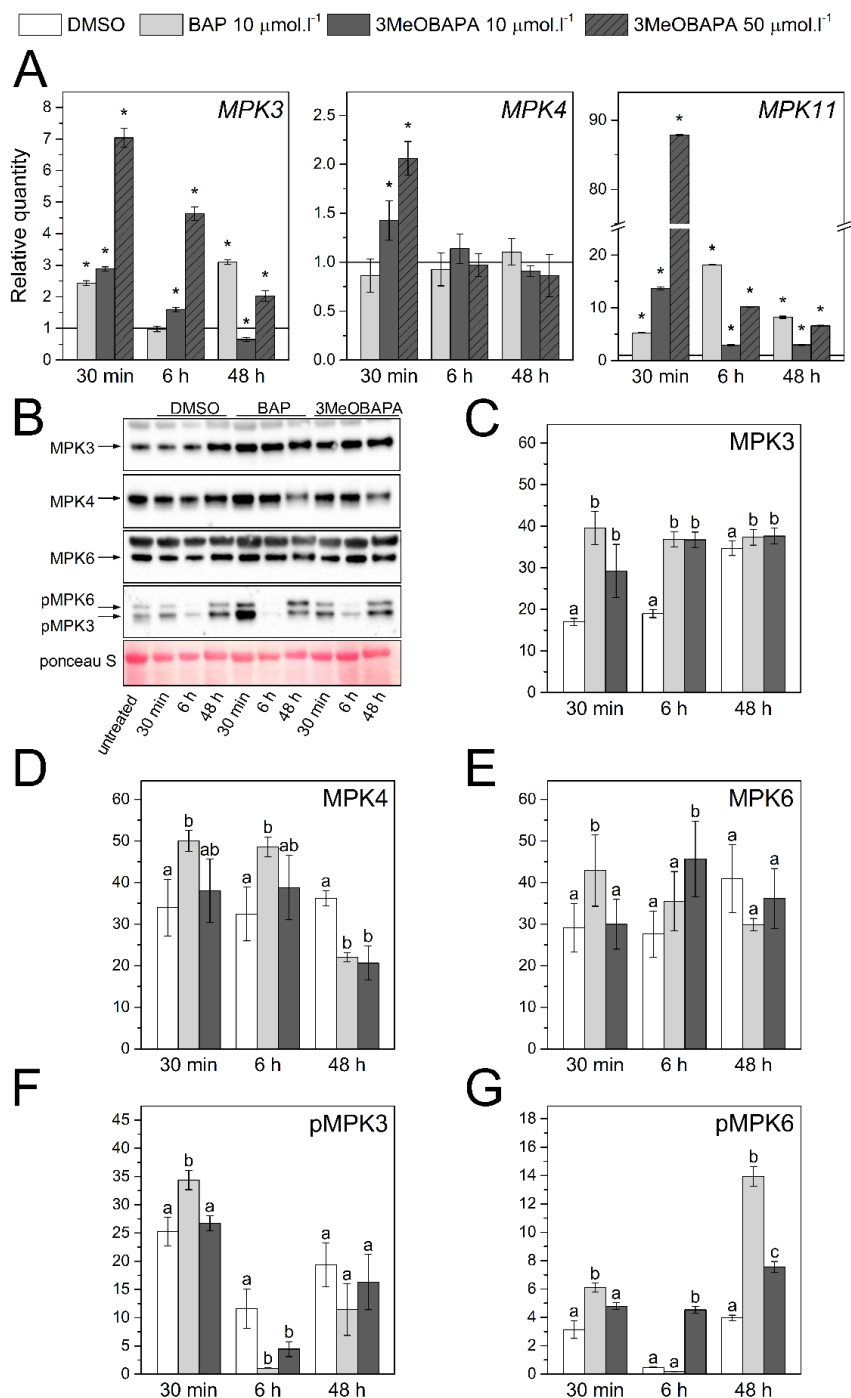
Fig. 10. (**A**) Expression profiles of *MPK3*, *MPK4* and *MPK11* in detached leaves treated by 0.1% DMSO or 10 μmol.l⁻¹ BAP or 3MeOBAPA; or 50 μmol.l⁻¹ 3MeOBAPA for 30 min, 6 h and 48 h quantified using qPCR. Means and SD are presented (n = 4). Asterisks indicate statistically significant difference of treated versus untreated (control) leaves ($p < 0.05$; Student´s unpaired *t*-test). (**B**) Immunoblots of Arabidopsis leaves incubated in 0.1% DMSO or 10 μmol.l⁻¹ BAP or 3MeOBAPA for 30 min, 6 h and 48 h and probed with anti-MPK3, anti-MPK4, anti-MPK6, anti-pERK phosphospecific antibodies recognizing the phosphorylated forms of MPK3 and MPK6 (pMPK3, pMPK6). Ponceau S staining was used for loading control to verify that equal quantities of all studied proteins were loaded onto each probed membrane. (**C-G**) Quantification of band densities from immunoblots (**C**) for MPK3, (**D**) MPK4, (**E**) MPK6, (**F**) phosphorylated MPK3; pMPK3 and (**G**) phospohorylated MPK6; pMPK6. In (**F**) and (**G**) the densities are normalized to the abundance of the corresponding MPKs. In (**C-G**) means and SD are presented. Different letters indicate statistically significant difference between treatments ($p < 0.05$; Student´s unpaired *t*-test). Reprinted and adapted with permission from Bryksová et al. (2020). Copyright (2020) American Chemical Society.

4.3 Ethylene, jasmonic acid and ROS as signalling agents

As already mentioned, 3MeOBAPA treatment (6-h) caused a strong upregulation of genes that are related to jasmonic acid (JA) and ethylene-dependent systemic resistance. To confirm activation of those defence response mechanisms by 3MeOBAPA, the ethylene production in 3MeOBAPA-treated leaves (for 48 h and 72 h) and content of JA forms after 48-h treatment was compared to mock-treated leaves (Fig. 11). In the case of ethylene, 3MeOBAPA treatment increased its production after both time periods (Fig. 11A). In the case of JA content, three forms were estimated: its precursor *cis*-(+)-12-oxo-phytodienoic acid (*cis*-OPDA), JA itself and its major biologically active form jasmonoyl-L-isoleucine (JA-Ile). Similarly to ethylene, the content of all JA forms was higher in 3MeOBAPA-treated leaves (Fig. 11B). The increased ethylene and JA content might have contributed to the 3MeOBAPA-induced PTI represented by activation of plant defensins (*PDF*s; Table 2). PDFs are part of plant innate immunity system directed against fungal pathogens and they are known to be induced by JA and ethylene (Stotz et al. 2009).

Additionally, expression of *RBOH* genes coding for NADPH oxidases Rbohs (respiratory burst oxidase homologs) was upregulated in 3MeOBAPA treated leaves (Table 2). Rbohs are important source of ROS in a response to pathogen attack in plants (Miller et al. 2009). ROS are known to be involved in various signalling networks of plant responses to stressors including MAPK cascades and JA- and ethylene- signalling pathways (for review see Sewelam et al. 2016). When production of overall ROS in Arabidopsis cell culture treated by 3MeOBAPA (10 and 50 μmol.l^{-1}) was measured using a standard DCFH-DA assay, 3MeOBAPA in both concentrations increased this production in 3 h of the treatment. Then the ROS production gradually decreased to pre-treatment levels (Fig. 11C). The increase of ROS production induced by short-term (30 min) 3MeOBAPA treatment was found also in detached Arabidopsis leaves using measurement of $O_2^{\cdot-}$ accumulation. $O_2^{\cdot-}$ were visualized using confocal microscopy and fluorescent probe dihydroethidium (DHE). The production of $O_2^{\cdot-}$ was higher in the case of 3MeOBAPA-treated leaves in comparison to mock-treated ones (Fig. 11D). The

increased ROS production (including O_2^-) as a result of 3MeOBAPA treatment indicates involvement of ROS signalling in early response to 3MeOBAPA.
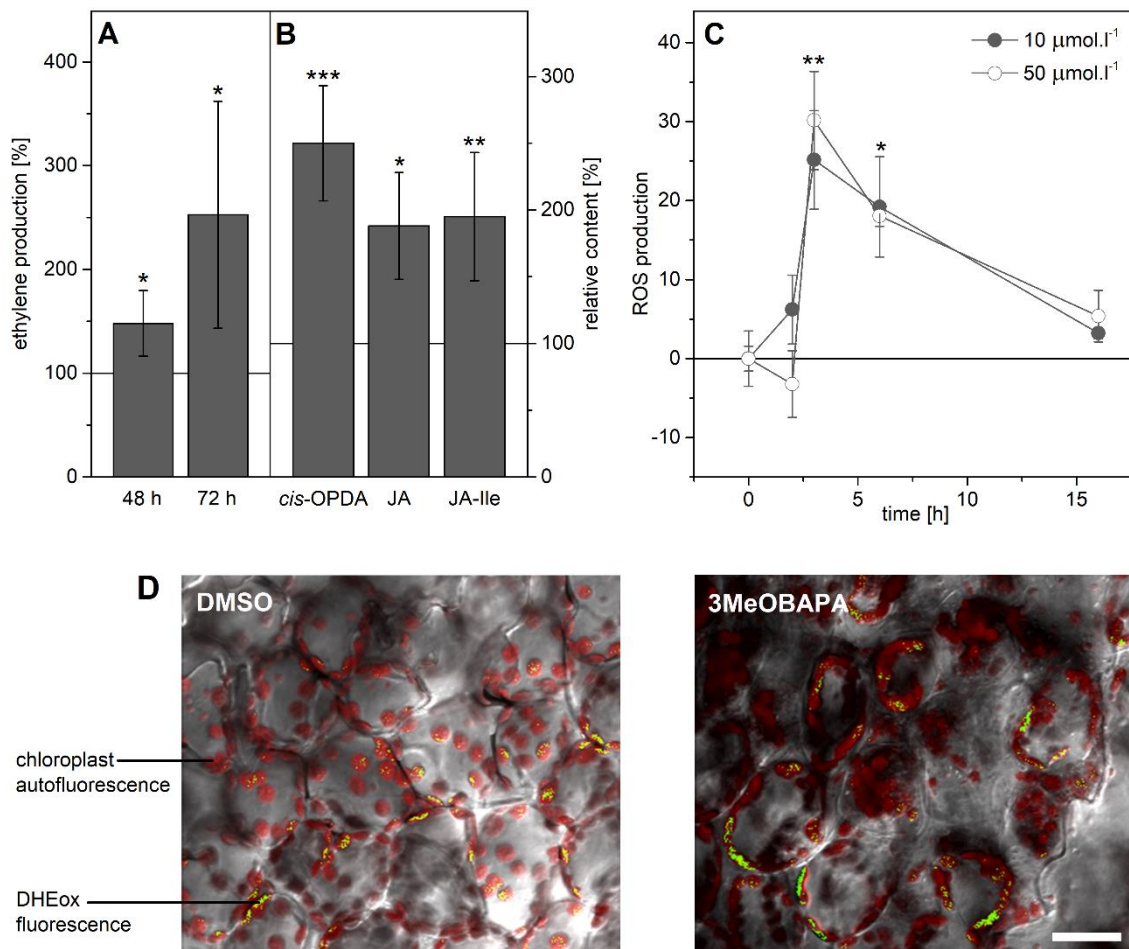

Fig. 11. (**A**) Ethylene production in detached Arabidopsis leaves treated by 10 μmol.l^{-1} 3MeOBAPA for 48 and 72 h compared to mock-treated leaves. (**B**) Relative content of *cis*-(+)-12-oxo-phytodienoic acid (*cis*-OPDA), jasmonic acid (JA) and jasmonoyl-L-isoleucine (JA-Ile) in detached Arabidopsis leaves treated by 10 μmol.l^{-1} 3MeOBAPA for 48 h compared to mock-treated leaves. (**C**) Overall ROS production in Arabidopsis cell cultures treated by 10 and 50 μmol.l^{-1} 3MeOBAPA for up to 16 h. In all charts means and SD are presented (n = 4-5). Asterisks indicate statistically significant difference between 3MeOBAPA treatment and mock (DMSO) treatment (***, $p < 0.001$; **, $p < 0.01$; *, $p < 0.05$, Student′s unpaired t-test**) (D**) *In vivo* imaging of O_2^- using fluorescent probe dihydroethidium (DHE; green) in detached leaves of Arabidopsis treated by 0.1% DMSO or 10 μmol.l^{-1} 3MeOBAPA for 30 min. Scale bar represent 50 μm. (B) and (C) were reprinted and adapted with permission from Bryksová et al. (2020). Copyright (2020) American Chemical Society.

4.4 Model of 3MeOBAPA action

Among others, the transcriptomic changes induced by 3MeOBAPA treatment suggested that 3MeOBAPA acts as a priming agent for the PTI response. To further confirm that 3MeOBAPA primes the PTI response in Arabidopsis seedlings, expression levels of *MPK3*, *MPK4*, *MPK6* and *MPK11* together with another PTI-responsive genes such as *FRK1* and transcription factors such as *WRKY 33* and *WRKY 53* (Eschen-Lippold et al. 2016) were evaluated using qPCR and compared with a response to flg 22 (Fig. 12).
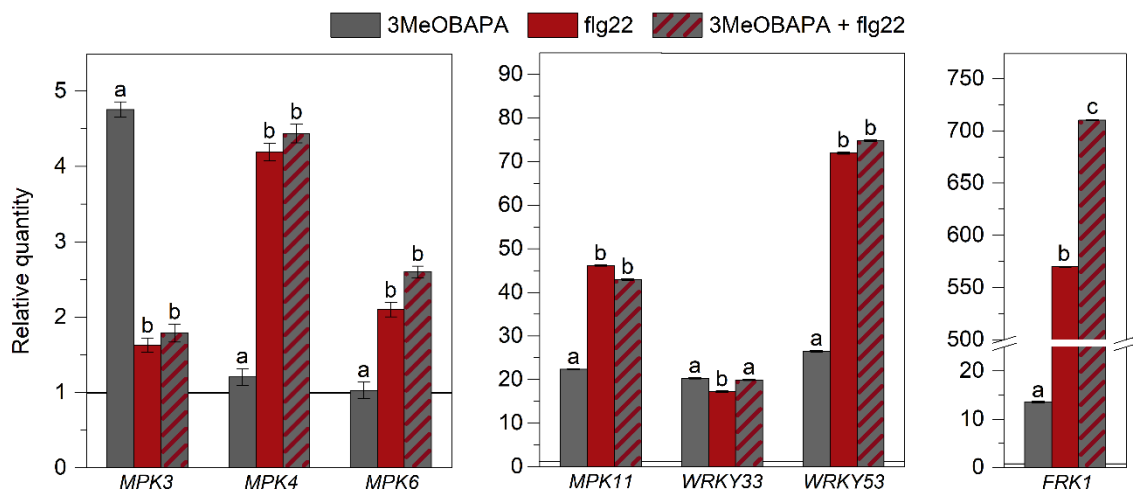

Fig. 12. The expression levels of *MPK3, MPK4, MPK6, MPK11, WRKY 33, WRKY 53* and *FRK1* in Arabidopsis seedlings treated with 10 μmol.l⁻¹ 3MeOBAPA and/or 1 μmol.l⁻¹ flg22 for 2h in comparison with mock-treated seedlings. Genes for elongation factor 1 alpha and actin 7 were used as reference genes. Means and SD are presented (each bar represents a biological pool of approximately 50 seedlings, n ≥ 4). Different letters indicate statistically significant difference between treatments ($p < 0.05$; Student´s unpaired t-test). Reprinted and adapted with permission from Bryksová et al. (2020). Copyright (2020) American Chemical Society.

As expected, flg22 primed these PTI-responsive genes (Fig. 12). In line with results from detached leaves (Fig. 10), in the 3MeOBAPA-treated seedlings expression level of *MPK11* was strongly increased (Fig. 12). Importantly, the 3MeOBAPA-treatment profoundly increased also expression level of the other PTI-responsible genes, although flg22 provoked much stronger effect, especially in the case of *FRK1*. Although treatment of 3MeOBAPA together with flg22 showed little effect in the case of *MPK*s and *WRKY*s, their downstream *FRK1* proved to be very sensitive to this combined treatment. A strong synergistic effect between flg22 and 3MeOBAPA was observed in the FLS2-initiated MAPK defence pathway (Fig. 12). Briefly, this pathway consists of plasma-membrane FLS2 receptor (PRR) whose activation via perception of flg22 stimulates the recruitment

of BAK1 (brassinosteroid-insensitive 1-associated receptor kinase) and BIK1 (Botrytis-induced kinase 1). These kinases are subsequently phosphorylated and released from the membrane complex. Then, the MAPK cascade is activated resulting in activation of TFs such as WRKY that induce responsive defence genes. Calcium-dependent protein kinases (CPKs) also play a role in activating the defence response via flg22. Together with BIK1 and Ca^{2+} influx via calcium-controlled channel and nucleotides (CNGC) they activate RBOH and related oxidative burst and ROS production (for detailed review see Bigeard et al. 2015, Withers & Dong 2017). Since all mentioned components of the flg22 signalling pathway together with EFR (PRR for another PAMP, elf18) are affected also by 3MeOBAPA treatment, it appears that PTI response plays dominant role in 3MeOBAPA-induced defence response alongside JA-ethylene signalling cascade-mediated expression of plant defensins. Based on above mentioned results a model of 3MeOBAPA action was proposed (Fig. 13).
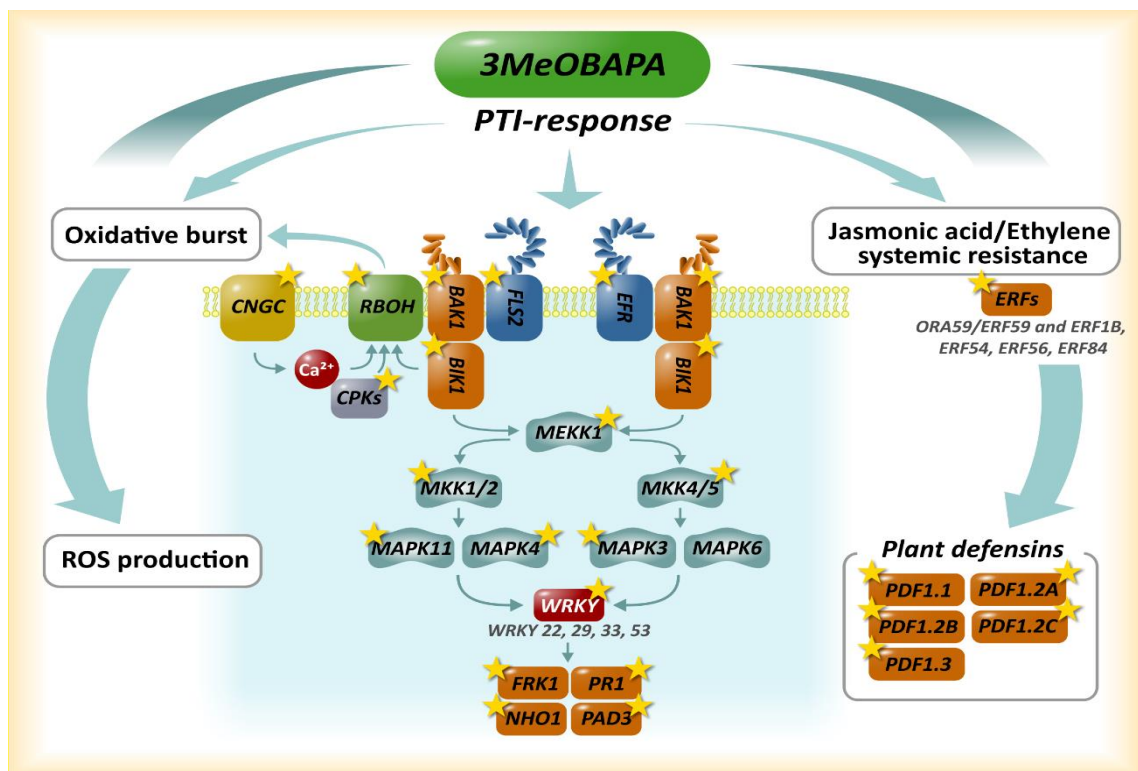
Fig. 13. Model of 3MeOBAPA mediated priming in Arabidopsis plants. Significantly upregulated genes (data from RNA-seq analysis and gene expression studies) are marked with a star. *ERF*, ethylene responsive factor; *PDF*, plant defensin; *FRK1*, *FLG-INDUCED RECEPTOR-LIKE KINASE*; *PR1*, *PATHOGENESIS RELATED1*; *NHO1*, *NONHOST RESISTANCE TO P.S. PHASEOLICOLA 1*; *PAD3*, *PHYTOALEXIN DEFICIENT 3*. Reprinted and adapted with permission from Bryksová et al. (2020). Copyright (2020) American Chemical Society.

4.5 3-MeOBAPA treatment and resistance to pathogens

To corroborate the predicted ability of 3MeOBAPA to enhance plant resistance to pathogens, field experiments with foliar application of 3MeOBAPA and also 3OHBAPA on wheat and barley plants were performed. The CK arabinosides were applied on plants at various growth stages such as tillering, beginning of stem elongation and start of flag leaf extending. The application of CK arabinosides effectively supressed infection by wheat leaf rusts and powdery mildew and foot rot diseases in the case of barley (Fig. 14).
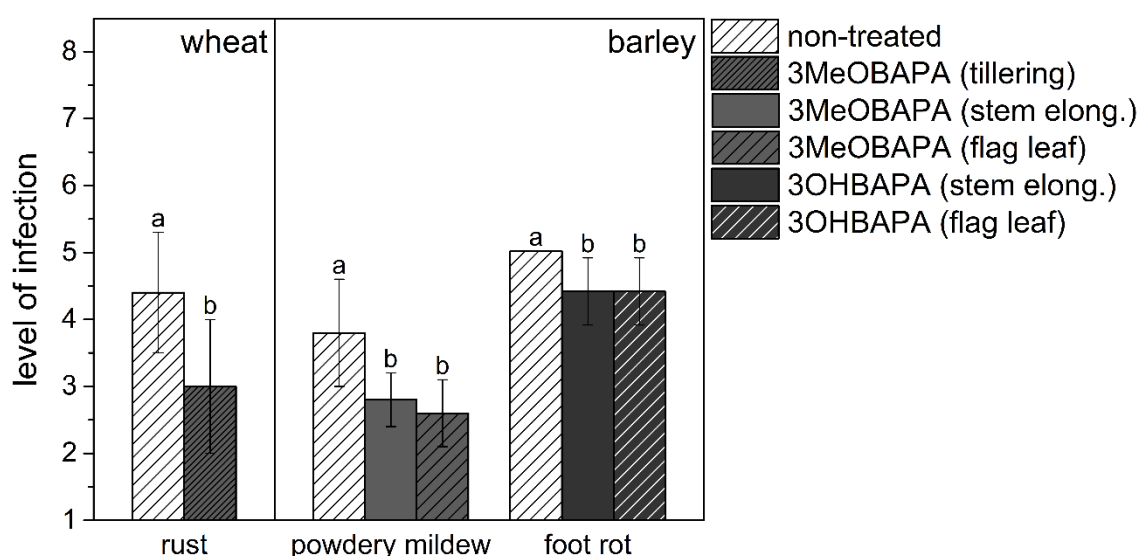
Fig. 14. Level of infection by wheat leaf rusts, powdery mildews and foot rots on 3MeOBAPA- and 3OHBAPA-treated field-grown plants of wheat and barley. Foliar application of 3MeOBAPA and 3OHBAPA (5 μmol.l^{-1}) was performed at a different plant growth stages: tillering, at the beginning of stem elongation (stem elong.) and start of flag leaf extending (flag leaf). The level of infection was evaluated according to standardized methodology (see chapter 3.9 Field trial experiments). Means and SD are presented (n = 5), different letters indicate statistically significant differences within treatment and plant species ($p < 5$). Reprinted and adapted with permission from Bryksová et al. (2020). Copyright (2020) American Chemical Society.

For the purpose of confirming 3MeOBAPA-induced protective effect against pathogens, we also performed experiments with *Botrytis cinerea* inoculation on 3MeOBAPA-treated Arabidopsis leaves and compared its effect with mock and BAP treatment. Although the effect of 3MeOBAPA was not as pronounced as expected, it suppressed the *B. cinerea* infection more effectively than BAP in both ways of treatment (the leaves were treated by placing the leaves in solution or by a petiole, Fig. 15). The development of *B. cinerea* on 3MeOBAPA- and mock-treated leaves was comparable. Since growth rate of *B. cinerea* is positively affected by ethylene (Zhu et al. 2012), the presumed protective action of 3MeOBAPA might be reduced due to higher ethylene production in the initial stages of treatment compared to mock-treated leaves (Fig. 11A**)**. Interestingly, the growth rate of *B. cinerea* was most pronounced in leaves treated by BAP (Fig. 15). The increased susceptibility of Arabidopsis plants to pathogens (*Hyaloperonospora arabidopsidis*) after exogenous application of BAP was also observed by Argueso et al. (2012).

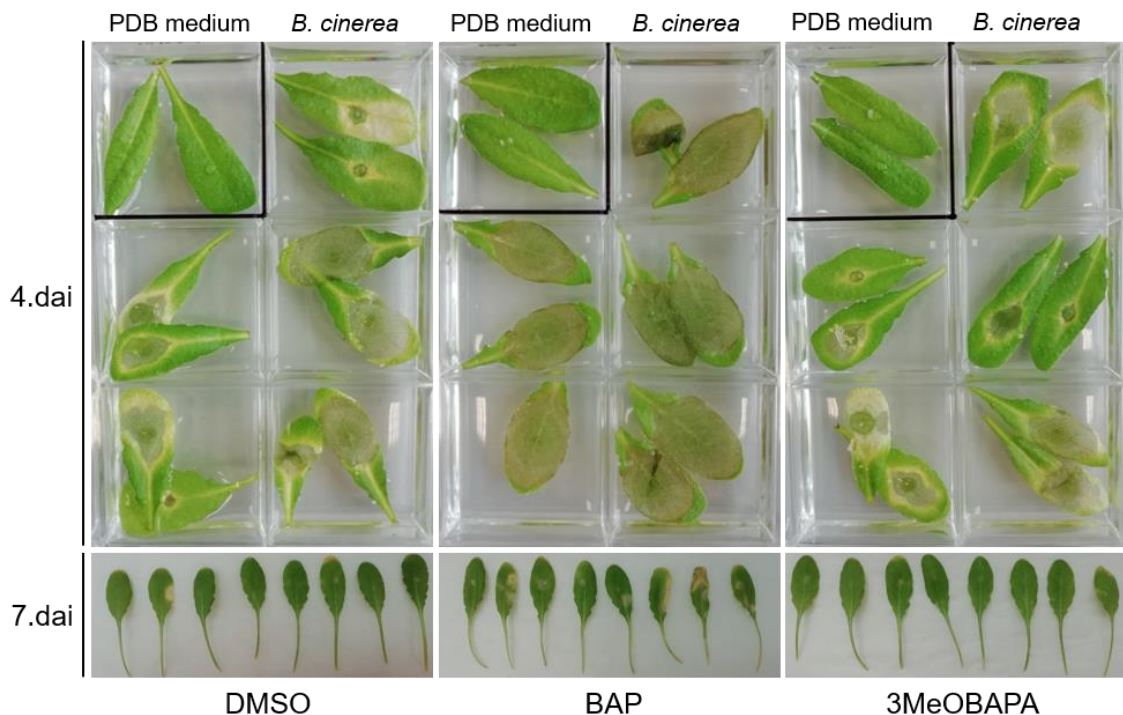**Fig. 15.** Development of *Botrytis cinerea* on detached Arabidopsis leaves treated by 0.1% DMSO, 10 μmol.l^{-1} BAP or 3MeOBAPA 4 days after inoculation in the case of leaves floating on the surface of the solutions and 7 days after inoculation in the case of leaves put in the solution by a petiole. PDB medium without conidia was used as a control ("PDB medium"). dai; day after inoculation.

4.6 Anti-senescence activity of CK arabinosides

Since defence mechanisms are high-cost, energy demanding and are accompanied by photosynthesis inhibition, long-term exposure to PAMP usually leads to plant fitness impairment (Gómez-Gómez et al. 1999, Göhre et al. 2012). In spite of that, 3OHBAPA and 3MeOBAPA were highly active in the wheat leaf senescence bioassay ($180 \pm 7\%$ and $119 \pm 8\%$, respectively, of BAP activity) suggesting that the prolonged exposure is not harmful, but on the contrary has protective effect against dark-induced senescence of detached leaves. Therefore, another experiments with detached darkened leaves were performed using leaves of wheat and Arabidopsis and longer incubation time (6 days in the dark instead of 4 days that are used in the wheat senescence bioassay) to see whether the anti-senescence effect will last during longer dark incubation. Effect of CK arabinosides on photosynthetic activity (namely PSII which is known to be markedly affected by senescence (e.g. Vlčková et al. 2006)) was also evaluated. Firstly, Chl content and the maximum quantum yield of photochemistry of PSII (F_V/F_M) as a widely used parameter reflecting PSII efficiency was measured. In the case of wheat the results were resembling wheat senescence bioassay – 3OHBAPA maintained Chl and also preserved PSII function very effectively while effect of 3MeOBAPA was similar to that of BAP (Table 3; Fig. 16). Interestingly, 3OHBAPA effectively maintained PSII function even when applied at concentration $1\ \mu mol.l^{-1}$ while in the case of BAP and 3MeOBAPA effective concentration was 10-times higher ($10\ \mu mol.l^{-1}$; Table 3). In Arabidopsis the Chl content was most effectively maintained in BAP-treated leaves. On the contrary, F_V/F_M was highest in 3MeOBAPA-treated leaves (Table 3; Fig. 16). Overall, the senescence-induced changes were more pronounced in Arabidopsis in comparison to wheat and to induce protective effect all compounds have to be applied at concentration $10\ \mu mol.l^{-1}$ (Table 3). For further experiments BAP, 3OHBAPA and 3MeOBAPA were applied at the concentration $10\ \mu mol.l^{-1}$ in both wheat and Arabidopsis.

Table 3. Chlorophyll (Chl) content and maximum quantum yield of photosystem II photochemistry (F_V/F_M) of freshly detached (0.dad) leaves of wheat and Arabidopsis and leaves incubated in 0.1% DMSO or BAP, 3OHBAPA and 3MeOBAPA at various concentrations in the dark for 6 days. Different letters indicate statistically significant difference at the tested concentrations. Means ± SD are presented (n = 5).

treatment	concentration	wheat		Arabidopsis	
		Chl content	F_V/F_M	Chl content	F_V/F_M
0.dad		28.24 ± 0.44	0.80 ± 0.00	15.24 ± 2.61	0.79 ± 0.01
DMSO	0.1 %	9.69 ± 2.14	0.06 ± 0.02	0.50 ± 0.16	0.14 ±0.07
BAP	100 nmol.l^{-1}	6.70 ± 1.07 [a]	0.11 ± 0.04 [a]	0.27 ± 0.13 [a]	0.18 ± 0.09 [a]
	1 μmol.l^{-1}	9.20 ± 1.68 [a]	0.20 ± 0.12 [a]	0.32 ± 0.09 [a]	0.16 ± 0.03 [a]
	10 μmol.l^{-1}	15.55 ± 2.39 [a]	0.59 ± 0.04 [a]	10.44 ± 2.71 [a]	0.24 ± 0.05 [a]
3OHBAPA	100 nmol.l^{-1}	5.99 ± 1.15 [a]	0.13 ± 0.09 [a]	0.34 ± 0.15 [a]	0.30 ± 0.12 [a]
	1 μmol.l^{-1}	14.25 ± 1.73 [c]	0.63 ± 0.08 [b]	1.31 ± 0.52 [b]	0.15 ± 0.02 [a]
	10 μmol.l^{-1}	23.10 ± 2.79 [b]	0.72 ± 0.01 [b]	3.74 ± 1.76 [c]	0.24 ± 0.13 [a]
3MeOBAPA	100 nmol.l^{-1}	6.10 ± 0.66 [a]	0.10 ± 0.06 [a]	0.36 ± 0.15 [a]	0.21 ± 0.04 [a]
	1 μmol.l^{-1}	6.54 ± 0.42 [b]	0.06 ± 0.08 [a]	0.53 ± 0.15 [a]	0.15 ± 0.03 [a]
	10 μmol.l^{-1}	12.90 ± 1.63 [a]	0.61 ± 0.07 [a]	8.87 ± 0.78 [b]	0.53 ± 0.11 [b]
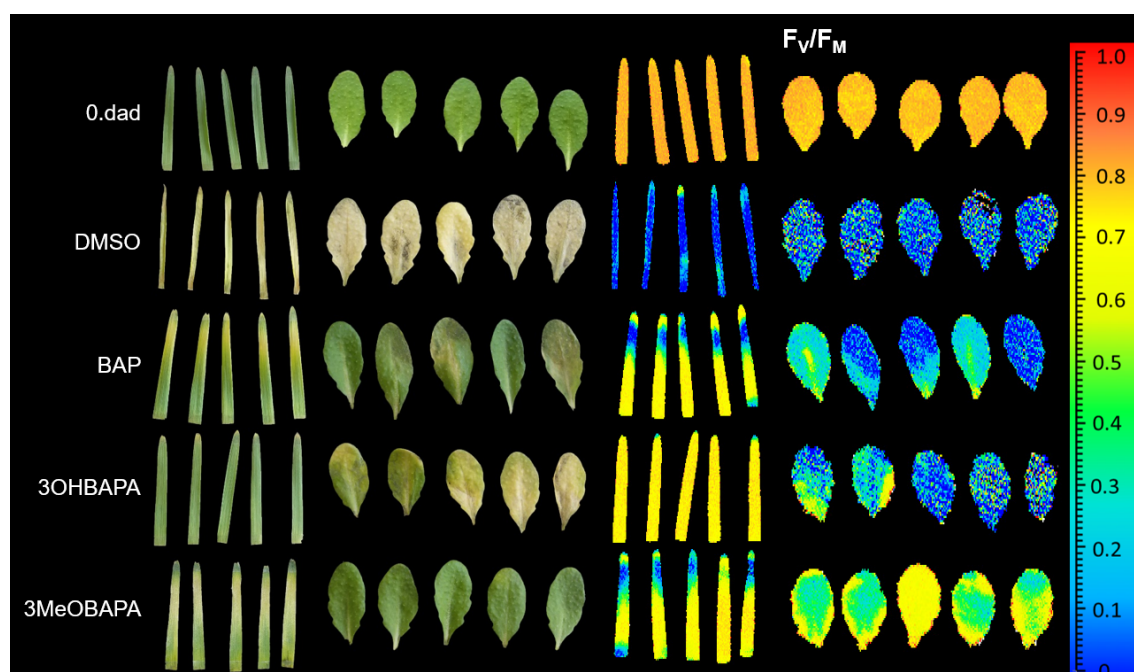
Fig. 16. Imaging of maximum quantum yield of photosystem II photochemistry (F_V/F_M) of freshly detached leaves of wheat and Arabidopsis (0.dad) and leaves incubated in 0.1% DMSO or 10 μmol.l^{-1} BAP, 3OHBAPA and 3MeOBAPA in the dark for 6 days.

Although decrease in Chl content is one of the most apparent and known marker of leaf senescence, content of other photosynthetic pigments such as carotenoids is also declining during senescence (Biswal 1995). In the case of carotenoid content in detached wheat and Arabidopsis leaves treated by BAP and CK arabinosides, the trend was comparable to that observed in Chl content (Fig. 17A, C)
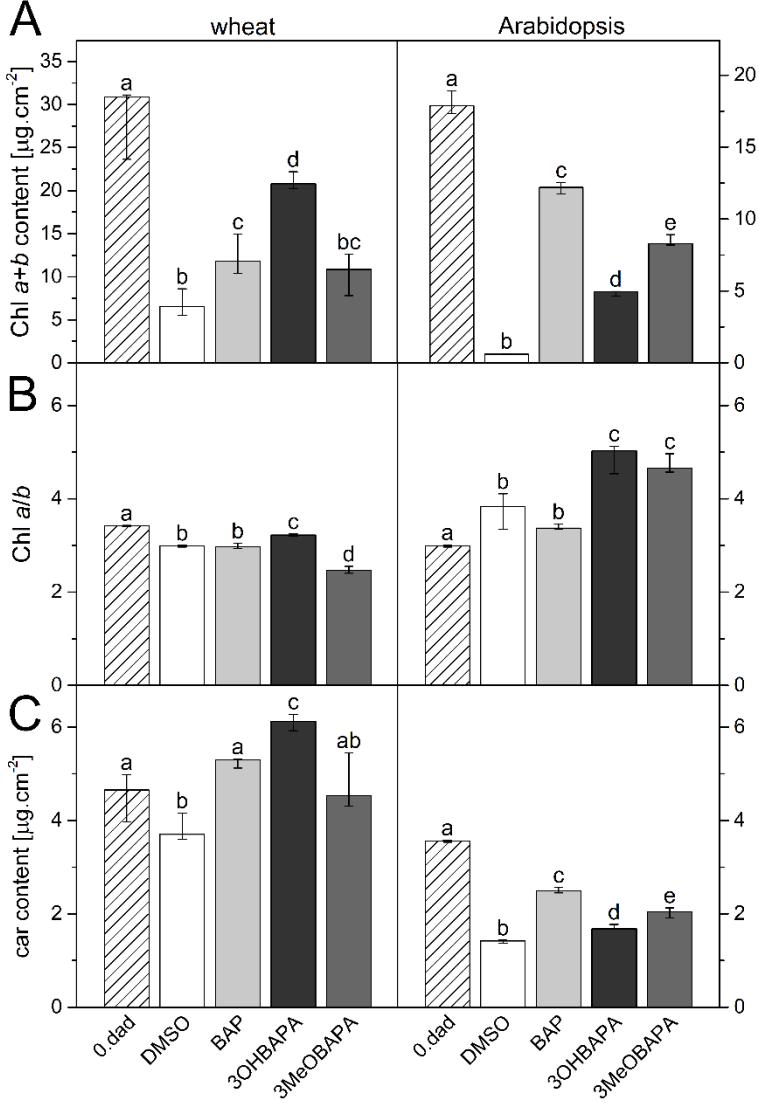
Figure 17. (**A**) Chlorophyll (Chl) *a+b* content; (**B**) Chl *a/b* ratio and (**C**) carotenoid (car) content in freshly detached leaves (0. dad) and leaves of wheat and Arabidopsis after 6 days of dark incubation in 0.1% DMSO or 10 µmol.l⁻¹ solutions of 6-benzylaminopurine (BAP), 3OHBAPA and 3MeOBAPA. Medians and quartiles are shown (n = 5). Different letters indicate a statistically significant difference between treatments within a plant species ($p < 0.05$; Student's unpaired *t*-test). Reprinted from Kučerová et al. (2020).

4.7 Chl degradation in 3MeOBAPA-treated Arabidopsis leaves

It is well known that CKs maintain Chl content in senescing leaves, although the exact molecular mechanism in Arabidopsis is not fully understood. However, it has been reported that CKs positively affect majority of Chl biosynthesis enzymes (reviewed by Cortleven & Schmülling 2015) and that application of BAP on detached dark-incubated rice leaves causes downregulation of some genes involved in Chl degradation (Liu et al. 2016, Talla et al. 2016). Based on the literature it seems that CKs in Arabidopsis conserve the Chl content in senescing leaves via maintained Chl biosynthesis rather than via inhibition of Chl degradation. However, in the case of 3MeOBAPA-treated detached Arabidopsis leaves, all of the genes coding for senescence-induced Chl degradation enzymes (Fig. 2) and also majority of the genes coding for Chl biosynthesis were downregulated (Table 4). This suggests a different mechanism of maintenance of Chl content by 3MeOBAPA and BAP and possibly the reason for the lower effectivity of 3MeOBAPA in this action.

Table 4. The expression level of some chlorophyll biosynthesis and degradation genes in Arabidopsis detached leaves after 48-h treatment with 10 μmol.l⁻¹ 3MeOBAPA.

Chlorophyll biosynthesis			Chlorophyll degradation		
gene ID	Gene name	Log$_2$ fold change	gene ID	Gene name	Log$_2$ fold change
AT1G03630	*PORC*	-0,84	AT4G13250	*NYC1*	-2,94
AT5G18660	*PCB2*	2,32	AT5G04900	*NOL*	-3,87
AT4G27440	*PORB*	-1,29	AT4G22920	*SGR1*	-1,01
AT2G26670	*HY1*	-2,82	AT1G31480	*SGR2*	-0,20
AT1G03475	*LIN2*	0,74	AT1G04620	*HCAR*	-1,72
AT1G44446	*CAO*	-2,01	AT4G27800	*PPH1*	-0,90
AT2G26540	*HEMD*	1,99	AT3G44880	*PAO*	-1,55
AT5G54190	*PORA*	-2,47	AT4G37000	*RCCR*	-0,86
AT1G08520	*CHLD*	-1,42	AT2G24820	*TIC55*	-2,49
AT3G14110	*FLU*	-1,40	AT3G03470	*CYP89A9*	-2,30
AT3G56940	*CRD1*	-1,48	AT4G16690	*MES16*	-3,01
AT4G01690	*PPO1*	-0,33	AT1G19670	*CLH1*	6,42
AT4G18480	*CHLI1*	-0,96	AT5G43860	*CLH2*	1,02
AT1G03475	*HEMF1*	0,74			
AT5G14220	*PPO2*	1,75			
AT5G63570	*GSA1*	1,34			

Interestingly, 3MeOBAPA strongly upregulated *CLH1* coding for chlorophyllase (Table 4), enzyme that catalyses the conversion of Chl to more hydrophilic compound, chlorophyllide. Chlorophyllase used to be considered the main enzyme of Chl degradation under stress conditions and during senescence (for recent review see Kuai et al. 2018). However, it has recently been revealed that CLH1 is not necessary for senescence-related chlorophyll breakdown (Schenk et al. 2007) and its main role lies rather in plant defence (Kariola et al. 2005, Hu et al. 2015). In Arabidopsis, silencing of *CLH1* increased plant susceptibility to necrotrophic fungus *Alternaria brassicicola* (Kariola et al., 2005). Contrarily, CLH1-overexpressing plants were toxic to larvae of *Spodoptera litura*, an insect herbivore. In intact cells, CLH1 is localized in endoplasmic reticulum and tonoplast, therefore is spatially separated from its substrate, chlorophyll. When plant tissue is damaged (e.g. by herbivores or necrotrophic fungi), cells are disrupted and CLH1 is capable to catalyse the hydrolysis of Chl to chlorophyllide (Hu et al., 2015). Similarly to other tetrapyrroles such as pheophorbide *a* (Vencl et al., 2009), chlorophyllide exerts toxic effects and acts as protecting agent in defence against insects (Hu et al., 2015). The strong upregulation of *CLH1* induced by 3MeOBAPA in Arabidopsis detached leaves suggests also an activation of this anti-herbivory system beside the PTI plant defence response.

4.8 Chloroplast maintenance

Since degradation of chloroplasts and changes in their structure occur during senescence (Zavaleta-Mancera et al. 1999), an effect of BAP and CK arabinosides on maintenance of chloroplasts was evaluated using confocal microscopy (Fig. 18). In the case of wheat, senescence-induced deterioration and aggregation of chloroplasts was most apparent in mock-treated leaves. Those changes were partially supressed in BAP- and 3MeOBAPA-treated leaves, while in 3OHBAPA the chloroplasts were highly maintained. In Arabidopsis mock-treated leaves, the autofluorescence of chloroplasts was no longer detectable suggesting complete chloroplast deterioration and the leaf tissue was severely impaired. This observation, together with results of pigment content (Fig. 17), implies more pronounced senescence in Arabidopsis compared to wheat. All used compounds supressed the senescence-induced changes, especially BAP and 3MeOBAPA.
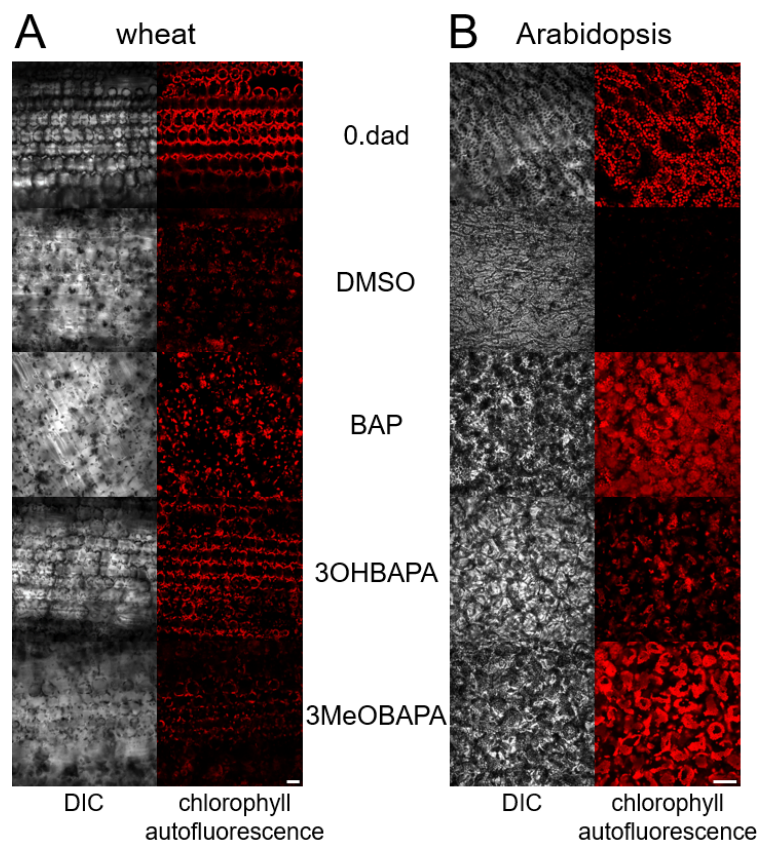

Figure 18. Confocal micrographs of freshly detached (0. dad) (**A**) wheat and (**B**) Arabidopsis leaves and leaves incubated in 0.1% DMSO or 10 μmol.l^{-1} solutions of BAP, 3MeOBAPA and 3OHBAPA in the dark for 6 days. Scale bars represent 50 μm. DIC, differential interference contrast. Reprinted from Kučerová et al. (2020).

4.9 PSII function

Measuring F_V/F_M affirmed that the CK arabinosides (especially 3OHBAPA in wheat and 3MeOBAPA in Arabidopsis) effectively maintain PSII function. To determine this action in more detailed way other Chl fluorescence parameters such as parameters derived from Chl fluorescence induction transient (OJIP curve) and quantum yields of Φ_P, Φ_{NPQ} and $\Phi_{f,D}$ (Fig. 19) were evaluated.

The OJIP curve was measured to monitor the rate of excitation supply to reaction center of PSII (RCII), reduction of primary electron acceptor of PSII (Q_A), and subsequent electron transport behind Q_A (Strasser et al. 2000) during the first (milli)seconds of illumination of dark-adapted leaves. In the mock-treated wheat leaves, both $(dV/dt)_0$ and V_J parameters increased indicating an acceleration of both excitation supply to RCII and Q_A reduction together with inhibition of electron transport behind Q_A. Almost the same increase in both parameters was found in the BAP- and 3MeOBAPA-treated leaves, but it was eliminated completely by 3OHBAPA (Fig. 19A, B). In the mock-treated Arabidopsis leaves $(dV/dt)_0$ decreased, while V_J increased to its maximal value (= 1). These changes indicate a strong impairment of PSII including minimal delivery of excitations to RCII and extreme inhibition of electron transfer from Q_A^-. The inhibition of the excitation supply to RCII could be related to the increased Chl a/b ratio (Fig. 17), which reflects higher degradation of LHCII compared to RCII (Leong & Anderson 1984). In the BAP-treated leaves, $(dV/dt)_0$ increased pronouncedly indicating stimulation of the excitation supply to RCII probably due to the suppression of preferential degradation of LHCII observed in mock-treated leaves (Fig. 17), whereas the electron transport behind Q_A^- was inhibited as $V_J = 0.98$ (Fig. 19A, B). 3OHBAPA maintained $(dV/dt)_0$ close to the value of freshly detached leaves, but it did not reduce the senescence-induced inhibition of electron transport behind Q_A ($V_J = 0.98$). On the other hand, 3MeOBAPA maintained both excitation supply to RCII and electron transport behind Q_A as values of $(dV/dt)_0$ and V_J were very similar to those of freshly detached leaves (Fig. 19A, B). The non-accelerated excitation supply to RCII corresponds to a higher degradation of LHCII in comparison to RCII indicated by increased Chl a/b ratio (Fig. 17) which is in line with the downregulation of genes coding for LHCII (Fig. 8). Interestingly, CK ribosides

synthesized by Vylíčilová et al. (2016) caused the upregulation of LHCII genes and an increase in the relative abundance of LHCII, implying a different mechanism of action of different types of CK derivatives such as CK arabinosides and CK ribosides (Vylíčilová et al. 2016).

Fig. 19. (**A**) The initial slope of the O–J Chl fluorescence rise (dV/dt)$_0$, (**B**) the relative variable fluorescence at the J step (V_J) and (**C**) quantum yields of photosystem II photochemistry (Φ_P), regulatory non-photochemical quenching (Φ_{NPQ}) and non-regulatory dissipation processes ($\Phi_{f,D}$) in freshly detached (0.dad) leaves and in detached leaves of wheat and Arabidopsis after six days in the dark-incubation in 0.1% DMSO, 10 µmol.l^{-1} solution of BAP, 3OHBAPA and 3MeOBAPA. Medians and quartiles are presented (n = 5-12). Different letters indicate a statistically significant difference between treatments within a plant species (*p* < 0.05; Student´s unpaired *t*-test). Reprinted from Kučerová et al. (2020).

Further information on senescence-induced changes in the PSII function was obtained by measurement of quantum yields Φ_P, Φ_{NPQ} and $\Phi_{f,D}$. These parameters, measured during exposition of leaves to actinic light, reflect the partitioning of absorbed light energy for PSII photochemistry (Φ_P) and for regulated (Φ_{NPQ}) and non-regulated ($\Phi_{f,D}$) non-photochemical processes (Lazár 2015). Steady-state values of Φ_P, Φ_{NPQ}, and $\Phi_{f,D}$ measured after a 7-min exposition of the senescent leaves to actinic light are discussed (Fig. 19C, Fig. 20). Decrease in Φ_P and Φ_{NPQ} and increase in $\Phi_{f,D}$ was found in mock-treated leaves of both wheat and Arabidopsis, while in Arabidopsis those changes were more pronounced (Fig. 19C, Fig. 20). These results again indicate very strong impairment of PSII function in senescent Arabidopsis leaves connected with the low ability of photosynthetic apparatus to regulate dissipation of excess light energy, which subsequently can result in oxidative damage (Triantaphylidès & Havaux 2009). The senescence-induced changes in the partitioning of absorbed light energy were partially reduced in the BAP-treated leaves of both wheat and Arabidopsis. The PSII photochemistry and regulatory non-photochemical quenching (Φ_P and Φ_{NPQ}, respectively) were more effective and the increase in the yield of non-regulated energy dissipation ($\Phi_{f,D}$) was lower compared to the mock-treated leaves (Fig. 19C, Fig. 20). Similarly to F_V/F_M (Table 3, Fig. 16) and OJIP transient parameters, the senescence-induced changes in the partitioning of absorbed light energy observed in mock-treated leaves were suppressed very effectively by 3OHBAPA in wheat and 3MeOBAPA in Arabidopsis (Fig. 19C, Fig. 20). While in these two cases CK arabinosides maintained the PSII function more effectively than BAP, protective effect of 3MeOBAPA in wheat and 3OHBAPA in Arabidopsis was comparable to that of BAP (Fig. 19C, Fig. 20). The high efficiency of 3MeOBAPA in Arabidopsis on the maintenance of the partitioning of absorbed light energy (documented by minimal changes of Φ_P, Φ_{NPQ} and $\Phi_{f,D}$; Fig. 19C, Fig. 20) could also be supported by the absence of increased delivery of excitations to RCII as it can contribute to the protection of photosynthetic apparatus from excess excitations.
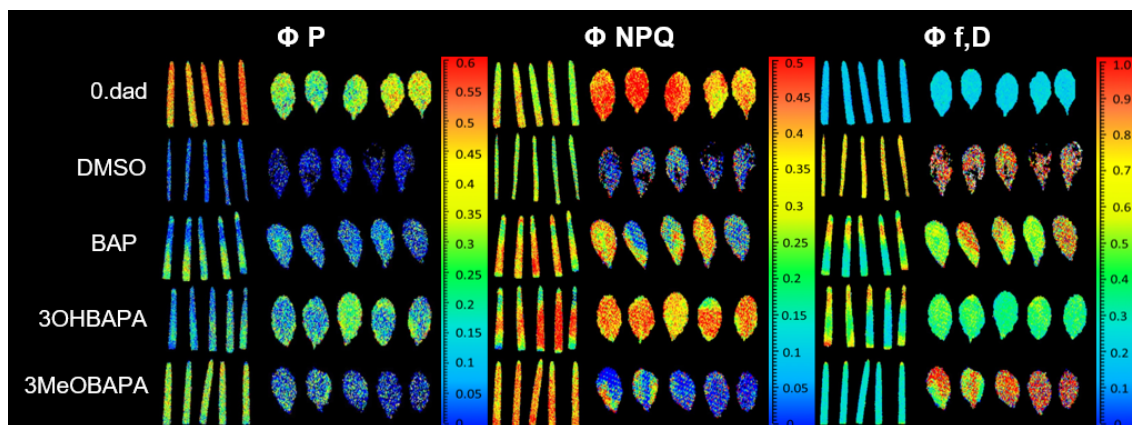
Fig. 20. Imaging of the effective quantum yield of photosystem II photochemistry (Φ_P), the quantum yield of regulatory light-induced non-photochemical quenching (Φ_{NPQ}) and the quantum yield of constitutive non-regulatory dissipation processes ($\Phi_{f,D}$) of freshly detached leaves (0.dad) and leaves incubated in 0.1% DMSO or 10 μmol.l^{-1} BAP, 3OHBAPA and 3MeOBAPA in the dark for 6 days. Steady-state values of Φ_P, Φ_{NPQ}, and $\Phi_{f,D}$ measured after a 7-min exposition of the senescent leaves to actinic light are presented.

In summary to the anti-senescence action of BAP and CK arabinosides, 3OHBAPA had the highest activity in wheat, followed by 3MeOBAPA and BAP, whose activity was similar. In Arabidopsis, 3MeOBAPA was less efficient than BAP in the maintenance of photosynthetic pigment content, but it was more effective in the maintenance of PSII function. At the same time, when compared to 3OHBAPA, 3MeOBAPA had higher anti-senescence activity, as documented by the changes in all studied parameters.

4.10 Ethylene production

It has been shown that different activity of anti-senescence compounds can be associated with their influence on ethylene production in the detached dark-incubated leaves (Nisler et al. 2018). As opposed to the positive effect of CKs on plant and leaf longevity, ethylene is known for being the accelerator of senescence (for recent review see Ceusters & Van de Poel 2018) and exogenous application of CKs stimulates the production of ethylene (Cary et al. 1995, for review see Zdarska et al. 2015). Thus, the rate of the stimulation of ethylene production by exogenously applied CK can co-determine a resultant senescence-delaying effect—i.e., the anti-senescence activity of CK. Therefore, we have evaluated the effect of the compounds on ethylene production in wheat and Arabidopsis leaves. As expected, the ethylene production in BAP-treated leaves was higher compared to the mock-treated leaves in both wheat and Arabidopsis

(Fig. 21). Interestingly, no stimulation of ethylene production was observed in the wheat leaves treated by 3OHBAPA and in Arabidopsis leaves treated by 3MeOBAPA, despite the increased ethylene production in shorterly (48 and 72 h) treated leaves (Fig. 11). A moderately stimulated ethylene production was observed in the 3MeOBAPA-treated wheat leaves and 3OHBAPA-treated leaves of Arabidopsis (Fig. 21). Thus, the differences in the rate of ethylene production corresponded generally to the quantitative differences of anti-senescence activity between BAP and CK arabinosides, as well as between 3OHBAPA and 3MeOBAPA: the lower the ethylene production, the higher the anti-senescence action.
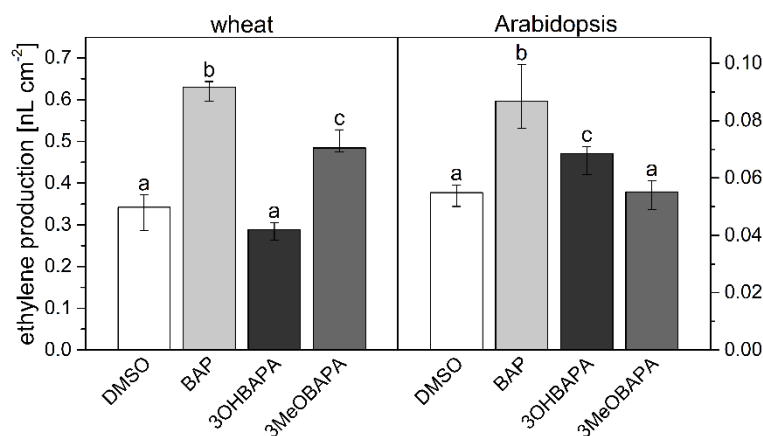
Fig. 21. Ethylene production in detached leaves of wheat and Arabidopsis incubated in 0.1% DMSO or 10 µmol.l⁻¹ solutions of BAP, 3OHBAPA and 3MeOBAPA and kept sealed in 8 ml vials in darkness for 6 days. Medians and quartiles are presented (n = 5–9). Different letters indicate a statistically significant difference between treatments within a plant species ($p < 0.05$; Student´s unpaired t-test). Reprinted Kučerová et al. (2020)

4.11 Senescence-related genes in 3MeOBAPA-treated Arabidopsis leaves

The transcriptomic analysis performed on 3MeOBAPA-treated (for 48 h) Arabidopsis leaves also revealed downregulation of some positive regulators of leaf senescence such as *SAG12*, *ORE1*, *ORE3* and *ORE9* (Weaver et al. 1998, Kim et al. 2011, 2018; Table 2) and upregulation of negative regulators of senescence such as *JAZ7* and *JAZ8* (Kim et al. 2018) confirming the anti-senescence activity of 3MeOBAPA at the molecular level. Upregulation was found also in the case of *JUB1*, *ELIP1* and *ELIP2* (Table 2). ELIPs (early-light induced proteins) belonging to the family of pigment-protein LHCs fulfil a protective function and prevent oxidative damage under conditions of excess

light (Hutin et al. 2003). Originally, the photoprotective function of ELIPs thought to consist in transient binding of free Chl and preventing formation of ROS, was predominantly found in developing leaves (e.g. Meyer & Kloppstech 1984). However, the protective role of ELIPs was reported also during senescence, although their upregulation was conditioned by the presence of light (Binyamin et al. 2001) and/or correlated with light intensity (Humbeck et al. 1994). Interestingly, 3MeOBAPA upregulated *ELIPs* even though the leaves were incubated in the dark. Thus, it seems that 3MeOBAPA had in a certain way similar effect to that of increased light, which is supported also by the reduction of LHCII/RCII ratio (indicated by increased Chl *a/b* ratio, Fig. 17), typical for leaf acclimation to higher light intensities. The mechanism of this unexpected effect of 3MeOBAPA remains to be elucidated.

The ROS-responsive transcription factor *JUB1* is considered to be a central longevity regulator in Arabidopsis which acts through modulation of H_2O_2 level in cells (Wu et al. 2012). It has been found that overexpression of *JUB1* not only delays senescence, but also enhances tolerance to abiotic stresses (Wu et al. 2012). An increased tolerance to various types of oxidative stress (including H_2O_2 treatment) has been reported also in detached leaves of Arabidopsis mutants *ore1*, *ore3* and *ore9* (Hye et al. 2004). Expression of both *JUB1* and *ORE*s was affected by 3MeOBAPA-treatment in Arabidopsis detached leaves (Table 2). It has also been shown that the inhibition of ethylene production not only delays leaf senescence but also enhances tolerance of plants to abiotic stresses, including H_2O_2- or HL- induced oxidative stress (Wi et al. 2010). Since no ethylene stimulation was found in 3OHBAPA-treated wheat leaves and 3MeOBAPA-treated Arabidopsis leaves (Fig. 21), this suggests, along with downregulation of *ORE*s and upregulation of *ELIP*s and *JUB1* induced by 3MeOBAPA treatment in Arabidopsis, protective function of CK arabinosides against oxidative damage. To confirm this hypothesis, we exposed the senescent leaves (kept in the dark for 6 days while incubated in BAP or CK arabinosides) to subsequent H_2O_2 or HL treatment to induce oxidative stress and investigated how the CK arabinosides affect a level of oxidative damage. For those experiments only the more effective CK arabinoside (meaning 3OHBAPA in wheat and 3MeOBAPA in Arabidopsis) was used to compare their effect with BAP.

4.12 Protection against induced oxidative damage

As mentioned above, for confirmation of the protective effect of CK arabinosides against oxidative damage, the senescent leaves were exposed to exogenous H_2O_2 (5 mmol.l^{-1}). The level of oxidative damage was evaluated using ultra-weak photon emission (UPE) as its intensity correlates with an extent of oxidative damage (Pospíšil et al. 2014). In wheat, the protective effect indicated by the lower UPE ratio was observed only in leaves treated with 3OHBAPA. In Arabidopsis, both BAP and 3MeOBAPA reduced the oxidative damage, 3MeOBAPA being more effective (Fig. 22).

Fig. 22. Ratio of ultra-weak photon emission (UPE) intensity after/before application of H_2O_2 in detached leaves of wheat and Arabidopsis dark-incubated for 6 days in 0.1% DMSO or 10 μmol.l^{-1} solutions of BAP, 3OHBAPA or 3MeOBAPA. Medians and quartiles are presented (n = 4). Different letters indicate a statistically significant difference between treatments within a plant species ($p < 0.05$; Student´s unpaired t-test). Reprinted from Kučerová et al. (2020).

In the following experiments, we exposed the senescent leaves to HL (500 μmol photons.m^{-2}.s^{-1}) and estimated cell membrane damage using the measurement of ion leakage by conductivity, accumulation of lipid hydroperoxides (LOOHs; as primary products of lipid peroxidation and markers of oxidative damage) by confocal microscopy, and maintenance of the maximal quantum yield of PSII photochemistry (F_V/F_M), which reflects the extent of photoinhibition or photodamage of PSII. The exposure of senescing mock-treated leaves to HL led to a strong oxidative damage, as indicated by progressive deterioration of cell membranes during 8 h of HL treatment (Fig. 23), and by LOOH accumulation (Fig. 24) and photoinhibition of PSII (Fig. 25) after 4 h of HL treatment.
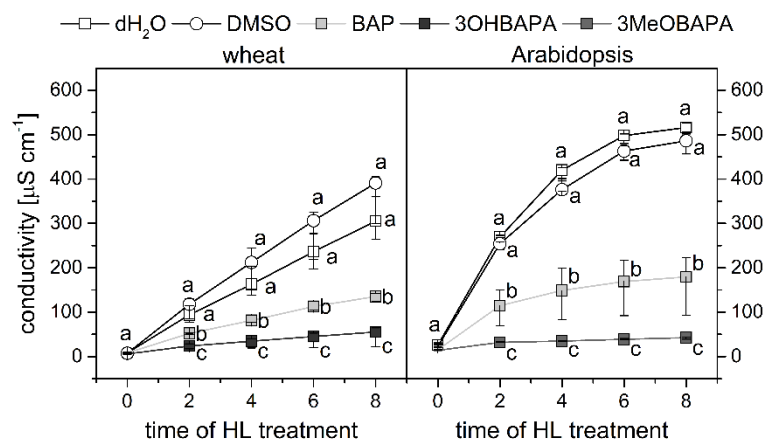
Fig. 23. Conductivity as a measure of cell membrane damage in wheat and Arabidopsis detached leaves incubated in deionized water (dH₂O), 0.1% DMSO, 10 μmol.l⁻¹ solutions of BAP, 3OHBAPA or 3MeOBAPA. Before high-light treatment (HL; 500 μmol photons.m⁻².s⁻¹) for up to 8 h leaves were incubated in the dark for 6 days. Medians and quartiles are presented (n = 7). Different letters indicate a statistically significant difference between treatments within a plant species (p < 0.05; Student′s unpaired t-test). Reprinted from Kučerová et al. (2020).

The oxidative damage was suppressed by the exogenous application of BAP, although its protective effect was quite low. The HL-induced membrane deterioration and PSII photoinhibition were attenuated in the BAP-treated leaves of both wheat and Arabidopsis; LOOH accumulation was reduced only in Arabidopsis (Figs. 23-25). It has been previously reported that action of CKs (including BAP) can switch from protective to damaging when their application is combined with excessive light conditions (Vlčková et al. 2006, Prokopová et al. 2010a). This negative CK effect is supposed to be a result of over-excitation of photosynthetic apparatus and related oxidative damage (Vlčková et al. 2006). We presume that was the case of the BAP-treated Arabidopsis leaves exposed to HL as the excitation supply to RCII in senescent leaves was increased (indicated by increased $(dV/dt)_0$; Fig. 19A) due to the higher LHCII/RCII ratio. The mentioned negative effect could reduce a protective action of BAP resulting in the relatively high oxidative damage indicated by LOOH accumulation (Fig. 24) and decrease in xanthophyll content (Fig. 26).
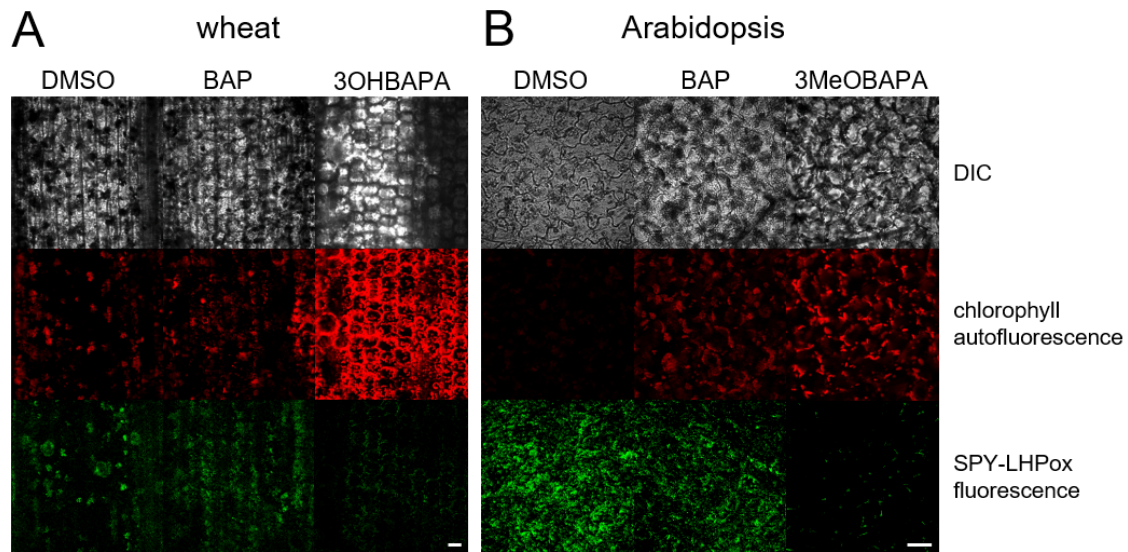
Fig. **24**. *In vivo* imaging of lipid hydroperoxides (LOOHs) using fluorescent probe SPY-LHP in (**A**) wheat and (**B**) Arabidopsis leaves kept in the dark for 6 days and subsequently exposed to high light (500 µmol photons.m^{-2}.s^{-1} for 4 h). Detached leaves were incubated in 10 µmol.l^{-1} solutions of BAP, 3OHBAPA or 3MeOBAPA. Scale bars represent 50 µm. DIC, differential interference contrast. Reprinted from Kučerová et al. (2020).

As we presumed, the CK arabinosides were more efficient than BAP in the protection of wheat and Arabidopsis leaves against HL-induced oxidative damage as indicated by the lower cell membrane deterioration, LOOH accumulation and PSII photoinhibition (Figs. 23-25). As chloroplast avoidance movement is one of the photoprotective mechanisms (for review see Li et al. 2009, Pinnola & Bassi 2018), its maintenance indicated by chloroplast positioning in the CK arabinoside-treated leaves exposed to HL (Fig. 24) could also contribute to the lower oxidative damage.

Fig. 25. (A) Imaging of maximum quantum yield of PSII photochemistry (F_V/F_M) before and after high-light treatment (HL; 500 μmol photons.m^{-2}.s^{-1} for 4 h) of freshly detached leaves and leaves incubated for 6 days in 0.1% DMSO or 10 μmol.l^{-1} solutions of BAP, 3OHBAPA or 3MeOBAPA; **(B)** the relative F_V/F_M values and **(C)** relative de-epoxidation state of xanthophylls (DEPS) in detached wheat and Arabidopsis leaves. The relative F_V/F_M and DEPS were calculated as a ratio of values measured after and before exposure to high light. In the column graphs, medians and quartiles estimated from presented values of individual leaves are shown (n = 5). Different letters indicate a statistically significant difference between treatments within a plant species ($p < 0.05$; Student´s unpaired t-test). Reprinted and adapted from Kučerová et al. (2020).

Nevertheless, we suppose that in case of the HL-treated wheat leaves the high protective effect of 3OHBAPA against oxidative damage consisted mainly in the completely maintained xanthophyll cycle (Fig. 25C) together with the high content of xanthophylls (Fig. 26). Both xanthophylls and xanthophyll cycle are well-known to have an important role in protection of leaves against HL, including senescent ones (Špundová et al. 2005). Xanthophylls are responsible for quenching triplet Chl excited states and singlet oxygen formed in LHC and RC complexes (for recent review see Pinnola & Bassi 2018). Within xantophyll cycle violaxanthin (V) is converted to antheraxathin (A) and zeaxanthin (Z) by violaxanthin-deepoxidase after its activation by decrease in thylakoid lumen pH and the excessive light energy is thermally dissipated (for review see Li et al. 2009, Triantaphylidès & Havaux 2009, Pinnola & Bassi 2018). Z itself is an effective ROS scavenger. Lutein is necessary for effective quenching of singlet oxygen, the major ROS involved in (photo)oxidative damage, while neoxanthin is believed to be effective in protecting PSII against O_2^{--} (Triantaphylidès & Havaux 2009, Ramel et al. 2012).

Unlike wheat, the xanthophyll cycle was only moderately more efficient in the 3MeOBAPA-treated Arabidopsis leaves in comparison with the BAP-treated ones (Fig. 25C), which corresponds to only slightly lower decrease in F_V/F_M after HL treatment (Fig. 25B). We suppose that the protective effect of 3MeOBAPA from PSII photoinhibition was related rather to the lower LHCII/RCII ratio and to the higher maintenance of xanthophylls during HL treatment (Fig. 26). The difference in the Chl *a/b* ratio observed in senescent leaves treated by BAP and 3MeOBAPA (Fig. 17) was deepened due to HL treatment (Fig. 26). Thehigher Chl *a/b* ratio in 3MeOBAPA-treated leaves reflects higher degradation of LHCII compared to RCII (Leong & Anderson 1984). Unlike only a little increased PSII photoprotection, 3MeOBAPA clearly surpassed BAP in the overall antioxidative effect as indicated by estimation of UPE, cell deterioration and LOOH accumulation (Fig. 22-24). This effective protection could be related to the above mentioned changes in gene expression, i.e., upregulation of *ELIPs* and *JUB1* and downregulation of *OREs* (Table 2). Interestingly, 3MeOBAPA has been shown to protect human dermal fibroblasts from UV-A and UV-B treatment (Doležal et al. 2016), thus the photoprotective activity of this compound may be more universal.
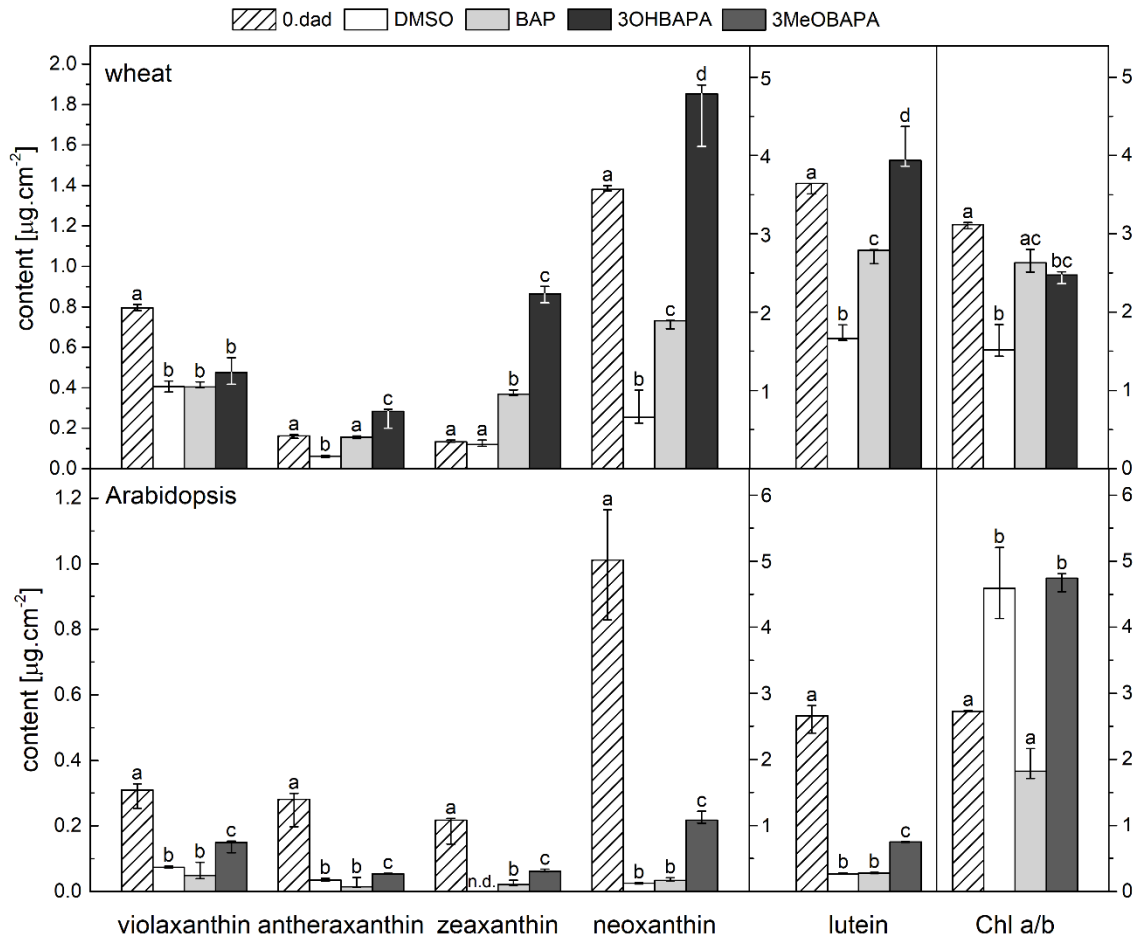
Fig. 26. Content of violaxanthin, antheraxanthin, zeaxanthin, neoxanthin and lutein; and chlorophyll *a/b* ratio in freshly detached leaves (0. dad) of wheat and Arabidopsis and in detached leaves incubated in 10 µmol.l⁻¹ solutions of BAP, 3OHBAPA or 3MeOBAPA. Leaves were kept in the dark for 6 days and subsequently exposed to high light (500 µmol photons.m⁻².s⁻¹ for 4 h). Medians and quartiles are presented (n = 3-5). Different letters indicate a statistically significant difference between treatments within a plant species (p<0.05, Student's unpaired *t*-test). n.d., not detectable.

4.13 On the mechanism of anti-senescence action of CK arabinosides

As can be seen from presented results, the unique mode of CK arabinosides' action differs from that of CKs. The CK arabinosides have only low activity in the Amaranthus and tobacco callus bioassays. However, their activity in the senescence bioassay was high, despite the fact that *in vitro* they did not activate the AHK3 receptor, which is considered to be the main receptor involved in CK-mediated delay of senescence (Riefler et al. 2006, Janečková et al. 2018) and protection during HL stress (Cortleven et al. 2014). The RNA-seq gene expression analysis (Fig. 3, Table 2) in Arabidopsis 3MeOBAPA-treated leaves revealed a broad range of transcriptomic changes typical for the activation of the PAMP-response: down-regulation of a number of photosynthetic genes and upregulation of defence genes. A similar response can be expected in BAPAs-treated wheat and barley plants, as their enhanced resistance to pathogens was observed in field trial experiments (Fig. 14). The upregulation of genes of defence regulons in the 3MeOBAPA-treated Arabidopsis leaves included jasmonate/ethylene-driven upregulation of PDFs and was accompanied by a significant elevation of endogenous levels of ethylene, ROS together with JA and its metabolites (Fig. 11).

However, despite the increased ethylene production in Arabidopsis leaves treated by 3MeOBAPA for 48 and 72 h, the ethylene production after 6 days of dark-incubation in appropriate solutions of the CK arabinosides was low (Fig. 21). As ethylene is known to promote leaf senescence (Ceusters & Van de Poel 2018) low ethylene production by CK arabinosides-treated senescing leaves might be one of the main reasons for the CK arabinosides' high anti-senescence activity. The differencies in ethylene production between early and long-term response to 3MeOBAPA treatment suggest that elevated production of ethylene have only signalling function and later it is attenuated.

It has been reported that the key transcription factor of ethylene signalling pathway EIN3 and its downstream target ORE1 directly activate genes of Chl degradation (Table 4). ORE1 also directly promotes ethylene synthesis and ethylene in turn accelerates leaf senescence through EIN3–ORE1 (Qiu et al. 2015). Since *EIN3* and *ORE1* were downregulated by 3MeOBAPA (Table 2), it indicates that the attenuation of this loop is involved in the anti-senescence activity of 3MeOBAPA. This activity is evidenced also by the downregulation of other positive regulators of senescence, such as *SAG12,*

ORE3, and *ORE9* (Table 2). In summary, the anti-senescence effect of CK arabinosides in Arabidopsis may be related to specific downregulation of the EIN3/ORE1 pathway which has been previously shown to be involved in leaf degreening through Chl catabolic genes regulation (Qiu et al. 2015).

Similarly to ethylene, JA is considered to be a positive regulator of leaf senescence. As mentioned, the level of JA and its metabolites was found to be increased in the 3MeOBAPA-treated Arabidopsis leaves (Fig. 11). However, similarly to ethylene, this increase was only temporary – it was observed after 48 h of the treatment (Fig. 11), while after 4 and 8 days the JA level was lower than that in the mock-treated leaves (Fig. 27). The transient increase in endogenous JA content appears to be involved in triggering the defence response by 3MeOBAPA and does not stimulate, but rather suppresses leaf senescence. This hypothesis is in line with the upregulation of the JA-signalling repressors *JAZ7* and *JAZ 8* (Table 2), as JAZ7 is known to be a specific negative regulator of dark-induced leaf senescence and together with JAZ8 suppresses the activation of *SAGs* including *SAG12* (Yu et al. 2016, Kim et al. 2018).
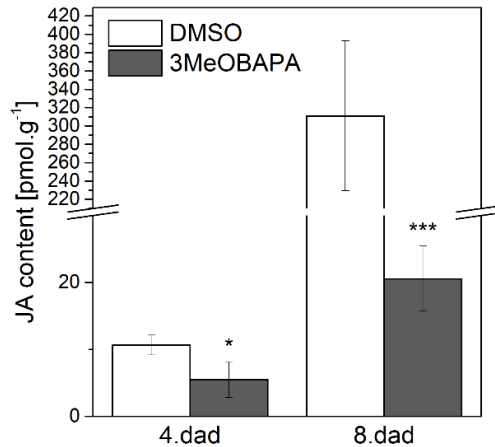
Fig. 27. Content of jasmonic acid (JA) in detached Arabidopsis leaves in 0.1% DMSO or 10 µmol.l^{-1} 3MeOBAPA for 4 and 8 days. Means and SD are presented (n = 4-5). Asterisks indicate statistically significant difference between 3MeOBAPA treatment and mock (DMSO) treatment (***, $p < 0.001$; **, $p < 0.01$; *, $p < 0.05$, Student´s unpaired t-test).

Consistent to ethylene and JA and its isoforms, the ROS content was increased shortly after application of 3MeOBAPA (Fig. 11) but was lower compared to mock-treatment in senescing leaves subsequently exposed to HL (Fig. 24), indicating that ROS in 3MeOBAPA-treated leaves play role in defence response signalling.

5 Conclusions and future perspectives

It is well known that leaf senescence can be suppressed by exogenous application of CKs. Nevertheless, under specific conditions CKs can possess negative effects and can even accelerate senescence. For this reason there are efforts to prepare compounds based on CKs that lack these effects and have other advantageous properties. Recently, two aromatic CK arabinosides, 3OHBAPA and 3MeOBAPA, have been synthesized and found to possess unique effects and mechanism of action. The RNA-seq profiling study that was performed on detached Arabidopsis leaves treated with 3MeOBAPA revealed that short (6 h) and extended (48 h) treatments with this compound result in the shift in transcriptional response toward defence. 3MeOBAPA affects genes involved in processes associated with plant innate immunity and its activation of MAPK signalling pathway together with oxidative burst and JA-ethylene signalling result in effective protection of field-grown plants against various pathogens. Interestingly, long-term incubation of leaves in 3OHBAPA and 3MeOBAPA solutions does not impair leaf fitness which is common in prolonged activation of defence response mechanisms, but on the contrary effectively delays senescence. CK arabinosides anti-senescence action in detached dark-adapted leaves differs quantitatively in wheat and Arabidopsis. In wheat, 3OHBAPA has higher protective effect than 3MeOBAPA, whereas in Arabidopsis, 3MeOBAPA is the more efficient derivative. We have found that the different anti-senescent activity of 3OHBAPA and 3MeOBAPA is coupled to different ethylene production in the treated leaves: the lower the ethylene production, the higher the anti-senescence activity. 3OHBAPA and 3MeOBAPA also protects efficiently the senescing leaves against oxidative damage induced by both H_2O_2 and high-light treatment, which could also be connected with the low level of ethylene production.

The specific effects described in this work represent evidence that CK arabinosides possess unique activity while acting through a mechanism different from that of classical CKs. Since they have high anti-senescence activity and protective effects under biotic and abiotic stress conditions they are promising substances for plant protection. However, further study is needed to elucidate the exact mechanism of their action. In future research, experiments using various Arabidopsis mutant plants are

planned to explore the mechanism of action in more detailed way. For example, due to possible involvement of OREs in 3MeOBAPA signalling pathway, the knockout mutants *ore1, ore3 and ore9* will be studied. Similarly, as the increased ROS production as an early response to 3MeOBAPA treatment is probably connected to upregulation of RBOH, experiments using *rbohD* and *rbohF* are planned to corroborate this relationship. In the near future, the research will also focus on more precise studies using different species of plant pathogens such as *Alternaria brassiciccola* as another necrotrophic pathogen beside *B. cinerea,* or *Pseudomonas syringae* DC3000 to evaluate effect of CK arabinosides on infection by biotrophic pathogens. Based on the literature and results obtained in this thesis, we presume that mechanism of Chl maintenance in senescing leaves treated by CK arabinosides and BAP differs. For this reason we would like to compare Chl degradation products and activity of Chl degradation enzymes in CK arabinosides- and BAP-treated senescing leaves. Importantly, comparative proteomic and transcriptomic analyses of leaves or seedlings treated by isoprenoid, aromatic and urea CKs together with corresponding derivatives are already in the process of preparation.

6 References

Amasino R (2005) 1955: Kinetin arrives. The 50th anniversary of a new plant hormone. *Plant Physiology* 138: 1177–1184.

Aremu AO, Bairu MW, Doležal K, Finnie JF, Van Staden J (2012) Topolins: A panacea to plant tissue culture challenges? *Plant Cell, Tissue and Organ Culture* 108: 1–16.

Argueso CT, Ferreira FJ, Epple P, To JPC, Hutchison CE, Schaller GE, Dangl JL, Kieber JJ (2012) Two-component elements mediate interactions between cytokinin and salicylic acid in plant immunity. *PLoS Genetics* 8: e1002448.

Arnoux P, Morosinotto T, Saga G, Bassi R, Pignol D (2009) A structural basis for the ph-dependent xanthophyll cycle in *Arabidopsis thaliana*. *Plant Cell* 21: 2036–2044.

Attaran E, Major IT, Cruz JA, Rosa BA, Koo AJK, Chen J, Kramer DM, He SY, Howe GA (2014) Temporal dynamics of growth and photosynthesis suppression in response to jasmonate signaling. *Plant Physiology* 165: 1302–1314.

Bairu MW, Jain N, Stirk WA, Doležal K, Van Staden J (2009) Solving the problem of shoot-tip necrosis in *Harpagophytum procumbens* by changing the cytokinin types, calcium and boron concentrations in the medium. *South African Journal of Botany* 75: 122–127.

Bairu MW, Stirk WA, Doležal K, Van Staden J (2007) Optimizing the micropropagation protocol for the endangered Aloe polyphylla: Can meta-topolin and its derivatives serve as replacement for benzyladenine and zeatin? *Plant Cell, Tissue and Organ Culture* 90: 15–23.

Bethke G, Pecher P, Eschen-Lippold L, Tsuda K, Katagiri F, Glazebrook J, Scheel D, Lee J (2012) Activation of the *Arabidopsis thaliana* Mitogen-activated protein kinase MPK11 by the flagellin-derived elicitor peptide, flg22. *Molecular Plant-Microbe Interactions* 25: 471–480.

Bhattacharjee S (2005) Reactive oxygen species and oxidative burst: Roles in stress, senescence and signal transduction in plants. *Current science* 89: 1113–1121.

Biddington ANL, Thomas TH (1973) A modified Amaranthus betacyanin bioassay for the rapid determination of cytokinins in plant extracts. *Planta* 111: 183–186.

Bigeard J, Colcombet J, Hirt H (2015) Signaling mechanisms in pattern-triggered

immunity (PTI). *Molecular Plant* 8: 521–539.

Bilgin DD, Zavala JA, Zhu J, Clough SJ, Ort DR, Delucia EH (2010) Biotic stress globally downregulates photosynthesis genes. *Plant, Cell and Environment* 33: 1597–1613.

Binyamin L, Falah M, Portnoy V, Soudry E, Gepstein S (2001) The early light-induced protein is also produced during leaf senescence of *Nicotiana tabacum*. *Planta* 212: 591–597.

Biswal B (1995) Carotenoid catabolism during leaf senescence and its control by light. *Journal of Photochemistry and Photobiology, B: Biology* 30: 3–13.

Breeze E, Harrison E, McHattie S, Hughes L, Hickman R, Hill C et al. (2011) High-resolution temporal profiling of transcripts during Arabidopsis leaf senescence reveals a distinct chronology of processes and regulation. *Plant Cell* 23: 873–894.

Bryksová M, Dabravolski S, Kučerová Z, Zavadil Kokáš F, Špundová M, Plíhalová L et al. (2020) Aromatic cytokinin arabinosides promote PAMP-like responses and positively regulate leaf longevity. *ACS Chemical Biology* 15: 1949–1963.

Buchanan-Wollaston V (1994) Isolation of cDNA clones for genes that are expressed during leaf senescence in Brassica napus. Identification of a gene encoding a senescence-specific metallothionein-like protein. *Plant Physiology* 105: 839–846.

Buchanan-Wollaston V, Page T, Harrison E, Breeze E, Pyung OL, Hong GN et al. (2005) Comparative transcriptome analysis reveals significant differences in gene expression and signalling pathways between developmental and dark/starvation-induced senescence in Arabidopsis. *Plant Journal* 42: 567–585.

Carimi F, Terzi M, De Michele R, Zottini M, Lo Schiavo F (2004) High levels of the cytokinin BAP induce PCD by accelerating senescence. *Plant Science* 166: 963–969.

Cary AJ, Liu Wennuan, Howell SH (1995) Cytokinin action is coupled to ethylene in its effects on the inhibition of root and hypocotyl elongation in *Arabidopsis thaliana* seedlings. *Plant Physiology* 107: 1075–1082.

Ceusters J, Van de Poel B (2018) Ethylene exerts species-specific and age-dependent control of photosynthesis. *Plant Physiology* 176: 2601–2612.

Choi J, Choi D, Lee S, Ryu CM, Hwang I (2011) Cytokinins and plant immunity: Old foes or new friends? *Trends in Plant Science* 16: 388–394.

Choi J, Huh SU, Kojima M, Sakakibara H, Paek KH, Hwang I (2010) The cytokinin-

activated transcription factor ARR2 promotes plant immunity via TGA3/NPR1-dependent salicylic acid signaling in arabidopsis. *Developmental Cell* 19: 284–295.

Cortleven A, Nitschke S, Klaumünzer M, AbdElgawad H, Asard H, Grimm B, Riefler M, Schmülling T (2014) A novel protective function for cytokinin in the light stress response is mediated by the ARABIDOPSIS HISTIDINE KINASE2 and ARABIDOPSIS HISTIDINE KINASE3 receptors. *Plant Physiology* 164: 1470–1483.

Cortleven A, Schmülling T (2015) Regulation of chloroplast development and function by cytokinin. *Journal of Experimental Botany* 66: 4999–5013.

Dai J, Gao H, Dai Y, Zou Q (2004) Changes in activity of energy dissipating mechanisms in wheat flag leaves during senescence. *Plant Biology* 6: 171–177.

Diaz-Mendoza M, Velasco-Arroyo B, Santamaria ME, González-Melendi P, Martinez M, Diaz I (2016) Plant senescence and proteolysis: Two processes with one destiny. *Genetics and Molecular Biology* 39: 329–338.

Doležal K, Popa I, Hauserová E, Spíchal L, Chakrabarty K, Novák O et al. (2007) Preparation, biological activity and endogenous occurrence of N6-benzyladenosines. *Bioorganic and Medicinal Chemistry* 15: 3737–3747.

Doležal K, Plíhalová L, Vylíčilová H, Zatloukal M, Plíhal O, Voller J, Strnad M, Bryksová M, Vostálová J, Rajnochová Svobodová A, Ulrichová J, Spíchal L (2016) 6-aryl-9-glycosylpurines and use thereof. U.S. Patent 10,100,077.

Eschen-Lippold L, Bethke G, Palm-Forster MAT, Pecher P, Bauer N, Glazebrook J, Scheel D, Lee J (2012) MPK11-a fourth elicitor-responsive mitogen-activated protein kinase in Arabidopsis thaliana. *Plant Signaling and Behavior* 7: 1203–1205.

Eschen-Lippold L, Jiang X, Elmore JM, Mackey D, Shan L, Coaker G, Scheel D, Lee J (2016) Bacterial AvrRpt2-like cysteine proteases block activation of the Arabidopsis mitogen-activated protein kinases, MPK4 and MPK11. *Plant Physiology* 171: 2223–2238.

Floková K, Tarkowská D, Miersch O, Strnad M, Wasternack C, Novák O (2014) UHPLC-MS/MS based target profiling of stress-induced phytohormones. *Phytochemistry* 105: 147–157.

Gajdošová S, Spíchal L, Kamínek M, Hoyerová K, Novák O, Dobrev PI et al. (2011) Distribution, biological activities, metabolism, and the conceivable function of *cis-*

zeatin-type cytokinins in plants. *Journal of Experimental Botany* 62: 2827–2840.

Gan S, Amasino RM (1995) Inhibition of leaf senescence by autoregulated production of cytokinin. *Science* 270: 1986–1988.

Gan S, Amasino RM (1997) Making sense of senescence: Molecular genetic regulation and manipulation of leaf senescence. *Plant Physiology* 113: 313–319.

Gepstein S, Sabehi G, Carp MJ, Hajouj T, Nesher MFO, Yariv I, Dor C, Bassani M (2003) Large-scale identification of leaf senescence-associated genes. *Plant Journal* 36: 629–642.

Gilmore AM, Björkman O (1994) Adenine nucleotides and the xanthophyll cycle in leaves - II. Comparison of the effects of CO2- and temperature-limited photosynthesis on photosystem II fluorescence quenching, the adenylate energy charge and violaxanthin de-epoxidation in cotton. *Planta* 192: 537–544.

Girondé A, Etienne P, Trouverie J, Bouchereau A, Le Cahérec F, Leport L et al. (2015) The contrasting N management of two oilseed rape genotypes reveals the mechanisms of proteolysis associated with leaf N remobilization and the respective contributions of leaves and stems to N storage and remobilization during seed filling. *BMC Plant Biology* 15.

Göhre V, Jones AME, Sklenář J, Robatzek S, Weber APM (2012) Molecular crosstalk between PAMP-triggered immunity and photosynthesis. *Molecular Plant-Microbe Interactions* 25: 1083–1092.

Gómez-Gómez L, Felix G, Boller T (1999) A single locus determines sensitivity to bacterial flagellin in *Arabidopsis thaliana*. *Plant Journal* 18: 277–284.

Gonzalez-Rizzo S, Crespi M, Frugier F (2006) The Medicago truncatula CRE1 cytokinin receptor regulates lateral root development and early symbiotic interaction with *Sinorhizobium meliloti*. *Plant Cell* 18: 2680–2693.

Guo Y, Cai Z, Gan S (2004) Transcriptome of Arabidopsis leaf senescence. *Plant, Cell and Environment* 27: 521–549.

Guo FQ, Crawford NM (2005) Arabidopsis nitric oxide synthase1 is targeted to mitochondria and protects against oxidative damage and dark-induced senescence. *Plant Cell* 17: 3436–3450.

Hann DR, Domínguez-Ferreras A, Motyka V, Dobrev PI, Schornack S, Jehle A et al.

(2014) The Pseudomonas type III effector HopQ1 activates cytokinin signaling and interferes with plant innate immunity. *New Phytologist* 201: 585–598.

Hauenstein M, Christ B, Das A, Aubry S, Hörtensteiner S (2016) A role for TIC55 as a hydroxylase of Phyllobilins, the products of chlorophyll breakdown during plant senescence. *Plant Cell* 28: 2510–2527.

Havé M, Marmagne A, Chardon F, Masclaux-Daubresse C (2017) Nitrogen remobilization during leaf senescence: Lessons from Arabidopsis to crops. *Journal of Experimental Botany* 68: 2513–2529.

Hendrickson L, Furbank RT, Chow WS (2004) A simple alternative approach to assessing the fate of absorbed light energy using chlorophyll fluorescence. *Photosynthesis Research* 82: 73–81.

Himelblau E, Amasino RM (2001) Nutrients mobilized from leaves of *Arabidopsis thaliana* during leaf senescence. *Journal of Plant Physiology* 158: 1317–1323.

Holub J, Hanuš J, Hanke DE, Strnad M (1998) Biological activity of cytokinins derived from Ortho- and Meta-hydroxybenzyladenine. *Plant Growth Regulation* 26: 109–115.

Hörtensteiner S, Kräutler B (2011) Chlorophyll breakdown in higher plants. *Biochimica et Biophysica Acta - Bioenergetics* 1807: 977–988.

Hu X, Makita S, Schelbert S, Sano S, Ochiai M, Tsuchiya T et al. (2015) Reexamination of chlorophyllase function implies its involvement in defense against chewing herbivores. *Plant Physiology* 167: 660–670.

Humbeck K, Kloppstech K, Krupinska K (1994) Expression of early light-inducible proteins in flag leaves of field-grown barley. *Plant Physiology* 105: 1217–1222.

Hutin C, Nussaume L, Moise N, Moya I, Kloppstech K, Havaux M (2003) Early light-induced proteins protect Arabidopsis from photooxidative stress. *Proceedings of the National Academy of Sciences of the United States of America* 100: 4921–4926.

Hye RW, Jin HK, Hong GN, Pyung OL (2004) The delayed leaf senescence mutants of Arabidopsis, *ore1*, *ore3*, and *ore9* are tolerant to oxidative stress. *Plant and Cell Physiology* 45: 923–932.

Inoue T, Higuchi M, Hashimoto Y, Seki M, Kobayashi M, Kato T, Tabata S, Shinozaki K, Kakimoto T (2001) Identification of CRE1 as a cytokinin receptor from Arabidopsis. *Nature* 409: 1060–1063.

Iqbal M, Ashraf M, Jamil A (2006) Seed enhancement with cytokinins: Changes in growth and grain yield in salt stressed wheat plants. *Plant Growth Regulation* 50: 29–39.

Janečková H, Husičková A, Ferretti U, Prčina M, Pilařová E, Plačková L, Pospíšil P, Doležal K, Špundová M (2018) The interplay between cytokinins and light during senescence in detached Arabidopsis leaves. *Plant Cell and Environment* 41: 1870–1885.

Janečková H, Husičková A, Lazár D, Ferretti U, Pospíšil P, Špundová M (2019) Exogenous application of cytokinin during dark senescence eliminates the acceleration of photosystem II impairment caused by chlorophyll *b* deficiency in barley. *Plant Physiology and Biochemistry* 136: 43–51.

Järvi S, Gollan PJ, Aro EM (2013) Understanding the roles of the thylakoid lumen in photosynthesis regulation. *Frontiers in Plant Science* 4: 434.

Juers DH, Matthews BW, Huber RE (2012) LacZ β-galactosidase: Structure and function of an enzyme of historical and molecular biological importance. *Protein Science* 21: 1792–1807.

Kalaji HM, Schansker G, Brestic M, Bussotti F, Calatayud A, Ferroni L et al. (2017) *Frequently asked questions about chlorophyll fluorescence, the sequel*.

Kalaji HM, Schansker G, Ladle RJ, Goltsev V, Bosa K, Allakhverdiev SI et al. (2014) Frequently asked questions about in vivo chlorophyll fluorescence: Practical issues. *Photosynthesis Research* 122: 121–158.

Kariola T, Brader G, Li J, Palva ET (2005) Chlorophyllase 1, a damage control enzyme, affects the balance between defense pathways in plants. *Plant Cell* 17: 282–294.

Khanna-Chopra R (2012) Leaf senescence and abiotic stresses share reactive oxygen species-mediated chloroplast degradation. *Protoplasma* 249: 469–481.

Kim JH, Chung KM, Woo HR (2011) Three positive regulators of leaf senescence in Arabidopsis, ORE1, ORE3 and ORE9, play roles in crosstalk among multiple hormone-mediated senescence pathways. *Genes and Genomics* 33: 373–381.

Kim J, Kim JH, Lyu J Il, Woo HR, Lim PO (2018) New insights into the regulation of leaf senescence in Arabidopsis. *Journal of Experimental Botany* 69: 787–799.

Kim HJ, Ryu H, Hong SH, Woo HR, Lim PO, Lee IC, Sheen J, Nam HG, Hwang I (2006)

Cytokinin-mediated control of leaf longevity by AHK3 through phosphorylation of ARR2 in Arabidopsis. *Proceedings of the National Academy of Sciences of the United States of America* 103: 814–819.

Kim J, Ryun Woo H, Gil Nam H (2016) Toward systems understanding of leaf senescence: An integrated multi-omics perspective on leaf senescence research. *Molecular Plant* 9: 813–825.

Koprna R, De Diego N, Dundálková L, Spíchal L (2016) Use of cytokinins as agrochemicals. *Bioorganic and Medicinal Chemistry* 24: 484–492.

Kuai B, Chen J, Hörtensteiner S (2018) The biochemistry and molecular biology of chlorophyll breakdown. *Journal of Experimental Botany* 69: 751–767.

Kučerová Z, Rác M, Mikulík J, Plíhal O, Pospíšil P, Bryksová M, Sedlářová M, Doležal K, Špundová M (2020) The anti-senescence activity of cytokinin arabinosides in wheat and Arabidopsis is negatively correlated with ethylene production. *International Journal of Molecular Sciences* 21: 8109.

Lazár D (2015) Parameters of photosynthetic energy partitioning. *Journal of Plant Physiology* 175: 131–147.

Leong TY, Anderson JM (1984) Adaptation of the thylakoid membranes of pea chloroplasts to light intensities. II. Regulation of electron transport capacities, electron carriers, coupling factor (CF1) activity and rates of photosynthesis. *Photosynthesis Research* 5: 117–128.

Li Z, Wakao S, Fischer BB, Niyogi KK (2009) Sensing and responding to excess light. *Annual Review of Plant Biology* 60: 239–260.

Lichtenthaler HK (1987) Chlorophylls and carotenoids: Pigments of photosynthetic biomembranes. *Methods in Enzymology* 148: 350–382.

Lim PO, Woo HR, Nam HG (2003) Molecular genetics of leaf senescence in Arabidopsis. *Trends in Plant Science* 8: 272–278.

Liu L, Li H, Zeng H, Cai Q, Zhou X, Yin C (2016) Exogenous jasmonic acid and cytokinin antagonistically regulate rice flag leaf senescence by mediating chlorophyll degradation, membrane deterioration, and senescence-associated genes expression. *Journal of Plant Growth Regulation* 35: 366–376.

Lomin SN, Krivosheev DM, Steklov MY, Osolodkin DI, Romanov GA (2012) Receptor

properties and features of cytokinin signaling. *Acta Naturae* 4: 31–45.

Maillard A, Diquélou S, Billard V, Laîné P, Garnica M, Prudent M, Garcia-Mina JM, Yvin JC, Ourry A (2015) Leaf mineral nutrient remobilization during leaf senescence and modulation by nutrient deficiency. *Frontiers in Plant Science* 6: 317.

Mayta ML, Hajirezaei MR, Carrillo N, Lodeyro AF (2019) Leaf senescence: the chloroplast connection comes of age. *Plants* 8: 1–18.

Meyer G, Kloppstech K (1984) A rapidly light-induced chloroplast protein with a high turnover coded for by pea nuclear DNA. *European Journal of Biochemistry* 138: 201–207.

Mik V, Szücová L, Šmehilová M, Zatloukal M, Doležal K, Nisler J et al. (2011a) N9-substituted derivatives of kinetin: Effective anti-senescence agents. *Phytochemistry* 72: 821–831.

Mik V, Szücová L, Spíchal L, Plíhal O, Nisler J, Zahajská L, Doležal K, Strnad M (2011b) N9-substituted N6-[(3-methylbut-2-en-1-yl)amino]purine derivatives and their biological activity in selected cytokinin bioassays. *Bioorganic and Medicinal Chemistry* 19: 7244–7251.

Miller G, Schlauch K, Tam R, Cortes D, Torres MA, Shulaev V, Dangl JL, Mittler R (2009) The plant NADPH oxidase RBOHD mediates rapid systemic signaling in response to diverse stimuli. *Science Signaling* 2.

Mittler R (2002) Oxidative stress, antioxidants and stress tolerance. *Trends in Plant Science* 7: 405–410.

Mittler R, Vanderauwera S, Gollery M, Van Breusegem F (2004) Reactive oxygen gene network of plants. *Trends in Plant Science* 9: 490–498.

Mok DW, Mok MC (2001) Cytokinin metabolism and action. *Annual Review of Plant Physiology and Plant Molecular Biology* 52: 89–118.

Naseem M, Philippi N, Hussain A, Wangorsch G, Ahmed N, Dandekara T (2012) Integrated systems view on networking by hormones in Arabidopsis immunity reveals multiple crosstalk for cytokinin. *Plant Cell* 24: 1793–1814.

Nisler J, Zatloukal M, Popa I, Doležal K, Strnad M, Spíchal L (2010) Cytokinin receptor antagonists derived from 6-benzylaminopurine. *Phytochemistry* 71: 823–830.

Nisler J, Zatloukal M, Sobotka R, Pilný J, Zdvihalová B, Novák O, Strnad M, Spíchal L

(2018) New urea derivatives are effective anti-senescence compounds acting most likely via a cytokinin-independent mechanism. *Frontiers in Plant Science* 9: 1225.

Noodén LD, Guiamét JJ, John I (1997) Senescence mechanisms. *Physiologia Plantarum* 101: 746–753.

Noodén LD, Hillsberg JW, Schneider MJ (1996) Induction of leaf senescence in *Arabidopsis thaliana* by long days through a light-dosage effect. *Physiologia Plantarum* 96: 491–495.

Oh MH, Kim JH, Zulfugarov IS, Moon YH, Rhew TH, Lee CH (2005) Effects of benzyladenine and abscisic acid on the disassembly process of photosystems in an Arabidopsis delayed-senescence mutant, *ore9*. *Journal of Plant Biology* 48: 170–177.

Pinnola A, Bassi R (2018) Molecular mechanisms involved in plant photoprotection. *Biochemical Society Transactions* 46: 467–482.

Plíhalová L, Vylíčilová H, Doležal K, Zahajská L, Zatloukal M, Strnad M (2016) Synthesis of aromatic cytokinins for plant biotechnology. *New Biotechnology* 33: 614–624.

Podlešáková K, Zalabák D, Čudejková M, Plíhal O, Szüčová L, Doležal K, Spíchal L, Strnad M, Galuszka P (2012) Novel cytokinin derivatives do not show negative effects on root growth and proliferation in submicromolar range. *PLoS ONE* 7: e39293.

Pospíšil P, Prasad A, Rác M (2014) Role of reactive oxygen species in ultra-weak photon emission in biological systems. *Journal of Photochemistry and Photobiology B: Biology* 139: 11–23.

Prokopová J, Mieslerová B, Hlaváčková V, Hlavinka J, Lebeda A, Nauš J, Špundová M (2010a) Changes in photosynthesis of *Lycopersicon* spp. plants induced by tomato powdery mildew infection in combination with heat shock pre-treatment. *Physiological and Molecular Plant Pathology* 74: 205–213.

Prokopová J, Špundová M, Sedlářová M, Husičková A, Novotný R, Doležal K, Nauš J, Lebeda A (2010b) Photosynthetic responses of lettuce to downy mildew infection and cytokinin treatment. *Plant Physiology and Biochemistry* 48: 716–723.

Pružinská A, Tanner G, Aubry S, Anders I, Moser S, Müller T et al. (2005) Chlorophyll breakdown in senescent Arabidopsis leaves. Characterization of chlorophyll catabolites and of chlorophyll catabolic enzymes involved in the degreening

reaction. *Plant Physiology* 139: 52–63.

Qiu K, Li Z, Yang Z, Chen J, Wu S, Zhu X et al. (2015) EIN3 and ORE1 accelerate degreening during ethylene-mediated leaf senescence by directly activating chlorophyll catabolic genes in Arabidopsis. *PLoS Genetics* 11: 1–20.

Ramel F, Birtic S, Cuiné S, Triantaphylidès C, Ravanat JL, Havaux M (2012) Chemical quenching of singlet oxygen by carotenoids in plants. *Plant Physiology* 158: 1267–1278.

Riefler M, Novak O, Strnad M, Schmülling T (2006) Arabidopsis cytokinin receptors mutants reveal functions in shoot growth, leaf senescence, seed size, germination, root development, and cytokinin metabolism. *Plant Cell* 18: 40–54.

Del Río LA (2015) ROS and RNS in plant physiology: An overview. *Journal of Experimental Botany* 66: 2827–2837.

Roháček K (2002) Chlorophyll fluorescence parameters: the definitions, photosynthetic meaning, and mutual relationships. *Photosynthetica* 40: 13–29.

Roháček K, Barták M (1999) Technique of the modulated chlorophyll fluorescence: Basic concepts, useful parameters, and some applications. *Photosynthetica* 37: 339–363.

Romanov GA, Kieber JJ, Schmülling T (2002) A rapid cytokinin response assay in Arabidopsis indicates a role for phospholipase D in cytokinin signalling. *FEBS Letters* 515: 39–43.

Romanov GA, Lomin SN, Schmülling T (2006) Biochemical characteristics and ligand-binding properties of Arabidopsis cytokinin receptor AHK3 compared to CRE1/AHK4 as revealed by a direct binding assay. *Journal of Experimental Botany* 57: 4051–4058.

Rosenvasser S, Mayak S, Friedman H (2006) Increase in reactive oxygen species (ROS) and in senescence-associated gene transcript (SAG) levels during dark-induced senescence of Pelargonium cuttings, and the effect of gibberellic acid. *Plant Science* 170: 873–879.

Rottet S, Devillers J, Glauser G, Douet V, Besagni C, Kessler F (2016) Identification of plastoglobules as a site of carotenoid cleavage. *Frontiers in Plant Science* 7: 1855.

Rulcová J, Pospíšilová J (2001) Effect of benzylaminopurine on rehydration of bean plants after water stress. *Biologia Plantarum* 44: 75–81.

Schenk N, Schelbert S, Kanwischer M, Goldschmidt EE, Dörmann P, Hörtensteiner S (2007) The chlorophyllases AtCLH1 and AtCLH2 are not essential for senescence-related chlorophyll breakdown in *Arabidopsis thaliana*. *FEBS Letters* 581: 5517–5525.

Schippers JHM, Schmidt R, Wagstaff C, Jing HC (2015) Living to die and dying to live: The survival strategy behind leaf senescence. *Plant Physiology* 169: 914–930.

Sedlářová M, Petřivalský M, Piterková J, Luhová L, Kočířová J, Lebeda A (2011) Influence of nitric oxide and reactive oxygen species on development of lettuce downy mildew in Lactuca spp. *European Journal of Plant Pathology* 129: 267–280.

Sewelam N, Kazan K, Schenk PM (2016) Global plant stress signaling: Reactive oxygen species at the cross-road. *Frontiers in Plant Science* 7: 187.

Simeonova E, Sikora A, Charzynska M, Mostowska A (2000) Aspects of programmed cell death during leaf senescence of mono- and dicotyledonous plants. *Protoplasma* 214: 93–101.

Smart BYCM (1994) Tansley Review No. 64 Gene expression during leaf senescence. *New Phytologist*: 419–448.

Spíchal L (2012) Cytokinins - Recent news and views of evolutionally old molecules. *Functional Plant Biology* 39: 267–284.

Spíchal L, Rakova NY, Riefler M, Mizuno T, Romanov GA, Strnad M, Schmülling T (2004) Two cytokinin receptors of Arabidopsis thaliana, CRE1/AHK4 and AHK3, differ in their ligand specificity in a bacterial assay. *Plant and Cell Physiology* 45: 1299–1305.

Spicher L, Kessler F (2015) Unexpected roles of plastoglobules (plastid lipid droplets) in vitamin K1 and E metabolism. *Current Opinion in Plant Biology* 25: 123–129.

Springer A, Kang C, Rustgi S, Von Wettstein D, Reinbothe C, Pollmann S, Reinbothe S (2016) Programmed chloroplast destruction during leaf senescence involves 13-lipoxygenase (13-LOX). *Proceedings of the National Academy of Sciences of the United States of America* 113: 3383–3388.

Špundová M, Popelkova H, Ilik P, Skotnica J, Novotný R, Nauš J (2003) Ultra-structural and functional changes in the chloroplasts of detached barley leaves senescing under dark and light conditions. *Journal of Plant Physiology* 160: 1051–1058.

Špundová M, Strzałka K, Nauš J (2005) Xanthophyll cycle activity in detached barley

leaves senescing under dark and light. *Photosynthetica* 43: 117–124.

Stotz HU, Thomson JG, Wang Y (2009) Plant defensins: defense, development and application. *Plant signaling & behavior* 4: 1010–1012.

Strasser R, Srivastava A, Tsimilli-Michael M (2000) The fluorescence transient as a tool to characterize and screen photosynthetic samples. In: *Probing Photosynthesis: Mechanism, Regulation & Adaptation.* Yunus M, Pathre U, Mohanty P, Eds. Taylor & Francis: New York, NY, USA. pp.445-483.

Strnad M (1997) The aromatic cytokinins. *Physiologia Plantarum* 101: 674–688.

Suzuki T, Miwa K, Ishikawa K, Yamada H, Aiba H, Mizuno T (2001) The Arabidopsis sensor His-kinase, AHK4, can respond to cytokinins. *Plant and Cell Physiology* 42: 107–113.

Swarbrick PJ, Schulze-Lefert P, Scholes JD (2006) Metabolic consequences of susceptibility and resistance (race-specific and broad-spectrum) in barley leaves challenged with powdery mildew. *Plant, Cell and Environment* 29: 1061–1076.

Szüčová L, Spíchal L, Doležal K, Zatloukal M, Greplová J, Galuszka P et al. (2009) Synthesis, characterization and biological activity of ring-substituted 6-benzylamino-9-tetrahydropyran-2-yl and 9-tetrahydrofuran-2-ylpurine derivatives. *Bioorganic and Medicinal Chemistry* 17: 1938–1947.

Talla SK, Panigrahy M, Kappara S, Nirosha P, Neelamraju S, Ramanan R (2016) Cytokinin delays dark-induced senescence in rice by maintaining the chlorophyll cycle and photosynthetic complexes. *Journal of Experimental Botany* 67: 1839–1851.

Tamary E, Nevo R, Naveh L, Levin-Zaidman S, Kiss V, Savidor A et al. (2019) Chlorophyll catabolism precedes changes in chloroplast structure and proteome during leaf senescence. *Plant Direct* 3: 1–18.

Tarkowská D, Doležal K, Tarkowski P, Åstot C, Holub J, Fuksová K, Schmülling T, Sandberg G, Strnad M (2003) Identification of new aromatic cytokinins in *Arabidopsis thaliana* and *Populus x canadensis* leaves by LC-(+)ESI-MS and capillary liquid chromatography/frit-fast atom bombardment mass spectrometry. *Physiologia Plantarum* 117: 579–590.

Thompson JE, Legge RL, Barber RF (1987) The role of free radicals in senescence and wounding. *New Phytologist* 105: 317–344.

To JPC, Kieber JJ (2008) Cytokinin signaling: two-components and more. *Trends in Plant Science* 13: 85–92.

Triantaphylidès C, Havaux M (2009) Singlet oxygen in plants: production, detoxification and signaling. *Trends in Plant Science* 14: 219–228.

Ueguchi C, Koizumi H, Suzuki T, Mizuno T (2001a) Novel family of sensor histidine kinase genes in *Arabidopsis thaliana*. *Plant and Cell Physiology* 42: 231–235.

Ueguchi C, Sato S, Kato T, Tabata S (2001b) The AHK4 gene involved in the cytokinin-signaling pathway as a direct receptor molecule in *Arabidopsis thaliana*. *Plant and Cell Physiology* 42: 751–755.

Vlčková A, Špundová M, Kotabová E, Novotný R, Doležal K, Nauš J (2006) Protective cytokinin action switches to damaging during senescence of detached wheat leaves in continuous light. *Physiologia Plantarum* 126: 257–267.

Vylíčilová H, Bryksová M, Matušková V, Doležal K, Plíhalová L, Strnad M (2020) Naturally occurring and artificial n9-cytokinin conjugates: From synthesis to biological activity and back. *Biomolecules* 10: 1–29.

Vylíčilová H, Husičková A, Spíchal L, Srovnal J, Doležal K, Plíhal O, Plíhalová L (2016) C2-substituted aromatic cytokinin sugar conjugates delay the onset of senescence by maintaining the activity of the photosynthetic apparatus. *Phytochemistry* 122: 22–33.

Weaver LM, Gan S, Quirino B, Amasino RM (1998) A comparison of the expression patterns of several senescence-associated genes in response to stress and hormone treatment. *Plant Molecular Biology* 37: 455–469.

Werbrouck SPO, Strnad M, Van Onckelen HA, Debergh PC (1996) Meta-topolin, an alternative to benzyladenine in tissue culture? *Physiologia Plantarum* 98: 291–297.

Werner T, Köllmer I, Bartrina I, Holst K, Schmülling T (2006) New insights into the biology of cytokinin degradation. *Plant Biology* 8: 371–381.

Wi SJ, Jang SJ, Park KY (2010) Inhibition of biphasic ethylene production enhances tolerance to abiotic stress by reducing the accumulation of reactive oxygen species in *Nicotiana tabacum*. *Molecules and Cells* 30: 37–49.

Withers J, Dong X (2017) Post-translational regulation of plant immunity. *Current Opinion in Plant Biology* 38: 124–132.

Woo HR, Goh CH, Park JH, De La Serve BT, Kim JH, Park Y Il, Nam HG (2002) Extended leaf longevity in the ore4-1 mutant of Arabidopsis with a reduced expression of a plastid ribosomal protein gene. *Plant Journal* 31: 331–340.

Woodward EJ, Marshal C (1988) Effects of plant growth regulators on tiller bud outgrowth in Barley (*Hordeum distichum* L.). *Annals of Botany* 61: 347–354.

Wu A, Allu AD, Garapati P, Siddiqui H, Dortay H, Zanor MI et al. (2012) JUNGBRUNNEN1, a reactive oxygen species-responsive NAC transcription factor, regulates longevity in Arabidopsis. *Plant Cell* 24: 482–506.

Yamada H, Suzuki T, Terada K, Takei K, Ishikawa K, Miwa K, Yamashino T, Mizuno T (2001) The arabidopsis AHK4 histidine kinase is a cytokinin-binding receptor that transduces cytokinin signals across the membrane. *Plant and Cell Physiology* 42: 1017–1023.

Yoshida S (2003) Molecular regulation of leaf senescence. *Current Opinion in Plant Biology* 6: 79–84.

Yu J, Zhang Y, Di C, Zhang Q, Zhang K, Wang C et al. (2016) JAZ7 negatively regulates dark-induced leaf senescence in Arabidopsis. *Journal of Experimental Botany* 67: 751–762.

Zatloukal M, Gemrotová M, Doležal K, Havlíček L, Spíchal L, Strnad M (2008) Novel potent inhibitors of *A. thaliana* cytokinin oxidase/dehydrogenase. *Bioorganic and Medicinal Chemistry* 16: 9268–9275.

Zavaleta-Mancera HA, López-Delgado H, Loza-Tavera H, Mora-Herrera M, Trevilla-García C, Vargas-Suárez M, Ougham H (2007) Cytokinin promotes catalase and ascorbate peroxidase activities and preserves the chloroplast integrity during dark-senescence. *Journal of Plant Physiology* 164: 1572–1582.

Zavaleta-Mancera HA, Thomas BJ, Thomas H, Scott IM (1999) Regreening of senescent Nicotiana leaves. II. Redifferentiation of plastids. *Journal of Experimental Botany* 50: 1683–1689.

Zdarska M, Dobisová T, Gelová Z, Pernisová M, Dabravolski S, Hejátko J (2015) Illuminating light, cytokinin, and ethylene signalling crosstalk in plant development. *Journal of Experimental Botany* 66: 4913–4931.

Zhang J, Li H, Xu B, Li J, Huang B (2016) Exogenous melatonin suppresses dark-induced

leaf senescence by activating the superoxide dismutase-catalase antioxidant pathway and down-regulating chlorophyll degradation in excised leaves of perennial ryegrass (*Lolium perenne* L.). *Frontiers in Plant Science* 7: 1500.

Zhu P, Xu L, Zhang C, Toyoda H, Gan SS (2012) Ethylene produced by *Botrytis cinerea* can affect early fungal development and can be used as a marker for infection during storage of grapes. *Postharvest Biology and Technology* 66: 23–29.

Zimmermann P, Zentgraf U (2005) The correlation between oxidative stress and leaf senescence during plant development. *Cellular and Molecular Biology Letters* 10: 515–534.

Zubo YO, Yamburenko M V., Selivankina SY, Shakirova FM, Avalbaev AM, Kudryakova N V. et al. (2008) Cytokinin stimulates chloroplast transcription in detached barley leaves. *Plant Physiology* 148: 1082–1093.

Zwack PJ, Rashotte AM (2013) Cytokinin inhibition of leaf senescence. *Plant Signaling and Behavior* 8: e24737.

7 Appendix

Bryksová M, Dabravolski S, **Kučerová Z**, Zavadil Kokáš F, Špundová M, Plíhalová L, Takáč T, Gruz J, Hudeček M, Hloušková V, Koprna R, Novák O, Strnad M, Plíhal O, Doležal K (2020) Aromatic cytokinin arabinosides promote PAMP-like responses and positively regulate leaf longevity. *ACS Chemical Biology* 15: 1949–1963.

Kučerová Z, Rác M, Mikulík J, Plíhal O, Pospíšil P, Bryksová M, Sedlářová M, Doležal K, Špundová M (2020) The anti-senescence activity of cytokinin arabinosides in wheat and Arabidopsis is negatively correlated with ethylene production. *International Journal of Molecular Sciences* 21: 8109.

Aromatic Cytokinin Arabinosides Promote PAMP-like Responses and Positively Regulate Leaf Longevity

Magdaléna Bryksová,[∇] Siarhei Dabravolski,[∇] Zuzana Kučerová,[∇] Filip Zavadil Kokáš, Martina Špundová, Lucie Plíhalová, Tomáš Takáč, Jiří Grúz, Martin Hudeček, Veronika Hloušková, Radoslav Koprna, Ondřej Novák, Miroslav Strnad, Ondřej Plíhal,* and Karel Doležal

ACCESS | Metrics & More | Article Recommendations | Supporting Information

ABSTRACT: Cytokinins are plant hormones with biological functions ranging from coordination of plant growth to the regulation of biotic and abiotic stress-related responses and senescence. The components of the plant immune system can learn from past elicitations by microbial pathogens and herbivores and adapt to new threats. It is known that plants can enter the primed state of enhanced defense induced by either natural or synthetic compounds. While the involvement of cytokinins in defense priming has been documented, no comprehensive model of their action has been provided to date. Here, we report the functional characterization of two aromatic cytokinin derivatives, 6-benzylaminopurine-9-arabinosides (BAPAs), 3-methoxy-BAPA and 3-hydroxy-BAPA, that proved to be effective in delaying senescence

in detached leaves while having low interactions with the cytokinin pathway. An RNA-seq profiling study on *Arabidopsis* leaves treated with 3-methoxy-BAPA revealed that short and extended treatments with this compound shifted the transcriptional response markedly toward defense. Both treatments revealed upregulation of genes involved in processes associated with plant innate immunity such as cell wall remodeling and upregulation of specific MAP kinases, most importantly *MPK11*, which is a MAPK module involved in stress-related signaling during the pathogen-associated molecular patterns (PAMPs) response. In addition, elevated levels of JA and its metabolites, jasmonate/ethylene-driven upregulation of *PLANT DEFENSIN 1.2* (*PDF1.2*) and other defensins, and also temporarily elevated levels of reactive oxygen species marked the plant response to 3-methoxy-BAPA treatment. Synergistic interactions were observed when plants were cotreated with 3-hydroxy-BAPA and the flagellin-derived bacterial PAMP peptide (flg22), leading to the enhanced expression of the PAMP-triggered immunity (PTI) marker gene *FRK1*. Our data collectively show that some BAPAs can sensitively prime the PTI responses in a low micromolar range of concentrations while having no observable negative effects on the overall fitness of the plant.
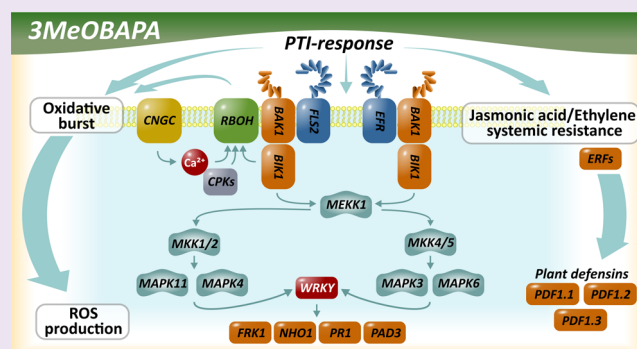
INTRODUCTION

Naturally occurring cytokinins (CKs) are purine-based molecules that promote cell division, regulate growth and differentiation, and orchestrate many physiological processes in plants.[1] They also help suppress leaf senescence[2,3] and are involved in complex phytohormone-regulated plant response mechanisms to various pathogens.[4] In plants, CKs can exist as free bases but are more commonly found in the form of glucosides, nucleosides, or nucleotides depending on the cell type, developmental phase, and environmental conditions. CK content and activity are tightly controlled by enzymatic degradation or glucosylation of free bases. Glucose conjugation to CKs may occur at the purine *N3*, *N7*, or *N9* atoms (*N*-glucosylation), generating terminal CK metabolites, or at the oxygen of the zeatin/dihydrozeatin side chain (*O*-glucosylation). Whereas CK *N*-glucosides are considered to be irreversibly deactivated, *O*-glucosides can be converted back

into active free bases by *β*-glucosidases.[5] Another way to selectively regulate plant physiology is to modulate plants CK status using cytokinin analogues or inhibitors that affect specific aspects of CK sensing and metabolism.[6−8]
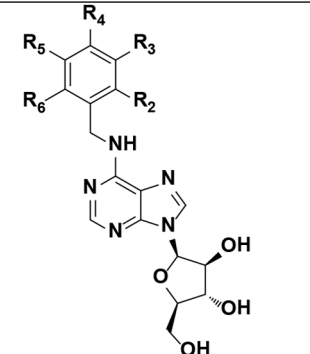
N⁶-benzylaminopurine (BAP) is an aromatic cytokinin (ArCK) that is widely used in micropropagation because of its low cost and high biological activity, which is largely due to its resistance to degradation.[9] For a relatively long period, most ArCKs were regarded as synthetic compounds with limited usefulness. However, a detailed characterization of plant

Table 1. Structure−Activity Relationship Studies of 6-Benzylaminopurine-9-β-D-arabinosides Tested in This Work[a]

			Amaranthus assay		Senescence assay		Tobacco callus assay	
			Optimal concentration (mol/L)	Relative activity (%)	Optimal concentration (mol/L)	Relative activity (%)	Optimal concentration (mol/L)	Relative activity (%)
# ID	MW	R_x =						
1	357.37	R_{2-6} = H	10^{-4}	19($\pm$1)	10^{-4}	138($\pm$5)	10^{-4}	34($\pm$5)
2	375.36	R_2 = F	10^{-4}	13($\pm$2)	10^{-4}	138($\pm$12)	10^{-4}	32($\pm$9)
3	375.36	R_3 = F	10^{-4}	31($\pm$7)	10^{-4}	140($\pm$9)	10^{-7}	15($\pm$4)
4	375.36	R_4 = F	10^{-4}	9($\pm$1)	10^{-4}	134($\pm$11)	10^{-4}	73($\pm$9)
5	391.81	R_2 = Cl	10^{-4}	15($\pm$2)	10^{-4}	99($\pm$6)	10^{-4}	20($\pm$2)
6	391.81	R_3 = Cl	10^{-4}	13($\pm$4)	10^{-4}	121($\pm$6)	10^{-4}	40($\pm$1)
7	391.81	R_4 = Cl	10^{-5}	10($\pm$3)	10^{-8}	13($\pm$1)	10^{-8}	12($\pm$2)
8	483.27	R_3 = I	10^{-4}	5($\pm$2)	10^{-8}	29($\pm$4)	10^{-7}	8($\pm$1)
9	483.27	R_4 = I	10^{-4}	12($\pm$4)	10^{-4}	53($\pm$4)	10^{-5}	12($\pm$2)
10	387.40	R_2 = CH$_3$O	10^{-4}	4($\pm$1)	10^{-4}	174($\pm$11)	10^{-4}	30($\pm$4)
11	387.40	R_3 = CH$_3$O	10^{-4}	7($\pm$2)	10^{-4}	119($\pm$8)	10^{-4}	26($\pm$3)
12	387.40	R_4 = CH$_3$O	10^{-5}	0	10^{-4}	40($\pm$3)	10^{-8}	23($\pm$5)
13	373.37	R_3 = OH	10^{-4}	8($\pm$1)	10^{-4}	180($\pm$7)	10^{-4}	32($\pm$2)
14	371.40	R_2 = CH$_3$	10^{-4}	5($\pm$1)	10^{-7}	49($\pm$5)	10^{-6}	22($\pm$3)
15	371.40	R_3 = CH$_3$	10^{-4}	4($\pm$1)	10^{-4}	152($\pm$7)	10^{-4}	36($\pm$5)
16	371.40	R_4 = CH$_3$	10^{-4}	0	10^{-7}	62($\pm$7)	10^{-6}	23($\pm$6)
17	372.39	R_2 = NH$_2$	10^{-5}	2($\pm$1)	10^{-7}	91($\pm$6)	10^{-4}	22($\pm$2)
18	425.37	R_3 = CF$_3$		n.t.		n.t.		n.t.
19	441.37	R_3 = OCF$_3$		n.t.		n.t.		n.t.
20	393.35	$R_{2,5}$ = F	10^{-4}	27($\pm$6)	10^{-4}	113($\pm$12)	10^{-9}	6($\pm$1)
21	393.35	$R_{3,5}$ = F	10^{-4}	15($\pm$3)	10^{-4}	156($\pm$11)	10^{-8}	29($\pm$5)

[a]All compounds except of **1** were modified at the benzyl ring with a single or double substitution (remaining R's are hydrogens). Relative activity of the newly synthesized cytokinin derivatives was assessed in standardized cytokinin bioassays: the Amaranthus assay, wheat leaf senescence, and tobacco callus assays. The reported values are activities expressed as percentages of the activity of the control compound (BAP), measured at the concentration yielding the maximum positive effect. Thus, a relative activity of 100% indicates that the given compound has the same activity as 10 μM BAP in the case of the Amaranthus betacyanin bioassay, 100 μM BAP in the case of the senescence bioassay, and 1 μM BAP in the case of the tobacco callus bioassay. n.t.: not tested.

regulators including the ArCKs 6-(2-hydroxybenzylamino)-purine (ortho-topolin), 6-(3-hydroxybenzylamino)purine (meta-topolin), and their ribosides revealed them to have strong activity in classical cytokinin bioassays.[10] Structure−activity relationship analyses established that the biological activity of these ArCKs depends on the position of the substituent on the benzyl ring and is commonly increased by the presence of a hydroxy or methoxy group in the meta position.[9,11]

Over the past decade, we have synthesized and evaluated several CK derivatives with different modifications at the N9-, C2-, C8-, and C6-positions of the purine moiety by exploiting combinatorial synthetic strategies.[3,9,12−15] In most of these derivatives, N9 substitution plays a central role because it prevents the unfavorable glucosylation that renders the final CK-N9-glucoside biologically inactive. To identify active derivatives resistant to N-glucosylation, N9-ribosylated BAP derivatives bearing variously substituted benzyl rings were

prepared and tested.[16] A series of kinetin-N9-substituted derivatives was prepared with various attached alkyl halides at N9 atom of purine exhibiting promising biological activities including the ability to reduce membrane lipid peroxidation, which is a typical symptom of senescence.[13] 2,6-Disubstituted BAPR derivatives with halogen substituents at the meta position of the benzyl ring exhibited significant activity in a detached wheat leaf senescence bioassay that correlated with their ability to reprogram the expression of many photosynthesis-related genes.[3] Several N9-tetrahydropyran-2-ylated and N9-tetrahydrofuran-2-ylated ArCKs were also synthesized and shown to exhibit strong antisenescent effects as well as significantly lower cytotoxicity in breast carcinoma cells (MCF-7) and human foreskin fibroblasts (BJ) than previously prepared N9-ribosides.[12] The metabolism of two ArCKs bearing a tetrahydropyranyl substituent at N9 atom, 6-benzylamino-9-(tetrahydropyran-2-yl)purine (BA9THPP) and 6-(3-methoxybenzylamino)-9-(tetrahydropyran-2-yl)-
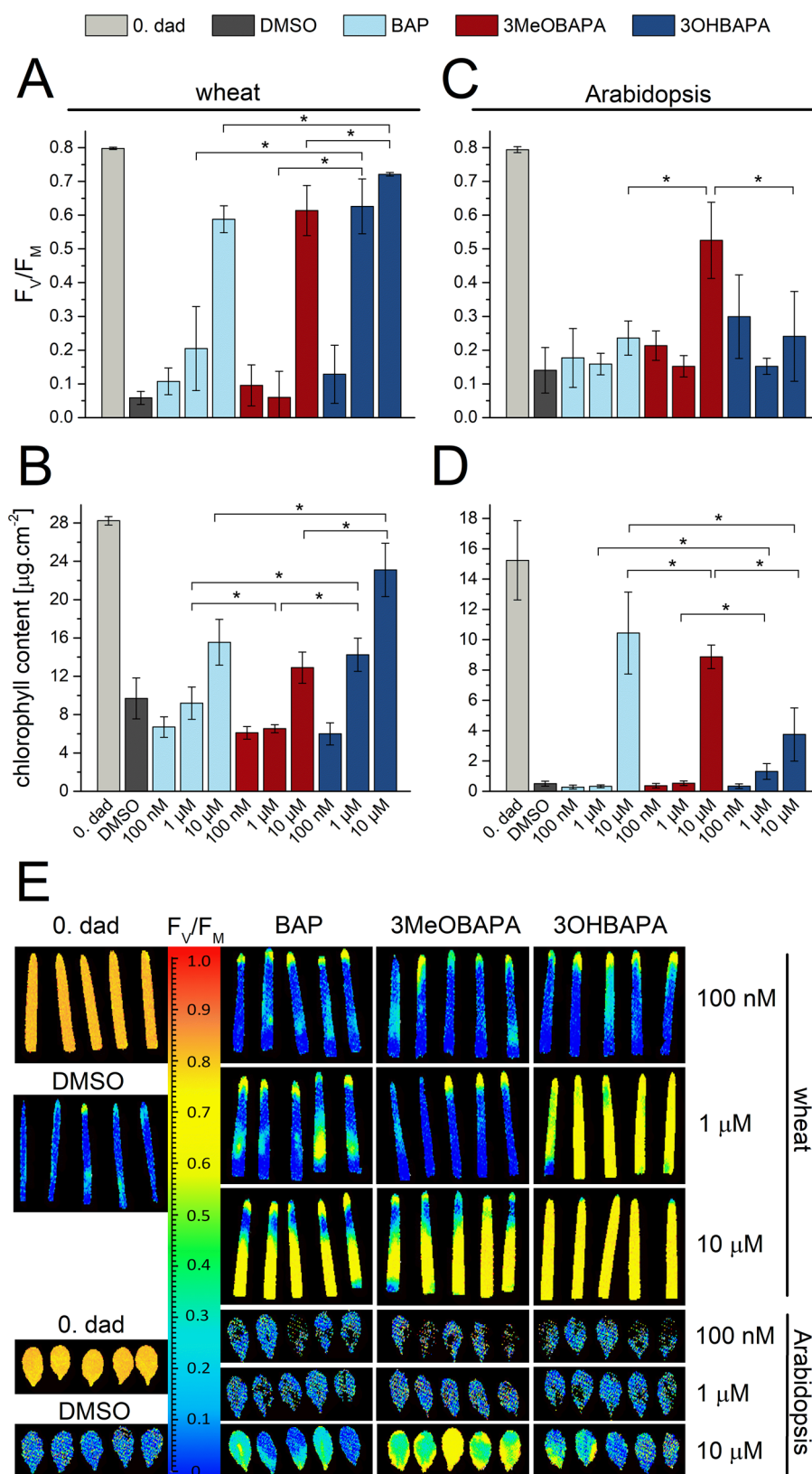
Figure 1. Effect of two 6-benzylaminopurine-9-β-D-arabinosides on detached wheat and *Arabidopsis* leaves. The maximum quantum yield of photosystem II photochemistry (F_V/F_M; A, C and E) and chlorophyll content (B, D) in leaves of wheat and *Arabidopsis* measured immediately after detachment (0. dad) and after 6 days' dark incubation in aqueous DMSO (0.1%) or aqueous DMSO solutions of BAP, 3-methoxy-BAP (3MeOBAPA), or 3-hydroxy-BAP (3OHBAPA). Concentration-dependent effect of BAP, 3-methoxy-BAP, and 3-hydroxy-BAP treatments is depicted as F_V/F_M in wheat leaves (E, top) and *Arabidopsis* leaves (E, bottom) using color-coding shown in the figure. The bar charts show means $\pm$ SD estimated from measurements of the individual leaves (n = 5) imaged in panel (E). Asterisks indicate statistically significant differences at the tested concentrations according to Student's unpaired t test ($P < 0.05$).

purine (3MeOBA9THPP), was studied in maize. The N9-THP substitution of the parental ArCK significantly enhanced the acropetal transport of these derivatives, enabling a slow gradual release of the active base from the synthetic precursor.[9]

Arabinosyl nucleosides such as fludarabine (9-β-D-arabinosyl-2-fluoroadenine, F-ara-A) and its derivatives are biologically active compounds with important antitumor activity.[17] In humans, several ArCK derivatives[16] and F-ara-A[18] seem to affect the differentiation of certain cancer cells by interfering with cell cycle regulation. Moreover, some of these adenine derivatives such as 6-chloropurine arabinoside possess potent activity against varicella-zoster virus (VZV) and other viruses.[19] Other arabinosyl nucleosides including (2'S)-2'-deoxy-2'-fluoro-5-ethynyluridine, F-ara-EdU exhibit selective DNA labeling but have negligible effects on genomic stability and function.[20] The activity of these compounds in plants has not yet been explored, but arabinose is a vital component of various lipopolysaccharides and oligosaccharides and is also found in antimicrobial flavonoids.[21]

One of the aims of this work was to create a new class of CK derivatives that retain the antisenescence activity of ArCKs without the negative effects on root/shoot development typically associated with CK use in plants.[12,22] The biological activity of the newly prepared CK derivatives was tested in standard CK bioassays and bacterial receptor assays. Two derivatives with strong senescence-delaying activity were further tested by performing chlorophyll fluorescence measurements to assess their ability to maintain photosynthetic function in detached wheat and *Arabidopsis* leaves. RNA-seq analysis of detached dark-incubated *Arabidopsis* leaves treated with one of these derivatives revealed significant reprogramming of gene expression leading to the primed state of enhanced defense with several marker genes of PAMP-triggered immunity (PTI) response being affected by either short or extended treatment with the compound. Our previous results showed that several ArCKs and their derivatives interact only weakly with CK receptors, suggesting that their antistress/antisenescent activity may be at least partly due to a parallel mechanism that is distinct from the standard CK pathway.[23] The results presented here show that ArCK arabinosides can significantly promote plant protective and defense mechanisms and that these actions are not significantly linked to the standard CK signaling pathway.

■ RESULTS AND DISCUSSION

6-Benzylaminopurines Substituted with β-D-Arabinose at the N9-Position (BAPAs) Show Antisenescence Activity in Plants. We prepared 21 novel BAPA derivatives with various substituents at different positions on the benzyl ring (Table 1) using established synthetic protocols (Supplementary Methods and Supplementary Table 1). Their activity was assessed using three classical cytokinin bioassays. The measured activities are reported relative to that of the natural aromatic cytokinin BAP (Table 1). None of the compounds exceeded 31% of the activity observed for BAP in the *Amaranthus* bioassay, suggesting they have only weak cytokinin-like activity. A similar pattern emerged in the tobacco callus bioassay: aside from compound **4**, whose relative activity was 73% of that of the BAP control, the compounds exhibited low or modest relative activities in the range of 6−40%. In stark contrast, several of the new BAPAs exhibited activity similar to (compounds **5**, **17**, and **20**) or greater than (compounds **1**, **2**, **3**, **4**, **6**, **10**, **11**, **13**, **15**, and **21**)

that of BAP in the wheat leaf senescence bioassay, in which the degree of senescence is evaluated based on the chlorophyll (Chl) content in dark-incubated detached wheat leaves. This indicated that the new BAPAs specifically affect physiological processes primarily related to senescence and/or stress without being active in the cytokinin pathway.

We also examined the new compounds' ability to activate cytokinin sensor histidine kinase (HK) receptor-linked signaling cascade by using a previously reported protocol[24] in which the *Arabidopsis* AHK3 and CRE1/AHK4 receptors[25,26] are overexpressed in the *Escherichia coli* KMI001 strain ($\Delta rcsC$, *cps::lacZ*), using β-galactosidase as a reporter gene. In line with the *Amaranthus* bioassay and tobacco callus bioassay results, none of the BAPAs triggered a cytokinin response from the AHK3 and CRE1/AHK4 receptors, demonstrating that BAPAs did not initiate the cytokinin signaling *in vitro*.

Thus, several of our new compounds, especially those bearing a substituent (*i.e.*, a fluorine/chlorine atom or a hydroxy/methoxy group) in the *meta* position on the benzyl ring, effectively delayed the onset of senescence but had negligible standard hormonal activity. This is particularly interesting because it is well-known that CK treatment can have adverse developmental effects.[27] While many of the new compounds exhibited promising activity in the senescence bioassay, some of them are unsuitable for use *in planta*. For example, the metabolic deactivation of compound **1** might be expected to proceed similarly to that of BAP, which is converted into inactive CK 9-glucosides that are probably responsible for the aberrant root formation mentioned above. Conversely, *meta*-topolin is metabolized via a different pathway, which results in its reversible conversion into a storage form that does not interfere with efficient root development.[11,22] We therefore selected two derivatives for further mechanistic investigation *in planta*: compounds **11** and **13**, which bear CH$_3$O− and −OH groups, respectively, in the *meta* position (Table 1). Despite having low activity in standard cytokinin activity tests (the *Amaranthus* and tobacco callus bioassays), these compounds exhibited either above average (**11**) or high (**13**) activity in the senescence assay (Table 1). Compound **13** (hereafter referred to as 3-hydroxy-BAPA) is structurally related to the naturally occurring ArCK *meta*-topolin,[28] while compound **11** (hereafter referred to as 3-methoxy-BAPA) is its methoxy analogue.

Influence of 3-Hydroxy-BAPA and 3-Methoxy-BAPA on the Maintenance of Photosynthetic Activity in Detached Wheat and *Arabidopsis* Leaves. The senescence bioassay results demonstrated that the chosen compounds suppress the Chl degradation in detached wheat leaves incubated in darkness (Table 1). To determine whether they also preserve photosynthetic activity (specifically, the activity of photosystem II (PSII), which decreases markedly during dark-induced senescence of detached leaves[3,29]), we measured the maximum quantum yield of PSII photochemistry (F_V/F_M) in wheat and *Arabidopsis* leaves kept in darkness for 6 days, together with the leaf Chl content. Wheat leaves treated with dimethyl sulfoxide (DMSO; negative control) exhibited low F_V/F_M values (Figure 1A and E), indicating only minimal PSII activity. However, wheat leaves treated with 3-methoxy-BAPA (10 μM) and 3-hydroxy-BAPA (1 and 10 μM) exhibited F_V/F_M values above 0.6, indicating effective preservation of PSII function. In *Arabidopsis*, a comparable effect was only found in leaves treated with 3-methoxy-BAPA at 10 μM, which generated a stronger protective response than the control
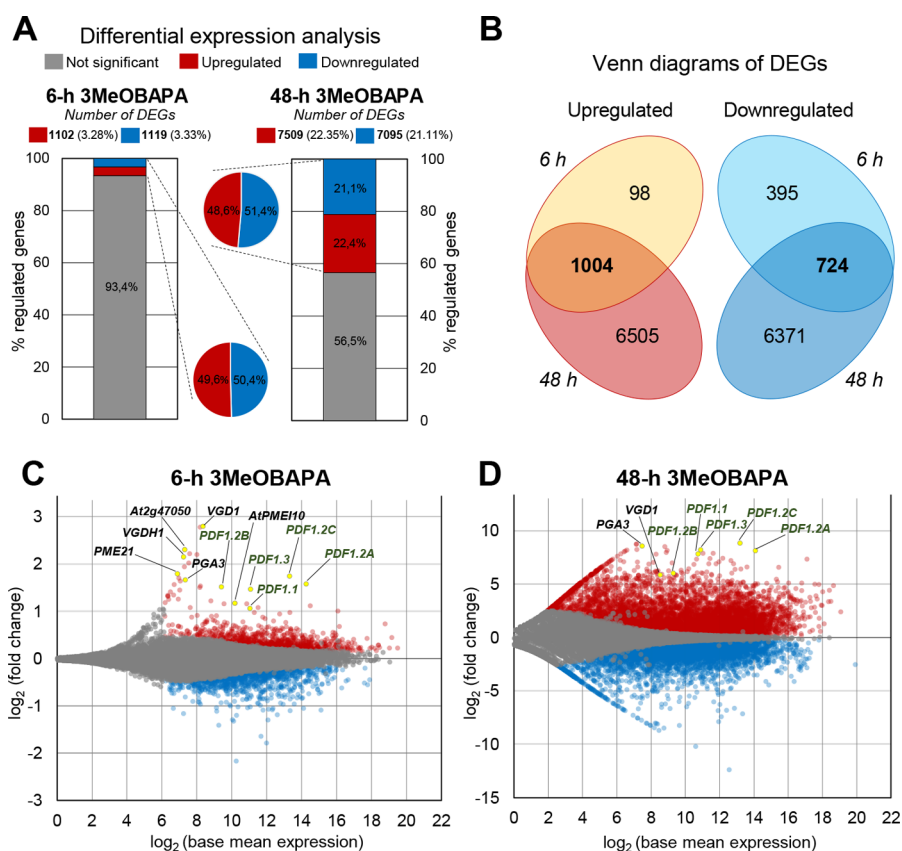
Figure 2. 3-Methoxy-BAPA treatment in *Arabidopsis* leaves shows a massive transcriptional reprogramming that significantly affects defense-related genes. (A, C, D) Differential expression analysis of genes affected by 3-methoxy-BAPA treatment (adjusted *P*-value < 0.05; data normalization and statistical evaluation was performed in the DESeq2 program). (B) Venn diagrams comparing gene expression in detached *Arabidopsis* leaves after short-term (6 h) and long-term treatment (48 h) with 10 μM 3-methoxy-BAPA. Both upregulated DEGs (left diagram) and downregulated DEGs (right diagram) are shown.

BAP treatment (Figure 1C and E). In wheat leaves, 3-hydroxy-BAPA had a significantly stronger protective effect on both Chl content and PSII function than 3-methoxy-BAPA (Figure 1A, B, and E top), which is consistent with its higher relative activity in the standard senescence bioassay (Table 1). In *Arabidopsis* leaves, 3-methoxy-BAPA was more effective than 3-hydroxy-BAPA in both Chl retention and maintenance of PSII function (Figure 1C, D, and E bottom). Whereas the effects of 3-methoxy-BAPA treatment at concentrations of 1 and 10 μM were similar in wheat, the minimum 3-methoxy-BAPA concentration needed to produce a protective effect in *Arabidopsis* was 10 μM.

Collectively, these results show that both compounds have significant senescence-delaying effects and that these effects are (quantitatively) species-specific. Whereas 3-hydroxy-BAPA exhibited stronger antisenescence activity in wheat, 3-methoxy-BAPA's protective effect proved to be more specific for *Arabidopsis* leaves, and the positive effect on the photosynthetic function in *Arabidopsis* was found to be superior to that exhibited by highly active aromatic cytokinin BAP. Therefore, 3-methoxy-BAPA was selected for use in a whole transcriptome differential expression study using *Arabidopsis* as a model system.

Whole Transcriptome Expression Changes in 3-Methoxy-BAPA-Treated *Arabidopsis* Leaves and GO Distribution Analysis. A high-throughput mRNA sequencing analysis (RNA-seq) of dark-incubated *Arabidopsis* leaves was performed to characterize the reprogramming of gene transcription induced by treating detached leaves with 3-methoxy-BAPA. We analyzed gene expression after short (6 h) and long (48 h) treatments with 10 μM 3-methoxy-BAPA (*i.e.*, the lowest concentration found to elicit a significant response in the preceding experiments) to clarify the molecular mechanisms of adaptation to short and extended treatment with the compound.

Overall, the transcriptome of 3-methoxy-BAPA-treated *Arabidopsis* leaves in the short term treatment was significantly different from that of DMSO treated control, with 1102 upregulated and 1119 downregulated genes based on an adjusted *P*-value of < 0.05 (Figure 2A). Extended treatment (*i.e.*, 48 h) led to a massive transcriptional reprogramming, with a much higher number of differentially expressed genes (DEGs) being affected: 7509 were upregulated and 7095 were downregulated. A comparison of DEGs obtained from the short-term treatment with genes coming from the extended treatment revealed a high overlap: more than 91% among upregulated DEGs and 65% among downregulated DEGs (Figure 2B).

Among the genes with the highest upregulation in both 3-methoxy-BAPA treatment were genes of defense regulons, namely, antifungal plant defensins (PDF; Figure 2C, D and Supplementary Table 2): *At5g44430* coding for defensin-like protein 1.2C (*PDF1.2C*), *At5g44420* coding for defensin-like protein 1.2A (*PDF1.2A*), *At2g26020* coding for defensin-like protein 1.2B (*PDF1.2B*), and *At2g26010* coding for defensin-like protein 1.3 (*PDF1.3*), all of which are important antifungal
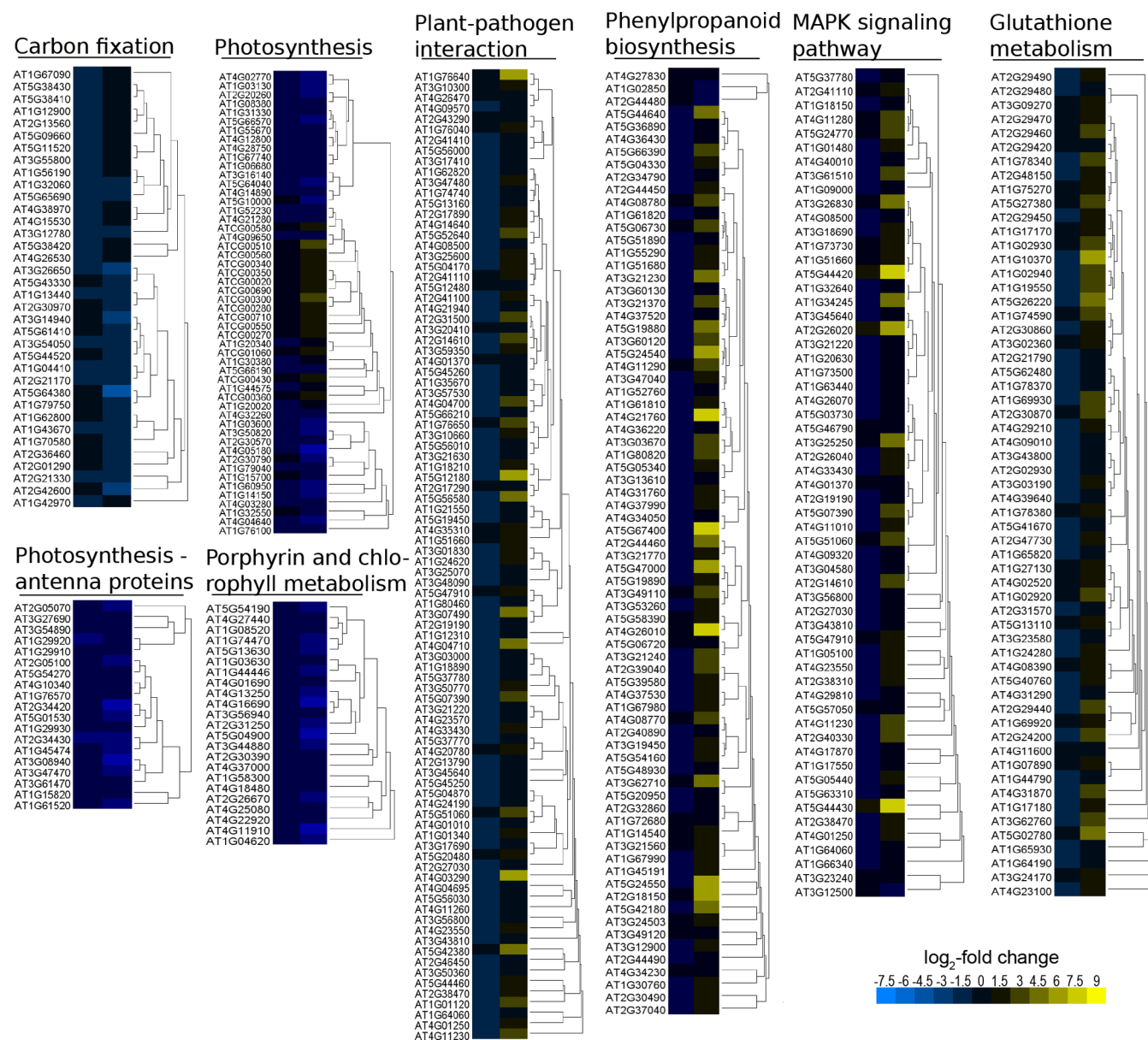
Figure 3. KEGG pathways over-representation analysis. Fold changes (log$_2$ scale) in expression of selected metabolic pathway genes are shown for the short-term (left columns) and long-term (right columns) treatment with 3-methoxy-BAPA. Genes were clustered using average-linkage hierarchical clustering. The metabolic pathways shown in the figure represent the most significantly affected group of genes related to carbon fixation (map00710), photosynthetic machinery (map00195 "Photosynthesis," map00196 "Photosynthesis - antenna proteins," map00860 "Porphyrin and chlorophyll metabolism," plant-pathogen interactions (map04626), MAPK signaling (map04016), phenylpropanoid biosynthesis (map00940), and glutathione metabolism (map00480) according to KEGG database. The log$_2$ fold change values are expressed as negative or positive numbers on the bar, and the color scale indicates which genes are up- (yellow) and downregulated (blue).

and antistress factors that comprise part of the innate immunity arsenal in plants.[30,31] We also detected strong transcription of several genes encoding inhibitors of pectin methylesterases (PMEI), especially in the short term treatment, including *At1g62760*, which encodes *AtPMEI10*, and *At2g47050* coding for a previously uncharacterized PMEI. Several PMEIs, together with their target pectin methylesterases (PME), were shown to play protective function by controlling the status of methylesterification of pectin during infection by necrotrophic pathogens.[32]

In addition, some tissue-specific PMEs and polygalacturonases (pectinases) were also upregulated including *At2g47040*, which encodes pectin methylesterase Vanguard1 (VGD1),[33] *At3g05610* coding for pathogen-induced PME21,[32]

and *At3g07830*, which codes for pectin lyase/polygalacturonase 3 (PGA3) (Supplementary Table 2). The unique expression pattern of specific PMEs and their inhibitory PMEIs together with the plant defensins strongly suggests that 3-methoxy-BAPA in the early stages of transcriptional reprogramming specifically regulates processes necessary for cell wall remodeling and consequent enhanced resistance to stresses and fungal pathogens in plants. It seems that the action of 3-methoxy-BAPA might be related to jasmonic acid (JA) and ethylene (ET) signaling as the expression of both PMEIs and defensins is regulated by JA/ET stress signaling pathway.[34]

On the other hand, over 30% of the 50 most strongly downregulated DEGs were related to photosynthesis, including 10 genes encoding subunits of the light-harvesting chlorophyll-

protein complexes (LHC) of PSII (*At1g29920, At2g34430, At3g27690, At2g05100, At2g05070, At1g29930, At5g54270, At3g08940, At2g34420,* and *At4g10340;* Supplementary Tables 2 and 3). These results are consistent with the hypothesis that 3-methoxy-BAPA activates defense responses because down-regulation of photosynthetic genes is a hallmark of plant responses to pathogens during the first few hours or days after a pathogen attack.[35]

To characterize the functions of the genes exhibiting differential expression following 3-methoxy-BAPA treatment, all genes were analyzed for enriched biological processes (BPs) or molecular functions (MFs) according to the Gene Ontology (GO) project and the distribution of GO terms was analyzed at level 6 and above. The results suggested that 3-methoxy-BAPA indeed affected JA/ET signaling pathways, as DEGs related to JA/ET-dependent systemic resistance[34] (*e.g., ORA59, PDF1.2,* and *MPK4*) as well as to various cell wall modifications including pectin catabolic processes (*e.g., VGD1, VGDH1, At3g01270, PME21, PME50,* and *CYP79B3*) were upregulated after the short-term treatment (Supplementary Tables 2 and 3). Conversely, in the fast responding group of downregulated DEGs, we observed a generally higher number of genes in the most affected GO categories, with clear enrichment of GO terms related to photosynthesis (Supplementary Table 3). Notably, over 50% of the DEGs were contained within one of annotated GO categories: light-harvesting complex, photosystem I, nonphotochemical quenching, and reductive pentose-phosphate cycle.

To look into complex pattern of DEGs coming particularly from the long-term treatment with 3-methoxy-BAPA, both GO and KEGG databases were used; the KEGG database, however, proved to be more useful in the enrichment analysis of biological processes and mapping of signaling pathways.[36] A hierarchical clustering analysis was performed to decipher the biological consequences of the observed upregulation of pathogen defense-related genes under both short- and long-term treatments. Consistent with the previous enrichment analysis, we observed eight major distinct clusters of transcripts with similar expression profiles (Figure 3). Genes encoding stromal proteins ("Carbon fixation") and thylakoid proteins ("Photosynthesis-antenna proteins," "Photosynthesis") were downregulated by both treatments (particularly after 48 h treatment, with a few exceptions; Figure 3), while plant defense response-related elements (*e.g.,* "Plant-pathogen interaction," "Phenylpropanoid biosynthesis," and "Gluta-thione metabolism") were significantly upregulated by the long-term treatment with 3-methoxy-BAPA. "MAPK-signaling pathway" stands out as a relevant category with several gene products annotated also within "Plant-pathogen interaction" category that reflects plant immunity response triggered by pathogen-associated molecular patterns (PAMPs), *i.e.,* PAMP-triggered imunity (PTI) (Figure 3). In line with the previous results, such reprogramming of the leaf transcriptome from photosynthesis toward defense suggests that 3-methoxy-BAPA induces plant responses similar to those triggered by pathogens or PAMPs (see *e.g.,* refs 37 and 38) and promotes PTI.

As has been known for some time, both exogenous and endogenous CKs can enhance plant resistance to pathogens[4,39,40] but the mechanism of their action in plant immunity remains unclear. CKs have been reported to promote PTI in *Arabidopsis.*[4,41] A model proposed by Choi *et al.*[39] suggests that CKs enhance defense responses (and consequently plant resistance to pathogens) via AHK2/AHK3 and ARR2

activation. We suggest that the activation of defense responses by 3-methoxy-BAPA is most likely not significantly related to the standard cytokinin pathway because 3-methoxy-BAPA was not recognized by AHK3 or CRE1/AHK4 *in vitro,* and neither short- nor long-term treatment with 3-methoxy-BAPA induced any significant upregulation of *ARR5* or most other cytokinin response regulators (with the exception of *ARR3* and *ARR7* upregulation in the long term treatment only) that are usually upregulated by other cytokinin derivatives.[3] This suggestion is also in line with the low CK activity of 3-methoxy-BAPA in the *Amaranthus* and tobacco callus bioassays.

It is generally accepted that the PTI responses in plants rely on MAPK modules that are activated by diverse biotic and abiotic stress conditions.[42] The activation of plasma mem-brane-localized pattern recognition receptors (PRRs) triggers defense response in affected cells. Genetic studies revealed that MEKK1-MKK1/2-MPK4 is the main module involved in PTI-mediated defense responses (reviewed in ref 43). Other MPKs that respond to elicitation in PTI include MPK3 and MPK6, possibly independently of MEKK1.[43] MPK11 was recently characterized as a fourth PAMP-activated MAPK that is involved in the stress signaling including a very sensitive response to flg22 (the PAMP derived from the bacterial motor protein flagellin) and other elicitors, acting in synergy with MPK4.[44,45]

Notably, in the "Plant-pathogen interaction" and "MAPK signaling pathway" groups of genes, we observed upregulation of several mitogen-activated protein-kinase (MAPK) signaling modules (*MPK3, MPK4, MPK6,* and *MPK11*) and their upstream MAPKKs (*MKK1, MKK2, MKK4, MKK5,* and *MKK6*) and MAPKKKs (*MEKK1, MAPKKK21, MAPKKK20,* and *MAPKKK19;* Figure 3). Further, typical PTI marker genes, which act downstream of MEKK1, were upregulated including several *RBOH*s (coding for respiratory burst oxidase homologues), *FLG22-INDUCED RECEPTOR-LIKE KINASE 1* (*FRK1*), pathogen-related WRKY transcription factors (*WRKY22, WRKY29, WRKY33,* and *WRKY53*) or patho-genesis-related protein 1 (*PR1*) (see, *e.g.,* ref 42).

These results corroborate our view that the PTI response was provoked by 3-methoxy-BAPA treatment through the standard MAPK cascade including also MPK11, an important MAPK module activated in the PTI signaling. Interestingly, *MPK11* was the single most upregulated MAPK module in our transcriptomic screenings, with a $\log_2$ fold change value of 2.57 after long-term 3-methoxy-BAPA treatment. In addition, *MPK4* was upregulated by both short- and long-term elicitation with 3-methoxy-BAPA. Long-term incubation with 3-methoxy-BAPA also induced significant upregulation of several other MPKs and their upstream MAPK regulators as well as their downstream elements.

3-Methoxy-BAPA Affects PTI through MAPK Signal-ing Cascades. In an attempt to verify that MAPK signaling pathways are involved in promoting PTI induced by 3-methoxy-BAPA, we further investigated the possible involve-ment of MAPK signaling modules in detached *Arabidopsis* leaves. Specifically, we examined the expression profiles of *MPK3, MPK4, MPK6,* and *MPK11* after the short- (6 h) and long-term (48 h) treatments, and also after 30 min treatment to evaluate earlier changes in their expression. While none of 3-methoxy-BAPA treatments induced statistically significant changes in *MPK6* expression profiles (data not shown), we observed a concentration-dependent effect on the expression patterns of *MPK3, MPK4,* and *MPK11* in detached *Arabidopsis*
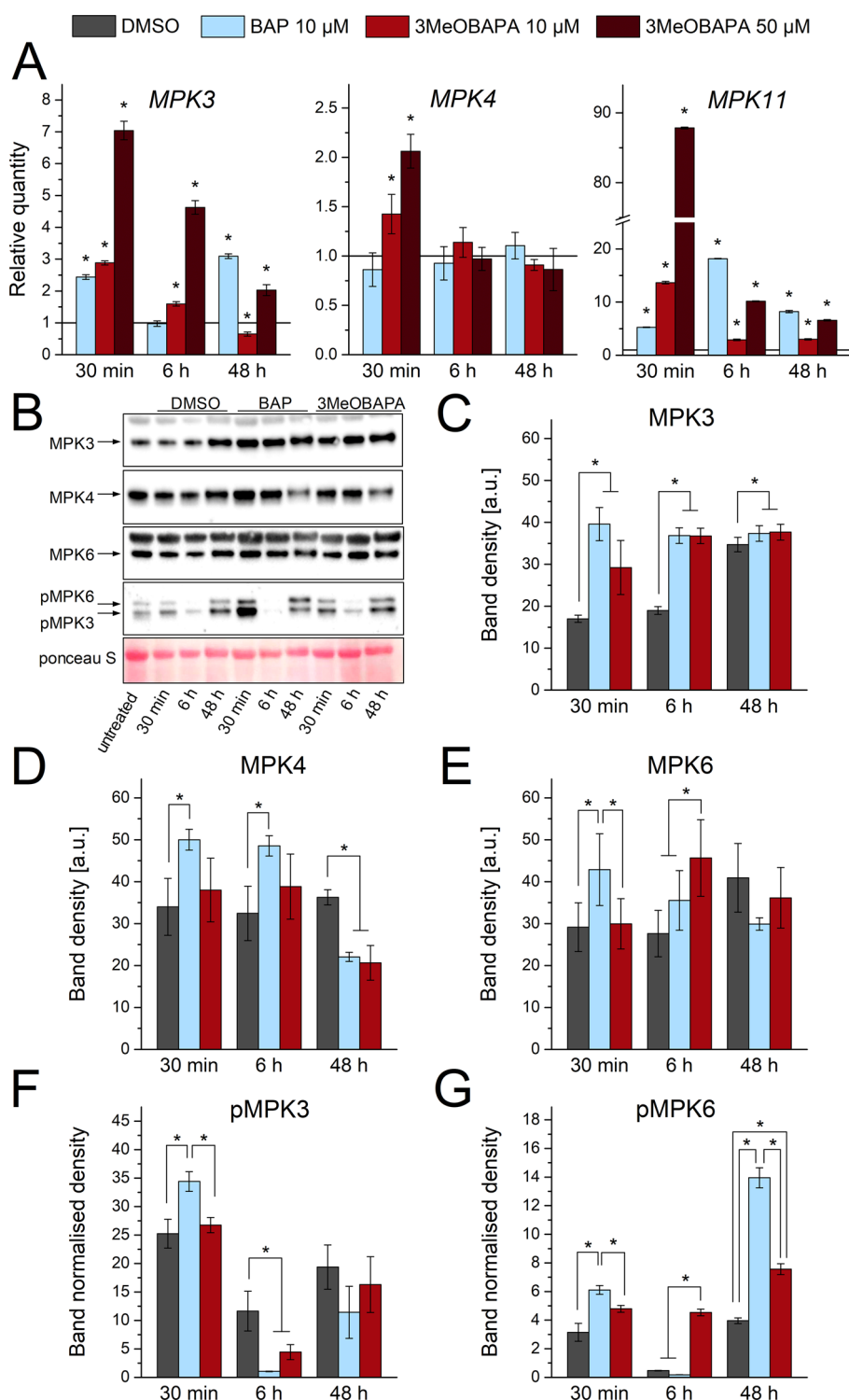
Figure 4. Expression profiles of selected *MPK* genes and MPK protein immunoblots following treatment. (A) Two 3-methoxy-BAPA concentrations were used: 10 and 50 μM; BAP was applied only at 10 μM. Changes in the expression versus the DMSO-treated control were followed by qPCR after time intervals ranging from 30 min to 48 h in detached *Arabidopsis* leaves ($n = 4$ biological replicates; at least two technical replicates were performed for each biological sample). (B) Immunoblots of *Arabidopsis* leaves incubated in aqueous DMSO (0.1%) or aqueous DMSO solutions of 10 μM BAP and 3-methoxy-BAPA (3MeOBAPA). Detached leaves were incubated with the above compounds for designated time periods, probed with anti-MPK3, anti-MPK4, and anti-MPK6, as well as anti-pERK phosphospecific antibodies recognizing the phosphorylated forms of MPK3 and MPK6 (pMPK3, pMPK6). Ponceau S staining was used for loading control to verify that equal quantities of all studied proteins were loaded onto each probed membrane. (C−G) Quantification of band densities from immunoblots (B) for MPK3 (C), MPK4 (D), MPK6 (E), and phosphorylated MPK3 (F) and MPK6 (G). In (F) and (G), the densities are normalized to the abundance of the corresponding MPKs. In all charts, means ± SD are presented, and Student's unpaired *t* test was used for statistical analyses ($P < 0.05$).
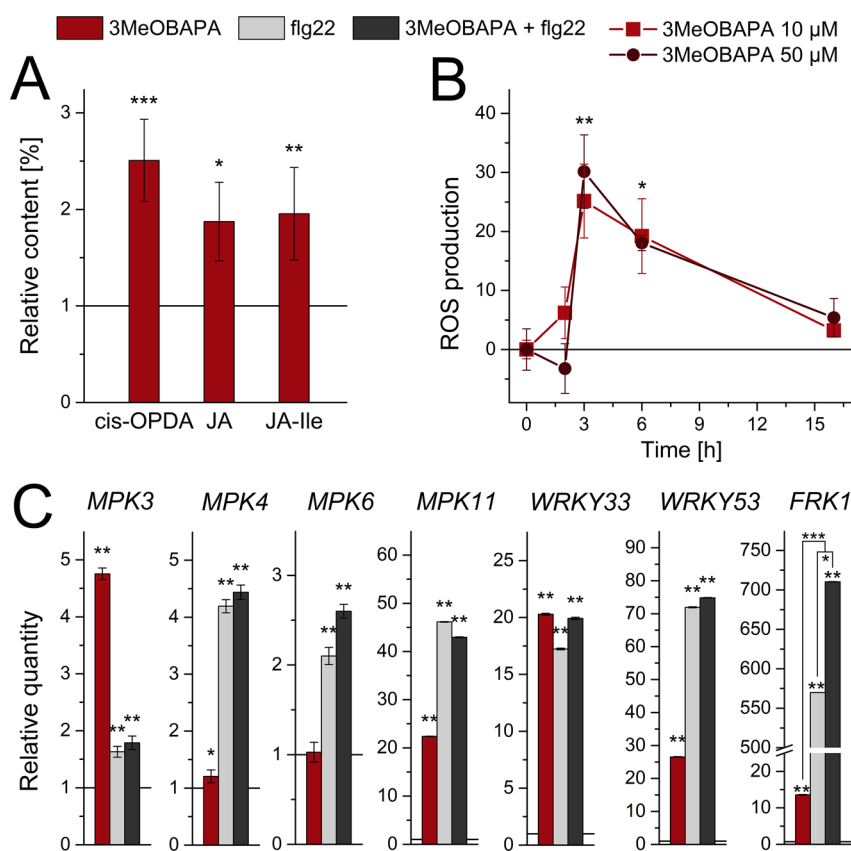
Figure 5. 3-Methoxy-BAPA treatment leads to changes in the intracellular content of jasmonic acid (JA) forms, ROS production and expression profiles of PTI-responsive genes. (A) Content of *cis*-(+)-12-oxo-phytodienoic acid (*cis*-OPDA), jasmonic acid (JA) and jasmonoyl-L-isoleucin (JA-Ile) in *Arabidopsis* leaves treated with 10 μM 3-methoxy-BAPA for 48 h versus the DMSO-treated leaves (n = 4). (B) ROS production in *Arabidopsis* cells treated with 10 μM or 50 μM 3-methoxy-BAPA as determined by DCFH-DA assay (n = 5); asterisks indicate significant difference between untreated (0 h) and treated cells with either 10 or 50 μM 3-methoxy-BAPA. (C) Effect of 3-methoxy-BAPA and bacterial elicitor peptide flg22 on the expression of PTI-responsive genes. Seven days old (DAG) *A. thaliana* Col-0 seedlings were treated with 10 μM 3-methoxy-BAPA and/or 1 μM flg22 for 2 h. The expression levels of *MPK3*, *MPK4*, *MPK6*, *MPK11*, *WRKY33*, *WRKY53*, and *FRK1* were analyzed in 3-methoxy-BAPA, flg22, and 3-methoxy-BAPA + flg22 treated plants versus the DMSO-treated control. Genes for elongation factor 1 alpha and actin 7 were used as reference genes. Each bar represents a biological pool of approximately 50 seedlings ($n \geq 4$). In all charts, means $\pm$ SD are presented, and Student's unpaired t test was used (*P < 0.05, **P < 0.01, ***P < 0.001).

leaves (Figure 4A). The effect of 3-methoxy-BAPA was generally strongest 30 min after its application, and it declined significantly after 6 h, suggesting a fast response mechanism. Strikingly, a dramatic increase of *MPK11* transcript levels was achieved by treatment with 50 μM 3-methoxy-BAPA; after 30 min incubation, we could observe almost 90-fold increase in *MPK11* expression levels followed by a modest decline at 6 h, but the levels stayed significantly elevated after 48 h treatment in line with our transcriptomic profiling results. Further, treatment with 3-methoxy-BAPA for 30 min increased the transcript accumulation of *MPK11* almost three times more strongly than treatment with BAP at the same concentration (Figure 4A).

Immunoblotting experiments showed that the abundance of MPK3 in BAP- as well as 3-methoxy-BAPA-treated leaves increased after treatments of both 30 min and 6 h (Figure 4B and C). The abundance of MPK4 increased significantly after BAP treatment but was only slightly elevated after treatment with 3-methoxy-BAPA for 30 min or 6 h (Figure 4B and D). The abundance of MPK6 slightly increased after 30 min of treatment with BAP and after 6 h of treatment with 3-methoxy-BAPA (Figure 4B and E). The abundance of the protein

product of the highly responsive *MPK11* could not be assessed due to unavailability of the respective antibody.

The phosphorylation of MPK3 and MPK6 was monitored using pTEpY, a specific anti phospho-p44/42 antibody.[46] The phosphorylation of MPK3 peaked after 30 min treatment with BAP or 3-methoxy-BAPA and decreased sharply after 6 h treatment. The level of MPK3 phosphorylation after 48 h treatment with BAP or 3-methoxy-BAPA did not differ significantly from that in the negative (DMSO) control (Figure 4F). This suggests that MPK3 status in response to 3-methoxy-BAPA changes rapidly and that there was a possible correlation between changes on the gene level (Figure 4A) to those on the corresponding (phospho-)protein level (Figures 4C and F). As with MPK3, MPK6 phosphorylation was observable after 30 min BAP treatment. However, unlike MPK3, MPK6 remained strongly phosphorylated after 48 h of incubation with either BAP or 3-methoxy-BAPA (Figure 4G) indicating possible involvement of MPK6 in long-term 3-methoxy-BAPA-induced responses.

Together, these results demonstrate that like BAP, 3-methoxy-BAPA can enhance the expression of several *MPK* genes, especially when applied in short (30 min) treatment. Treatment with this compound increased the protein-level
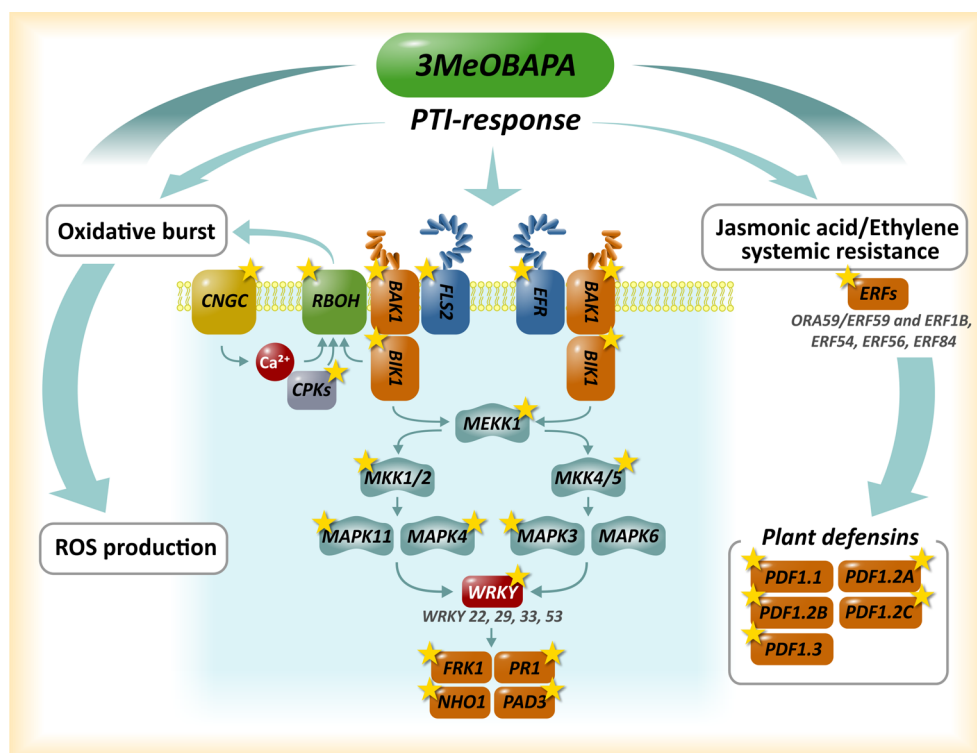
Figure 6. Hypothetical model of 3-methoxy-BAPA-mediated priming in *Arabidopsis* plants. The model is based on data from our RNA-seq transcriptomics and gene expression studies (significantly upregulated genes are marked with a star), data from the KEGG pathway database, and references cited throughout the text. Priming (either short or extended treatment with 3-methoxy-BAPA) leads to JA/ET stress signaling and expression of plant defensins, to the oxidative burst and production of ROS, and the backbone of the PTI responses is characterized by activation of the MAPK signaling pathway, leading to the expression of *FLG22-INDUCED RECEPTOR-LIKE KINASE 1* (*FRK1*), *PATHOGENESIS RELATED 1* (*PR1*), *NONHOST RESISTANCE TO P. S. PHASEOLICOLA 1* (*NHO1*), and *PHYTOALEXIN DEFICIENT 3* (*PAD3*).

expression of MPK3 and (to lesser degrees) MPK4 and MPK6. However, the effect of 3-methoxy-BAPA is better understood by considering the phosphorylation status of these MAPKs. Elicitation with 3-methoxy-BAPA had a considerably stronger effect than BAP treatment on the expression profile of *MPK11*, a stress signaling MAPK module belonging to the PAMP-triggered pathway.

Toward an Integrative Model of 3-methoxy-BAPA Action in Plants. Our data suggest that treatment of *Arabidopsis* leaves with 3-methoxy-BAPA promotes PTI defense pathways in several ways. In the short term response, the plant utilizes defense-related JA/ET pathway through *ORA59/ERF59* and *ERF1B* transcription factors,[34] and subsequent upregulation of downstream plant defensins *PDF1.1*, *PDF1.2*, and *PDF1.3* and others (Figure 2C). Notably, PDF1.2 (with isoforms 1.2A, 1.2B, and 1.2C) seems to be of particular importance, because it is primarily induced in leaves upon pathogen attack, probably through MPK3/6-EIN3-ERF1-PDF1.2 pathway.[47]

To corroborate our transcriptomic results suggesting the activation of JA/ET pathways by 3-methoxy-BAPA, we estimated the content of three JA forms (JA, its precursor *cis*-(+)-12-oxo-phytodienoic acid (*cis*-OPDA), and the major biologically active form, jasmonoyl-L-isoleucine (JA-Ile)). The content of all three forms was significantly higher in leaves treated with 3-methoxy-BAPA (10 μM) for 48 h compared to the negative control (DMSO) (Figure 5A), which in turn may lead to enhanced JA biosynthesis and signaling. All JA forms might have contributed to the 3-methoxy-BAPA-induced PTI

response including *cis*-OPDA that was found to be an active player in defense responses.[48]

The formation of active JA forms within the PAMP-response is typically preceded by an accumulation of reactive oxygen species (ROS) that also help to induce the cell wall integrity/remodeling processes (as observed in the GO enrichment analysis; see Supplementary Table 3) and protect the plant from biotic or abiotic stresses. NADPH oxidase (mostly known as respiratory burst oxidase homologue, RBOH), whose expression was also stimulated by 3-methoxy-BAPA, is thought to be a key player in the PAMP-induced ROS accumulation (for a review, see *e.g.*, ref 49).

To see whether the redox state of plant cells responds to 3-methoxy-BAPA treatment, we took advantage of an available *A. thaliana* suspension cell culture. Using a standard 2′-7′-dichlorodihydrofluorescein diacetate (DCFH-DA) assay, we quantified the production of ROS in 3-methoxy-BAPA-treated *Arabidopsis* cells with either a high (50 μM) or low (10 μM) concentration of the compound (Figure 5B). Interestingly, both treatments resulted in a comparably significant increase in the ROS production 3 h after the elicitation, which was followed by a slow decrease back to the pretreatment levels after 16 h of treatment. Thus, in the early stages of the response to 3-methoxy-BAPA, temporally elevated levels of ROS seem to be involved in signaling defense responses in concert with other pathways.

It is well-known that plant defense against pathogens can be enhanced by both synthetic and natural compounds including PAMPs and also by CKs (for a recent review, see *e.g.*, ref 50). This effect is collectively referred to as defense priming. In the

primed state, the plant defense response to pathogen attack, often initiated by PAMP receptors including FLS2 (the receptor specific for bacterial flg22) and EFR (the bacterial EF-Tu receptor), is faster and stronger as compared to nonprimed plants. The complex molecular mechanism of priming comprises upregulation of the mentioned PAMP receptors and FLS2 co-receptor BAK1,[51] activation of a hierarchical MPK signal cascade including MEKK1, MKK4/5, MPK3/6 and MPK 11,[44,45] and upregulation of WRKY.[42] It is suggested that defense priming induces an "open chromatin" configuration at promoter regions of PTI-responsive genes[52] enabling a more effective defense gene response to a subsequent triggering stimulus (such as PAMP).

The transcriptomic changes induced by 3-methoxy-BAPA treatment in detached *Arabidopsis* leaves suggested that 3-methoxy-BAPA acts as a priming agent for the PTI response. To further confirm whether 3-methoxy-BAPA primes the PTI response in *Arabidopsis* plants, we evaluated expression levels of *MPK3*, *MPK4*, *MPK6*, and *MPK11* and other typical PTI-responsive genes including flg22-induced *FRK1* and transcription factors *WRKY33* and *WRKY53*.[45] As expected, priming of the expression of these PTI-responsive genes was also observed after treatment with flg22 (Figure 5C). In line with our results obtained with 3-methoxy-BAPA-treated detached leaves (Figure 4A), we could observe relatively strong elevation of *MPK11* expression levels and somewhat weaker effects on the expression pattern of *MPK3* and *MPK4*. Importantly, the effect of 3-methoxy-BAPA treatment proved to be significant with other examined PTI-response marker genes, although flg22, unsurprisingly, provoked a much stronger effect in the case of *FRK1*. While combined treatment of 3-methoxy-BAPA/flg22 showed little effect in the cases of MPKs and WRKYs, their downstream *FRK1* proved to be very sensitive to the combined treatment: a strong synergistic effect between the elicitor peptide flg22 and 3-methoxy-BAPA was observed in the FLS2-initiated MAPK defense pathway (Figure 5C). This leads us to the conclusion that the PTI response appears to have a dominant role in 3-methoxy-BAPA-induced defense response alongside JA/ET defense signaling cascade-mediated expression of plant defensins (Figure 6). We thus propose a model in which 3-methoxy-BAPA primes and upregulates expression of pattern recognition receptors (PRRs), such as FLS2 and EFR1, and downstream components of this signaling cascades as explained above, in agreement with our transcriptomic and gene expression analyses (Figure 6). Priming of this signaling pathway then leads to a sensitive response to bacterial peptide flg22 through *FRK1* in combined 3-methoxy-BAPA/flg22 cotreatments (Figure 5C).

The predicted ability of 3-methoxy-BAPA (and BAPAs generally) to prime plants should enhance plant resistance to pathogens. Indeed, a foliar application of both 3-methoxy-BAPA and 3-hydroxy-BAPA on field-grown wheat and barley plants in various growth stages (tillering, beginning of stem elongation, and start of flag leaf extending) significantly suppressed infection by several fungal pathogens (Figure 7). This protective effect in primed plants does not necessarily lead to impaired plant fitness and growth (unlike typical defense responses), as evidenced by a significantly increased number of tillers per plant observed for barley plants, and slightly increased (but statistically nonsignificant) number of spikes per square meter and grain yield (Supplementary Table 4).
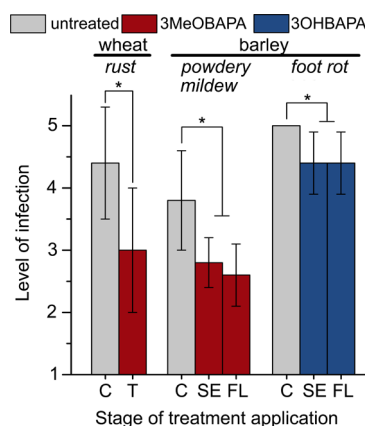

Figure 7. Effect of 3-methoxy-BAPA (3MeOBAPA) and 3-hydroxy-BAPA (3OHBAPA) treatment on the level of pathogen infection in winter wheat and spring barley plants in field-plot experiments. Plants were evaluated at the beginning of heading (wheat leaf rusts *Puccinia striiformis* syn. *Puccinia glumarum*, *Puccinia recondita* f. sp. *tritici*, *Puccinia graminis*; barley powdery mildew *Blumeria graminis* syn. *Erysiphe graminis*) or early milk ripeness (barley foot rot diseases *Gaeumannomyces graminis* syn. *Ophiobolus graminis*, *Ramulispora herpotrichoides* syn. *Pseudocercosporella herpotrichoides*, teleomorpha *Tapesia yallundae*, *Fusarium* spp., *Rhizoctonia* spp.). The 5 μM solutions were applied as a foliar spray at different plant growth stages: tillering (T), at the beginning of stem elongation (SE), and at the beginning of flag leaf extending (FL). The level of infection versus the untreated control (C) was evaluated according to the standardized methodology; for details, see Supplementary Methods. Means ± SD are presented ($n = 5$); asterisks indicate statistically significant difference according to Student's unpaired t test ($P < 0.05$).

While activation of early defense response by PAMPs can protect plants from pathogen attacks, prolonged PAMP exposure can worsen plant fitness because of the persistent stimulation of high-cost defense mechanisms and simultaneous inhibition of photosynthesis. For example, treating *Arabidopsis* seedlings with flg22 for 7 days reduced growth and inhibited PSII photochemistry.[38] However, the treatment of detached *Arabidopsis* leaves with 3-methoxy-BAPA had no negative effect on PSII function after 6 h, 48 h (data not shown), or even after 6 days (Figure 1C and E). On the contrary, 6 day treatment with BAPAs maintained high PSII function in both *Arabidopsis* and wheat leaves as compared with the negative control.

■ CONCLUSIONS

Our results show that BAPAs can emerge as a new type of priming agents in plants with a good potential for manipulating plant PAMP responses through specific elicitation of MAPK modules and series of repair and defense response mechanisms. The promotion of these defense mechanisms is linked with JA/ET stress signaling that may be directly related to enhanced levels of JA and its metabolites in response to 3-methoxy-BAPA treatment. Further, temporarily elevated levels of ROS seem to play a role in the early stages of priming with the compound. The downregulation of several photosynthetic genes, particularly in the immediate aftermath of 3-methoxy-BAPA treatment, was observed, but the prolonged elicitation with 3-methoxy-BAPA resulted in a good preservation of chlorophyll levels and significantly improved photosynthetic function. These beneficial effects also delayed the onset of senescence in BAPAs treated *Arabidopsis* and wheat leaves. In

addition, our field trial experiments with 3-methoxy-BAPA and 3-hydroxy-BAPA suggested that application of this type of compounds provides positive effects that may occur through the above mechanisms and protects the plant against some fungal pathogens. We believe that our approach will help integrate existing results on the role of ArCKs with a new methodology aimed at characterization of their lesser-known functions, such as the promotion of plant resistance to pathogens.

■ METHODS

Plant Material and Sample Preparation. *Arabidopsis thaliana* (L.) Heynh (*Arabidopsis*) and *Triticum aestivum* L. cv. Aranka (wheat) plants were used. For isolation of total RNA or total protein from detached leaves, *Arabidopsis* plants (ecotype Columbia, Col-0) were grown in soil for 6 weeks in a controlled growth chamber at 22/20 °C under short-day conditions: 8 h light (120 μmol photons m^{-2} s^{-1})/16 h dark cycle. Subsequently, leaves of similar size and chlorophyll content were cut and immediately subjected to the treatment. At least 20 detached leaves were submerged in 1 x MS medium supplemented with DMSO (0.1%) or DMSO solutions of BAP or 3-methoxy-BAPA and left incubated in given MS medium for either 30 min, 6 h or 48 h in darkness. After incubation, detached leaves were frozen in liquid nitrogen and used for RNA or protein isolation; 150 mg of liquid nitrogen-ground material was used per isolation.

For isolation of total RNA from seedlings, *Arabidopsis* Col-0 plants were grown on 1/2 × MS agar plates in a controlled growth chamber at 22/20 °C under long-day conditions: 16 h light (120 μmol photons m^{-2} s^{-1})/8 h dark cycle. Seedlings (5 DAG) were transferred into the 1/2 × liquid MS medium for another 3 days under constant shaking (60 rpm). Seedlings were then treated with 10 μM 3-methoxy-BAPA, 1 μM flg22 or both and 0.1% DMSO (negative control) for 2 h. Seedlings were frozen in liquid nitrogen and immediately used for RNA isolation.

Cytokinin Bioassays. The prepared compounds were tested in three classical cytokinin bioassays: the tobacco callus assay, *Amaranthus* assay, and detached wheat leaf senescence assay. In all cases, their biological activity was compared to that of natural cytokinin BAP. The bioassays were performed as described[7] using 6-well microtiter plates with each well containing 3 mL of MS medium and 0.1 g of callus tissue in the case of the tobacco callus bioassay.

Photosynthetic Activity of Detached Wheat and *Arabidopsis* Leaves. Spring wheat plants used in these experiments were grown on an artificial medium composed of perlite and Hoagland's solution in a growth chamber at 25 °C under a 16 h light (120 μmol photons m^{-2} s^{-1})/8 h dark cycle for 7 days. Then segments were cut off from the primary leaves 4 cm from the leaf tip. The basal ends of the leaf segments were placed in 100 nM, 1 μM, or 10 μM solutions of BAP, 3-methoxy-BAPA, or 3-hydroxy-BAPA dissolved in 0.1% DMSO, or in a 0.1% DMSO solution in distilled water (negative control). *A. thaliana* (Col-0) plants were grown in soil in a growth chamber at 22/20 °C under an 8 h light (120 μmol photons m^{-2} s^{-1})/16 h dark cycle for 6 weeks, after which the sixth and seventh rosette leaves were detached from the plants and placed in the above-mentioned solutions. The wheat leaf segments as well as *Arabidopsis* leaves were then kept in darkness at 24 °C for 6 days. The Chl content was estimated analytically as described previously.[29] Chl fluorescence parameters were measured on the adaxial side of the leaf segments at RT using a FluorCam 700MF imaging system (PSI). Before the Chl fluorescence measurement, the control leaves were dark-adapted for 30 min. The minimal fluorescence of the dark-adapted leaf sample (F_0) was determined by applying several microseconds-long measuring flashes (red light, 0.1 μmol photons m^{-2} s^{-1}) at the beginning of the procedure. The maximal fluorescence of the dark-adapted sample (F_M) was measured using a 1.6 s saturating pulse (white light, 850 μmol photons m^{-2} s^{-1}). The maximum quantum yield of PSII photochemistry was calculated as $F_V/F_M = (F_M - F_0)/F_M$.

RNA-seq Analysis. Plant cDNA sequencing libraries were prepared using 3.5 μg of total RNA per sample with the Illumina TruSeq Stranded mRNA Sample Preparation Kit (Illumina) in accordance with the standard procedure. Two independent replicate samples per condition were used to generate cDNA libraries. Prepared libraries were validated using a DNA 1000 chip with a 2100 Bioanalyzer (Agilent Technologies) instrument, and all concentrations were assessed using a Kapa Library Quantification Kit (Kapa Biosystems, Roche). Prepared libraries were pooled to a final concentration of 12 pM for cluster generation and sequencing. The clusters were generated using an Illumina TruSeq SR Cluster Kit v3 cBot HS and sequenced on a HiSeq SR Flow Cell v3 (50 bp reads) with a HiSeq 2500 Sequencing System (Illumina). Two independent libraries were prepared for each condition at each time point from two biological replicates. The quality control of reads generated by sequencing was performed with FASTQC v.0.11.5,[53] and reads were mapped to the reference genome of *A. thaliana* v.25 obtained from Ensembl[54] using a TopHat v.2.0.12 splice-read mapper[55] with default parameters. The reads mapped to the transcripts annotated in the reference genome were quantified using HTSeq v.0.6.0[53] with respect to the stranded library. The tests for differential gene expression were performed using the DESeq2 package.[56] Gene ontology (GO) analysis was performed using the Blas2GO v.3.0 program.[57] HemI software was used to generate heat maps.[58]

Quantitative PCR Analysis. Expression profiling of genes coding for MPKs and PTI-marker genes was done as described previously.[6] Briefly, 5 μg of total RNA isolated using RNAqueousH kit and treated twice with TURBO DNase-freeTM kit (Life Technologies) was used for first strand cDNA synthesis by RevertAidTM H Minus M-MuLV RT and oligo-dT (Fermentas). Diluted cDNA samples were used as templates in real-time PCR reactions containing gb SG PCR Master Mix (Generi Biotech) and 300 nM of each primers. RNA samples were isolated from four biological replicates and transcribed in four independent reactions and each cDNA sample was run in at least two technical replications on StepOnePlusTM Real-Time PCR System in a default program (Life Technologies). Ct values were normalized with respect to actin 2 and elongation factor 1 genes. Expression values were determined and statistically evaluated with DataAssist v3.0 Software (Life Technologies). The Benjamini and Hochberg false discovery rate was used to obtain adjusted p-values for unpaired t test.

Immunoblotting Analyses of MAPKs. Detached *Arabidopsis* leaves were homogenized in liquid nitrogen to a fine powder. Proteins were extracted by adding ice-cold 50 mM HEPES (pH 7.5) containing 75 mM NaCl, 1 mM EGTA, 1 mM MgCl$_2$, 10% (v/v) glycerol, 1 mM DTT, and Complete EDTA-free protease inhibitor cocktail (Roche). After 15 min incubation on ice, the extracts were centrifuged at 13000g at 4 °C for 15 min and the protein amount was quantitated in supernatants. Extracts were proportionally mixed to give a protein concentration of 1.5 mg protein/mL with 4-fold concentrated Laemmli buffer (final concentration 62.5 mM Tris-HCl, pH 6.8, 2% (w/v) SDS, 10% (v/v) glycerol, 300 mM 2-mercaptoethanol), heat-denatured at 95 °C for 5 min, and centrifuged to remove undissolved components. An amount of 15 μg of each protein was loaded on 12% PAGE gels. After electrophoresis, the proteins were transferred to nitrocellulose membranes using the TransBlot Turbo (BioRad) semidry transfer system. To validate the protein transfer, membranes were stained with Ponceau S. Afterward, they were blocked overnight in 15% (v/v) commercial blocking solution (Western blocking reagent; Roche) diluted in Tris-HCl buffered saline with 0.1% (v/v) Tween-20 (TBS-T) and then incubated overnight with anti-MPK3 (1:3000), anti-MPK4 (1:1000), and anti-MPK6 (1:10000) antibodies (all from Merck) and anti-phospho p44/42 MAPK antibody (Erk1/2,Thr202/Tyr204) (Cell SignalingTechnology), all prepared in TBS-T with 4% (v/v) Western blocking reagent (Roche). After repeated washing in TBS-T, membranes were incubated with a HRP-conjugated secondary antibody (F(ab′)2-goat anti-rabbit IgG (H+L) secondary antibody, HRP; Thermo Fisher Scientific) diluted to 1:5000 in 4% (v/v) Western blocking reagent (Roche). The signal was developed after washing with TBS-T using Clarity ECL Western Blotting Substrate

(BioRad) and recorded with the ChemiDoc documentation system (BioRad). Band densities were quantified using ImageLab (BioRad). The densities of phosphorylated MPK3 and MPK6 were normalized to the abundance of the corresponding MPKs (see Figure 4F and G). All immunoblot analyses were performed using at least three biological replicates. Student's t test was used to evaluate the statistical significance of differences.

Quantification of Jasmonic Acid Forms. Detached seventh or eighth leaves of *Arabidopsis* (Col-0) plants (grown for 6 weeks under the same conditions as plants used for measurement of photosynthetic activity) were put into 0.1% DMSO or 10 μM 3-methoxy-BAPA solutions by a petiole for 48 h. Subsequently, the samples were frozen in liquid nitrogen and stored at −80 °C before measurement. Endogenous levels of jasmonates (jasmonic acid, JA; jasmonoyl-L-isoleucine, JA-Ile; and *cis*-12-oxo-phytodienoic acid, *cis*-OPDA) were determined in 30−40 mg of plant material according to the method described previously.[59] All experiments were repeated in five biological replicates. Briefly, the phytohormones were extracted using 10% methanol with a cocktail of stable isotope-labeled standards added as follows: 10 pmol of $[^2H_6]$JA and $[^2H_2]$JA-Ile, and 20 pmol of $[^2H_5]$OPDA (all from Olchemim) per sample. The extracts were purified using Oasis HLB columns (30 mg/1 mL, Waters) and then evaporated to dryness under a stream of nitrogen. Jasmonate levels were quantified by ultrahigh performance liquid chromatography-electrospray tandem mass spectrometry (an Acquity UPLC I-Class System coupled to a Xevo TQ-S MS, all from Waters) using stable isotope-labeled internal standards as a reference.

ROS Measurements. *Arabidopsis* cells of PSB-D suspension culture in conical flasks were cultivated in the dark at 25 °C, under constant shaking (130 rpm), and subcultured every 7 days (1:5) in a cell suspension medium (1 × MS with 3% sucrose, 1 mg mL^{-1} NAA, 50 ug/mL kinetin). The generation of ROS in PSB-D culture was determined with DCFH-DA (2′,7′-dichlorofluorescin diacetate) (Merck). Cells were treated with either 10 μM or 50 μM 3-methoxy-BAPA, or 0.1% DMSO (negative control) for designated time periods. Briefly, cells were loaded with 10 μM DCFH-DA and the fluorescence was detected after 10 min using a microplate reader (Tecan Infinite M200) operating at excitation and emission wavelengths of 485 and 525 nm, respectively.

■ ASSOCIATED CONTENT

Ⓢ Supporting Information

The Supporting Information is available free of charge at https://pubs.acs.org/doi/10.1021/acschembio.0c00306.

> Physicochemical properties and chemical purity of the BAPA series; most strongly upregulated and down-regulated differentially expressed genes regulated by 3-methoxy-BAPA; most strongly affected gene ontology (GO) terms assigned to upregulated or downregulated differentially expressed genes; effects of 3-methoxy-BAPA and 3-hydroxy-BAPA application on field-grown wheat and barley plants in terms of grain yield and other growth parameters; information about primer design; and references (PDF)

■ AUTHOR INFORMATION

Corresponding Author

Ondřej Plíhal − *Department of Molecular Biology, Centre of the Region Haná for Biotechnological and Agricultural Research, Faculty of Science and Laboratory of Growth Regulators, Institute of Experimental Botany of the Czech Academy of Sciences & Faculty of Science, Palacký University, CZ-78371 Olomouc, Czech Republic;* ⓞ orcid.org/0000-0003-0645-2019; Phone: +420 585634373; Email: ondrej.plihal@upol.cz

Authors

Magdaléna Bryksová − *Department of Chemical Biology and Genetics, Centre of the Region Haná for Biotechnological and Agricultural Research, Faculty of Science, Palacký University, CZ-78371 Olomouc, Czech Republic*

Siarhei Dabravolski − *Department of Molecular Biology, Centre of the Region Haná for Biotechnological and Agricultural Research, Faculty of Science, Palacký University, CZ-78371 Olomouc, Czech Republic*

Zuzana Kučerová − *Department of Biophysics, Centre of the Region Haná for Biotechnological and Agricultural Research, Faculty of Science, Palacký University, CZ-78371 Olomouc, Czech Republic*

Filip Zavadil Kokáš − *Department of Molecular Biology, Centre of the Region Haná for Biotechnological and Agricultural Research, Faculty of Science, Palacký University, CZ-78371 Olomouc, Czech Republic; Regional Centre for Applied Molecular Oncology (RECAMO), Masaryk Memorial Cancer Institute, CZ-65653 Brno, Czech Republic*

Martina Špundová − *Department of Biophysics, Centre of the Region Haná for Biotechnological and Agricultural Research, Faculty of Science, Palacký University, CZ-78371 Olomouc, Czech Republic*

Lucie Plíhalová − *Department of Chemical Biology and Genetics, Centre of the Region Haná for Biotechnological and Agricultural Research, Faculty of Science and Laboratory of Growth Regulators, Institute of Experimental Botany of the Czech Academy of Sciences & Faculty of Science, Palacký University, CZ-78371 Olomouc, Czech Republic*

Tomáš Takáč − *Department of Cell Biology, Centre of the Region Haná for Biotechnological and Agricultural Research, Faculty of Science, Palacký University, CZ-78371 Olomouc, Czech Republic;* ⓞ orcid.org/0000-0002-1569-1305

Jiří Grúz − *Laboratory of Growth Regulators, Institute of Experimental Botany of the Czech Academy of Sciences & Faculty of Science, Palacký University, CZ-78371 Olomouc, Czech Republic;* ⓞ orcid.org/0000-0002-8546-9697

Martin Hudeček − *Laboratory of Growth Regulators, Institute of Experimental Botany of the Czech Academy of Sciences & Faculty of Science, Palacký University, CZ-78371 Olomouc, Czech Republic*

Veronika Hloušková − *Laboratory of Growth Regulators, Institute of Experimental Botany of the Czech Academy of Sciences & Faculty of Science, Palacký University, CZ-78371 Olomouc, Czech Republic*

Radoslav Koprna − *Department of Chemical Biology and Genetics, Centre of the Region Haná for Biotechnological and Agricultural Research, Faculty of Science, Palacký University, CZ-78371 Olomouc, Czech Republic*

Ondřej Novák − *Laboratory of Growth Regulators, Institute of Experimental Botany of the Czech Academy of Sciences & Faculty of Science, Palacký University, CZ-78371 Olomouc, Czech Republic*

Miroslav Strnad − *Laboratory of Growth Regulators, Institute of Experimental Botany of the Czech Academy of Sciences & Faculty of Science, Palacký University, CZ-78371 Olomouc, Czech Republic*

Karel Doležal − *Department of Chemical Biology and Genetics, Centre of the Region Haná for Biotechnological and Agricultural Research, Faculty of Science and Laboratory of Growth Regulators, Institute of Experimental Botany of the Czech Academy of Sciences & Faculty of Science, Palacký University, CZ-78371 Olomouc, Czech Republic*

Complete contact information is available at:
https://pubs.acs.org/10.1021/acschembio.0c00306

■ REFERENCES

(1) Kieber, J. J., and Schaller, G. E. (2018) Cytokinin signaling in plant development. *Development 145*, dev149344.

(2) Zwack, P. J., and Rashotte, A. M. (2013) Cytokinin inhibition of leaf senescence. *Plant Signaling Behav. 8*, No. e24737.

(3) Vylíčilová, H., Husičková, A., Spíchal, L., Srovnal, J., Doležal, K., Plíhal, O., and Plíhalova, L. (2016) C2-substituted aromatic cytokinin sugar conjugates delay the onset of senescence by maintaining the activity of the photosynthetic apparatus. *Phytochemistry 122*, 22–33.

(4) Choi, J., Choi, D., Lee, S., Ryu, C. M., and Hwang, I. (2011) Cytokinins and plant immunity: old foes or new friends? *Trends Plant Sci. 16*, 388–394.

(5) Brzobohatý, B., Moore, I., Kristoffersen, P., Bako, L., Campos, N., Schell, J., and Palme, K. (1993) Release of active cytokinin by a beta-glucosidase localized to the maize root meristem. *Science 262*, 1051–1054.

(6) Zatloukal, M., Gemrotová, M., Doležal, K., Havlíček, L., Spíchal, L., and Strnad, M. (2008) Novel potent inhibitors of *A. thaliana* cytokinin oxidase/dehydrogenase. *Bioorg. Med. Chem. 16*, 9268–9275.

(7) Spíchal, L., Werner, T., Popa, I., Riefler, M., Schmülling, T., and Strnad, M. (2009) The purine derivative PI-55 blocks cytokinin action via receptor inhibition. *FEBS J. 276*, 244–253.

(8) Motte, H., Galuszka, P., Spíchal, L., Tarkowski, P., Plíhal, O., Šmehilová, M., Jaworek, P., Vereecke, D., Werbrouck, S., and Geelen, D. (2013) Phenyl-adenine, identified in an LSH4-assisted chemical screen, is a potent compound for shoot regeneration through the inhibition of CKX activity. *Plant Physiol. 161*, 1229–1241.

(9) Podlešáková, K., Zálábak, D., Čudejková, M., Plíhal, O., Szücová, L., Doležal, K., Spíchal, L., Strnad, M., and Galuszka, P. (2012) Novel cytokinin derivatives do not show negative effects on root growth and proliferation in submicromolar range. *PLoS One 7*, No. e39293.

(10) Holub, J., Hanuš, J., Hanke, D. E., and Strnad, M. (1998) Biological activity of hydroxybenzyladenines. *Plant Growth Regul. 26*, 109–115.

(11) Aremu, A. O., Bairu, M. W., Szücová, L., Finnie, J. F., and Van Staden, J. (2012) The role of *meta*-topolins on the photosynthetic pigment profiles and foliar structures of micropropagated 'Williams' bananas. *J. Plant Physiol. 169*, 1530–1541.

(12) Szücová, L., Spíchal, L., Doležal, K., Zatloukal, M., Greplová, J., Galuszka, P., Kryštof, V., Voller, J., Popa, I., Massino, F. J., Jørgensen, J. E., and Strnad, M. (2009) Synthesis, characterization and biological activity of ring-substituted 6-benzylamino-9-tetrahydropyran-2-yl and

(13) Mik, V., Szücová, L., Šmehilová, M., Zatloukal, M., Doležal, K., Nisler, J., Grúz, J., Galuszka, P., Strnad, M., and Spíchal, L. (2011) N9-substituted derivatives of kinetin: effective anti-senescence agents. *Phytochemistry 72*, 821–831.

(14) Mik, V., Szücová, L., Spíchal, L., Plíhal, O., Nisler, J., Zahajská, L., Doležal, K., and Strnad, M. (2011) N9-substituted N6-[(3-methylbut-2-en-1-yl)amino]purine derivatives and their biological activity in selected cytokinin bioassays. *Bioorg. Med. Chem. 19*, 7244–7251.

(15) Plíhalová, L., Vylíčilová, H., Doležal, K., Zahajská, L., Zatloukal, M., and Strnad, M. (2016) Synthesis of aromatic cytokinins for plant biotechnology. *New Biotechnol. 33*, 614–624.

(16) Doležal, K., Popa, I., Kryštof, V., Spíchal, L., Fojtíková, M., Holub, J., Lenobel, R., Schmülling, T., and Strnad, M. (2006) Preparation and biological activity of 6-benzylaminopurine derivatives in plants and human cancer cells. *Bioorg. Med. Chem. 14*, 875–884.

(17) Lubecka-Pietruszewska, K., Kaufman-Szymczyk, A., Stefanska, B., Cebula-Obrzut, B., Smolewski, P., and Fabianowska-Majewska, K. (2014) Clofarabine, a novel adenosine analogue, reactivates DNA methylation-silenced tumour suppressor genes and inhibits cell growth in breast cancer cells. *Eur. J. Pharmacol. 723*, 276–287.

(18) Sampath, D., Shi, Z., and Plunkett, W. (2002) Inhibition of cyclin-dependent kinase 2 by the Chk1-Cdc25A pathway during the S-phase checkpoint activated by fludarabine: dysregulation by 7-hydroxystaurosporine. *Mol. Pharmacol. 62*, 680–688.

(19) Maruyama, T., Sato, Y., Oto, Y., Takahashi, Y., Snoeck, R., Andrei, G., Witvrouw, M., and De Clercq, E. (1996) Synthesis and antiviral activity of 6-chloropurine arabinoside and its 2'-deoxy-2'-fluoro derivative. *Chem. Pharm. Bull. 44*, 2331–2334.

(20) Neef, A. B., and Luedtke, N. W. (2011) Dynamic metabolic labeling of DNA *in vivo* with arabinosyl nucleosides. *Proc. Natl. Acad. Sci. U. S. A. 108*, 20404–20409.

(21) Rattanachaikunsopon, P., and Phumkhachorn, P. (2007) Bacteriostatic effect of flavonoids isolated from leaves of *Psidium guajava* on fish pathogens. *Fitoterapia 78*, 434–436.

(22) Werbrouck, S. P., van der Jeugt, B., Dewitte, W., Prinsen, E., Van Onckelen, H. A., and Debergh, P. C. (1995) The metabolism of benzyladenine in *Spathiphyllum floribundum* 'Schott Petite' in relation to acclimatisation problems. *Plant Cell Rep. 14*, 662–665.

(23) Doležal, K., Popa, I., Hauserová, E., Spíchal, L., Chakrabarty, K., Novák, O., Kryštof, V., Voller, J., Holub, J., and Strnad, M. (2007) Preparation, biological activity and endogenous occurrence of N6-benzyladenosines. *Bioorg. Med. Chem. 15*, 3737–3747.

(24) Spíchal, L., Rakova, N. Y., Riefler, M., Mizuno, T., Romanov, G. A., Strnad, M., and Schmülling, T. (2004) Two cytokinin receptors of *Arabidopsis thaliana*, CRE1/AHK4 and AHK3, differ in their ligand specificity in a bacterial assay. *Plant Cell Physiol. 45*, 1299–1305.

(25) Suzuki, T., Miwa, K., Ishikawa, K., Yamada, H., Aiba, H., and Mizuno, T. (2001) The Arabidopsis sensor His-kinase, AHK4, can respond to cytokinins. *Plant Cell Physiol. 42*, 107–113.

(26) Yamada, H., Suzuki, T., Terada, K., Takei, K., Ishikawa, K., Miwa, K., Yamashino, T., and Mizuno, T. (2001) The Arabidopsis AHK4 histidine kinase is a cytokinin-binding receptor that transduces cytokinin signals across the membrane. *Plant Cell Physiol. 42*, 1017–1023.

(27) Kurepa, J., Shull, T. E., and Smalle, J. A. (2019) Antagonistic activity of auxin and cytokinin in shoot and root organs. *Plant Direct 3*, No. e00121.

(28) Tarkowská, D., Doležal, K., Tarkowski, P., Astot, C., Holub, J., Fuksová, K., Schmülling, T., Sandberg, G., and Strnad, M. (2003) Identification of new aromatic cytokinins in *Arabidopsis thaliana* and *Populus* x *canadensis* leaves by LC-(+)ESI-MS and capillary liquid chromatography/frit-fast atom bombardment mass spectrometry. *Physiol. Plant. 117*, 579–590.

(29) Vlčková, A., Špundová, M., Kotabová, E., Novotný, R., Doležal, K., and Nauš, J. (2006) Protective cytokinin action switches to

damaging during senescence of detached wheat leaves in continuous light. *Physiol. Plant.* 126, 257−267.

(30) Thomma, B. P., Cammue, B. P., and Thevissen, K. (2002) Plant defensins. *Planta* 216, 193−202.

(31) Lay, F. T., and Anderson, M. A. (2005) Defensins–components of the innate immune system in plants. *Curr. Protein Pept. Sci.* 6, 85−101.

(32) Lionetti, V., Fabri, E., De Caroli, M., Hansen, A. R., Willats, W. G. T., Piro, G., and Bellincampi, D. (2017) Three pectin methylesterase inhibitors protect cell wall integrity for Arabidopsis immunity to *Botrytis*. *Plant Physiol.* 173, 1844−1863.

(33) Jiang, L., Yang, S. L., Xie, L. F., Puah, C. S., Zhang, X. Q., Yang, W. C., Sundaresan, V., and Ye, D. (2005) VANGUARD1 encodes a pectin methylesterase that enhances pollen tube growth in the Arabidopsis style and transmitting tract. *Plant Cell* 17, 584−596.

(34) Yang, J., Duan, G., Li, C., Liu, L., Han, G., Zhang, Y., and Wang, C. (2019) The crosstalks between jasmonic acid and other plant hormone signaling highlight the involvement of jasmonic acid as a core component in plant response to biotic and abiotic stresses. *Front. Plant Sci.* 10, 1349.

(35) Bilgin, D. D., Zavala, J. A., Zhu, J., Clough, S. J., Ort, D. R., and DeLucia, E. H. (2010) Biotic stress globally downregulates photosynthesis genes. *Plant, Cell Environ.* 33, 1597−1613.

(36) Kanehisa, M., Sato, Y., Kawashima, M., Furumichi, M., and Tanabe, M. (2016) KEGG as a reference resource for gene and protein annotation. *Nucleic Acids Res.* 44, D457−D462.

(37) Attaran, E., Major, I. T., Cruz, J. A., Rosa, B. A., Koo, A. J., Chen, J., Kramer, D. M., He, S. Y., and Howe, G. A. (2014) Temporal dynamics of growth and photosynthesis suppression in response to jasmonate signaling. *Plant Physiol.* 165, 1302−1314.

(38) Göhre, V., Jones, A. M., Sklenář, J., Robatzek, S., and Weber, A. P. (2012) Molecular crosstalk between PAMP-triggered immunity and photosynthesis. *Mol. Plant-Microbe Interact.* 25, 1083−1092.

(39) Choi, J., Huh, S. U., Kojima, M., Sakakibara, H., Paek, K. H., and Hwang, I. (2010) The cytokinin-activated transcription factor ARR2 promotes plant immunity via TGA3/NPR1-dependent salicylic acid signaling in Arabidopsis. *Dev. Cell* 19, 284−295.

(40) Prokopová, J., Špundová, M., Sedlářová, M., Husičková, A., Novotný, R., Doležal, K., Nauš, J., and Lebeda, A. (2010) Photosynthetic responses of lettuce to downy mildew infection and cytokinin treatment. *Plant Physiol. Biochem.* 48, 716−723.

(41) Naseem, M., Philippi, N., Hussain, A., Wangorsch, G., Ahmed, N., and Dandekar, T. (2012) Integrated systems view on networking by hormones in Arabidopsis immunity reveals multiple crosstalk for cytokinin. *Plant Cell* 24, 1793−1814.

(42) Asai, T., Tena, G., Plotnikova, J., Willmann, M. R., Chiu, W. L., Gomez-Gomez, L., Boller, T., Ausubel, F. M., and Sheen, J. (2002) MAP kinase signalling cascade in Arabidopsis innate immunity. *Nature* 415, 977−983.

(43) Rodriguez, M. C., Petersen, M., and Mundy, J. (2010) Mitogen-activated protein kinase signaling in plants. *Annu. Rev. Plant Biol.* 61, 621−649.

(44) Bethke, G., Pecher, P., Eschen-Lippold, L., Tsuda, K., Katagiri, F., Glazebrook, J., Scheel, D., and Lee, J. (2012) Activation of the *Arabidopsis thaliana* mitogen-activated protein kinase MPK11 by the flagellin-derived elicitor peptide, flg22. *Mol. Plant-Microbe Interact.* 25, 471−480.

(45) Eschen-Lippold, L., Jiang, X., Elmore, J. M., Mackey, D., Shan, L., Coaker, G., Scheel, D., and Lee, J. (2016) Bacterial AvrRpt2-like cysteine proteases block activation of the Arabidopsis mitogen-activated protein kinases, MPK4 and MPK11. *Plant Physiol.* 171, 2223−2238.

(46) Piater, L. A., Nürnberger, T., and Dubery, I. A. (2004) Identification of a lipopolysaccharide responsive erk-like MAP kinase in tobacco leaf tissue. *Mol. Plant Pathol.* 5, 331−341.

(47) Meng, X., Xu, J., He, Y., Yang, K.-Y., Mordorski, B., Liu, Y., and Zhang, S. (2013) Phosphorylation of an ERF transcription factor by Arabidopsis MPK3/MPK6 regulates plant defense gene induction and fungal resistance. *Plant Cell* 25, 1126−1142.

(48) Stintzi, A., Weber, H., Reymond, P., Browse, J., and Farmer, E. E. (2001) Plant defense in the absence of jasmonic acid: the role of cyclopentenones. *Proc. Natl. Acad. Sci. U. S. A.* 98, 12837−12842.

(49) Hu, C. H., Wang, P. Q., Zhang, P. P., Nie, X. M., Li, B. B., Tai, L., Liu, W. T., Li, W. Q., and Chen, K. M. (2020) NADPH oxidases: the vital performers and center hubs during plant growth and signaling. *Cells* 9, 437.

(50) Cortleven, A., Leuendorf, J. E., Frank, M., Pezzetta, D., Bolt, S., and Schmülling, T. (2019) Cytokinin action in response to abiotic and biotic stresses in plants. *Plant, Cell Environ.* 42, 998−1018.

(51) Chinchilla, D., Zipfel, C., Robatzek, S., Kemmerling, B., Nürnberger, T., Jones, J. D. G., Felix, G., and Boller, T. (2007) A flagellin-induced complex of the receptor FLS2 and BAK1 initiates plant defense. *Nature* 448, 497−500.

(52) Po-Wen, C., Singh, P., and Zimmerli, L. (2013) Priming of the Arabidopsis pattern-triggered immunity response upon infection by necrotrophic *Pectobacterium carotovorum* bacteria. *Mol. Plant Pathol.* 14, 58−70.

(53) Anders, S., Pyl, P. T., and Huber, W. (2015) HTSeq–a Python framework to work with high-throughput sequencing data. *Bioinformatics* 31, 166−169.

(54) Cunningham, F., Amode, M. R., Barrell, D., Beal, K., Billis, K., Brent, S., Carvalho-Silva, D., Clapham, P., Coates, G., Fitzgerald, S., Gil, L., Girón, C. G., Gordon, L., Hourlier, T., Hunt, S. E., Janacek, S. H., Johnson, N., Juettemann, T., Kähäri, A. K., Keenan, S., Martin, F. J., Maurel, T., McLaren, W., Murphy, D. N., Nag, R., Overduin, B., Parker, A., Patricio, M., Perry, E., Pignatelli, M., Riat, H. S., Sheppard, D., Taylor, K., Thormann, A., Vullo, A., Wilder, S. P., Zadissa, A., Aken, B. L., Birney, E., Harrow, J., Kinsella, R., Muffato, M., Ruffier, M., Searle, S. M., Spudich, G., Trevanion, S. J., Yates, A., Zerbino, D. R., and Flicek, P. (2015) Ensembl 2015. *Nucleic Acids Res.* 43, D662−669.

(55) Kim, D., Pertea, G., Trapnell, C., Pimentel, H., Kelley, R., and Salzberg, S. L. (2013) TopHat2: accurate alignment of transcriptomes in the presence of insertions, deletions and gene fusions. *Genome Biol.* 14, R36.

(56) Love, M. I., Huber, W., and Anders, S. (2014) Moderated estimation of fold change and dispersion for RNA-seq data with DESeq2. *Genome Biol.* 15, 550.

(57) Conesa, A., Götz, S., García-Gómez, J. M., Terol, J., Talón, M., and Robles, M. (2005) Blast2GO: a universal tool for annotation, visualization and analysis in functional genomics research. *Bioinformatics* 21, 3674−3676.

(58) Deng, W., Wang, Y., Liu, Z., Cheng, H., and Xue, Y. (2014) HemI: a toolkit for illustrating heatmaps. *PLoS One* 9, No. e111988.

(59) Floková, K., Tarkowská, D., Miersch, O., Strnad, M., Wasternack, C., and Novák, O. (2014) UHPLC-MS/MS based target profiling of stress-induced phytohormones. *Phytochemistry* 105, 147−157.

Aromatic cytokinin arabinosides promote PAMP-like responses and positively regulate leaf longevity

Magdaléna Bryksová[1,#], Siarhei Dabravolski[2,#], Zuzana Kučerová[3,#], Filip Zavadil Kokáš[2,4], Martina Špundová[3], Lucie Plíhalová[1,5], Tomáš Takáč[6], Jiří Grúz[5], Martin Hudeček[5], Veronika Hloušková[5], Radoslav Koprna[1], Ondřej Novák[5], Miroslav Strnad[5], Ondřej Plíhal[2,5,*], and Karel Doležal[1,5]

[1] Department of Chemical Biology and Genetics, Centre of the Region Haná for Biotechnological and Agricultural Research, Faculty of Science, Palacký University, Šlechtitelů 27, 78371 Olomouc, Czech Republic.

[2] Department of Molecular Biology, Centre of the Region Haná for Biotechnological and Agricultural Research, Faculty of Science, Palacký University, Šlechtitelů 27, 78371 Olomouc, Czech Republic.

[3] Department of Biophysics, Centre of the Region Haná for Biotechnological and Agricultural Research, Faculty of Science, Palacký University, Šlechtitelů 27, 78371 Olomouc, Czech Republic.

[4] Regional Centre for Applied Molecular Oncology (RECAMO), Masaryk Memorial Cancer Institute, Žlutý kopec 7, 65653 Brno, Czech Republic.

[5] Laboratory of Growth Regulators, Faculty of Science, Institute of Experimental Botany of the Czech Academy of Sciences & Palacký University, Šlechtitelů 27, 78371 Olomouc, Czech Republic.

[6] Department of Cell Biology, Centre of the Region Haná for Biotechnological and Agricultural Research, Faculty of Science, Palacký University, Šlechtitelů 27, 78371 Olomouc, Czech Republic.

[*] Corresponding Author: ondrej.plihal@upol.cz

Supporting Information
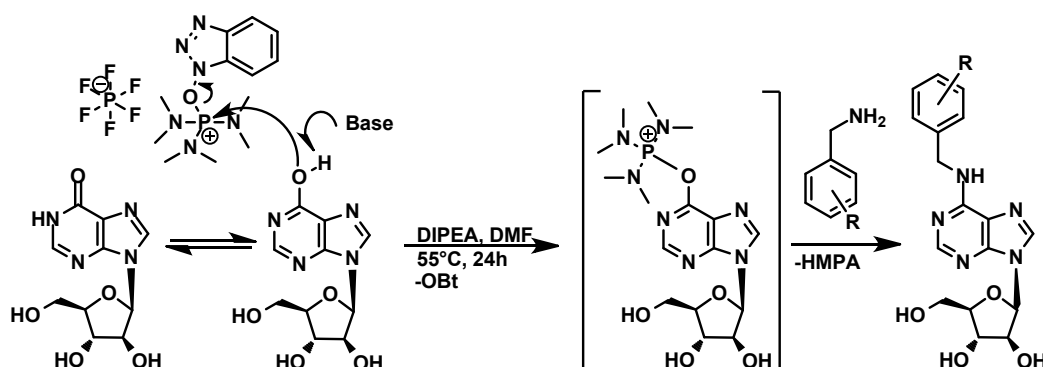
Supplementary Methods

Synthesis of prepared derivatives

The synthesis of BAPAs was achieved according to the following general reaction scheme given here:

9-(β-ᴅ-arabinofuranosyl)hypoxantine (100 mg, 0.37 mmol) and BOP (196 mg, 0.37 mmol) were mixed together in DMF (2 ml). Subsequently, the appropriate benzylamine (0.37 mmol) and DIPEA (97 μl, 0.44 mmol) were added. The reaction mixture was stirred under an argon atmosphere in an oil bath at 60 °C for 24 h then evaporated using a rotary evaporator. MeOH with a drop of chloroform was added to the distillation residue and the mixture was sonicated. The resulted white solid was isolated by filtration and re-crystallized from EtOH. The identity and purity of the synthesized compounds was confirmed by elemental and melting point analysis, analytical thin layer chromatography, high performance liquid chromatography, ES+MS spectrometry, and ^{1}H NMR (Supplementary Table 1).

^{1}H NMR data for the new compounds (DMSO-d6, 500 MHz) δ ppm:

Compound **1**:

3.55-3.75 (m,3H), 4.09 (t,J=4,5Hz,2H), 4.66 (bs,2H), 5.05 (t,J=5,5Hz,1H), 5.48 (d,J=4,5Hz,1H), 5.57 (d,J=5Hz,1H), 6.21 (d,J=4Hz,1H), 7.12-7.32 (m,5H), 8.14 (s,1H), 8.16 (s,1H), 8.32 (bs,1H)

Compound **2**:

3.55-3.68 (m,2H), 3.74 (d,J=3,5Hz,1H), 4.10 (s,2H), 4.71 (bs,2H), 5.05 (d,J=4,5Hz,1H), 5.49 (s,1H), 5.58 (d,J=3,5Hz,1H), 6.23 (d,J=3,5Hz,1H), 7.03-7.32 (m,4H), 8.15 (s,1H), 8.18 (s,1H), 8.30 (bs,1H)

Compound **3**:

3.55-3.67 (m,2H), 3.74 (d,J=4Hz,1H), 4.10 (s,2H), 4.67 (bs,2H), 5.05 (t,J=4,5Hz,1H), 5.48 (d,J=4Hz,1H), 5.57 (d,J=3,5Hz,1H), 6.22 (d,J=4Hz,1H), 6.98 (t,J=6Hz,1H), 7.06-7.16 (m,2H), 7.25-7.33 (m,1H), 8.15 (s,1H), 8.18 (s,1H), 8.37 (bs,1H)

Compound **4**:

3.55-3.66 (m,2H), 3.73 (d,J=4,5 Hz,1H), 4.07-4.11 (m,2H), 4.62 (bs,2H), 5.06 (t,J=5,5 Hz,1H), 5.49 (d,J=4,5 Hz,1H), 5.57 (d,J=5 Jz,1H), 6.22 (d,J=5 Hz,1H), 7.07 (t,J=8,5 Hz,2H), 7.33 (t,J=5,5 Hz,2H), 8.16 (s,2H), 8.34 (bs,1H)

Compound **5**:

3.54-3.80 (m,3H), 4.10 (bs,2H), 4.71 (bs,2H), 5.06 (bs,1H), 5.49 (d,J=3,5Hz,1H), 5.60 (d,J=4Hz,1H), 6.23 (d,J=4Hz,1H) 7.21 (d,J=4Hz,3H), 7.37-7.44 (m,1H), 8.13 (s,1H), 8.20 (s,1H), 8.34 (bs,1H)

Compound **6**:

3.54-3.65 (m,2H), 3.74 (bs,1H), 4.09 (bs,2H), 4.65 (bs,2H), 5.11 (bs,1H), 5.56 (bs,2H), 6.21 (d, J=4,5 Hz,1H), 7.21-7.35 (m,4H), 8.15 (s,1H), 8.17 (s,1H), 8.37 (s,1H)

Compound **7**:

3.56-3.67 (m,2H), 3.73 (bs,1H), 4.09 (bs,2H), 4.63 (bs,2H), 5.05 (t,J=4,5Hz,1H), 5.48 (d,J=3Hz,1H), 5.57 (d,J=4,5Hz,1H), 6.22 (d,J=4Hz,1H), 7.30 (s,4H), 8.14 (s,1H), 8.17 (s,1H), 8.36 (bs,1H)

Compound **8**:

3.75-3.79 (m,2H), 4.13 (t,J=5 Hz,3H), 4.64 (bs,2H), 5.23 (bs, 1H), 5.66 (bs,2H), 6.25 (d,J=5,5 Hz,1H), 7.09 (t,J=7,5 Hz,1H), 7.33 (d,J=7,5 Hz,1H), 7.55 (d,J=8 Hz,1H), 7.68 (s,1H), 8.18 (s,1H), 8.21 (s,1H), 8.36 (bs,1H)

Compound **9**:

3.54-3.65 (m,2H), 3.72 (d,J=4Hz,1H), 4.09 (t,J=4,5Hz,2H), 4.58 (bs,2H), 5.04 (t,J=5Hz,1H), 5.48 (d,J=4Hz,1H), 5.56 (d,J=4,5Hz,1H), 6.21 (d,J=4Hz,1H), 7.09 (d,J=8,5Hz,2H), 7.59 (d,J=8Hz,2H), 8.13 (s,1H), 8.16 (s,1H), 8.34 (bs,1H)

Compound **10**:

3.55-3.68 (m,2H), 3.74 (d,J=4Hz,1H), 3.79 (s,3H), 4.10 (s,2H), 4.62 (bs,2H), 5.07 (bs,1H), 5.50 (s,1H), 5.59 (s,1H), 6.23 (d,J=4Hz,1H), 6.79 (t,J=8Hz,1H), 6.93 (d,J=7,5Hz,1H), 7.05 (d,J=6,5Hz,1H), 7.16 (t,J=8Hz,1H), 8.06 (s,1H), 8.11 (s,1H), 8.17 (bs,1H)

Compound **11**:

3.56-3.79 (m,6H), 4.10 (s,2H), 4.63 (bs,2H), 5.06 (s,1H), 5.49 (s,1H), 5.58 (s,1H), 6.22 (d,J=2,5Hz,1H), 6.72 (d,J=6Hz,1H), 6.86 (d,J=8Hz,2H), 7.15 (t,J=8Hz,1H), 8.15 (s,1H), 8.17 (s,1H), 8.30 (bs,1H)

Compound **12**:

3.52-3.75 (m,6H), 4.03-4.12 (m,2H), 4.56 (bs,2H), 5.00-5.09 (m,1H), 5.44-5.59 (m,2H), 6.15-6.24 (m,1H), 6.79 (d,J=8,5Hz,2H), 7.16-7.26 (m,2H), 8.12 (s,1H), 8.14 (s,1H), 8.24 (bs,1H)

Compound **13**:

3.54-3.67 (m,2H), 3.74 (d,J=3,5Hz,1H), 4.10 (s,2H), 4.57 (bs,2H), 5.06 (s,1H), 5.49 (s,1H), 5.58 (d,J=3,5Hz,1H), 6.22 (d,J=3Hz,1H), 6.54 (d, J=7,5Hz,1H), 6.65-6.74 (m,2H), 7.02 (t,J=7,5Hz,1H), 8.14 (s,1H), 8.16 (s,1H), 8.26 (bs,1H), 9.20 (s,1H)

Compound **14**:

3.54-3.76 (m,6H), 4.03-4.15 (m,2H), 4.62 (bs,1H), 5.04 (t,J=5,5Hz,1H), 5.49 (d,J=4,5Hz,2H), 5.59 (d,J=6Hz,2H), 6.12-6.25 (m,1H), 7.01-7.18 (m,2H), 7.99 (s,1H), 8.10 (s,1H), 8.12 (s,1H), 8.23 (bs,1H)

Compound **15**:

3.55-3.78 (m,6H), 4.06-4.15 (m,2H), 4.62 (bs,2H), 5.14 (t,J=5,5HZ,1H), 5.56 (d,J=4Hz,1H), 5.62 (d,J=5Hz,1H), 6.22 (d,J=4Hz,1H), 6.96 (d,J=7Hz,1H), 7.04-7.15 (m,3H), 8.14 (s,1H), 8.16 (s,1H), 8.26 (bs,1H)

Compound **16**:

3.54-3.77 (m,6H), 4.09 (s,2H), 4.61 (bs,2H), 5.05(t,J=5,5Hz,1H), 5.48 (d,J=3,5Hz,1H), 5.57 (d,J=4,5Hz,1H), 6.21 (d,J=4Hz,1H), 7.04 (d,J=7,5Hz,2H), 7.17 (d,J=7,5Hz,2H), 8.13 (s,1H), 8.15 (s,1H), 8.26 (bs,1H)

Compound **17**:

3.57-3.70 (m,2H), 3.76 (d,J=4 Hz,1H), 4.12 (s,2H), 4.51 (bs,2H), 5.09 (t,J=5 Hz,1H), 5.19 (s,2H), 5.52 (d,J=4 Hz,1H), 5.59 (d,J=5 Hz,1H), 6.25 (d,J=4 Hz,1H), 6.45 (t,J=7 Hz,1H), 6.59 (d,J=8 Hz,1H), 6.90 (t,J=7 Hz,1H), 7.07 (d,J=7,5 Hz,1H), 8.20 (s,3H)

Compound **18**:

3.55-3.76 (m,3H), 4.06-4.13 (m,2H), 4.73 (bs,2H), 5.05 (t,J=5Hz,1H), 5.48 (d,J=4,5Hz,1H), 5.56(d,J=5,5Hz,1H), 6.22 (d,J=5Hz,1H), 7.46-7.68 (m,4H), 8.15 (s,1H), 8.18 (s,1H), 8.44 (bs,1H)

Compound **19**:

3.56-3.76 (m,3H), 4.05-4.14 (m,2H), 4.68 (bs,2H), 5.05 (t,J=5,5Hz,1H), 5.48 (d,J=4,5Hz,1H), 5.57 (d,J=5,5Hz,1H), 6.22 (d,J=4,5Hz,1H), 7.15 (d,J=8Hz,1H), 7.25-7.42 (m,3H), 8.15 (s,1H), 8.18 (s,1H), 8.40 (bs, 1H)

Compound **20**:

3.54-3.76 (m,3H), 4.03-4.15 (m,2H), 4.68 (bs,2H), 5.05 (t,J=5,5Hz,1H), 5.48 (d,J=4Hz,1H), 5.56 (d,J=5Hz,1H), 6.23 (d,J=4,5Hz,1H), 7.02-7.22 (m,3H), 8.16 (s,1H), 8.19 (s,1H), 8.34 (bs,1H)

Compound **21**:

3.40-3.53 (m,2H), 3.60 (d,J=2,5 Hz,1H), 3.95 (s,2H), 4.52 (bs,2H), 4.91 t,J=5Hz,1h), 5.35 (d,J=2Hz,1H), 5.42 (d,J=4Hz,1H), 6.09 (d,J=3Hz,1H), 6.79-6.92 (m,3H), 8.02 (s,1H), 8.05 (s,1H), 8.26 (bs,1H)

General procedures

Elemental analyses were performed using an EA1112 CHN analyzer (Thermo Finnigan, Thermofisher Scientific). Melting points were determined on a Buchi Melting Point B-540 apparatus and are uncorrected. Analytical thin-layer chromatography (TLC) was carried out using silica gel 60 WF$_{254}$ plates (Merck) with CHCl$_3$/MeOH (4:1, v/v) as the solvent. The purity of the synthesized compounds was determined as described previously [1]. Briefly, samples were dissolved in methanol (1 mg ml^{-1}) and then diluted to a concentration of 10 μg ml^{-1} in the initial mobile phase. 10 μl of the resulting solution was injected onto a thermostated (25 °C) RP column (150 mm × 2.1 mm, 5 μm C18 Symmetry, Waters) and analyzed using an Alliance 2695 Separations Module high-performance liquid chromatograph coupled to a PDA 2996 detector (Waters) with detection at wavelengths of 210–400 nm. The chromatograph's effluent was directed into the ion source of a benchtop quadrupole orthogonal acceleration time-of-flight Q-TOF Micro tandem mass spectrometer (Waters). HPLC elution was performed at a flow rate of 0.3 ml min^{-1} using a linear gradient of 15 mM ammonium formate at pH 4.0 (mobile phase A) and pure methanol (mobile phase B). The proportion of B in the mobile phase was initially 10% and was increased linearly to 90% over 24 min, after which isocratic elution was performed with 90% B. The column was then re-equilibrated under the initial conditions (10% B) for 10 min. The electrospray source was maintained at 120 °C with a capillary voltage of +3.0 kV, a cone voltage of +20 V, and a desolvation temperature of 300 °C. Nitrogen was used as both the desolvation gas (500 l h^{-1}) and the cone gas (50 l h^{-1}). The mass spectrometer was operated in positive (ESI+) ionization mode and data were acquired in the 50–1000 m/z range. The mass spectrometer was directly coupled to a MassLynx 4.1 data system. ^{1}H NMR spectra were measured on a JEOL 500 ECA instrument at 500 MHz. Samples were prepared by dissolving the compounds in DMSO-d_6. Tetramethylsilane (TMS) was used as the internal standard.

KEGG pathway over-representation analysis

For the visual interpretation of transcriptomic data from 3-methoxy-BAPA treatments, the KEGG database was employed (https://www.kegg.jp). KEGG Mapper was used for processing of KO annotation data [2].

Bacterial cytokinin assay

E. coli strain KMI001 (*ΔrcsC, cps::lacZ*), harboring either the plasmid pIN-III-AHK4 or pSTV28-AHK3, which express the Arabidopsis histidine kinases CRE1/AHK4 or AHK3 [3, 4] was used in the experiments. Activity of β-galactosidase was measured using 4-methylumbelliferyl β-D-galactopyranoside as a substrate after overnight growth in the presence of CK [5]. In addition, live-cell cytokinin-binding assay with radiolabeled *t*Z as a competitor was performed as previously described [6]. Homogenous bacterial suspensions with OD_{600} values of 0.8 and 1.2 were found to be optimal for CRE1/AHK4 and AHK3 cultures, respectively. The competition reaction was allowed to proceed with 2 nM [2-^{3}H]*t*Z and various concentrations of the tested compounds for 30 min at 4 °C. When binding equilibrium was reached, the suspension was centrifuged (6000 x g), the supernatant was removed, and the bacterial pellet was resuspended in the scintillation cocktail (Beckman).

Effect of 3-methoxy-BAPA and 3-hydroxy-BAPA on infection level in field trial experiments

An effect of 3-methoxy-BAPA and 3-hydroxy-BAPA was tested in field trials on winter wheat (cv. Turandot; Selgen, Czech Republic) and spring barley (cv. Francin; Selgen, Czech Republic) performed near Olomouc, Czech Republic (GPS: 49.5748542N, 17.2851261E; altitude 218 m) in a growth season 2017/2018. The 5 µM solution of 3-methoxy-BAPA or 3-hydroxy-BAPA was applied as a foliar spray on wheat at a growth stage of tillering (BBCH 25 [7]) and on barley at stage of beginning of stem elongation (BBCH 30-33 [7]) or start of flag leaf extending (BBCH 39-41 [7]) in amount of 300 ml per 10 m^2. A level of infection was evaluated at a growth stage of beginning of heading (BBCH 51 [7]) in the case of wheat and leaf rusts and barley and powdery mildew or at growth stage of early milk ripeness (BBCH 73 [7]) in the case of barley and foot rot diseases. The evaluation of each variant was carried out on 5 plots (n = 5), 20 plants were evaluated from each plot. The level of infection was evaluated according the following scales:

i)   for wheat and leaf rusts (namely *Puccinia striiformis* syn. *Puccinia glumarum*, *Puccinia recondita* f. sp. *tritici*, *Puccinia graminis*): 1 – without infection; 2 – a few clusters of chlorosis; 3 – clusters to 1 % of leaf area; 4 – clusters from 1 to 3 % of leaf area; 5 - clusters from 3 to 5 % of leaf area, beginning of strips; 6 – clusters and strips from 5 to 15 % of leaf area;

ii)   for barley and powdery mildew (*Blumeria graminis* syn. *Erysiphe graminis*): 1 – without symptoms; 2 – mycelium at max. 1 % of leaf area; 3 – mycelium at 1 – 5 % of leaf area; 4 – mycelium at 5 – 10 % of leaf area; 5 - mycelium at 10 – 30 % of leaf area;

iii)   for barley and foot rot diseases (*Gaeumannomyces graminis* syn. *Ophiobolus graminis*, *Ramulispora herpotrichoides* syn. *Pseudocercosporella herpotrichoides*, teleomorpha *Tapesia yallundae*, *Fusarium* spp., *Rhizoctonia* spp.): 1 – without symptoms; 3 – brown spots to 5 % of stem perimeter; 5 – brown spots from 5 to 25 % of stem perimeter.

In the end of each experiment, a number of tillers per plant was determined with 50 randomized plants of the variant (10 plants from each plot). A number of spikes per 0.25 m^2 was counted and converted to 1 m^2. After harvest, grain yield was determined.

Supplementary Tables

Supplementary Table 1. Elemental analysis, ES+ mass spectrometry analysis, melting points and HPLC purity of prepared BAPA derivatives.

Compound	Elemental analysis calculated/found			Mp (°C)	ES-MS	HPLC (%)
	% of C	% of H	% of N		[M+H$^+$]	
1	57.1/55.9	5.3/4.9	19.6/19.0	191-193	358	>98
2	54.4/52.6	4.8/4.7	18.7/18.0	191-193	376	>98
3	54.4/54.0	4.8/4.7	18.7/18.8	224-225	376	>98
4	54.4/52.9	4.8/4.9	18.7/18.0	190-192	376	>98
5	52.1/51.7	4.6/4.7	17.9/17.6	226-229	393	>99
6	52.1/51.9	4.6/4.6	17.9/17.4	240-242	393	>98
7	52.1/52.3	4.6/4.4	17.9/17.2	181-183	393	>99
8	42.3/41.8	3.8/3.6	14.5/14.1	221-223	484	>98
9	42.3/42.2	3.8/3.8	14.5/13.8	182-184	484	>98
10	55.8/55.6	5.5/5.5	18.1/17.9	224-225	388	>98
11	55.8/55.4	5.5/5.4	18.1/17.9	236-238	388	>99
12	55.8/55.7	5.5/5.5	18.1/17.9	182-183	388	>99
13	54.7/53.9	5.1/5.0	18.8/18.3	235-238	374	>98
14	58.2/57.9	5.7/5.4	18.9/18.8	224-227	372	>98
15	58.2/57.4	5.7/5.3	18.9/18.9	216-218	372	>99
16	58.2/58.0	5.7/5.4	18.9/18.6	173-177	372	>98
17	54.8/54.2	5.4/5.3	22.6/21.8	193-196	373	>98
18	50.8/49.9	4.3/3.9	16.5/15.8	182-184	426	>98
19	49.0/48.6	4.1/3.9	15.9/15.4	175-176	442	>98
20	51.9/51.2	4.4/4.3	17.8/17.6	214-216	394	>98
21	51.9/51.4	4.4/3.7	17.8/17.3	236-237	394	>98

Supplementary Table 2. Overview of DEGs regulated by 3-methoxy-BAPA. The table lists the 50 most strongly upregulated and downregulated genes (adjusted P-value < 0.05), respectively, that showed the highest absolute log$_2$ fold change (log$_2$FC) after 6 h dark-incubation of detached Arabidopsis leaves with 10 µM 3-methoxy-BAPA.

UPREGULATED DEGs		
AGI number	**Description**	**log$_2$ FC**
At2g47040	Vanguard 1/Pectinesterase 5 [Source:Uniprot/SWISSPROT 3BAcc:Q5MFV8]	**2.80**
At3g01270	Probable pectate lyase 7 [Source:Uniprot/SWISSPROT 3BAcc:Q9SRH4]	**2.79**
At2g47050	Plant invertase/pectin methylesterase inhibitor superfamily protein [Source:TAIR 3BAcc:47050]	**2.31**
At3g07820	Pectin lyase-like superfamily protein [Source:TAIR 3BAcc:07820]	**2.22**
At3g28750	Hypothetical protein	**2.21**
At2g47030	Plant invertase/pectin methylesterase inhibitor superfamily protein (VGDH1) [Source:Uniprot/SWISSPROT 3BAcc:O80722]	**2.16**
At4g35010	Beta-galactosidase 11 (BGAL11) [Source:Uniprot/SWISSPROT 3BAcc:Q9SCV1]	**2.03**
At3g62230	F-box protein At3g62230/DUO1-ACTIVATED F-BOX 1 [Source:Uniprot/SWISSPROT 3BAcc:Q9M1Q1]	**1.95**
At3g05610	Probable pectinesterase/pectinesterase inhibitor 21 [Source:Uniprot/SWISSPROT 3BAcc:Q8GX86]	**1.80**
At5g44430	PLANT DEFENSIN 1.2C (PDF1.2C)/Defensin-like protein 17 [Source:Uniprot/SWISSPROT 3BAcc:Q9FI22]	**1.75**
At1g55560	SKU5 similar 14/SKS14 [Source:TAIR 3BAcc:55560]	**1.71**
At1g02790	Exopolygalacturonase 4 (PGA4) [Source:Uniprot/SWISSPROT 3BAcc:P49062]	**1.67**

At5g39880	Transmembrane protein [Source:TAIR 3BAcc:39880]	**1.64**
At5g44420	PLANT DEFENSIN 1.2A/Defensin-like protein 16 [Source:Uniprot/SWISSPROT 3BAcc:Q9FI23]	**1.58**
At5g07430	Pectin lyase-like superfamily protein/Probable pectinesterase 50 [Source:Uniprot/SWISSPROT 3BAcc:Q9LY17]	**1.57**
At1g07260	UDP-glycosyltransferase 71C3 (UGT71C3) [Source:Uniprot/SWISSPROT 3BAcc:Q9LML7]	**1.54**
At2g26020	PLANT DEFENSIN 1.2B/Putative defensin-like protein 15 [Source:Uniprot/SWISSPROT 3BAcc:O80994]	**1.52**
At5g19580	Glyoxal oxidase-related protein [Source:TAIR 3BAcc:19580]	**1.51**
At2g26010	PLANT DEFENSIN 1.3/Defensin-like protein 14 [Source:Uniprot/SWISSPROT 3BAcc:O80995]	**1.47**
At5g45880	Pollen Ole e 1 allergen and extensin family protein [Source:TAIR 3BAcc:45880]	**1.45**
At5g50030	Plant invertase/pectin methylesterase inhibitor superfamily protein [Source:TAIR 3BAcc:50030]	**1.42**
At3g01240	Splicing regulatory glutamine/lysine-rich-like protein	**1.35**
At3g62710	Glycosyl hydrolase family protein [Source:TAIR 3BAcc:62710]	**1.35**
At5g04180	Alpha carbonic anhydrase 3 (ATACA3) [Source:Uniprot/SWISSPROT 3BAcc:Q9FYE3]	**1.33**
At5g12960	Proline-tRNA ligase (DUF1680) [Source:TAIR 3BAcc:12960]	**1.33**
At5g26700	RmlC-like cupins superfamily protein/Probable germin-like protein subfamily 2 member 5 [Source:Uniprot/SWISSPROT 3BAcc:O65252]	**1.26**
At1g05580	Cation/H(+) antiporter 23 2C chloroplastic (CHX23) [Source:Uniprot/SWISSPROT 3BAcc:Q8VYD4]	**1.26**
At5g58390	Peroxidase superfamily protein [Source:Uniprot/SWISSPROT 3BAcc:Q9LVL2]	**1.23**
At1g61566	Protein RALF-like 9 (RALFL9) [Source:Uniprot/SWISSPROT 3BAcc:Q3ECL0]	**1.19**
At1g62760	Pectin methylesterase inhibitor (ATPMEI10) [Source:TAIR 3BAcc:AT1G62760]	**1.18**
At1g06160	Ethylene-responsive transcription factor ERF094/Ethylene responsive factor 59 [Source:Uniprot/SWISSPROT 3BAcc:Q9LND1]	**1.16**
At2g04460	Transposable element gene [Source:TAIR 3BAcc:04460]	**1.16**
At5g61160	Agmatine coumaroyltransferase/Anthocyanine 5-aromatic acyltransferase 1 [Source:Uniprot/SWISSPROT 3BAcc:Q9FNP9]	**1.13**
At3g20470	Glycine-rich protein 5 [Source:TAIR 3BAcc:AT3G20470]	**1.09**
At1g59950	NAD(P)-linked oxidoreductase superfamily protein [Source:TAIR 3BAcc:59950]	**1.08**
At1g75830	PLANT DEFENSIN 1.1 (PDF1.1)/Defensin-like protein 13 [Source:Uniprot/SWISSPROT 3BAcc:P30224]	**1.06**
At4g16260	Putative beta-1,3-endoglucanase [Source:TAIR 3BAcc:16260]	**1.01**
At2g41180	Sigma factor binding protein 2 2C chloroplastic (SIB2) [Source:Uniprot/SWISSPROT 3BAcc:O80669]	**0.98**
At3g49110	Peroxidase 33 (PRX33) [Source:Uniprot/SWISSPROT 3BAcc:P24101]	**0.98**
At2g43590	Chitinase family protein [Source:TAIR 3BAcc:43590]	**0.95**
At3g28153	Transposable element gene [Source:TAIR 3BAcc:28153]	**0.92**
At2g43580	Chitinase family protein [Source:TAIR 3BAcc:43580]	**0.91**
At1g61563	Protein RALF-like 8 (RALFL8) [Source:Uniprot/SWISSPROT 3BAcc:Q1ECR9]	**0.90**
At3g43828	Transposable element gene [Source:TAIR 3BAcc:43828]	**0.90**
At1g15415	Protein phosphatase 2A (PP2A) B'gamma subunit [Source:TAIR 3BAcc:15415]	**0.88**
At2g31141	Hypothetical protein	**0.88**
At2g28210	Alpha carbonic anhydrase 2 (ATACA2) [Source:TAIR 3BAcc:28210]	**0.85**
At3g13400	SKU5 similar 13/SKS13 [Source:TAIR 3BAcc:13400]	**0.82**
At2g22320	Hypothetical protein	**0.82**
At1g66390	Transcription factor MYB90 [Source:Uniprot/SWISSPROT 3BAcc:Q9ZTC3]	**0.81**

DOWNREGULATED DEGs

At4g36850	PQ-loop repeat family protein / transmembrane family protein [Source:TAIR 3BAcc:At4g36850]	**-2.16**
At1g29920	Chlorophyll a/b binding protein 2 (LHCB1.2) [Source:Uniprot/SWISSPROT 3BAcc:Q8VZ87]	**-1.78**

At2g34430	Light-harvesting chlorophyll-protein complex II subunit B1 [Source:TAIR 3BAcc:At2g34430]	**-1.64**
At3g27690	Photosystem II light harvesting complex gene 2.3 [Source:TAIR 3BAcc:At3g27690]	**-1.40**
At2g05100	Photosystem II light harvesting complex gene 2.1 [Source:TAIR 3BAcc:At2g05100]	**-1.32**
At1g29910	Light-harvesting chlorophyll a/b binding protein 1.2 [Source:TAIR 3BAcc:At1g29910]	**-1.29**
At2g05070	Photosystem II light harvesting complex gene 2.2 [Source:TAIR 3BAcc:At2g05070]	**-1.29**
At3g19390	Granulin repeat cysteine protease family protein [Source:TAIR 3BAcc:At3g19390]	**-1.20**
At3g19710	Methionine aminotransferase BCAT4 [Source:Uniprot/SWISSPROT 3BAcc:Q9LE06]	**-1.18**
At1g62510	Bifunctional inhibitor/lipid-transfer protein/seed storage 2S albumin superfamily protein [Source:TAIR 3BAcc:At1g62510]	**-1.16**
At4g21650	Subtilase 3. 13 (SBT3.13) [Source:TAIR 3BAcc:At4g21650]	**-1.11**
At5g65690	Phosphoenolpyruvate carboxykinase 2 (PCK2) [Source:TAIR 3BAcc:At5g65690]	**-1.09**
At5g24490	30S ribosomal protein 2C putative [Source:TAIR 3BAcc:At5g24490]	**-1.08**
At1g29930	Chlorophyll a/b binding protein 1 2C chloroplastic/Light-harvesting chlorophyll a/b protein 1.3 [Source:Uniprot/SWISSPROT 3BAcc:P04778]	**-1.08**
At5g54270	Light-harvesting chlorophyll B-binding protein 3 [Source:TAIR 3BAcc:At5g54270]	**-1.08**
At5g38420	Ribulose bisphosphate carboxylase small chain 2B 2C chloroplastic (RBCS2B) [Source:Uniprot/SWISSPROT 3BAcc:P10797]	**-1.06**
At4g25580	CAP160 protein [Source:TAIR 3BAcc:At4g25580]	**-1.05**
At1g16410	Dihomomethionine N-hydroxylase/Cytochrome P450 79F1 (CYP79F1) [Source:Uniprot/SWISSPROT 3BAcc:Q949U1]	**-1.05**
At4g26260	Myo-inositol oxygenase 4 (MIOX4) [Source:Uniprot/SWISSPROT 3BAcc:Q8H1S0]	**-1.05**
At3g26060	Peroxiredoxin Q 2C chloroplastic [Source:Uniprot/SWISSPROT 3BAcc:Q9LU86]	**-1.03**
At5g02160	FTSH5 interacting protein [Source:TAIR 3BAcc:At5g02160]	**-1.03**
At5g64040	Photosystem I reaction center subunit N 2C chloroplastic [Source:Uniprot/SWISSPROT 3BAcc:P49107]	**-1.02**
At3g22740	Homocysteine S-methyltransferase 3 [Source:Uniprot/SWISSPROT 3BAcc:Q8LAX0]	**-1.01**
At2g10940	Bifunctional inhibitor/lipid-transfer protein/seed storage 2S albumin superfamily protein [Source:TAIR 3BAcc:AT2G10940]	**-0.99**
At3g08940	Chlorophyll a-b binding protein CP29.2 2C chloroplastic/LHCB4.2 [Source:Uniprot/SWISSPROT 3BAcc:Q9XF88]	**-0.98**
At4g01330	Protein kinase superfamily protein [Source:TAIR 3BAcc:At4g01330]	**-0.97**
At1g30280	Chaperone DnaJ-domain superfamily protein/Auxilin-like 7 [Source:TAIR 3BAcc:At1g30280]	**-0.96**
At2g20670	Putative sugar phosphate exchanger (DUF506) [Source:TAIR 3BAcc:At2g20670]	**-0.96**
At2g34420	Photosystem II light harvesting complex gene B1B2 [Source:TAIR 3BAcc:At2g34420]	**-0.95**
At1g68560	Alpha-xylosidase 1 (ATXYL1)/Altered xyloglucan 3 (AXY3) [Source:Uniprot/SWISSPROT 3BAcc:Q9S7Y7]	**-0.94**
At4g08870	Arginine amidohydrolase 2 2C mitochondrial [Source:Uniprot/SWISSPROT 3BAcc:Q9ZPF5]	**-0.93**
At5g23010	Methylthioalkylmalate synthase 1 2C chloroplastic [Source:Uniprot/SWISSPROT 3BAcc:Q9FG67]	**-0.93**
At3g50800	Hypothetical protein	**-0.93**
At2g46740	L-gulonolactone oxidase 5 [Source:Uniprot/SWISSPROT 3BAcc:O81030]	**-0.92**
At5g63450	Cytochrome P450 94B1 [Source:Uniprot/SWISSPROT 3BAcc:Q9FMV7]	**-0.92**
At4g03060	Alkenyl hydroxalkyl producing 2 (AOP2) [Source:TAIR 3BAcc:At4g03060]	**-0.91**
At5g55150	F-box SKIP23-like protein (DUF295) [Source:Uniprot/SWISSPROT 3BAcc:Q9FLP7]	**-0.90**
At1g12900	Glyceraldehyde-3-phosphate dehydrogenase GAPA2 2C chloroplastic [Source:Uniprot/SWISSPROT 3BAcc:Q9LPW0]	**-0.89**
At3g02020	Aspartokinase 3 2C chloroplastic [Source:Uniprot/SWISSPROT 3BAcc:Q9S702]	**-0.88**
At1g68010	Glycerate dehydrogenase HPR 2C peroxisomal [Source:Uniprot/SWISSPROT 3BAcc:Q9C9W5]	**-0.86**
At3g46780	Plastid transcriptionally active 16 [Source:TAIR 3BAcc:AT3G46780]	**-0.86**

At5g14740	Beta carbonic anhydrase 2 2C chloroplastic [Source:Uniprot/SWISSPROT 3BAcc:P42737]	**-0.85**
At1g32060	Phosphoribulokinase 2C chloroplastic [Source:Uniprot/SWISSPROT 3BAcc:P25697]	**-0.85**
At4g10340	Light-harvesting complex of Photosystem II 5 (LHCB5) [Source:Uniprot/SWISSPROT 3BAcc:Q9XF89]	**-0.85**
At4g28040	Nodulin MtN21-like transporter family protein/WAT1-related protein [Source:Uniprot/SWISSPROT 3BAcc:Q9SUD5]	**-0.85**
At1g01620	Aquaporin PIP1;3 [Source:Uniprot/SWISSPROT 3BAcc:Q08733]	**-0.84**
At5g57550	Probable xyloglucan endotransglucosylase/hydrolase protein 25 [Source:Uniprot/SWISSPROT 3BAcc:Q38907]	**-0.84**
At2g13360	L-Serine: glyoxylate aminotransferase (SGAT) [Source:Uniprot/SWISSPROT 3BAcc:Q56YA5]	**-0.84**
At2g46820	Curvature thylakoid 1B 2C chloroplastic (CURT1B) [Source:Uniprot/SWISSPROT 3BAcc:Q8LCA1]	**-0.84**
At5g13630	Magnesium-chelatase subunit ChlH 2C chloroplastic/ABA-binding protein (ABAR) [Source:Uniprot/SWISSPROT 3BAcc:Q9FNB0]	**-0.84**

Supplementary Table 3. The most strongly affected gene ontology (GO) terms assigned to upregulated or downregulated differentially expressed genes (adjusted *P*-value < 0.05) in Arabidopsis leaves treated with 3-methoxy-BAPA for 6 h.

GO number	Domain	Description	Total #	Affected genes (%)
Up-regulated				
GO:0009861	BP	jasmonic acid and ethylene-dependent systemic resistance	13	23.1
GO:0016653	MF	oxidoreductase activity, acting on NAD(P)H, heme protein as acceptor	9	22.2
GO:0047893	MF	flavonol 3-O-glucosyltransferase activity	11	18.2
GO:0004089	MF	carbonate dehydratase activity	14	14.3
GO:0006026	BP	aminoglycan catabolic process	24	12.5
GO:0046348	BP	amino sugar catabolic process	24	12.5
GO:1901072	BP	glucosamine-containing compound catabolic process	24	12.5
GO:0006032	BP	chitin catabolic process	24	12.5
GO:0080043	MF	quercetin 3-O-glucosyltransferase activity	24	12.5
GO:0016998	BP	cell wall macromolecule catabolic process	27	11.1
GO:0071456	BP	cellular response to hypoxia	26	7.7
GO:0071804	BP	cellular potassium ion transport	43	7.0
GO:0009817	BP	defense response to fungus, incompatible interaction	44	6.8
GO:0004364	MF	glutathione transferase activity	54	5.6
GO:0019722	BP	calcium-mediated signaling	55	5.5
Down-regulated				
GO:0030076	CC	light-harvesting complex	26	61.5
GO:0009522	CC	photosystem I	42	59.5
GO:0010196	BP	nonphotochemical quenching	7	57.1
GO:0019253	BP	reductive pentose-phosphate cycle	20	55.0
GO:0009765	BP	photosynthesis, light harvesting	39	53.9
GO:0016168	MF	chlorophyll binding	38	52.6
GO:0019685	BP	photosynthesis, dark reaction	21	52.4
GO:0015977	BP	carbon fixation	22	50.0
GO:0042549	BP	photosystem II stabilization	6	50.0
GO:0009533	CC	chloroplast stromal thylakoid	8	50.0
GO:0008187	MF	poly-pyrimidine tract binding	18	44.4
GO:0008266	MF	poly(U) RNA binding	18	44.4
GO:0009773	BP	photosynthetic electron transport in photosystem I	48	41.7
GO:0018298	BP	protein-chromophore linkage	41	41.5

GO:0009523	CC	photosystem II	68	39.7

GO, gene ontology; BP, biological process; CC, cellular component; MF, molecular function.

Detached Arabidopsis leaves were treated with 10 µM 3-methoxy-BAPA or an equivalent volume of buffer containing 0.1% DMSO (negative control) for 6 h in darkness. The most strongly affected GO terms at level 6 or higher are shown. Percentages of DEGs are calculated based on the total number of genes in *Arabidopsis thaliana* genome annotated with the same GO number (total #).

Supplementary Table 4. Effect of the treatment with 3-methoxy-BAPA (3MeOBAPA) and 3-hydroxy-BAPA (3OHBAPA) on the grain yield, number of tillers and number of spikes in winter wheat / spring barley plants. The same plants were used in field-plot experiments evaluating the level of plant infection by fungal pathogens (see Figure 7). The 5 µM solutions were applied as a foliar spray at different plant growth stages (tillering, the beginning of stem elongation, the beginning of flag leaf extending). The values in bold italics show statistically significant difference between treated and non-treated plants ($P < 0.01$). n.d., not determined.

	Compound (growth stage during application)	Grain yield		Number of tillers per plant		Number of spikes per m^2	
		[t ha^{-1}]	[%]		[%]		[%]
wheat	non-treated	6.72	100	5.9	100	432	100
	3MeOBAPA (tillering)	6.48	96	6.3	107	470	109
barley	non-treated	8.53	100	3.8	100	698	100
	3MeOBAPA (stem elongation)	8.78	103	*4.7*	*124*	748	107
	3MeOBAPA (flag leaf extending)	8.67	102	n.d.	n.d.	721	103
	3OHBAPA (stem elongation)	8.62	101	4.2	111	688	99
	3OHBAPA (flag leaf extending)	8.86	104	n.d.	n.d.	686	98

Supplementary Table 5. Primers for expression profiling of *A. thaliana* MAPK genes.

Gene	AGI No.	Primers 5′ - 3′
Housekeeping genes (Endogenous controls)		
Act2	*At3g18780*	TGGTCGTACAACCGGTATTGTG ATCAGTAAGGTCACGTCCAGCAA
Act7	*At5g09810*	CTAGAGACAGCCAAGAGCAGTTC GTTTCATGGATTCCAGGAGCTTC
EF1α	*At5g60390*	TGAGCACGCTCTTCTTGCTTTCA GGTGGTGGCATCCATCTTGTTACA
MAPK/PTI marker genes		
MPK3	*At3g45640*	GACAGAGTTGCTTGGCACACCGA GGCTGACGTGGGAAGTTGGGA
MPK4	*At4g01370*	TGTCGGCTGGTGCAGTCGATTT TGGCACAACGCCTCATCAACTGT
MPK6	*At2g43790*	ACAGCTTCCACCTTATCCTCGCCA TGGGCCAATGCGTCTAAAACTGTG
MPK11	*At1g01560*	TTCTTAAGAAGCGACAACGCTAG ATTGACCGACATGTTTGGGAATC
FRK1	*At2g19190*	GAGACTATTTGGCAGGTAAAAGGT AGGAGGCTTACAACCATTGTG
WRKY33	*At2g38470*	GGGAAACCCAAATCCAAGA GTTTCCCTTCGTAGGTTGTGA
WRKY53	*At4g23810*	CGGAAGTCCGAGAAGTGAAG TCTGACCACTTTGGTAACATCTTT

Supplementary References

1. Gucký, T., Jorda, R., Zatloukal, M., Bazgier, V., Berka, K., Řezníčková, E., Béres, T., Strnad, M., and Kryštof, V. (2013) A novel series of highly potent 2,6,9-trisubstituted purine cyclin-dependent kinase inhibitors, *J. Med. Chem. 56*, 6234-6247.
2. Kanehisa, M., Sato, Y., Kawashima, M., Furumichi, M., and Tanabe, M. (2016) KEGG as a reference resource for gene and protein annotation, *Nucleic Acids Res. 44*, D457-462.
3. Suzuki, T., Miwa, K., Ishikawa, K., Yamada, H., Aiba, H., and Mizuno, T. (2001) The Arabidopsis sensor His-kinase, AHK4, can respond to cytokinins, *Plant Cell Physiol. 42*, 107-113.
4. Yamada, H., Suzuki, T., Terada, K., Takei, K., Ishikawa, K., Miwa, K., Yamashino, T., and Mizuno, T. (2001) The Arabidopsis AHK4 histidine kinase is a cytokinin-binding receptor that transduces cytokinin signals across the membrane, *Plant Cell Physiol. 42*, 1017-1023.
5. Spíchal, L., Rakova, N. Y., Riefler, M., Mizuno, T., Romanov, G. A., Strnad, M., and Schmülling, T. (2004) Two cytokinin receptors of Arabidopsis thaliana, CRE1/AHK4 and AHK3, differ in their ligand specificity in a bacterial assay, *Plant Cell Physiol. 45*, 1299-1305.
6. Romanov, G. A., Spíchal, L., Lomin, S. N., Strnad, M., and Schmülling, T. (2005) A live cell hormone-binding assay on transgenic bacteria expressing a eukaryotic receptor protein. *Anal. Biochem. 347*, 129–134.
7. Meier, U. (2001). Growth stages of mono- and dicotyledonous plants. BBCH Monograph, Federal Biological Research Centre for Agriculture and Forestry, Bonn.

Article

The Anti-Senescence Activity of Cytokinin Arabinosides in Wheat and Arabidopsis Is Negatively Correlated with Ethylene Production

Zuzana Kučerová [1] , Marek Rác [1], Jaromír Mikulík [2], Ondřej Plíhal [2], Pavel Pospíšil [1],
Magdaléna Bryksová [3] , Michaela Sedlářová [4] , Karel Doležal [2,3] and Martina Špundová [1,*]

[1] Department of Biophysics, Centre of the Region Haná for Biotechnological and Agricultural Research, Faculty of Science, Palacký University, Šlechtitelů 27, CZ-78371 Olomouc, Czech Republic; zuzana.kucerova@upol.cz (Z.K.); marek.rac@upol.cz (M.R.); pavel.pospisil@upol.cz (P.P.)

[2] Laboratory of Growth Regulators, Faculty of Science, Palacký University and Institute of Experimental Botany AS CR, Šlechtitelů 27, CZ-78371 Olomouc, Czech Republic; jaromir.mikulik@upol.cz (J.M.); ondrej.plihal@upol.cz (O.P.); karel.dolezal@upol.cz (K.D.)

[3] Department of Chemical Biology and Genetics, Centre of the Region Haná for Biotechnological and Agricultural Research, Faculty of Science, Palacký University, Šlechtitelů 27, CZ-78371 Olomouc, Czech Republic; magdalena.bryksova@upol.cz

[4] Department of Botany, Faculty of Science, Palacký University, Šlechtitelů 27, CZ-78371 Olomouc, Czech Republic; michaela.sedlarova@upol.cz

* Correspondence: martina.spundova@upol.cz; Tel.: +420-585-634-512

check for
updates

Abstract: Leaf senescence, accompanied by chlorophyll breakdown, chloroplast degradation and inhibition of photosynthesis, can be suppressed by an exogenous application of cytokinins. Two aromatic cytokinin arabinosides (6-benzylamino-9-β-ᴅ-arabinofuranosylpurines; BAPAs), 3-hydroxy- (3OHBAPA) and 3-methoxy- (3MeOBAPA) derivatives, have recently been found to possess high anti-senescence activity. Interestingly, their effect on the maintenance of chlorophyll content and maximal quantum yield of photosystem II (PSII) in detached dark-adapted leaves differed quantitatively in wheat (*Triticum aestivum* L. cv. Aranka) and Arabidopsis (*Arabidopsis thaliana* L. (Col-0)). In this work, we have found that the anti-senescence effects of 3OHBAPA and 3MeOBAPA in wheat and Arabidopsis also differ in other parameters, including the maintenance of carotenoid content and chloroplasts, rate of reduction of primary electron acceptor of PSII (Q_A) as well as electron transport behind Q_A, and partitioning of absorbed light energy in light-adapted leaves. In wheat, 3OHBAPA had a higher protective effect than 3MeOBAPA, whereas in Arabidopsis, 3MeOBAPA was the more efficient derivative. We have found that the different anti-senescent activity of 3OHBAPA and 3MeOBAPA was coupled to different ethylene production in the treated leaves: the lower the ethylene production, the higher the anti-senescence activity. 3OHBAPA and 3MeOBAPA also efficiently protected the senescing leaves of wheat and Arabidopsis against oxidative damage induced by both H_2O_2 and high-light treatment, which could also be connected with the low level of ethylene production.

Keywords: cytokinin derivative; ethylene; senescence; chlorophyll fluorescence; wheat; Arabidopsis; phytohormone; oxidative stress; photosystem II

1. Introduction

Phytohormones cytokinins (CKs) have a crucial role in almost all stages of plant growth and development, including senescence. Senescence is a highly organized and controlled process that is characterized by dramatic structural and functional changes, such as degradation of photosynthetic

pigments and inhibition of photosynthesis (e.g., [1–3]), and by extensive changes in gene expression [4]. An exogenous application of CKs typically delays senescence-induced decreases in chlorophyll (Chl) and carotenoid content, inhibition of photosynthesis, degradation of proteins, pigment–protein complexes and whole chloroplasts, as well as membrane deterioration (e.g., [3,5–9]). The anti-senescence activity of CKs is related to the downregulation of senescence-associated genes (*SAGs*) [10] and upregulation of genes encoding components of photosynthetic light-harvesting complexes [11].

From an agricultural point of view, leaf senescence is one of the major traits that negatively affects crop production, and therefore the delay of this process represents an ideal target for improving crop yield and quality [12]. One of the natural CKs that is used both in agriculture [13] and biotechnology is the aromatic CK 6-benzylaminopurine (BAP), mainly because of its activity, affordability, and stability in plants [14,15]. BAP has significant anti-senescence activity and its exogenous application effectively delays senescence-induced changes (e.g., [3,8,9]). However, under certain conditions, BAP can have negative effects on primary root development, lateral root branching, or shoot formation in vitro (e.g., [16–19]). When applied at higher concentrations or in combination with light, BAP can even accelerate senescence [11,20,21]. These findings led to the search for aromatic CK derivatives that would not exhibit these negative effects on plant growth and development [22]. Several previously prepared compounds have been shown to be more efficient in delaying senescence than unmodified BAP, including those with hydroxy- or methoxy-groups introduced to the benzyl ring (e.g., [5,23,24]).

In our previous work, novel 6-benzylamino-9-β-ᴅ-arabinofuranosylpurines (BAPAs) were synthesized [25] and their unique mode of action has been described [26]. BAPAs have high anti-senescence activity, but they have generally low interactions with the CK pathway and thus also very low activity in other CK-regulated processes and no negative effects on root/shoot development [26]. We have observed that the application of BAPAs induced a massive transcriptional reprogramming from photosynthesis toward defense responses, including the elicitation of several MAPK modules, suggesting an induction of a pathogen-associated molecular patterns (PAMP)-like response [26]. This response was accompanied by delaying senescence. A comparison of the anti-senescence activity of two selected BAPAs, 3-hydroxy- (3OHBAPA) and 3-methoxy- (3MeOBAPA) derivatives (see Figure 1), indicated that their protective effect during senescence (maintenance of Chl content and maximal quantum yield of photosystem II (PSII)) differs quantitatively in wheat and Arabidopsis: 3OHBAPA had higher protective effect in wheat, while in Arabidopsis 3MeOBAPA was more efficient.
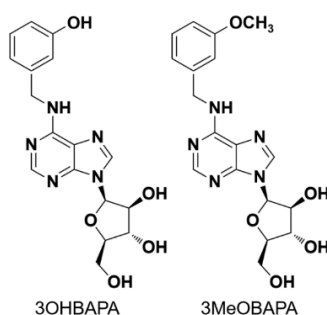

Figure 1. Structure of 6-(3-hydroxybenzylamino)-9-β-ᴅ-arabinofuranosylpurine (3OHBAPA, left) and 6-(3-methoxybenzylamino)-9-β-ᴅ-arabinofuranosylpurine (3MeOBAPA, right).

Here, we have investigated whether the different effects of 3OHBAPA and 3MeOBAPA on the senescence of detached wheat (*Triticum aestivum* L. cv. Aranka) and *Arabidopsis thaliana* L. (Col-0) leaves will also manifest in the maintenance of other parameters related to photosynthetic apparatus and its function. We have evaluated the changes in carotenoid content and chloroplasts, rate of reduction of primary electron acceptor of PSII (Q_A) and electron transport behind Q_A, and changes in the partitioning of absorbed light energy in light-adapted leaves. We have also explored the possibility that the different anti-senescent activity of 3OHBAPA and 3MeOBAPA in both plant models is related

to a different level of ethylene production in the treated leaves, as ethylene is known to co-determine the progression of senescence in plant samples treated by anti-senescence compounds [27]. Finally, we have evaluated whether 3OHBAPA and 3MeOBAPA can protect senescing leaves of wheat and Arabidopsis against oxidative damage induced by both H_2O_2 and high-light treatment.

2. Results and Discussion

2.1. Senescence-Induced Changes in Detached Leaves of Wheat and Arabidopsis

The decrease in photosynthetic pigment content, deterioration of chloroplasts, and the loss of photosynthetic activity are typical phenomena of leaf senescence [1–3,7]. In our case, after six days of dark-induced senescence of detached wheat and Arabidopsis leaves, the content of Chl decreased significantly (Figure 2A). In line with our previous results [26], the decline in Chl content was more pronounced in the case of Arabidopsis leaves, which reflected a higher progression of senescence compared to wheat (Figure 2A). A similar trend was observed in the decrease in carotenoid content (Figure 2C). The relative rate of degradation of Chl *a* and Chl *b* differed between the leaves of wheat and Arabidopsis, as evidenced by different changes in the Chl *a/b* ratio (Figure 2B). The decrease in the ratio found in wheat indicated a higher degradation of Chl *a*, while in the Arabidopsis leaves Chl *b* degraded faster, which resulted in a higher Chl *a/b* ratio (Figure 2B).
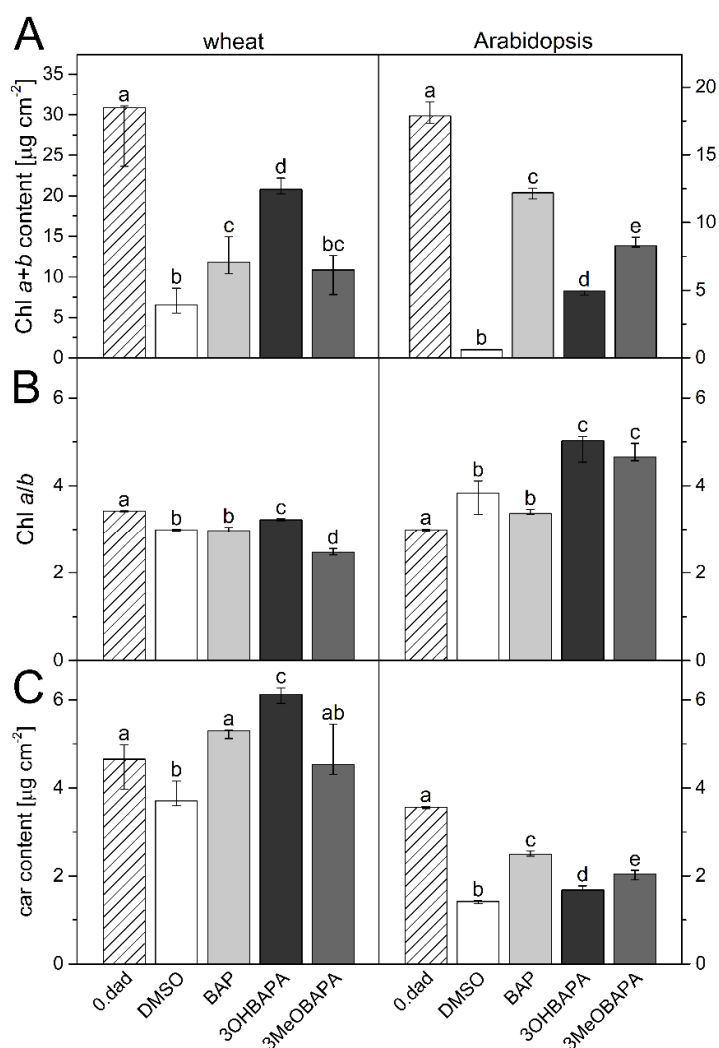
Figure 2. (**A**) Chlorophyll (Chl) *a+b* content; (**B**) Chl *a/b* ratio and (**C**) carotenoid (car) content in control (0. dad) and detached leaves of wheat and Arabidopsis after 6 days of dark incubation in 0.1% DMSO

or 10-µmol·L^{-1} solutions of 6-benzylaminopurine (BAP), 3OHBAPA and 3MeOBAPA. Medians and quartiles are shown (*n* = 5). Different letters indicate a statistically significant difference between treatments within a plant species (*p* < 0.05; Student's unpaired *t*-test).

Since the progressive decline in photosynthetic pigment contents suggests chloroplast degradation, confocal microscopy was performed to compare the chloroplast integrity in freshly detached leaves ("0. dad") and in the leaves senescing for six days in the dark ("DMSO"; Figure 3). In senescing wheat leaves, the chloroplasts were still partially preserved, although their deterioration and aggregation was apparent (Figure 3A). In Arabidopsis, chloroplast autofluorescence was no longer detectable (Figure 3B), suggesting chloroplast degradation, which implies, together with apparent impairment of tissue structure, more advanced senescence compared to wheat.
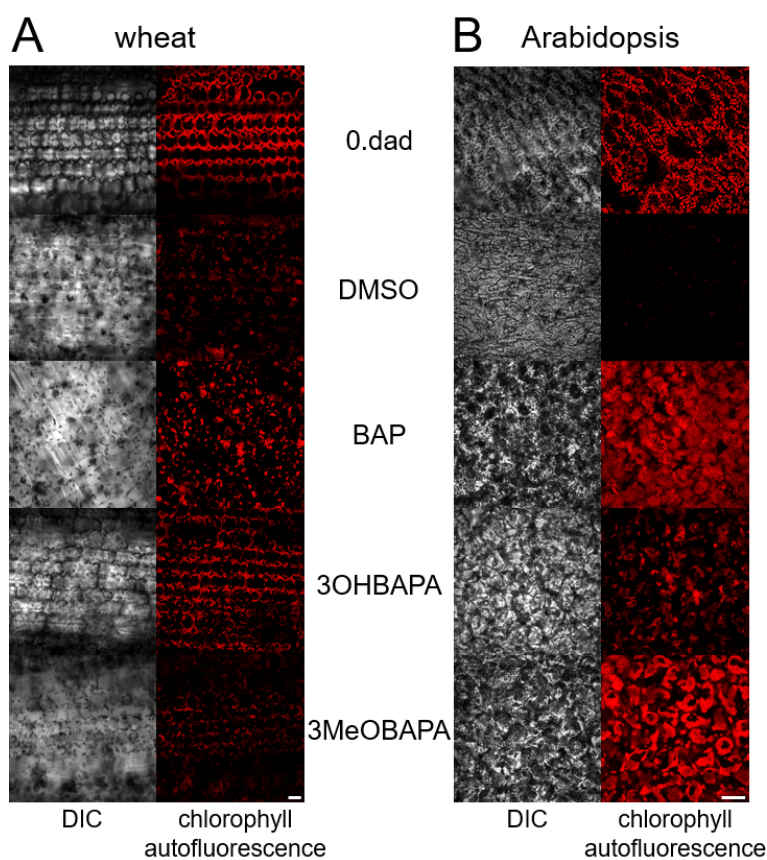
Figure 3. Confocal micrographs of freshly detached (0. dad) (**A**) wheat and (**B**) Arabidopsis leaves and leaves incubated in 0.1% DMSO or 10-µmol·L^{-1} solutions of BAP, 3MeOBAPA and 3OHBAPA in the dark for 6 days. Scale bars represent 50 µm. DIC, differential interference contrast.

The different extent of senescence in wheat and Arabidopsis was also manifested at the level of PSII function, whose maintenance was estimated from the measurement of Chl fluorescence parameters (Figure 4). We measured Chl fluorescence induction transient (OJIP curve) to monitor the rate of excitation supply to reaction center (RCII), reduction of primary electron acceptor of PSII (Q$_A$), and subsequent electron transport behind Q$_A$ [28] during the first (milli)seconds of illumination of dark-adapted leaves. In wheat leaves, both (dV/dt)$_0$ and V$_J$ parameters increased (Figure 4A,B), indicating the acceleration of excitation supply to RCII and Q$_A$ reduction and inhibition of electron transport behind Q$_A$. Unlike in wheat, a decrease in (dV/dt)$_0$ was found in Arabidopsis leaves, while V$_J$ increased to its maximal value (=1). These changes indicate a strong impairment of PSII, involving minimal delivery of excitations to RCII as well as extreme inhibition of electron transfer from Q$_A^-$. In the senescent Arabidopsis leaves, the inhibition of the excitation supply to RCII could

be partially related to the increased Chl *a/b* ratio (Figure 2B), which reflects higher degradation of light-harvesting complexes of PSII (LHCII) compared to RCII [29].
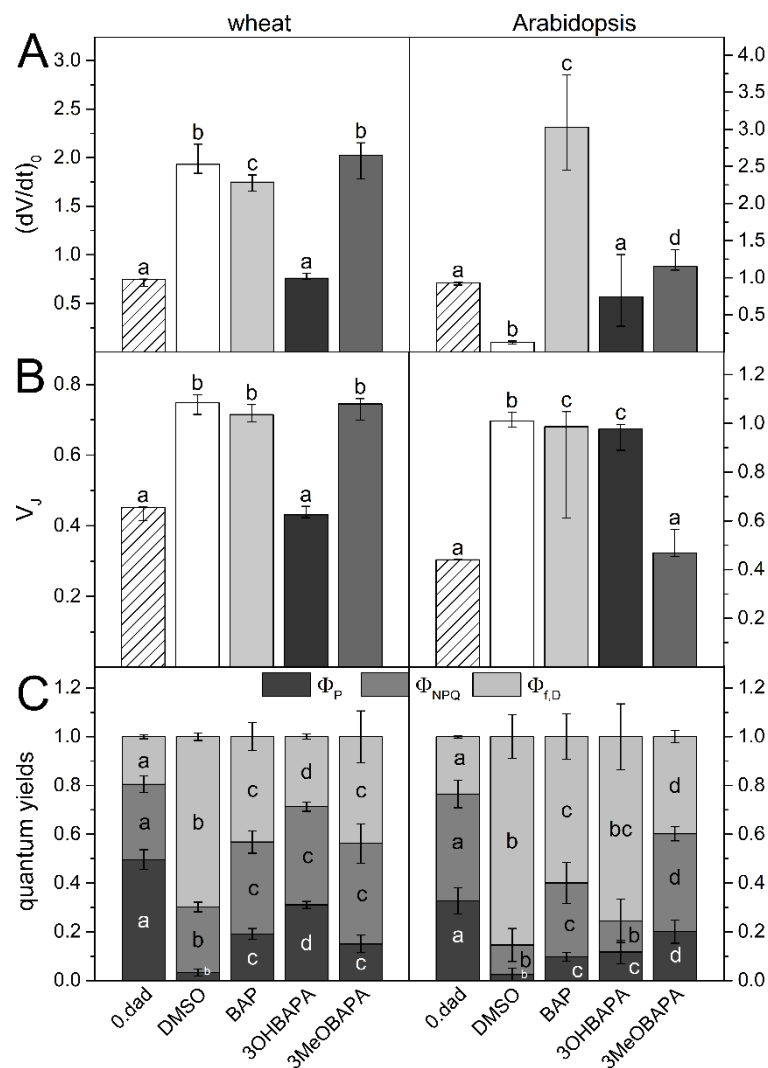

Figure 4. (**A**) The initial slope of the O–J Chl fluorescence rise (dV/dt)$_0$, (**B**) the relative variable fluorescence at the J step (V$_J$) and (**C**) quantum yields of photosystem II (PSII) photochemistry (Φ_P), regulatory non-photochemical quenching (Φ_{NPQ}) and non-regulatory dissipation processes ($\Phi_{f,D}$) in control (0. dad) and detached leaves of wheat and Arabidopsis after 6 days of dark-incubation in 0.1% DMSO or 10-μmol$\cdot$L^{-1} solutions of BAP, 3OHBAPA and 3MeOBAPA. Medians and quartiles are presented (*n* = 5–12). Different letters indicate a statistically significant difference between treatments within a plant species (*p* < 0.05; Student's unpaired *t*-test).

Further information on senescence-induced changes in the PSII function was obtained by measurement of quantum yields Φ_P, Φ_{NPQ} and $\Phi_{f,D}$. These parameters, measured during exposition of leaves to actinic light, reflect the partitioning of absorbed light energy for PSII photochemistry (Φ_P) and for regulated (Φ_{NPQ}) and non-regulated ($\Phi_{f,D}$) non-photochemical processes [30]. Steady-state values of Φ_P, Φ_{NPQ}, and $\Phi_{f,D}$ measured after a 7-min exposition of the senescent leaves to actinic light are presented (Figure 4C). A higher decrease in Φ_P and Φ_{NPQ}, and a more pronounced increase in $\Phi_{f,D}$ was found in Arabidopsis compared to wheat (Figure 4C). These results again indicate very strong impairment of PSII function in senescent Arabidopsis leaves connected with the low ability of photosynthetic apparatus to regulate dissipation of excess light energy, which subsequently can result in oxidative damage [31].

2.2. Comparison of the Anti-Senescence Activity of BAP and CK Arabinosides in Wheat and Arabidopsis Leaves

It is well known that the senescence-induced changes can be effectively delayed by the exogenous application of CKs. The aromatic cytokinin BAP is known to be stable in plants and highly active in delaying senescence (e.g., [3,5,8,9]). In line with the previously published results, the exogenous application of BAP slowed down the senescence-induced decrease in Chl and carotenoid content and partially suppressed deterioration of chloroplasts in both wheat and Arabidopsis (Figures 2 and 3). However, the effect of BAP on parameters reflecting PSII function during the initial phase of transition of photosynthetic apparatus from a dark- to light-adapted state (the OJIP transient) was not so convincing. The only distinct effect of BAP was found for $(dV/dt)_0$ in Arabidopsis. Unlike in the mock-treated leaves ("DMSO"), in the BAP-treated leaves the parameter $(dV/dt)_0$ increased pronouncedly, indicating faster excitation delivery, probably due to the suppression of the preferential degradation of LHCII observed in the mock-treated Arabidopsis leaves. A minimal protective effect of BAP on excitation delivery to RCII, reduction in Q_A and electron transport behind Q_A was found in the wheat leaves (Figure 4A,B). A similar effect of BAP has already been reported by Špundová [32] in wheat, but only 7 days after leaf detachment. In leaves senescing for 4 days, BAP significantly protected electron transfer behind Q_A, as indicated by the non-increased V_J. Since a pronounced protective effect of BAP on excitation delivery to RCII $(dV/dt)_0$ and electron transport behind Q_A (V_J) was also found by Janečková [3] in detached leaves of barley senescing for 4 days, it seems that BAP protects these photosynthetic reactions especially at earlier stages of senescence and later its effect weakens.

The senescence-induced changes in the partitioning of absorbed light energy were partially reduced in the BAP-treated leaves. The PSII photochemistry and regulatory non-photochemical quenching were more effective and the increase in the yield of non-regulated energy dissipation was lower compared to the mock-treated leaves (Figure 4C). This protective effect of BAP on PSII photochemistry corresponds with the maintenance of the maximal quantum yield of PSII photochemistry (F_V/F_M) found in our previous work [26].

Based on the estimation of overall Chl content in detached leaves of wheat and Arabidopsis, we have recently found that CK arabinosides have similar or even higher anti-senescence activity than BAP [25,26]. Two of them, 3OHBAPA and 3MeOBAPA derivatives, have been found to have a strong positive effect on F_V/F_M (measured in the dark-adapted state of the senescent leaves) [26]. Interestingly, this effect differed quantitatively in wheat and Arabidopsis. 3OHBAPA had a higher protective effect in wheat, while 3MeOBAPA was more effective in Arabidopsis. In both plant species, the CK arabinosides were more effective in the maintenance of PSII function than BAP [26].

In this work, we have compared the effect of 3OHBAPA, 3MeOBAPA and BAP on senescence-induced changes in other parameters that characterize the status of photosynthetic apparatus. Among the treated senescing leaves, relative differences in carotenoid contents corresponded to those of Chl (compare Figure 2A,C). In wheat, the carotenoid content was maintained similarly in BAP- and 3MeOBAPA-treated leaves, whereas in leaves treated with 3OHBAPA many more carotenoids (even more than in the freshly detached leaves) were found, confirming the more positive effect of this CK arabinoside. In Arabidopsis, the efficiency of 3MeOBAPA was lower in comparison with BAP, but higher when compared to 3OHBAPA (Figure 2C). Similar trends were found at the level of chloroplast integrity, evaluated by confocal microscopy (Figure 3). In the case of wheat, senescence-induced deterioration of chloroplasts was similar in the BAP- and 3MeOBAPA-treated leaves, whereas in the leaves treated by 3OHBAPA chloroplasts were better preserved (Figure 3A). On the contrary, in Arabidopsis, the protective effect of 3OHBAPA was the weakest (Figure 3B).

The senescence-induced impairment of PSII function was suppressed almost completely by 3OHBAPA in wheat and 3MeOBAPA in Arabidopsis. The excitation supply to RCII, Q_A reduction and electron transport behind Q_A were highly maintained, as indicated by the unchanged values of $(dV/dt)_0$ and V_J compared to non-senescent leaves (Figure 4A,B). Interestingly, in the 3MeOBAPA-treated leaves of Arabidopsis, the excitation supply into RCII was not accelerated (as in the BAP-treated leaves, Figure 4A), which corresponds to a higher degradation of LHCII compared to RCII, indicated also

by the increased Chl *a/b* ratio (Figure 2B). This result is in line with the RNA-seq gene expression analysis in our previous study, where we have shown that the genes encoding LHCII components were downregulated in 3MeOBAPA-treated leaves [26]. The absence of increased delivery of excitations to RCII could contribute to the protection of photosynthetic apparatus from excess excitations and to the maintenance of the partitioning of absorbed light energy documented by minimal changes of Φ_P, Φ_{NPQ} and $\Phi_{f,D}$ (Figure 4C). Interestingly, CK ribosides synthesized by Vylíčilová [11] caused the upregulation of LHCII genes and an increase in the relative abundance of LHCII [11], implying a different mechanism of action of CK arabinosides and CK ribosides.

In summary, 3OHBAPA had the highest anti-senescence activity in wheat, followed by 3MeOBAPA and BAP, whose activity was similar. In Arabidopsis, 3MeOBAPA was less efficient than BAP in the maintenance of photosynthetic pigment content, but it was more efficient in the maintenance of PSII function. At the same time, when compared to 3OHBAPA, 3MeOBAPA had higher anti-senescence activity, as documented by the changes in all studied parameters.

It has been shown that different activity of anti-senescence compounds can be associated with their influence on ethylene production in the detached dark-incubated leaves [27]. It is known that the exogenous application of CKs stimulates the production of ethylene [33,34]. As opposed to the positive effect of CKs on plant and leaf longevity, ethylene is known for being the accelerator of senescence [35]. Thus, the rate of the stimulation of ethylene production by exogenously applied CK can co-determine a resultant senescence-delaying effect—i.e., the anti-senescence activity of CK.

We have evaluated the effect of the compounds on ethylene production in wheat and Arabidopsis leaves. As expected, the ethylene production in BAP-treated leaves was higher compared to the mock-treated leaves (Figure 5). Interestingly, no stimulation of ethylene production was observed in the wheat leaves treated by 3OHBAPA and in Arabidopsis leaves treated by 3MeOBAPA. A moderately stimulated ethylene production was observed in the 3MeOBAPA-treated wheat leaves and 3OHBAPA-treated leaves of Arabidopsis (Figure 5). Thus, the differences in the rate of ethylene production corresponded generally to the quantitative differences of anti-senescence activity between BAP and BAPAs, as well as between 3OHBAPA and 3MeOBAPA: the lower the ethylene production, the higher the anti-senescence activity.
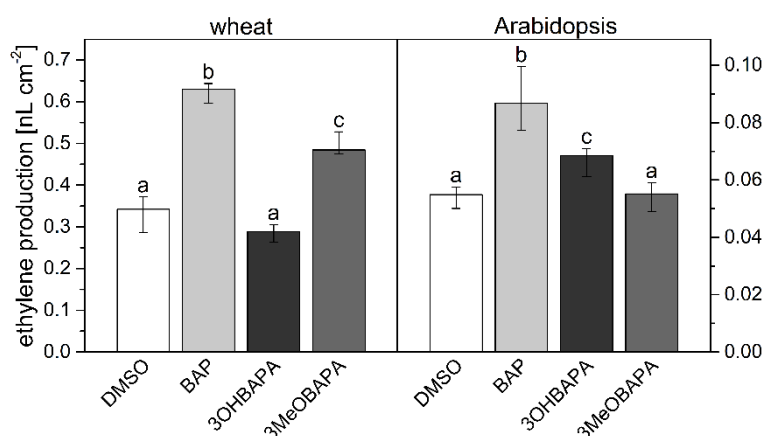

Figure 5. Ethylene production in detached leaves of wheat and Arabidopsis incubated in 0.1% DMSO or 10-μmol·L^{-1} solutions of BAP, 3OHBAPA and 3MeOBAPA and kept sealed in 8-mL vials in darkness for 6 days. Medians and quartiles are presented (*n* = 5–9). Different letters indicate a statistically significant difference between treatments within a plant species ($p < 0.05$; Student's unpaired *t*-test).

2.3. Species-Specific Effects of BAPAs Treatment in the Protection Against Induced Oxidative Damage

It has been shown that the inhibition of ethylene production not only suppresses leaf senescence, but it also enhances the tolerance of plants to abiotic stresses, including H_2O_2- and high light (HL)-induced oxidative stress [36]. As no stimulation of ethylene production was found in wheat leaves

treated by 3OHBAPA and Arabidopsis leaves treated by 3MeOBAPA (Figure 5), we hypothesized that the mentioned BAPA treatments could provide a more efficient protection of leaves against oxidative damage induced by H_2O_2- and HL-treatment than the BAP treatment.

For a comparison of the protective effect of CK arabinosides and BAP, senescent leaves were exposed to exogenous H_2O_2 (5 mmol·L^{-1}) and the level of oxidative damage was evaluated using ultra-weak photon emission (UPE) [37]. In the mock-treated leaves, the H_2O_2 treatment caused pronounced oxidative damage as indicated by the high UPE ratio (Figure 6). In wheat, the protective effect indicated by the lower UPE ratio was observed only in leaves treated with 3OHBAPA. In Arabidopsis, both BAP and 3MeOBAPA reduced the oxidative damage, 3MeOBAPA being more effective (Figure 6).
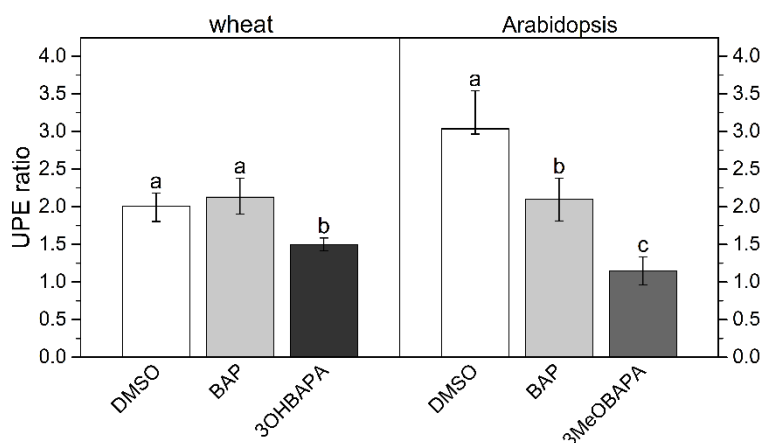
Figure 6. Ratio of ultra-weak photon emission (UPE) intensity after/before application of H_2O_2 in detached leaves of wheat and Arabidopsis dark-incubated for 6 days in 0.1% DMSO or 10-μmol·L^{-1} solutions of BAP, 3OHBAPA or 3MeOBAPA. Medians and quartiles are presented (*n* = 4). Different letters indicate a statistically significant difference between treatments within a plant species (*p* < 0.05; Student's unpaired *t*-test).

In the following experiment, we exposed the senescent leaves to HL (500 μmol photons·m^{-2}·s^{-1}) and estimated cell membrane damage using the measurement of ion leakage by conductivity, accumulation of lipid hydroperoxides (LOOHs; as primary products of lipid peroxidation and markers of oxidative damage) by confocal microscopy, and maintenance of the maximal quantum yield of PSII photochemistry (F_V/F_M), which reflects the extent of photoinhibition or photodamage of PSII. The exposure of senescing leaves to HL led to a strong oxidative damage, as indicated by progressive deterioration of cell membranes during 8 h of HL treatment (Figure 7), and by LOOH accumulation (Figure 8) and photoinhibition of PSII (Figure 9) after 4 h of HL treatment. The oxidative damage was suppressed by the exogenous application of BAP, although its protective effect was quite low. The HL-induced membrane deterioration and PSII photoinhibition were attenuated in the BAP-treated leaves of both wheat and Arabidopsis; LOOH accumulation was reduced only in Arabidopsis (Figures 7–9).
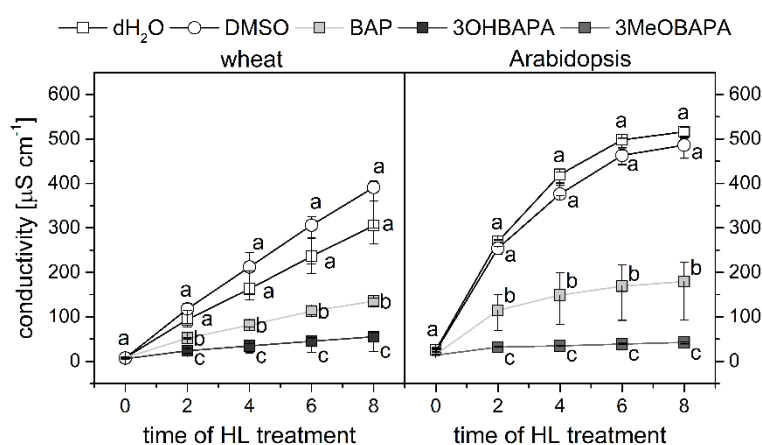
Figure 7. Conductivity as a measure of cell membrane damage in wheat- and Arabidopsis-detached leaves incubated in deionized water (dH$_2$O), 0.1% DMSO, 10-µmol·L^{-1} solutions of BAP, 3OHBAPA or 3MeOBAPA. Before high-light treatment (HL; 500 µmol photons·m^{-2}·s^{-1}) for up to 8 h leaves were incubated in the dark for 6 days. Medians and quartiles are presented (*n* = 7). Different letters indicate a statistically significant difference between treatments within a plant species and particular time point (*p* < 0.05; Student's unpaired *t*-test).
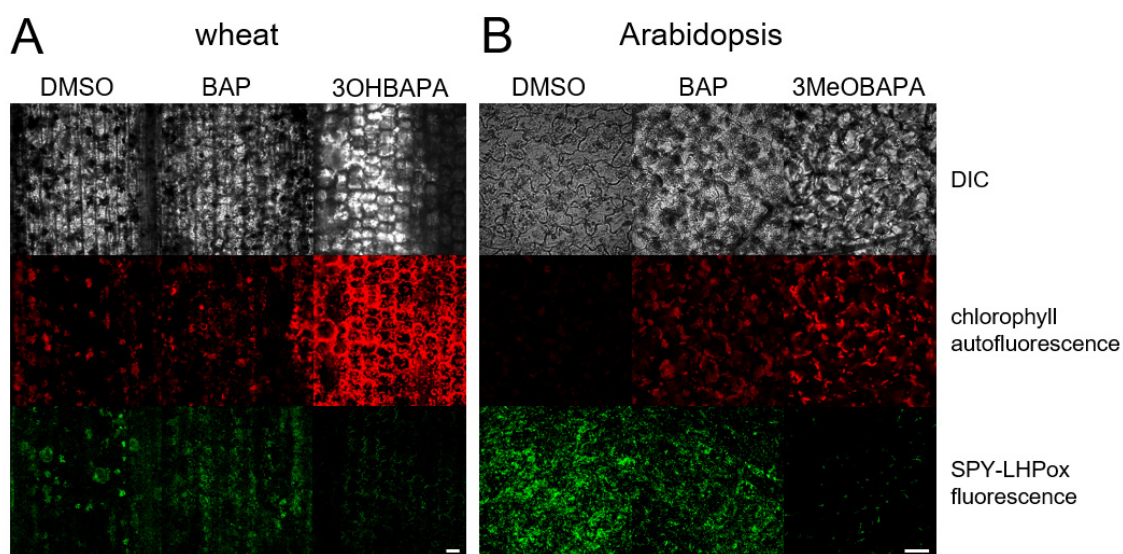
Figure 8. In vivo imaging of lipid hydroperoxides (LOOHs) using fluorescent probe SPY-LHP in (**A**) wheat and (**B**) Arabidopsis leaves kept in the dark for 6 days and subsequently exposed to high light (500 µmol photons·m^{-2}·s^{-1}) for 4 h. Detached leaves were incubated in 0.1% DMSO or 10-µmol·L^{-1} solutions of BAP, 3OHBAPA or 3MeOBAPA. Scale bars represent 50 µm. DIC, differential interference contrast.

As expected, 3OHBAPA in wheat and 3MeOBAPA in Arabidopsis were more effective in the protection of senescing leaves from oxidative damage than BAP. BAPAs markedly reduced the HL-induced cell membrane damage (Figure 7), accumulation of LOOHs (Figure 8), as well as PSII photoinhibition (Figure 9). We suppose that in the case of HL-treated wheat leaves, the high protective effect of 3OHBAPA can be mainly ascribed to the completely maintained xanthophyll cycle (Figure 9C) together with the high content of xanthophylls (Figure 10), both of which are known to be important for photoprotection [38,39].
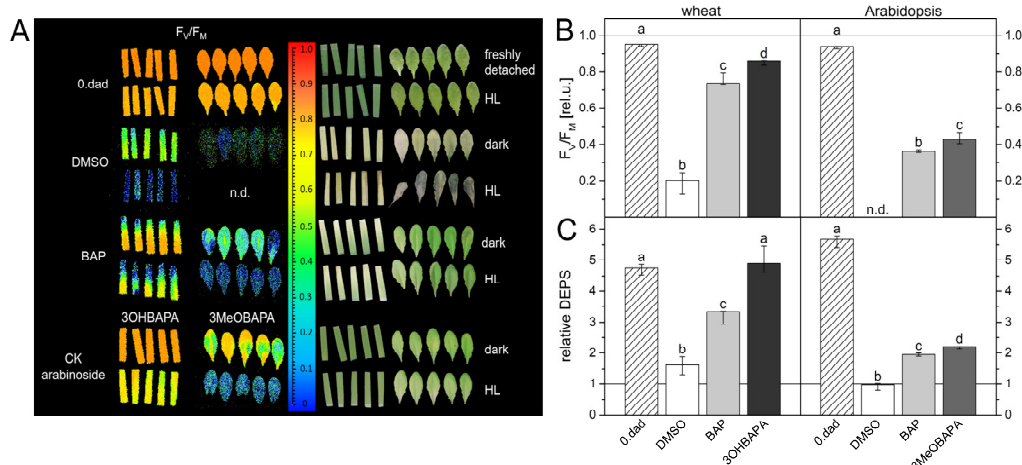
Figure 9. (**A**) Imaging of maximum quantum yield of PSII photochemistry (F_V/F_M) before and after high-light treatment (HL; 500 μmol photons·m^{-2}·s^{-1} for 4 h) of freshly detached leaves and leaves incubated for 6 days in 0.1% DMSO or 10-μmol·L^{-1} solutions of BAP, 3OHBAPA or 3MeOBAPA; (**B**) the relative F_V/F_M values and (**C**) relative de-epoxidation state of xanthophylls (DEPS) in detached wheat and Arabidopsis leaves. The relative F_V/F_M and DEPS were calculated as a ratio of values measured after and before exposure to high light. In the column graphs, medians and quartiles estimated from presented values of individual leaves are shown (*n* = 5). Different letters indicate a statistically significant difference between treatments within a plant species (*p* < 0.05; Student's unpaired *t*-test).

In Arabidopsis, the xanthophyll cycle was only moderately stimulated in the 3MeOBAPA-treated leaves exposed to HL (Figure 9), so the protective effect of 3MeOBAPA seems to be associated with the lower excitation delivery to RCII (due to the decreased LHCII/RCII ratio) (Figure 4A) and to the maintenance of xanthophylls during HL treatment (Figure 10). On the other hand, the lower protection of the BAP-treated senescent leaves could be related to the increased excitation supply to RCII (Figure 4A) due to the maintained LHCII/RCII ratio. Under HL, photosynthetic apparatus in the BAP-treated senescent leaves was most probably overexcited, which could contribute to the lower protective effect of BAP against oxidative damage. This finding is consistent with our previous work, where we have shown that under excessive light conditions, the protective action of exogenous CKs on senescent leaves can switch to damaging [7,21] due to the overexcitation of photosynthetic apparatus and oxidative damage [7].

The effective anti-oxidative protection by BAPAs could be related to the upregulation of *JUB1*, *ELIP1* and *ELIP2* detected in the 3MeOBAPA-treated Arabidopsis leaves (Table S1). The ROS-responsive transcription factor *JUB1* is considered to be a central longevity regulator in Arabidopsis that acts through the modulation of H_2O_2 level in cells [40]. It has been found that the overexpression of *JUB1* not only delays senescence, but also enhances tolerance to abiotic stresses [40].

Early-light-induced proteins (ELIPs) belong to the family of pigment-protein LHCs and fulfill a protective function and prevent oxidative damage under conditions of excess light [41]. The photoprotective function of ELIPs is based on the transient binding of free Chl and was originally thought to be important predominantly for developing leaves (e.g., [42]). However, the protective role of ELIPs was also reported during senescence, although their upregulation was conditioned by the presence of light [43] and/or correlated with light intensity [44]. Surprisingly, 3MeOBAPA upregulated *ELIPs* even in the dark, indicating that some aspects of 3MeOBAPA actions are similar to the effect of increased light. Additionally, the reduction in the LHCII/RCII ratio, observed in 3MeOBAPA-treated leaves, is typical for leaf acclimation to high-light intensities. This 3MeOBAPA-induced response may help leaves to cope with subsequent (photo)oxidative stress. Additionally, 3MeOBAPA has been shown to protect human dermal fibroblasts from UV-A and UV-B treatment [25], thus the protective

activity of this compound may be more universal. The mechanism of this 3MeOBAPA effect remains to be elucidated.
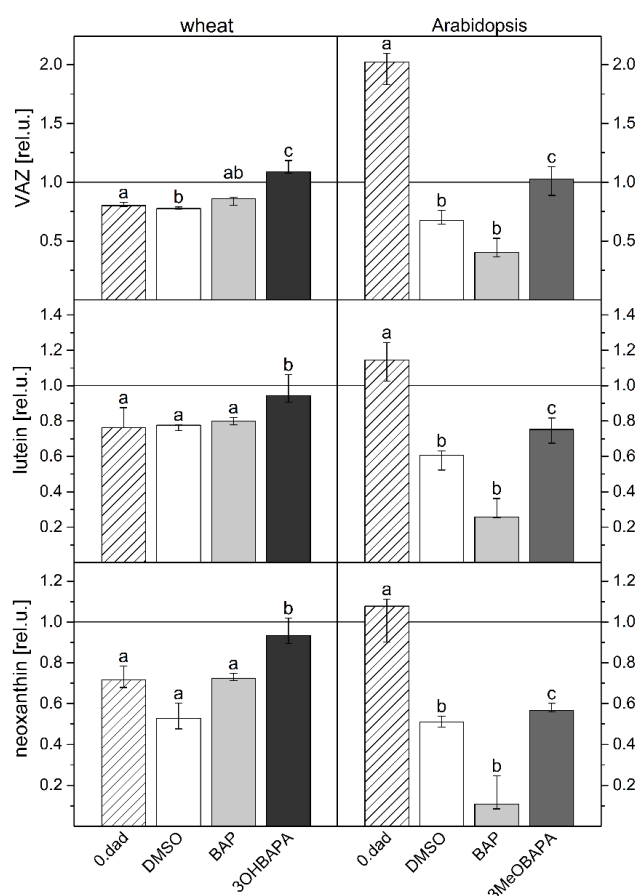

Figure 10. Violaxanthin, antheraxanthin, zeaxanthin (VAZ), lutein, and neoxanthin content (relative to the value before high-light treatment) in control (0. dad) and detached leaves of wheat and Arabidopsis incubated in 0.1% DMSO or 10-μmol·L^{-1} solutions of BAP, 3OHBAPA or 3MeOBAPA. Leaves were kept in the dark for 6 days and subsequently exposed to high light (500 μmol photons·m^{-2}·s^{-1} for 4 h). Medians and quartiles are presented (n = 4–5). Different letters indicate a statistically significant difference between treatments within a plant species ($p < 0.05$; Student's unpaired *t*-test).

2.4. On the Mechanism of Specific Anti-Senescence Activity of CK Arabinosides

In our previous work, we have shown that the unique mode of CK arabinosides' action differs from that of CKs. The CK arabinosides were shown to have only low activity in the *Amaranthus* and callus CK bioassays [25,26]. However, their activity in the senescence bioassay was high, despite the fact that in vitro they did not activate the AHK3 receptor [26], which is considered to be the main receptor involved in CK-mediated delay of senescence [2,45] and protection during HL stress [46]. The RNA-seq gene expression analysis performed by Bryksová [26] in Arabidopsis 3MeOBAPA-treated leaves revealed a broad range of transcriptomic changes typical for the activation of the PAMP-response: downregulation of a number of photosynthetic genes and upregulation of many defense genes. A similar response can be expected in BAPAs-treated wheat and barley plants, as their enhanced resistance to pathogens was observed in field trial experiments [26].

The upregulation of genes of defense regulons in the 3MeOBAPA-treated Arabidopsis leaves included jasmonate/ethylene-driven upregulation of plant defensins and was accompanied by a significant elevation of endogenous levels of jasmonic acid (JA) and its metabolites [26]. However, as we have demonstrated here, the ethylene production in the BAPA-treated leaves was low, which might

be one of the main reasons for the BAPAs' high anti-senescence activity, as ethylene is known to promote leaf senescence [35]. It has been reported that the key transcription factor of the ethylene signaling pathway *EIN3* and its downstream target *ORE1* directly activate genes of Chl degradation. *ORE1* also directly promotes ethylene synthesis and ethylene in turn accelerates leaf senescence through *EIN3–ORE1* [47]. *EIN3* and *ORE1* were downregulated by 3MeOBAPA (Table S1), which indicates that the attenuation of this loop is involved in the anti-senescence activity of 3MeOBAPA. This activity is also evidenced by the downregulation of other positive regulators of senescence, such as *SAG12*, *ORE3*, and *ORE9* (Table S1). In summary, in this work we show for the first time that the anti-senescence effect of CK arabinosides in Arabidopsis may be related to specific downregulation of the *EIN3–ORE1* pathway which has been previously shown to be involved in leaf degreening through Chl catabolic gene regulation [47].

Similarly to ethylene, JA is considered to be a positive regulator of leaf senescence. As mentioned, the level of JA and its metabolites was found to be increased in the 3MeOBAPA-treated Arabidopsis leaves [26]. However, this increase was only temporary—it was observed after 48 h of the treatment [26], while after 4 days the JA level was lower than that in the mock-treated leaves (unpublished data). The transient increase in endogenous JA content appears to be involved in triggering the defense response by 3MeOBAPA and does not stimulate, but rather suppresses, leaf senescence. This hypothesis is in line with the upregulation of the JA-signalling repressors *JAZ7* and *JAZ 8* (Table S1), as JAZ7 is known to be a specific negative regulator of dark-induced leaf senescence and together with JAZ8 suppresses the activation of *SAGs* including *SAG12* [48,49].

The specific effects of CK arabinosides described in this work represent further evidence that they act through a mechanism different from that of classical CKs. Because they have high anti-senescence activity and protective effects under stress conditions and simultaneously do not impair root development, they are promising substances for plant protection. However, further study is needed to elucidate the exact mechanism of their action.

3. Materials and Methods

3.1. Plant Material

Plants of spring wheat (*Triticum aestivum* L. cv. Aranka) were grown on an artificial medium composed of perlite and Hoagland's solution in a growth chamber at 25 °C under a 16-h light (120 µmol photons·m^{-2}·s^{-1})/8-h dark cycle for 7 days. Then segments were cut off from the primary leaves, 4 cm from the leaf tip. The basal end of the leaf segment was placed into a well of 96-well plate with 200 µL of 10-µmol·L^{-1} solutions of BAP, 3OHBAPA or 3MeOBAPA dissolved in 0.1% dimethylsulfoxide (DMSO; Sigma-Aldrich, St. Louis, MO, USA) or with 0.1% DMSO solution in deionized water (mock control). 3OHBAPA and 3MeOBAPA (Figure 1) were prepared as described previously [25,26]. The segments were kept in darkness at 24 °C for 6 days. Plants of *Arabidopsis thaliana* L. (Col-0) were grown in a soil (Potgrond H, Klasmann-Deilmann, Geeste, Germany) in a growth chamber under an 8-h light (120 µmol photons·m^{-2}·s^{-1})/16-h dark cycle and at 22 °C/20 °C for 6 weeks. Then the 7th and 8th rosette leaves were detached from the plants and incubated in a six-well plate with 5 mL of the solutions described above. Freshly detached Arabidopsis and wheat leaves were used as control (0. day after detachment; dad).

3.2. High-Light Treatment

After six days in the dark, wheat leaf segments and Arabidopsis leaves incubated in the solutions described above were exposed to high-light (HL; white light, 500 µmol photons·m^{-2}·s^{-1}) for up to 8 h to induce photo-oxidative stress. In the case of wheat, edges of the segments were cut off and the rectangular middle part (2 cm long) of the leaf segment was placed into solutions prior to the HL treatment.

3.3. Determination of Chlorophyll, Carotenoid and Xanthophyll Content

Following estimation of their area, leaf samples were frozen in liquid nitrogen, stored at −80 °C and subsequently homogenized using 80% acetone and a small amount of $MgCO_3$. Homogenate was centrifuged at 3600× *g* for 15 min at 4 °C. The supernatant was used for spectrophotometric (Unicam UV 500, Thermo Spectronics, Cambridge, UK) estimation of Chl and carotenoid contents according to Lichtenthaler [50] and for quantification of xanthophylls (violaxantin, V; anteraxantin, A; zeaxantin, Z; neoxantin; lutein) by a reversed-phase high-performance liquid chromatography (HPLC) using Alliance e 2695 HPLC System (Waters, Milford, MA, USA) equipped with 2998 Photodiode Array detectors. The separation was carried out using a gradient system (1.5 mL·min^{-1} at 25 °C) on a LiChrospher® 100 RP-18 (5 μm) LiChroCART® 250-4 (Merck, Darmstadt, Germany). Quantification was performed by absorbance at the following wavelength: 437 (neoxanthin), 441 (violaxanthin), 446 (antheraxanthin), 447 (lutein), and 454 nm (zeaxanthin) using standards purchased from DHI Lab Products (Hørsholm, Denmark). The de-epoxidation state of xanthophylls (DEPS) was calculated as DEPS = (A + Z)/(V + A + Z) [51].

3.4. Confocal Laser Scanning Microscopy

Confocal microscopy was performed on detached leaves kept in the dark for 6 days and on leaves subsequently exposed to HL for 4 h. Using fluorescent probe SPY-LHP (swallow-tailed perylene derivative; Dojindo Molecular Technologies, Rockville, MD, USA), lipid hydroperoxides (LOOHs) were localized. Wheat and Arabidopsis leaves were cut into pieces (approximately 2 mm × 2 mm) and incubated in 50 μmol·L^{-1} SPY-LHP in HEPES buffer (10 m μmol·L^{-1}, pH 7.5) in the dark at room temperature for 30 min. Afterward, the samples were visualized by a confocal microscope (FV1000, Olympus Czech Group, Prague, Czech Republic). The excitation of fluorochrome was performed using a 488-nm line of argon laser. The signal was detected through a 505–550-nm emission filter. The morphology of tissues was visualized by a 405-nm diode laser excitation in transmitted light detection module with differential interference contrast (DIC) filters, while chloroplasts by a 543-nm helium–neon laser excitation with emission recorded with a 655–755-nm bandpass filter. The proper intensity of the laser was set according to unstained samples at the beginning of each experiment [52]. During the image postprocessing in FV10-ASW 4.0 Viewer software (Olympus Czech Group, Prague, Czech Republic), the contrast of the SPY-LHP channel was increased to 3 in the case of wheat and to 4 in the case of Arabidopsis. Five replicates were performed and representative images are presented.

3.5. Chlorophyll Fluorescence Parameters (PSII Functioning)

Chl fluorescence induction transient (OJIP curve) and Chl fluorescence quenching analysis were measured at room temperature from the adaxial side of the leaves using a Plant Efficiency Analyser (Hansatech Instruments, Norfolk, UK) and FluorCam imaging system (PSI, Drásov, Czech Republic), respectively. The control leaves and HL-treated leaves were dark-adapted for 30 min prior to the measurement. In the case of senescent leaves, dark adaptation was not necessary due to their incubation in the dark.

The OJIP transient was measured in the middle of leaf segments with excitation light (red light, 4300 μmol photons·m^{-2}·s^{-1}) lasting 1 s. The initial slope of the O–J Chl fluorescence rise $(dV/dt)_0$ and the relative variable fluorescence at the J step (V_J) were evaluated. The $(dV/dt)_0$ parameter, defined as the maximal rate of accumulation of closed (i.e., reduced) RCII, was calculated as $(dV/dt)_0 = 4 (F_{300μs} - F_{50μs})/F_V$, where $F_{300μs}$ and $F_{50μs}$ are fluorescence intensities at the indicated times of the transient, and F_V is variable fluorescence ($F_V = F_P - F_0$, where F_P is fluorescence intensity at P step and F_0 is minimal fluorescence) [28]. The V_J parameter reflects a fraction of reduced RCII and was calculated as $V_J = (F_J - F_0)/F_V$, where F_J is fluorescence intensity at 2 ms (J-step).

A FluorCam imaging system was used for the measurement of quantum yields Φ_P, Φ_{NPQ} and $\Phi_{f,D}$ reflecting the proportion of three different types of energy usage by PSII (their sum equals 1; [30]) in light-adapted state of senescent leaves, and for measurement of changes in maximum quantum yield of PSII photochemistry ($F_V/F_M = (F_M - F_0)/F_M$) after HL treatment (4 h). The effective quantum yield of PSII photochemistry for the light-adapted state was calculated as $\Phi_P = (F_M' - F_t)/F_M'$. The quantum yield of regulatory light-induced non-photochemical quenching was calculated as $\Phi_{NPQ} = (F_t/F_M') - (F_t/F_M)$. The quantum yield of constitutive non-regulatory dissipation processes was calculated as $\Phi_{f,D} = F_t/F_M$. The minimal fluorescence of the dark-adapted leaf sample (F_0) was determined by applying several μ-seconds-long measuring flashes (red light, 0.1 μmol photons·m^{-2}·s^{-1}) at the beginning of the procedure. The maximal fluorescence of the dark-adapted sample (F_M) was measured using the 1.6-s saturating pulse (white light, 850 μmol photons·m^{-2}·s^{-1}). After 2 min of dark relaxation the sample was exposed to actinic light (red light, 200 μmol photons·m^{-2}·s^{-1}) and series of saturating pulses (the 1st pulse at the 3rd second of actinic light, 6 pulses in a 23-s interval, 3 pulses in a 47-s interval and the last 2 pulses in a 70-s interval) to measure the maximal fluorescence in the light-adapted sample (F_M'). The actual fluorescence signal at the time *t* of actinic illumination (F_t) was measured immediately prior to the application of saturating pulse. The last measured (steady-state) values of Φ_P, Φ_{NPQ} and $\Phi_{f,D}$ are presented.

3.6. Ethylene Production

The detached leaves of wheat and Arabidopsis were put into 10-μmol·L^{-1} solutions of BAP, 3OHBAPA, 3MeOBAPA, or into 0.1% DMSO solution in distilled water and kept sealed in 8-mL vials in darkness for 6 days. Subsequently, 1.5 mL of air was collected from each vial and reduced to 1 mL before injection to gas-chromatograph Agilent GC 6890 (Agilent Technologies, Santa Clara, CA, USA) equipped with a flame ionization detector and 50-m capillary column (HP-AL/S stationary phase, 15 μm, i.d. = 0.535). The injection temperature was set to 200 °C, oven temperature to 40 °C, and the detector temperature to 220 °C. The measurements were performed in triplicate from three different test tubes of each variant.

3.7. Ultra-Weak Photon Emission

Two-dimensional imaging of ultra-weak photon emission (UPE) [53] was measured from the adaxial side of the leaves kept in the dark for 6 days before and after their treatment with 5-mmol·L^{-1} H_2O_2. After the first UPE measurement, the leaf segments were let to dry off for 30 min under common laboratory conditions and then put into the H_2O_2 solution. After 3 h of H_2O_2 incubation, the second UPE measurement was performed while the leaves remained in the H_2O_2 solution. A ratio of UPE of the leaf after and before the H_2O_2 incubation was estimated. The UPE was detected by a highly sensitive CCD camera VersArray 1300B (Princeton Instruments Trenton, NJ, USA) equipped with an objective (F mount Nikkor 50 mm, f/1.2, Nikon, Tokyo, Japan). The CCD element was cooled down to −104 °C to reduce the background noise, the accumulation time of each measurement was 30 min. The UPE of the leaf represents the average number of counts from the leaf surface.

3.8. Ion Leakage

For the determination of the extent of ion leakage from leaf tissue as a measure of cell membrane damage, circular (diameter of 1 cm) or rectangular (2 cm long) segments were cut out from Arabidopsis leaves or wheat leaf segments, respectively. Groups of six leaf discs or eight rectangular segments (one group represents one sample) were put into 6-well plates containing 3.5 mL of deionized water and incubated under HL (500 μmol photons·m^{-2}·s^{-1}) for up to 8 h to induce oxidative damage in cell membranes. The conductivity of the solutions was measured after 2, 4, 6 and 8 h of the HL treatment with a conductivity meter (GMH 3430, Greisinger, Regenstauf, Germany). As DMSO is known to affect the membrane fluidity and permeability for ions, deionized water was used as a mock control as well to exclude effect of DMSO on the membrane permeability.

Author Contributions: Z.K. and M.Š. designed the experiments, analyzed and interpreted the data and wrote the article. Z.K. prepared samples for all experiments, performed Chl fluorescence and ion leakage measurements. M.R. performed UPE analysis and confocal microscopy. J.M. performed analysis of ethylene production. P.P. performed pigment analysis by HPLC. M.B. synthesized the CK arabinosides. M.S. supervised the confocal microscopy measurement. K.D. supervised the CK arabinoside synthesis and experimental design. O.P. contributed to the critical revision of the manuscript. All authors have read and agreed to the published version of the manuscript.

Abbreviations

A	antheraxanthin
AHK	Arabidopsis histidine kinase
BAP	6-benzylaminopurine
car	carotenoid
Chl	chlorophyll
CK	cytokinin
dad	day after detachment
DEPS	de-epoxidation state of xanthophylls
DIC	differential interference contrast
DMSO	dimethylsulfoxide
$(dV/dt)_0$	the initial slope of the O–J Chl fluorescence rise
F_V/F_M	the maximum quantum yield of photosystem II photochemistry
HL	high light
JA	jasmonic acid
LHCII	light-harvesting complexes of photosystem II
LOOH	lipid hydroperoxide
OJIP	chlorophyll fluorescence induction transient
PSII	photosystem II
Q_A	primary electron acceptor of photosystem II
RCII	reaction center of photosystem II
SAG	senescence-associated gene
UPE	ultra-weak photon emission
V	violaxanthin
V_J	the relative variable fluorescence at the J step of OJIP curve
Z	zeaxanthin
3OHBAPA	6-(3-hydroxybenzylamino)-9-β-D-arabinofuranosylpurine
3MeOBAPA	6-(3-methoxybenzylamino)-9-β-D-arabinofuranosylpurine
$\Phi_{f,D}$	the quantum yield of constitutive non-regulatory dissipation processes
Φ_{NPQ}	the quantum yield of regulatory light-induced non-photochemical quenching
Φ_P	the effective quantum yield of photosystem II photochemistry (for the light-adapted state)

References

1. Špundová, M.; Popelková, H.; Ilík, P.; Skotnica, J.; Novotný, R.; Nauš, J. Ultra-structural and functional changes in the chloroplasts of detached barley leaves senescing under dark and light conditions. *J. Plant Physiol.* **2003**, *160*, 1051–1058. [CrossRef] [PubMed]

2. Janečková, H.; Husičková, A.; Ferretti, U.; Prčina, M.; Pilařová, E.; Plačková, L.; Pospíšil, P.; Doležal, K.; Špundová, M. The interplay between cytokinins and light during senescence in detached Arabidopsis leaves. *Plant Cell Environ.* **2018**, *41*, 1870–1885. [CrossRef] [PubMed]

3. Janečková, H.; Husičková, A.; Lazár, D.; Ferretti, U.; Pospíšil, P.; Špundová, M. Exogenous application of cytokinin during dark senescence eliminates the acceleration of photosystem II impairment caused by chlorophyll b deficiency in barley. *Plant Physiol. Biochem.* **2019**, *136*, 43–51. [CrossRef] [PubMed]

4. Breeze, E.; Harrison, E.; McHattie, S.; Hughes, L.; Hickman, R.; Hill, C.; Kiddle, S.; Kim, Y.S.; Penfold, C.A.; Jenkins, D.; et al. High-resolution temporal profiling of transcripts during Arabidopsis leaf senescence reveals a distinct chronology of processes and regulation. *Plant Cell* **2011**, *23*, 873–894. [CrossRef] [PubMed]

5. Holub, L.; Hanuš, J.; Hanke, D.E.; Strnad, M. Biological activity of cytokinins derived from *ortho*- and *meta*-hydroxybenzyladenine. *Plant Growth Regul.* **1998**, *26*, 109–115. [CrossRef]

6. Oh, M.H.; Kim, J.H.; Zulfugarov, I.S.; Moon, Y.H.; Rhew, T.H.; Lee, C.H. Effects of benzyladenine and abscisic acid on the disassembly process of photosystems in an *Arabidopsis* delayed-senescence mutant, *ore9*. *J. Plant Biol.* **2005**, *48*, 170–177. [CrossRef]

7. Vlčková, A.; Špundová, M.; Kotabová, E.; Novotný, R.; Doležal, K.; Nauš, J. Protective cytokinin action switches to damaging during senescence of detached wheat leaves in continuous light. *Physiol. Plant.* **2006**, *126*, 257–267. [CrossRef]

8. Zavaleta-Mancera, H.A.; López-Delgado, H.; Loza-Tavera, H.; Mora-Herrera, M.; Trevilla-García, C.; Vargas-Suárez, M.; Ougham, H. Cytokinin promotes catalase and ascorbate peroxidase activities and preserves the chloroplast integrity during dark-senescence. *J. Plant Physiol.* **2007**, *164*, 1572–1582. [CrossRef] [PubMed]

9. Liu, L.; Li, H.; Zeng, H.; Cai, Q.; Zhou, X.; Yin, C. Exogenous jasmonic acid and cytokinin antagonistically regulate rice flag leaf senescence by mediating chlorophyll degradation, membrane deterioration, and senescence-associated genes expression. *J. Plant Growth Regul.* **2016**, *35*, 366–376. [CrossRef]

10. Weaver, L.M.; Gan, S.; Quirino, B.; Amasino, R.M. A comparison of the expression patterns of several senescence-associated genes in response to stress and hormone treatment. *Plant Mol. Biol.* **1998**, *37*, 455–469. [CrossRef]

11. Vylíčilová, H.; Husičková, A.; Spíchal, L.; Srovnal, J.; Doležal, K.; Plíhal, O.; Plíhalová, L. C2-substituted aromatic cytokinin sugar conjugates delay the onset of senescence by maintaining the activity of the photosynthetic apparatus. *Phytochemistry* **2016**, *122*, 22–33. [CrossRef]

12. Schippers, J.H.M.; Schmidt, R.; Wagstaff, C.; Jing, H.C. Living to die and dying to live: The survival strategy behind leaf senescence. *Plant Physiol.* **2015**, *169*, 914–930. [CrossRef]

13. Koprna, R.; De Diego, N.; Dundálková, L.; Spíchal, L. Use of cytokinins as agrochemicals. *Bioorg. Med. Chem.* **2016**, *24*, 484–492. [CrossRef]

14. Galuszka, P.; Popelková, H.; Werner, T.; Frébortová, J.; Pospíšilová, H.; Mik, V.; Köllmer, I.; Schmülling, T.; Frébort, I. Biochemical characterization of cytokinin oxidases/dehydrogenases from *Arabidopsis thaliana* expressed in *Nicotiana tabacum* L. *J. Plant Growth Regul.* **2007**, *26*, 255–267. [CrossRef]

15. Aremu, A.O.; Bairu, M.W.; Doležal, K.; Finnie, J.F.; Van Staden, J. Topolins: A panacea to plant tissue culture challenges? *Plant Cell Tissue Organ Cult.* **2012**, *108*, 1–16. [CrossRef]

16. Woodward, E.J.; Marshall, C. Effects of plant-growth regulators and nutrient supply on tiller bud outgrowth in barley (*Hordeum distichum* L.). *Ann. Bot.* **1998**, *61*, 347–354. [CrossRef]

17. Werbrouck, S.P.O.; Strnad, M.; Van Ockelen, H.A.; Debergh, P.C. Meta-topolin, an alternative to benzyladenine in tissue culture? *Physiol. Plant.* **1996**, *98*, 291–297. [CrossRef]

18. Iqbal, M.; Ashraf, M.; Jamil, A. Seed enhancement with cytokinins: Changes in growth and grain yield in salt stressed wheat plants. *Plant Growth Regul.* **2006**, *50*, 29–39. [CrossRef]

19. Bairu, M.W.; Stirk, W.A.; Doležal, K.; Van Staden, J. Optimizing the micropropagation protocol for the endangered *Aloe polyphylla*: Can *meta*-topolin and its derivatives serve as replacement for benzyladenine and zeatin? *Plant Cell Tissue Organ. Cult.* **2007**, *90*, 15–23. [CrossRef]

20. Rulcová, J.; Pospíšilová, J. Effect of benzylaminopurine on rehydration of bean plants after water stress. *Biol. Plant.* **2001**, *44*, 75–81. [CrossRef]

21. Prokopová, J.; Špundová, M.; Sedlářová, M.; Husičková, A.; Novotný, R.; Doležal, K.; Nauš, J.; Lebeda, A. Photosynthetic responses of lettuce to downy mildew infection and cytokinin treatment. *Plant Physiol. Biochem.* **2010**, *48*, 716–723. [CrossRef] [PubMed]

22. Plíhalová, L.; Vylíčilová, H.; Doležal, K.; Zahajská, L.; Zatloukal, M.; Strnad, M. Synthesis of aromatic cytokinins for plant biotechnology. *N. Biotechnol.* **2016**, *33*, 614–624. [CrossRef] [PubMed]

23. Tarkowská, D.; Doležal, K.; Tarkowski, P.; Åstot, C.; Holub, J.; Fuksová, K.; Schmülling, T.; Sandberg, G.; Strnad, M. Identification of new aromatic cytokinins in *Arabidopsis thaliana* and *Populus x canadensis* leaves by LC-(+)ESI-MS and capillary liquid chromatography frit-fast atom bombardment mass spectrometry. *Physiol. Plant.* **2003**, *117*, 579–590. [CrossRef] [PubMed]

24. Szüčová, L.; Spíchal, L.; Doležal, K.; Zatloukal, M.; Greplová, J.; Galuszka, P.; Kryštof, V.; Voller, J.; Popa, I.; Massino, F.J.; et al. Synthesis, characterization and biological activity of ring-substituted 6-benzylamino-9-tetrahydropyran-2-yl and 9-tetrahydrofuran-2-ylpurine derivatives. *Bioorg. Med. Chem.* **2009**, *17*, 1938–1947. [CrossRef]

25. Doležal, K.; Plíhalová, L.; Vylíčilová, H.; Zatloukal, M.; Plíhal, O.; Voller, J.; Strnad, M.; Bryksová, M.; Vostálová, J.; Rajnochová Svobodová, A.; et al. 6-aryl-9-glycosylpurines and use thereof. U.S. Patent 10,100,077, 16 October 2018.

26. Bryksová, M.; Dabravolski, S.; Kučerová, Z.; Zavadil Kokáš, F.; Špundová, M.; Plíhalová, L.; Takáč, T.; Grúz, J.; Hudeček, M.; Hloušková, V.; et al. Aromatic cytokinin arabinosides promote PAMP-like responses and positively regulate leaf longevity. *ACS Chem. Biol.* **2020**, *15*, 1949–1963. [CrossRef]

27. Nisler, J.; Zatloukal, M.; Sobotka, R.; Pilný, J.; Zdvihalová, B.; Novák, O.; Strnad, M.; Spíchal, L. New urea derivatives are effective anti-senescence compounds acting most likely via a cytokinin-independent mechanism. *Front. Plant Sci.* **2018**, *9*, 1225. [CrossRef]

28. Strasser, R.J.; Srivastava, A.; Tsimilli-Michael, M. The fluorescence transient as a tool to characterize and screen photosynthetic samples. In *Probing Photosynthesis: Mechanism, Regulation & Adaptation*; Yunus, M., Pathre, U., Mohanty, P., Eds.; Taylor & Francis: New York, NY, USA, 2000; pp. 443–480.

29. Leong, T.-Y.; Anderson, J.M. Adaptation of the thylakoid membranes of pea chloroplasts to light intensities. II. Regulation of electron transport capacities, electron carriers, coupling factor (CF1) activity and rates of photosynthesis. *Photosynth. Res.* **1984**, *5*, 117–128. [CrossRef]

30. Lazár, D. Parameters of photosynthetic energy partitioning. *J. Plant Physiol.* **2015**, *175*, 131–147. [CrossRef]

31. Triantaphylidès, C.; Havaux, M. Singlet oxygen in plants: Production, detoxification and signalling. *Trends Plant Sci.* **2009**, *14*, 219–228. [CrossRef]

32. Špundová, M.; Vlčková, A.; Doležal, K.; Habertová, A.; Nauš, J.; Strnad, M. Effect of meta-topolin and bohemine derived from benzylaminopurine on PSII function in artificially senescing wheat leaves. In *Proceedings of the 12th International Congress on Photosynthesis*; CSIRO Publishing: Collingwood, Victoria, Australia, 2001; S22-012.

33. Cary, J.A.; Liu, W.; Howell, S.H. Cytokinin action is coupled to ethylene in its effects on the inhibition of root and hypocotyl elongation in *Arabidopsis thaliana* seedlings. *Plant Physiol.* **1995**, *107*, 1075–1082. [CrossRef]

34. Zdarska, M.; Dobisová, T.; Gelová, Z.; Pernisová, M.; Dabravolski, S.; Hejátko, J. Illuminating light, cytokinin, and ethylene signalling crosstalk. *J. Exp. Bot.* **2015**, *66*, 4913–4931. [CrossRef] [PubMed]

35. Ceusters, J.; Van de Poel, B. Ethylene exerts species-specific and age-dependent control of photosynthesis. *Plant Physiol.* **2018**, *176*, 2601–2612. [CrossRef] [PubMed]

36. Wi, S.J.; Jang, S.J.; Park, K.Y. Inhibition of biphasic ethylene production enhances tolerance to abiotic stress by reducing the accumulation of reactive oxygen species in *Nicotiana tabacum*. *Mol. Cells* **2010**, *30*, 37–49. [CrossRef] [PubMed]

37. Pospíšil, P.; Prasad, A.; Rác, M. Role of reactive oxygen species in ultra-weak photon emission in biological systems. *J. Photoch Photobiol. B* **2014**, *139*, 11–23. [CrossRef] [PubMed]

38. Li, Z.; Wakao, S.; Fischer, B.B.; Niyogi, K.K. Sensing and responding to excess light. *Annu Rev. Plant Biol.* **2009**, *60*, 239–260. [CrossRef] [PubMed]

39. Pinnola, A.; Bassi, R. Molecular mechanisms involved in plant photoprotection. *Biochem. Soc. Trans.* **2018**, *46*, 467–482. [CrossRef]

40. Wu, A.; Allu, A.D.; Garapati, P.; Siddiqui, H.; Dortay, H.; Zanor, M.I.; Asensi-Fabado, M.A.; Munné-Bosch, S.; Antonio, C.; Tohge, T.; et al. JUNGBRUNNEN1, a reactive oxygen species-responsive NAC transcription factor, regulates longevity in Arabidopsis. *Plant Cell* **2012**, *24*, 482–506. [CrossRef]

41. Hutin, C.; Nussaume, L.; Moise, N.; Moya, I.; Kloppstech, K.; Havaux, M. Early light-induced proteins protect Arabidopsis from photooxidative stress. *Proc. Natl. Acad. Sci. USA* **2003**, *100*, 4921–4926. [CrossRef]

42. Meyer, G.; Kloppstech, K. A rapidly light-induced chloroplast protein with a high turnover coded for by pea nuclear DNA. *Eur. J. Biochem.* **1984**, *138*, 201–207. [CrossRef]

43. Binyamin, L.; Falah, M.; Portnoy, V.; Soudry, E.; Gepstein, S. The early light-induced protein is also produced during leaf senescence of *Nicotiana tabacum*. *Planta* **2001**, *212*, 591–597. [CrossRef]

44. Humbeck, K.; Kloppstech, K.; Krupinska, K. Expression of early-light inducible proteins in flag leaves of field-grown barley. *Plant Physiol.* **1994**, *105*, 1217–1222. [CrossRef]

45. Riefler, M.; Novák, O.; Strnad, M.; Schmülling, T. Arabidopsis cytokinin receptor mutants reveal functions in shoot growth leaf senescence, seed size, germination, root development, and cytokinin metabolism. *Plant Cell* **2016**, *18*, 40–54. [CrossRef] [PubMed]

46. Cortleven, A.; Nitschke, S.; Klaumünzer, M.; Abdelgawad, H.; Asard, H.; Grimm, B.; Riefler, M.; Schmülling, T. A novel protective function for cytokinin in the light stress response is mediated by the Arabidopsis histidine kinase2 and Arabidopsis histidine kinase3 receptors. *Plant Physiol.* **2014**, *164*, 1470–1483. [CrossRef] [PubMed]

47. Qiu, K.; Li, Z.; Yang, Z.; Chen, J.; Wu, S.; Zhu, X.; Gao, S.; Gao, J.; Ren, G.; Kuai, B.; et al. EIN3 and ORE1 accelerate degreening during ethylene-mediated leaf senescence by directly activating chlorophyll catabolic genes in *Arabidopsis*. *PLoS Genet.* **2015**, *11*, e1005399. [CrossRef]

48. Yu, J.; Zhang, Y.; Di, C.; Zhang, Q.; Zhang, K.; Wang, C.; You, Q.; Yan, H.; Dai, S.Y.; Yuan, J.S.; et al. JAZ7 negatively regulates dark-induced senescence in Arabidopsis. *J. Exp. Bot.* **2016**, *67*, 751–762. [CrossRef] [PubMed]

49. Kim, J.; Kim, J.H.; Lyu, J.I.; Woo, H.R.; Lim, P.O. New insights into the regulation of leaf senescence in Arabidopsis. *J. Exp. Bot.* **2018**, *69*, 787–799. [CrossRef] [PubMed]

50. Lichtenthaler, H.K. Chlorophylls and carotenoids: Pigments of photosynthetic biomembranes. *Methods Enzymol.* **1987**, *148*, 350–382. [CrossRef]

51. Gilmore, A.M.; Björkman, O. Adenine nucleotides and the xanthophyll cycle in leaves—I. Effects of CO_2- and temperature-limited photosynthesis on adenylate energy charge and violaxanthin de-epoxidation. *Planta* **1994**, *192*, 526–536. [CrossRef]

52. Sedlářová, M.; Petřivalský, M.; Piterková, J.; Luhová, L.; Kočířová, J.; Lebeda, A. Influence of nitric oxide and reactive oxygen species on development of lettuce downy mildew in *Lactuca* spp. *Eur. J. Plant Pathol.* **2011**, *129*, 267–280. [CrossRef]

53. Prasad, A.; Pospíšil, P. Towards the two-dimensional imaging of spontaneous ultra-weak photon emission from microbial, plant and animal cells. *Sci. Rep.* **2013**, *3*, 1211. [CrossRef]

Suppl. Table 1 The expression level of selected genes involved in senescence regulation and protection against oxidative damage in *Arabidopsis thaliana* L. (AT, Col-0) after 48 h treatment with 10 µmol L^{-1} 3MeOBAPA. Gene ID, name and description and log2 fold change of mock-treated and 3MeOBAPA-treated transcript abundance are listed. RNA-seq gene expression analysis was performed within our previous study [26].

ID	Log2 fold change	Gene name	description
AT5G45890	-12.35	*SAG12*	SENESCENCE-ASSOCIATED GENE 12
AT5G03280	-0.93	*EIN2, ORE3*	ETHYLENE INSENSITIVE 2, ORESARA 3
AT3G20770	-0.69	*EIN3*	ETHYLENE INSENSITIVE 3
AT5G39610	-1.30	*ORE1*	ORESARA 1
AT2G42620	-1.66	*ORE9*	ORESARA 9
AT2G43000	4.14	*JUB1*	JUNGBRUNNEN 1
AT3G22840	5.02	*ELIP1*	EARLY-LIGHT INDUCED PROTEIN 1
AT4G14690	3.71	*ELIP2*	EARLY-LIGHT INDUCED PROTEIN 2
AT1G30135	5.19	*JAZ8*	JASMONATE-ZIM-DOMAIN PROTEIN 7
AT2G34600	1.13	*JAZ7*	JASMONATE-ZIM-DOMAIN PROTEIN 8